

524 /2
1999



ISSN - 0132 - 1447

BULLETIN

OF THE GEORGIAN ACADEMY
OF SCIENCES

საქართველოს
მეცნიერებათა აკადემიის

გოაგბე

VOLUME 160, NUMBER 2
SEPTEMBER-OCTOBER

1999

T B I L I S I
თბილისი

The Journal is founded in 1940

BULLETIN

OF THE GEORGIAN ACADEMY OF SCIENCES

is a scientific journal, issued bimonthly in
Georgian and English languages

Editor-in-Chief

Academician **Albert N. Tavkhelidze**

Editorial Board

T. Andronikashvili,

T. Beridze (Deputy Editor-in-Chief),

I. Gamkrelidze,

T. Gamkrelidze,

R. Gordeziani (Deputy Editor-in-Chief),

G. Gvelesiani,

I. Kiguradze (Deputy Editor-in-Chief),

T. Kopaleishvili,

G. Kvesitadze,

J. Lominadze,

R. Metreveli,

D. Muskhelishvili (Deputy Editor-in-Chief),

T. Oniani,

M. Salukvadze (Deputy Editor-in-Chief),

G. Tsitsishvili,

T. Urushadze,

M. Zaalishvili

Executive Manager - L. Gverdtsiteli

Editorial Office:

Georgian Academy of Sciences

52, Rustaveli Avenue,

Tbilisi, 380008,

Republic of Georgia

Telephone : + 995 32 99.75.93

Fax : + 995 32 99.88.23

E-mail : **BULLETIN@PRESID.ACNET.GE**

CONTENTS

MATHEMATICS

Z. Khechinashvili. Mean Square Optimal Hedging Strategies for Currency Option	197
V. Kokilashvili. On the Compactness of Weak Singular Integral Operators on Regular Curves	199
N. Vakhania, V. Kvaratskhelia. Absolute and Unconditional Convergence in l_1	201
K. Gelashvili. On One Randomized Method of Directional Derivative Computation	204
E. Khmaladze. A Non-Abelian Tensor Product Modulo q of Lie Algebras	207
Z. Rostomashvili. Remark to the Projective Geometry over Rings and Corresponding Lattices	211

MATHEMATICAL PHYSICS

T.Burchuladze, R.Rukhadze, Yu.Bezhuashvili. On the Fundamental Solutions of the System of Equations for Oscillation of Hemitropic Micropolar for Two-Dimensional Case	213
---	-----

CYBERNETICS

G.Karumidze, G.Giorgadze, D.Goshadze, E. Kordzaia, T.Tsitlidze. On One Parametric Method for Mathematical Programming Problems Solving	217
L. Kadagishvili. Recognition of Images by Quadtree Method	219
O.Tavdishvili, T.Sulaberidze. Statistical Approach to Image Segmentation	223
N.Archvadze, E.Dekanosidze, J. Vakhtangadze, M.Nizharadze, N.Papunashvili, M.Pkhovelishvili, M.Tsuladze. System of Tutorial Courses Building	226
T. Ebralidze, N. Ebralidze. The Self-Excited Oscillation Hydraulic System (The Hydraulic Motor)	228

PHYSICS

A.Bichinashvili, M.Zviadadze, T.Mkhatrishvili, V.Achelashvili, I.Bendiashvili. The Formation of the Thermosensitive Equipment on the Basis of γ -Mn Alloy	231
S. Gotoshia, L. Gotoshia. Laser Raman Spectroscopy of A^3B^3 Amorphous Binary and Ternary Semiconductors Synthesized by Ion Implantation	234
V. Jakeli, Z. Kachlishvili, E. Khizanishvili. Electrothermal Ionization Mechanism and Impurity Breakdown	238
N.Margiani, T.Medoidze, J.Nakaidze, T.Nakaidze, G.Nakashidze, G.Tsintsadze. Fabrication and Investigation of the High-Temperature Superconducting Wires and Electromagnetic Solenoids	241
M.Dzhibladze, Z.Melikishvili, V.Bykov, T.Sanadze. The Interaction of Photon Clusters with Matter	244
M. Elizbarashvili, N. Kekelidze, M. Metskhvarishvili, Y. Metskhvarishvili. Investigation of the Internal Conversion Electrons Spectrum for the ^{154}Gd 123.07 keV γ -Transition	248
J.Mebonia, M.Abusaini, P.Saralidze, K.Sulakadze, G.Skhirtladze. Mechanism of Nucleon-Deuteron Elastic Scattering	251

GEOPHYSICS

- Z. Kereselidze, I. Gabisonia. On the Specificity of a Large-Scale Electric Field Modelling on the Boundary of the Dayside of the Earth's Magnetosphere 255
- Z. Khvedelidze, A. Topchishvili. Calculations of Radiation Balance in View of a Landscape Peculiarity 259
- I. Shengelia. A Model of the Spectral Diffuse Radiation Field for Georgia 262

ANALYTICAL CHEMISTRY

- Sh. Shatirishvili. High Performance Liquid Chromatography for Determination of Phenol Carboxylic Acids in Wine Materials 266
- R. Revia, G. Makharadze, G. Supatashvili. Preconcentration of Fulvic Acid from Aqueous Media Using Nonionic Surfactants 269

ORGANIC CHEMISTRY

- I. Chikvaizde, Sh. Samsoniya, T. Narindoshvili. Azocoupling Reactions of 2-(diphenylmethane-4-yl)indole and 2-(diphenylethane-4-yl)indole 272
- M. Trapaidze, E. Chkhaidze, Sh. Samsoniya. Conversion of 2,7-naphthilendihydrazine. 275

PHYSICAL CHEMISTRY

- G. Chakhtauri, M. Gverdtsiteli, N. Tssetsadze, E. Gelashvili. Graph "Asymmetric Star" and its Application for Algebraic-Chemical Study of Reactions of Coordination Compounds 277
- G. Makharadze, G. Sidamonidze, T. Kopperia, M. Gudavadze, N. Goliadze. The Infrared Spectrum of Humic Acids Isolated from Sediments 281

ELECTROCHEMISTRY

- R. Kvaratskhelia, E. Kvaratskhelia. Voltammetry of Oxalic Acid at the Solid Electrodes in Aqueous Solutions and Mixed Media 285
- G. Agladze, G. Gordadze, N. Koiava, N. Niozadze. Experimental Study of Current and Potential Distribution on Bipolar Electrode 289

GEOLOGY

- D. Shengelia. Again about the Atsghara Tectonic Wedge 292

MACHINE BUILDING SCIENCE

- M. Chelidze. Influence of Electromagnetic Disturbing Force on Dynamic Stability of Vibration 295

ENERGETICS

- V. Kashakashvili. On the Optimal Structure of Georgian Power System 299

PLANT GROWING

- N. Lomtadze. Biological Peculiarities of Seeds Germination of Japanese Medlar Turkish Varieties in Humid Subtropical Zone of Georgia 302

BOTANY

- I. Grigolia, A. Tsitsvidze. Some Peculiarities of Pine Growth, Development and Cultivation in Eastern Georgia 305
- M. Iashvili, N. Melia, L. Gabedava, L. Zhgenti. On Ultrastructural Study of Somatic and Generative Cells in some Subnival Belt Plants of Kazbegi 308

HUMAN AND ANIMAL PHYSIOLOGY

- T. Oniani, N. Darchia, I. Gvilia, N. Lortkipanidze, L. Maisuradze, L. Oniani, M. Eliava, V. Moliadze. The Effect of Food Deprivation on the Sleep-Wakefulness Cycle in Rodents 311

BIOPHYSICS

- G. Mikadze, M. Melikishvili, M. Zaalishvili. The Tropomyosin Molecule Domain Potentiating Actomyosin Contraction 315

BIOCHEMISTRY

- I. Pagava, G. Grigorashvili. Study of Biological Value of a Protein Concentrate from Grape Pomace 318
- B. Arziani. On some Regularities of Phenol-Peptide Conjugates Formation 320
- I. Abdushelishvili, V. Phiriashvili, B. Arziani, V. Ugrekhelidze. Influence of Copper on the Hydroxylation of Exogenous Benzoic Acid in Pea Seedlings 323
- N. Moseshvili, N. Aleksidze. Distribution of Soluble Proteins with Lectin Activity in Different Organs of *Mentha pulegium* and Biological Characteristics 327

MICROBIOLOGY AND VIROLOGY

- A. Gujabidze, T. Macharashvili, N. Gabashvili. Ecologo-physiologic Groups of Bacteria Formed on the Coatings of Certain Materials 331
- D. Pataraya, L. Basilashvili, M. Bagalishvili, M. Kikvidze, M. Betsiashvili, N. Nutsubidze. Influence of Nodule Bacteria and Different Microorganisms on Soybean Growth 334
- N. Tsilosani. The Use of a Biological Object, Bacteriophage in Trassing 337
- N. Goginashvili. The Increase of Insectine Effectiveness by Weakening Insects Chitinous Barriers 341

ZOOLOGY

- N. Jimsheleishvili, N. Bagaturia, I. Eliava. Two Species of Dorylaimida (Nematoda) New for Georgian Fauna 344

PARASITOLOGY AND HELMINTHOLOGY

- B. Kurashvili. To the Problem of Localization of Echinococcus Larval Stage in Animal and Human Organisms 347

CYTOLOGY

- A. Mamardashvili. On the Problem of Metabolic Correlation between Nucleus and Cytoplasm in Neutrophils of Alcoholic Patients 350



- M. Gagua, D. Dzidziguri, E. Mikadze, V. Bakhutashvili. Study of Plaferon
 LB Influence on White Rat Hepatocytes Morphofunctional Activity 352

HYDROBIOLOGY

- J. Oniani, A. Kudriashov, E. Esebuia, Kh. Mebonia. Biological Monitoring of
 Ecological Danger of Sewage Waters of Various Production Activities 355
- V. Yurin, J. Oniani, L. Abadovskaia, E. Esebuia, G. Ermolenko. Comparison of
 Electroalgalogical Testing Results with the Data of other Testing Procedures
 Using Hydrobionates 358

EXPERIMENTAL MEDICINE

- S. Mgebrishvili. Denture Functional Efficiency during Orthopedic Treatment of
 Secondary Complete Adenty 361
- T. Shatilova, M. Beraia. Glaucoma with Normal Pressure and Blood Circulation
 Disorders in Carotid Artery 364
- K. Gogilashvili, M. Ivericli. Evaluation of Decompensated Caries Reoccurrence Risk 368
- L. Danelishvili, E. Shilakadze. Drug-Resistance of *M. tuberculosis* and the Future
 Challenges of Bacteriological Service in Georgia 370
- M. Jebashvili. The Importance of Psychoadaptational and Personality Peculiarities in
 Development of Early Menopause 373

PALAEOBIOLOGY

- L. Gabunia, O. Bendukidze. On the First Find of the Land Mammal Remains in the
 Paleogene Deposits of Tbilisi Environs 375

ECOLOGY

- M. Murvanidze. To the Study of Quantitative Dynamics of Oribatid Mites (Acari,
 Oribatei) in Urban Conditions 377
- K. Tabagari, M. Tsitskishvili, N. Lomsadze. Strontium-90 and Cesium-137 Content
 in Food Products of Georgia 380

PHILOLOGY

- G. Tevzadze. The Calculation Rule of Real Rhythm Variants of Various Rhythmic
 Structures 383
- O. Petriashvili. Distinctive Features of Literary Grotesque 386
- M. Khukhunaishvili-Tsiklauri. On Genetic Roots of Tamar According to Folklore
 Materials 389

HISTORY

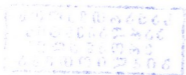
- T. Evdoshvili. Armenian Historical Source of Tamerlan's First Invasions of Georgia 392

LINGUISTICS

- V. Lekiasvili. On the Semantics of Linguistic Units 396

HISTORY OF ART

- A. Arveladze. To the Problem of Correlation of the Pianist's Hearing and Moving
 System 398



Z. Khechinashvili

Mean Square Optimal Hedging Strategies for Currency Option

Presented by Corr. Member of the Academy N.Vakhania, February 8, 1999

ABSTRACT. In this paper we consider the currency market where the foreign savings account process expressed in domestic currency and discount by domestic savings account represent a martingale with respect to the initial measure. We find hedging strategies for the European contingent claim to be optimal in the sense of square criterion.

Key words: Gaussian martingale, mean square optimal hedging strategies, currency market, contingent claim.

All the processes are defined on the filtered probability space $(\Omega, \mathcal{F}, (\mathcal{F}_t)_{t \geq 0}, P)$. The foreign stock price, i.e. the price in domestic currency of one unit of foreign currency is given by the following stochastic process

$$S_t = S_0 e^{N_t - \mu \langle N \rangle_t}, \quad S_0 > 0, \quad (1)$$

where $N = (N_t, \mathcal{F}_t)_{t \geq 0}$ is the right-continuous Gaussian martingale with the compensator $\langle N \rangle$. Assume, that the foreign and domestic interest rates r_f and r_d are some non-negative constants and savings accounts satisfy the equalities

$$B_t^f = e^{r_f \langle N \rangle_t}, \quad B_t^d = e^{r_d \langle N \rangle_t}. \quad (2)$$

Let's consider European call option [1] with contingent claim $f(S_T) = (S_T - K)^+$ on the foreign currency, where K and T are the given exercise price and expiry date and $f = f(x)$, $x \in (0, \infty)$ is a Borel function satisfying the condition

$$f(x) \leq c(1 + x^{p_1})x^{-p_2}, \quad (3)$$

where c, p_1, p_2 are some nonnegative constants.

Our aim is to find self-financing hedging strategies [2] optimal in the sense of the following square criterion

$$\inf_{\pi \in SF} E \left(\frac{f(S_T)}{e^{r_d \langle N \rangle_T}} - X_T^* \right)^2, \quad (4)$$

where X_T^* is the discounted wealth process and inf is taken by the all self-financing strategies. Such approach was developed, for example, in [2]. Let us $\mu = r_d - r_f - \frac{1}{2}$, then the process:

$$S_t^* = \tilde{B}_t^f (B_t^d)^{-1} = S_0 e^{N_t - \frac{1}{2} \langle N \rangle_t}, \quad t \in [0, T] \quad (5)$$

represents the martingale and for the hedging of currency option in the sense of criterion (4) theorems which received in [3] may be used. We receive the following theorem.

Theorem 1. Let's define the currency market by formulas (1), (2). Assume, that the

$\mu = r_d - r_f - \frac{1}{2}$ and $\Delta N_T = 0$. For the European standard call option with contingent claim $f(S_T) = (S_T - K)^+$, which satisfies condition (3), optimal in the sense of criterion (4) self-financing hedging strategy is

$$\begin{aligned} \gamma_t^* = & \frac{1}{e^{r_f(N)_T}} \Phi \left(\frac{\ln \frac{S_{t-}^*}{K} + (r_d - r_f + \frac{1}{2})(\langle N \rangle_T - \langle N \rangle_{t-}) + (r_d - r_f)\langle N \rangle_{t-}}{\sqrt{\langle N \rangle_T - \langle N \rangle_{t-}}} \right) - \\ & - \frac{e^{\Delta(N)_t} a_t^{-1} \sigma_t}{e^{r_f(N)_T} (e^{\Delta(N)_t} - 1)} \Phi \left(\frac{-a_t (\ln \frac{K}{S_{t-}^*} + I_t^{(1)})}{\sqrt{1 + \sigma_t^2}} \right) + \frac{K a_t^{-1} \sigma_t}{S_{t-}^* e^{r_d(N)_T} (e^{\Delta(N)_t} - 1)} \times \\ & \Phi \left(\frac{-a_t (\ln \frac{K}{S_{t-}^*} + I_t^{(2)})}{\sqrt{1 + \sigma_t^2}} \right) - \frac{1}{S_{t-}^* (e^{\Delta(N)_t} - 1)} \times \\ & \left[\frac{S_{t-}^*}{e^{r_f(N)_T}} \Phi \left(\frac{\ln \frac{S_{t-}^*}{K} + (r_d - r_f + \frac{1}{2})(\langle N \rangle_T - \frac{1}{2}\langle N \rangle_{t-})}{\sqrt{\langle N \rangle_T - \langle N \rangle_{t-}}} \right) - \right. \\ & \left. - \frac{K}{e^{r_d(N)_T}} \Phi \left(\frac{\ln \frac{S_{t-}^*}{K} + (r_d - r_f - \frac{1}{2})(\langle N \rangle_T + \frac{1}{2}\langle N \rangle_{t-})}{\sqrt{\langle N \rangle_T - \langle N \rangle_{t-}}} \right) \right], \end{aligned}$$

where

$$\begin{aligned} I_t^{(1)} &= (r_f - r_d - \frac{1}{2})(\langle N \rangle_T + \frac{1}{2}\langle N \rangle_t) - \frac{3}{2}\Delta(N)_t, \quad a_t = (\langle N \rangle_T - \langle N \rangle_t)^{-\frac{1}{2}} \\ I_t^{(2)} &= (r_f - r_d + \frac{1}{2})(\langle N \rangle_T - \frac{1}{2}\langle N \rangle_t) + \Delta(N)_t, \quad \sigma_t^2 = a_t^2 (\Delta(N)_t). \end{aligned}$$

Tbilisi I. Javakishvili State University

REFERENCES

1. F.Black, M. Sholes. Journal of political Economy, May/June, 1973, 637-657.
2. M.Musela, M. Rutkowski. Applications of mathematics. 36. Springer-Verlag, Berlin Heidelberg, N-Y, 1997.
3. O. Glonti, Z. Khechinashvili. Proc. A. Razmadze Math. Inst., Tbilisi, 1997, 115, 33-43.

Corr. Member of the Academy V. Kokilashvili

On the Compactness of Weak Singular Integral Operators on Regular Curves

Presented July 5, 1999

ABSTRACT. The compactness criterion for a weak singular integral operator on curves is derived.

Key words: weak singular integral operator, compactness, regular curve.

Let Γ be a rectifiable Jordan curve on the complex plane C . Let ν be the arc length measure on Γ .

Γ is said to be regular, if the following Alfers-Carleson condition is satisfied: there exists a constant $c > 0$ such that

$$D(z, r) \leq cr, \quad z \in \Gamma, \quad r > 0,$$

where $D(z, r) = B(z, r) \cap \Gamma$, $B(z, r) = \{w \in C: |z - w| < r\}$.

It is well known (see [1]), that the Cauchy integral operator is continuous in $L^p(\Gamma)$, ($1 < p < \infty$), if and only if Γ is regular.

Let us consider the weak singular integral operator

$$T_\gamma f(t) = \int_\Gamma \frac{f(\tau)}{|t - \tau|^{1-\gamma}} d\nu, \quad 0 < \gamma < 1.$$

In [2] we proved the following

Theorem 1. Let $1 < p < \gamma^{-1}$ and $q = p(1 - p\gamma)^{-1}$. Then T_γ is bounded from $L^p(\Gamma)$ into $L^q(\Gamma)$ if and only if Γ is regular.

This theorem is analogous to Hardy-Littlewood and Sobolev's results.

In this note we consider the compactness problem for T_γ . The following statement is true:

Theorem 2. Suppose that Γ belongs to some bounded domain. Assume also that $1 < p < \gamma^{-1}$. Then for the compactness of T_γ from $L^p(\Gamma)$ into $L^s(\Gamma)$ for some s , $p \leq s < p(1 - p\gamma)^{-1}$, it is necessary and sufficient that Γ be regular.

Note that this Theorem becomes invalid when $s = q$.

Now we will consider the similar problem in weighted Lebesgue spaces. Let ρ be an integrable, almost everywhere positive function on Γ . Then we define the weighted space $L^p(\Gamma, \rho)$ ($1 < p < \infty$) with the norm

$$\|f\|_{L^p(\Gamma, \rho)} = \left(\int_\Gamma |f(t)|^p \rho(t) d\nu \right)^{1/p}.$$

Note that in [3] we announced the necessary and sufficient condition for the compact-

ness of the potential operator T_γ from L_w^p into L_v^q ($1 < p < q < \infty$). The similar criteria work also for the operator T_γ which is considered in the present paper. But now our aim is to get a sufficient condition which is more easy to verify.

Theorem 3. Let Γ be a regular curve in the bounded domain. Assume also that $1 < p < \gamma^{-1}$ and $p < s < q$, where $q = p(1 - p\gamma)^{-1}$.

Then operator T_γ is compact from $L_w^p(\Gamma)$ into $L_v^s(\Gamma)$ if the condition

$$\sup_{\substack{z \in \Gamma \\ r > 0}} \left(\int_{D(z, 2r)} w^{1-p'}(t) dV \right)^{1/p'} \left(\int_{\Gamma \setminus D(z, r)} \frac{v(t)}{|z-t|^{(1-\sigma)s}} dV \right)^{1/s} < \infty,$$

with $\sigma = p^{-1} - s^{-1}$, is fulfilled.

Georgian Academy of Sciences
 A.Razmadze Mathematical Institute

REFERENCES

1. G. David. Ann.Sci. Ecole Norm. Sup. 17, 1984, 157-189.
2. V. Kokilashvili. Trudy Tbilis. Math. Inst. Razmadze, 76, 1985, 100-106.
3. D.E. Edmunds, V. Kokilashvili. Proc. A.Razmadze Math. Inst., 117,1998,123-125.



Corr. Member of the Academy N. Vakhania, V. Kvaratskhelia

Absolute and Unconditional Convergence in l_1

Presented May 12, 1999

ABSTRACT. One of the consequences of the famous Dvoretzky-Rogers theorem (1950) is the existence of an unconditionally convergent series in l_1 that fails to converge absolutely. The first direct proof of this fact was given by M. S. Macphail (1947). We give a simple and elementary example for this kind of series.

Key words: absolute convergence, unconditional convergence.

1. Let X be a real Banach space. The series $\sum x_k$, $x_k \in X$, is called absolutely convergent if $\sum \|x_k\| < \infty$, and is called unconditionally convergent if $\sum x_{\pi(k)}$ converges for any rearrangement π of the set of positive integers (in which case it has the same limit for all rearrangements). We consider convergence in norm topology. It is easy to show, applying the Cauchy criterion and obvious equality $\|x\| = \sup\{|(x^*, x)| : x^* \in X^*, \|x^*\| \leq 1\}$, that the series $\sum x_k$ unconditionally converges if (and only if, but we do not need the converse):

$$(a) \sum |(x^*, x_k)| < \infty \text{ for all } x^* \in X^* \quad \text{and} \quad (b) \limsup_{n \rightarrow \infty} \sup_{\|x^*\| \leq 1} \sum_{k=n}^{\infty} |(x^*, x_k)| = 0.$$

Absolute convergence implies obviously unconditional convergence. It is well-known that the converse statement is true for $X = R^1$ and, therefore, for any finite-dimensional Banach space. The situation is quite different if X is infinite-dimensional. A famous result of A. Dvoretzky and C. A. Rogers (1950) states that for any infinite-dimensional X and any sequence (c_k) of positive real numbers with $\sum c_k^2 < \infty$ there exists an unconditionally convergent series $\sum x_k$ such that $\|x_k\| = c_k$ for all k . Therefore (taking $c_k = \frac{1}{k}$) in any infinite-dimensional X there exists an unconditionally convergent series that fails to converge absolutely. Such series can easily be constructed in many standard Banach spaces. If, for example, $X = l_p$, $1 < p < \infty$, then clearly the series with $x_k = \frac{e_k}{k}$, where (e_k) denotes the natural basis in l_p gives an example. The case of the space l_1 is far more difficult. Existence of a series in l_1 which converges unconditionally but does not converge absolutely was first proved by M. S. Macphail [1] three years before Dvoretzky-Rogers

result came out. Afterwards other, easier proofs appeared (see [2]). However, as far as we know, a concrete elementary example in l_1 was not found in literature. In the present note we give a simple and elementary example of this type using a construction that might be useful for other problems of this kind as well.

2. Let

$$\Delta^{(1)} = \begin{vmatrix} 1, & 1 \\ 1, & -1 \end{vmatrix}, \quad \Delta^{(n+1)} = \begin{vmatrix} \Delta^{(n)}, & \Delta^{(n)} \\ \Delta^{(n)}, & -\Delta^{(n)} \end{vmatrix}, \quad n = 1, 2, \dots$$

It is easily seen that $\Delta^{(n)}$ is for any n a $2^n \times 2^n$ square matrix with entries $\Delta_{\bar{k}i}^{(n)}$ equal to $+1$ or -1 . It can easily be shown by a simple inductive reasoning that distinct columns of $\Delta^{(n)}$ are mutually orthogonal vectors of R^{2^n} . Therefore, for any n we have the equality

$$\sum_{k=1}^{2^n} \Delta_{\bar{k}i}^{(n)} \Delta_{\bar{k}j}^{(n)} = 2^n \delta_{ij}, \quad (1)$$

where δ_{ij} is the Kronecker delta.

Let further $N = \bigcup_{n=1}^{\infty} I_n$ be the partition of the set N of positive integers into the sections $I_n = [2^n - 1, 2^n, \dots, 2^{n+1} - 2]$, $n = 1, 2, \dots$ and let (δ_n) be a given sequence of positive numbers. Any positive integer k belongs to one of the sections I_n , i. e. has the form $k = 2^n - 2 + \bar{k}$, where $\bar{k} = 1, 2, \dots, 2^n$. For such k we set

$$d_k = \delta_n \sum_{i=1}^{2^n} \Delta_{\bar{k}i}^{(n)} e_{2^n - 2 + i}, \quad k \in I_n, \quad (2)$$

where (e_k) is the natural basis in l_1 or, equivalently, we denote

$$d_k = \delta_n (\overbrace{0, 0, \dots, 0}^{2^n - 2}, \Delta_{\bar{k}1}^{(n)}, \Delta_{\bar{k}2}^{(n)}, \dots, \Delta_{\bar{k}2^n}^{(n)}, 0, 0, \dots, 0).$$

The elements d_k depend on the given sequence (δ_k) . However, for the sake of simplicity, this dependence is not reflected in the notation.

Clearly, $d_k \in l_1$ for any $k = 1, 2, \dots$ whatever the sequence (δ_k) is. Our aim is to choose (δ_k) so that the series $\sum d_k$ unconditionally converges in l_1 but does not converge absolutely. We first give two simple and elementary technical facts.

Lemma. For any given $k \in I_n$ ($n = 1, 2, \dots$) and $f \in l_1^* = l_\infty$ we have

(i) $\|d_k\| = 2^n \delta_n,$

(ii) $\sum_{k \in I_n} |(f, d_k)|^2 \leq 2^{2n} \delta_n^2 \|f\|_{l_\infty}^2.$

Proof. (i) We use the (same) notation e_j for the element of l_∞ having 1 at j -th place

and 0 at other places. Writing the sum $\sum_{j=1}^{\infty}$ as $\sum_{m=1}^{\infty} \sum_{j \in I_m}$ and using relation (2) gives

$$\|d_k\| = \sum_{j=1}^{\infty} |(e_j, d_k)| = \delta_n \sum_{m=1}^{\infty} \sum_{j \in I_m} \left| \sum_{i=1}^{2^n} \pm(e_j, e_{2^n-2+i}) \right|,$$

and it is enough to note that for any $j \in I_m$

$$\left| \sum_{i=1}^{2^n} \pm(e_j, e_{2^n-2+i}) \right| = \left| \sum_{i \in I_n} \pm(e_j, e_i) \right| = \delta_{mn}.$$

Proof. (ii). Recall that k and n are connected by the condition $k \in I_n$. According to relation (2) we have

$$\sum_{k \in I_n} (f, d_k)^2 = \delta_n^2 \sum_{i, j=1}^{2^n} (f, e_{2^n-2+i})(f, e_{2^n-2+j}) \sum_{k \in I_n} \Delta_{ki}^{(n)} \Delta_{kj}^{(n)}$$

and relation (1) ends the proof since it gives

$$\sum_{k \in I_n} (f, d_k)^2 = 2^n \delta_n^2 \sum_{i=1}^{2^n} (f, e_{2^n-2+i})^2 \leq 2^{2n} \delta_n^2 \|f\|_{l_\infty}^2.$$

Now we are ready to choose the sequence (δ_n) . We claim we can take $\delta_n = 2^{-cn}$ with $3/2 < c < 2$. Indeed, statement (i) of the Lemma shows that the series $\sum d_k$ with $\delta_n = 2^{-cn}$, $c < 2$, does not converge absolutely. To show unconditional convergence we verify conditions (a) and (b) above. For $f \in l_\infty$ we have by virtue of Holder inequality

$$\sum_k |(f, d_k)| = \sum_{n=1}^{\infty} \sum_{k \in I_n} |(f, d_k)| \leq \sum_{n=1}^{\infty} 2^{\frac{n}{2}} \left[\sum_{k \in I_n} (f, d_k)^2 \right]^{1/2},$$

and statement (ii) of the Lemma gives the verification of condition (a). Condition (b) can be verified analogously after the following preliminary observation:

$$\sum_{k=n}^{\infty} |(f, d_k)| \leq \sum_{k=2^m-1}^{\infty} |(f, d_k)| = \sum_{j=m}^{\infty} \sum_{k \in I_j} |(f, d_k)| \leq \sum_{j=m}^{\infty} 2^{\frac{j}{2}} \left[\sum_{k \in I_j} (f, d_k)^2 \right]^{1/2},$$

where m is the integer part of $\log_2(n+1)$.

Thus the series $\sum d_k$ with $\delta_n = 2^{-cn}$, $3/2 < c < 2$, gives the required example.

Georgian Academy of Sciences

N. Muskhelishvili Institute of Computational Mathematics

REFERENCES

1. *M.S.Macphail*. Bull. of the AMS, **53**, 2, 1947, 121-123.
 2. *M.I.Kadets, V.M.Kadets*. Rearrangements of series in Banach spaces, Transl. Math. Monographs, **86**, AMS, Providence, RI, 1991.

K. Gelashvili

On One Randomized Method of Directional Derivative Computation

Presented by Member of the Academy G.Kharatishvili, July 20, 1998

ABSTRACT. We present one method of directional derivative computation, which does not use the operation of multiplication of vector and scalar on the domain of values of functions and which is applicable to large class of functions by its randomized nature.

Key words: directional derivative, randomization, directedness.

The present method takes into account an element of randomness, so it is applicable to large class of functions and more safe than determinate methods. It uses only the binary operation from the algebraic structure of the domain of values.

Let X and Y be Banach spaces, O be the open subset in X , $f:O \rightarrow Y$, $x \in O$ and $h \in X$. As usual, if there exists

$$\lim_{\lambda \rightarrow 0^+} \lambda^{-1} (f(x + \lambda h) - f(x)), \quad (1)$$

then it is called the derivative of f in x with direction h and denoted by $f'(x; h)$

$$\Xi = \{ \xi = \{ \xi_i \}_{i=1}^{n(\xi)} \subset (0, 1] \mid n(\xi) \in \mathbb{N}, \sum_{i=1}^{n(\xi)} \xi_i = 1 \},$$

and for each $\xi \in \Xi$, $|\xi| = \max \{ \xi_i \}_{i=1}^{n(\xi)}$. Ξ and its each subset of the form $\{ \xi \in \Xi \mid |\xi| \leq |\bar{\xi}| \}$, $\bar{\xi} \in \Xi$, are directed sets with the relation $\xi \leq \bar{\xi}$ ($\bar{\xi} \geq \xi$) meaning $|\xi| \geq |\bar{\xi}|$.

Proposition 1. Let X and Y be Banach spaces, O be the open subset in X , $f:O \rightarrow Y$, $x \in O$, $h \in X$ and there exists $f'(x; h)$. Then for each $\xi \in \Xi$, such that the directedness

$$\left\{ \sum_{i=1}^{n(\xi)} (f(x + \xi_i h) - f(x)) \right\}_{\bar{\xi} \leq \xi \in \Xi}, \quad (2)$$

is defined correctly, (2) converges to $f'(x; h)$.

Proof. $\exists \eta > 0$ such, that $x + \tau h \in O$, $\forall \tau \in [0, \eta]$. By conditions,

$$f(x + \tau h) - f(x) - \tau f'(x; h) = o(\tau),$$

$$\lim_{\tau \rightarrow 0^+} \text{Sup} \{ |o(\tau)|/\tau \mid 0 < \tau \leq s \} = 0; \quad (3)$$

Here $|\cdot|$ denotes the norm, $o(t)$ is an infinitesimal function of higher order than t .

When $\xi \in \Xi$ and $|\xi| \leq \eta$, we have:

$$\begin{aligned} & \sum_{i=1}^{n(\xi)} (f(x + \xi_i h) - f(x)) - f'(x; h) = \\ & |(\xi_1 f'(x, h) + o(\xi_1)) + \dots + (\xi_{n(\xi)} f'(x, h) + o(\xi_{n(\xi)})) - f'(x; h)| = \\ & = |o(\xi_1) + \dots + o(\xi_{n(\xi)})| \leq \\ & \leq \xi_1 \frac{|o(\xi_1)|}{\xi_1} + \dots + \xi_{n(\xi)} \frac{|o(\xi_{n(\xi)})|}{\xi_{n(\xi)}} \leq \\ & \leq \text{Sup}\left\{ \frac{|o(\tau)|}{\tau} \mid 0 < \tau \leq |\xi| \right\}. \end{aligned}$$

thus, for each $\bar{\xi} \in \Xi$ such that $|\bar{\xi}| \leq \eta$, (2) converges to $f'(x; h)$ according (3).

Proposition 2. Let X and Y be Banach spaces, O be the open subset in X , $f: O \rightarrow Y$, $x \in O$, $h \in X$,

$$\lim_{\tau \rightarrow 0+} (f(x + \tau h) - f(x)) = 0$$

and (2) is convergent in Y for some $\bar{\xi} \in \Xi$. Then there exists $f'(x; h)$ and it is the limit of (2).

Proof. Let $\bar{\xi} \in \Xi$ and (2) be convergent. Taking $\eta = |\bar{\xi}|$, we see that (as (2) is correctly defined) $x + \tau h \in O, \forall \tau \in [0, \eta]$.

Denote the integer part of number $s \geq 0$ by $\text{int}(s)$ and let us consider the function:

$$\tau(\tau^{-1} - \text{int}(\tau^{-1})) = 1 - \tau \text{int}(\tau^{-1}), \forall \tau \geq 0.$$

$0 \leq \tau^{-1} - \text{int}(\tau^{-1}) \leq 1$, so

$$1 - \tau \text{int}(\tau^{-1}) \rightarrow 0 \text{ when } \tau \rightarrow 0+. \quad (4)$$

Taking into account the conditions of proposition, from (4) follows

$$f(x + (1 - \tau \text{int}(\tau^{-1}))h) - f(x) \rightarrow 0 \text{ when } \tau \rightarrow 0+.$$

Let us estimate $\tau^{-1}(f(x + \tau h) - f(x))$ and verify its convergence to the limit of (2) when $\tau \rightarrow 0+$.

$$\begin{aligned} & \tau^{-1}(f(x + \tau h) - f(x)) = \\ & = \text{int}(\tau^{-1})(f(x + \tau h) - f(x)) + (\tau^{-1} - \text{int}(\tau^{-1}))(f(x + \tau h) - f(x)) = \\ & = \text{int}(\tau^{-1})(f(x + \tau h) - f(x)) + (f(x + (1 - \tau \text{int}(\tau^{-1}))h) - f(x)) - \\ & - (f(x + (1 - \tau \text{int}(\tau^{-1}))h) - f(x)) + (\tau^{-1} - \text{int}(\tau^{-1}))(f(x + \tau h) - f(x)). \end{aligned} \quad (5)$$

By conditions, the last two summands on the right side of (5) converge to zero, when $\tau \rightarrow 0+$. Let us verify, that sum of the first two summands

$$v(\tau) = \text{int}(\tau^{-1})(f(x+\tau h) - f(x)) + (f(x + (1-\tau \text{int}(\tau^{-1}))h) - f(x))$$

converges to the limit of (2), when $\tau \rightarrow 0+$.

By virtue of (4), there exists $\eta_1 \in (0, \eta)$ such that $x + (1-\tau \text{int}(\tau^{-1}))h \in O$, $\forall \tau \in [0, \eta_1]$. Let us define $\{\tau \rightarrow \xi(\tau)\}: (0, \eta_1) \rightarrow \Xi$ as follows: to every $\tau \in (0, \eta_1)$ there corresponds

$$\xi(\tau) = \{(\xi(\tau))_i\}_{i=1}^{\text{int}(\tau^{-1})+1}$$

such that:

$$(\xi(\tau))_i = \tau, \quad i \in \{1, \dots, \text{int}(\tau^{-1})\},$$

$$(\xi(\tau))_{\text{int}(\tau^{-1})+1} = 1 - \tau \text{int}(\tau^{-1}).$$

By construction,

$$\tau \rightarrow 0+ \Rightarrow |\xi(\tau)| \rightarrow 0,$$

$$\tau_1 \leq \tau_2 \Rightarrow \xi(\tau_1) \geq \xi(\tau_2)$$

and

$$v(\tau) = \sum_{i=1}^{\text{int}(\tau^{-1})+1} (f(x + (\xi(\tau))_i h) - f(x)).$$

Thus, $\{v(\tau)\}_{\tau \in (0, \eta)}$ is subdirectedness of (2) (the terminology of present paper is coordinated with [1]). At the same time it converges to $f'(x; h)$ by virtue of (5), therefore $f'(x; h)$ is the limit of (2).

Remark 1. The proofs of propositions show that the requirement of openness of O can be made weak.

Remark 2. Let $f: R \rightarrow R$ be totally discontinuous additive function (such function can be easily constructed by using Hamel-bases). When $h \neq 0$, the condition $\lim_{\tau \rightarrow 0+} (f(x + \tau h) - f(x)) = 0$ of proposition 2 does not hold and there does not exist $f'(x; h)$, $\forall x \in R$.

As we see, the Proposition 1 shows the way of directional derivative computation, and Proposition 2 indicates the borders of action of our method.

Tbilisi I. Javakhishvili State University

REFERENCES

1. I.Gogodze, K.Gelashvili. *Memoirs on Diff. Equat. and Mat. Physics*, **11**, 1997, 47-66.



E. Khmaladze

A Non-Abelian Tensor Product Modulo q of Lie Algebras

Presented by Corr. Member of the Academy Kh. Inassaridze, August 10, 1998

ABSTRACT. The notion of tensor product modulo q of two P -crossed modules, where q is a positive integer and P is a Lie algebra, is introduced and some properties are given.

Key words: Lie algebra, tensor product, exterior product, crossed module.

A generalized non-abelian tensor product modulo q of groups was introduced by D. Conduche and C. Rodriguez-Fernandez in [1]. It is clear that one should be able to develop an analogous theory of tensor product modulo q for other algebraic structures such as Lie algebras. Using G. Ellis's non-abelian tensor product of Lie algebras [2], we introduce a non-abelian tensor product modulo q of Lie algebras and investigate its properties.

Let Λ be a commutative ring with identity. We shall use the term Lie algebra to mean a Lie algebra over Λ ; we shall use $[\]$ to denote the Lie bracket. We denote by q a non-negative integer.

Let M and N be two Lie algebras. By an action of M on N we mean Λ -bilinear map $M \times N \rightarrow N$, $(m, n) \mapsto {}^m n$, satisfying

$$\begin{aligned} [{}^m, m']_n &= m({}^{m'} n) - m'({}^m n), \\ {}^m [n, n'] &= [{}^m n, n'] + [n, {}^m n'] \end{aligned}$$

for all $m, m' \in M, n, n' \in N$. Note that any Lie algebra acts on its ideal by Lie multiplication.

Definition 1. [3]. In the context of Lie algebras, a P -crossed module is a Lie homomorphism $\partial : M \rightarrow N$ together with an action of P on M such that

$$\begin{aligned} \partial({}^p m) &= [p, \partial(m)], \\ \partial({}^{(m)} m') &= [m, m'] \end{aligned}$$

for all $m, m' \in M, p \in P$.

Let $\mu : M \rightarrow P$ and $\nu : N \rightarrow P$ be two P -crossed modules and consider the pullback

$$\begin{array}{ccc} M \times_P N & \xrightarrow{\pi_2} & N \\ \pi_1 \downarrow & & \downarrow \nu \\ M & \xrightarrow{\mu} & P \end{array}$$

Let $K = M \times_P N = \{(m, n) | m \in M, n \in N, \mu(m) = \nu(n)\}$. In this diagram each Lie algebra acts on any other via its image in the Lie algebra P .

Definition 2. The tensor product modulo q , $M \otimes^q N$, of the P -crossed modules μ and ν is the Lie algebra generated by the symbols $m \otimes n$ and $\{k\}$, $m \in M, n \in N, k \in K$ with

the following relations

$$\lambda(m \otimes n) = \lambda n \otimes n = m \otimes \lambda n, \quad (1)$$

$$(m + m') \otimes n = m \otimes n + m' \otimes n \quad (2)$$

$$m \otimes (n + n') = m \otimes n + m \otimes n',$$

$$[m, m'] \otimes n = m \otimes^{m'} n - m' \otimes^m n, \quad (3)$$

$$m \otimes (n + n') = {}^{n'} m \otimes n - {}^n m \otimes n'$$

$$[m \otimes n, m' \otimes n'] = -{}^n m \otimes^{m'} n' \quad (4)$$

$$[\{k\}, m \otimes n] = {}^{qk} m \otimes n + m \otimes^{qk} n, \quad (5)$$

$$\{\lambda k + \lambda' k'\} = \lambda \{k\} + \lambda' \{k'\}, \quad (6)$$

$$\{\{k\}, \{k'\}\} = \pi_1(qk) \otimes \pi_2(qk), \quad (7)$$

$$\{(-{}^n m, {}^m n)\} = q(m \otimes n) \quad (8)$$

for all $m, m' \in M, n, n' \in N, k, k' \in K, \lambda, \lambda' \in \Lambda$

Let $M \circ N$ be the submodule of $M \otimes^q N$ generated by the elements $m \otimes n$ with $\mu(m) = \nu(n)$. $M \circ N$ is an ideal of $M \otimes^q N$.

Definition 3. The exterior product modulo q , $M\Delta^q N$, of the two P -crossed modules μ and ν is the quotient $M \otimes^q N / M \circ N$.

In other words, the Lie algebra $M\Delta^q N$ is the quotient of the tensor product $M \otimes^q N$ by the relation

$$\pi_1(k) \otimes \pi_2(k) = 0, \quad k \in K. \quad (9)$$

Let $m \wedge n$ be the image of $m \otimes n$ in $M\Delta^q N$ by the canonical homomorphism from $M \otimes^q N$ to $M\Delta^q N$.

Lemma 4. We have two Lie homomorphisms $x: M \check{\Delta}^q N \otimes M$ and $x': M \check{\Delta}^q N \otimes N$ defined by

$$x(m \otimes n) = -{}^n m, \quad x(\{k\}) = p_1(qk);$$

$$\xi(m \otimes n) = {}^m n, \quad \xi(\{k\}) = \pi_2(qk).$$

Furthermore, these homomorphisms act through $M\Delta^q N$.

Remark 5. Let $\partial = (\xi, \xi'): M \otimes^q N \rightarrow M\Delta^q N \rightarrow M \times_p N$ be the canonical Lie homomorphism, given for $x \in M \otimes^q N$, by $\partial(x) = (\xi(x), \xi'(x))$. In the case $q = 1$ the map ∂ is an isomorphism.

Lemma 6. (i) Let $m, m', m'' \in M$ and $n, n', n'' \in N$ be such that $\mu(m) = \nu(n) = \nu(n'')$ and $\mu(m') = \mu(m'') = \nu(n')$ then $qm'' \otimes qn'' = -qm \otimes qn' = qm' \otimes qn$.

(ii) Let $k, k' \in K$ and suppose $[k, k'] = 0$, then $q(\pi_1(k) \otimes \pi_2(k')) = 0$.

Recall that the non-abelian tensor product of Lie algebras, $M \otimes N$ is the Lie algebra generated by elements $m \otimes n, m \in M, n \in N$ and subject to relations (1) - (4) [2]. Furthermore, exterior product, $M \wedge N$ introduced in [2] is the Lie algebra generated by elements $m \wedge n, m \in M, n \in N$ and subject to relations (1) - (4) and (9).

Proposition 7. Let $[M, N]$ be the submodule of $K = M \times_p N$ generated by the elements of the form $(-{}^n m, {}^m n), m \in M, n \in N$. Then $[M, N]$ is an ideal of K and there is a commutative diagram

$$\begin{array}{ccccccc} M \otimes N & \xrightarrow{\varphi} & M \otimes^q N & \rightarrow & K/[M, N] & \rightarrow & 1 \\ & & \downarrow & & \parallel & & \\ M \wedge N & \xrightarrow{\psi} & M\Delta^q N & \rightarrow & K/[M, N] & \rightarrow & 1 \end{array}$$

with exact rows.

Remark 8. The ideal $[M, N]$ of the Lie algebra K contains the commutator $[K, K]$ of

K since, for $k, k' \in K$

$$[k, k'] = (-\pi_2(k'))\pi_1(k), \pi_1(k)\pi_2(k').$$

There is an action of the Lie algebra P on the Lie algebra $M \otimes^q N$ (resp. $M \Delta^q N$) given by ${}^p(m \otimes n) = {}^p m \otimes n + m \otimes {}^p n$ (resp. ${}^p(m \wedge n) = {}^p m \wedge n + m \wedge {}^p n$) and ${}^p\{k\} = \{{}^p k\}$ for $m \in M, n \in N, p \in P, k \in K$.

Following [4] (see also [1]) we have the definition:

Definition 9. A crossed square is a commutative diagram of Lie algebras

$$\begin{array}{ccc} H & \xrightarrow{\lambda} & M \\ \lambda' \downarrow & & \downarrow \mu \\ N & \xrightarrow{\nu} & P \end{array}$$

endowed with an action of P on each Lie algebra and a bilinear function $h : M \times N \rightarrow H$ such that

(i) μ, ν and $\alpha = \nu\lambda' = \mu\lambda$ are crossed modules, and the maps $\lambda\lambda'$ preserve the actions of P ;

- (ii) $\lambda h(m, n) = -{}^n m, \lambda' h(m, n) = {}^m n$;
- (iii) $h(\lambda(l), n) = -{}^n l, h(m, \lambda'(l)) = {}^m l$;
- (iv) $h([m, m'], n) = h(m, {}^{m'} n) - h(m', {}^m n)$;
 $h(m, [n, n']) = h({}^n m, n) - h({}^m m', n)$;
- (v) $h({}^n m, {}^{m'} n) = -[h(m, n), h(m', n)]$;
- (vi) ${}^p h(m, n) = h({}^p m, n) + h(m, {}^p n)$

for all $m, m' \in M, n, n' \in N, p \in P, l \in H$.

Lemma 10. The square

$$\begin{array}{ccc} M \times_P N & \xrightarrow{\pi_2} & N \\ \pi_1 \downarrow & & \downarrow \nu \\ M & \xrightarrow{\mu} & P \end{array}$$

with $h(m, n) = (-{}^n m, {}^m n)$ is a crossed square.

Lemma 11. The squares

$$\begin{array}{ccc} M \otimes N & \xrightarrow{\xi} & N \\ \xi \downarrow & & \downarrow \nu \\ M & \xrightarrow{\mu} & P \end{array} \quad \text{and} \quad \begin{array}{ccc} M \wedge N & \xrightarrow{\xi} & N \\ \xi \downarrow & & \downarrow \nu \\ M & \xrightarrow{\mu} & P \end{array}$$

with $\xi(m \otimes n) = -{}^n m, \xi(m \otimes n) = {}^m n$ and $h(m, n) = m \otimes n$ (resp. $h(m, n) = m \wedge n$) are crossed squares.

Lemma 12. For $m \in M, n \in N, k \in K$ we have the following relations:

$$\begin{aligned} {}^m\{k\} &= m \otimes \pi_2(qk), \\ {}^n\{k\} &= -\pi_1(qk) \otimes n. \end{aligned}$$

Proposition 13. The squares



$$\begin{array}{ccc}
 M \otimes^q N & \xrightarrow{\xi'} & N \\
 \xi \downarrow & & \downarrow^v \text{ and } \xi \downarrow \\
 M & \xrightarrow{\mu} & P
 \end{array}
 \quad
 \begin{array}{ccc}
 M \Delta^q N & \xrightarrow{\xi'} & N \\
 & & \downarrow^v \\
 M & \xrightarrow{\mu} & P
 \end{array}$$

with $h(m,n) = m \otimes n$ (resp. $h(m,n) = m \wedge n$) are crossed squares.

Lemma 14. With the action induced by the image of K in P the Lie homomorphism $\partial : M \otimes^q N \rightarrow M \times_P N$ is a crossed module. Furthermore, ∂ factor through a homomorphism $\partial' : M \Delta^q N \rightarrow K$ which is also a crossed module.

Theorem 15. Let p be a positive integer and let $q' = pq$. Then:

- (i) We have a Lie homomorphism $\varphi' : M \otimes^{q'} N \rightarrow M \otimes^q N$ given by $\varphi'(m \otimes n) = m \otimes n$ and $\varphi'(\{k\}) = \{pk\}$ for $m \in M, n \in N, k \in K$.
 (ii) The Lie homomorphism φ' induces a Lie homomorphism $\psi' : M \Delta^{q'} N \rightarrow M \Delta^q N$.

Recall from [2] that the actions of M on N and of N on M are compatible, if ${}^{(m)}n' = [n', m]$ and ${}^{(n)}m' = [m', n]$ for all $m, m' \in M, n, n' \in N$.

It is easy to see that the actions of two P -crossed modules M and N on each other via P are compatible.

Let M and N be two Lie algebras with compatible actions on each other. We shall denote by $[M, N]^N$ or $[N, M]^N$ the submodule of N generated by the elements of the form ${}^m n, m \in M, n \in N$. It follows from the compatibility condition that $[M, N]^N$ is an ideal of N .

According to the definition of the Peiffer product of groups (see [1, 5, 6,]) we have:

Definition 16. The Peiffer product, $M \bowtie N$, of two Lie algebras M and N with compatible actions on each other is the quotient of the coproduct $M * N$ by the relations: $[m, n] = {}^m n, [n, m] = {}^n m$ for $m \in M, n \in N$.

As a consequence of the compatibility condition the actions of $M * N$ on M and on N factor through $M \bowtie N$ and the canonical maps $M \rightarrow M \bowtie N$ and $N \rightarrow M \bowtie N$ are crossed modules. So we can define a tensor product modulo q of two Lie algebras M and N , acting on each other compatibly, considering them as $M \bowtie N$ -crossed modules.

Theorem 17. If M and N act trivially on each other (i.e. $[M, N]^N = \{0\}, [N, M]^N = \{0\}$), then there is an isomorphism

$$M \otimes^q N \cong (M^{ab} / qM^{ab}) \otimes_{\Lambda^1 q\Lambda} (N^{ab} / qN^{ab}),$$

where $M^{ab} = M/[M, M]$, $N^{ab} = N/[N, N]$, and $[M, M], [N, N]$ are commutators of M and N respectively.

Georgian Academy of Sciences
 A. Razmadze Mathematical Institute

REFERENCES

1. D. Conduche, C. Rodrigues-Fernandez. Journal of Pure and Applied Algebra, 78, 1992, 139-160.
2. G.J. Ellis. Glasgow Math. J., 33, 1991, 101-120.
3. C. Kassel, J.-L. Loday. Ann. Inst. Fourier (Grenoble) 33, 1982, 119-142.
4. R. Brown, J.-L. Loday. Topology 26, 3, 1987, 311-335.
5. J.H. Whitehead. Ann. of Math., 42, 1941, 409-428.
6. N.D. Gilbert, P.J. Higgins. Glasgow Math. J., 31, 1989, 17-29.



Z. Rostomashvili

Remark to the Projective Geometry over Rings and Corresponding Lattices

Presented by Corr. Member of the Academy Kh. Inassaridze, May 24, 1999

ABSTRACT. For the projective geometries over ring we construct the correspondence of these geometries and modular lattices with certain condition.

Key words: projective geometry, lattice, ring, height function.

In [1] G.-A. Faure and A. Frolicher introduced natural notion of morphisms between projective geometries and classical correspondence of projective geometries with certain lattices which are extended into equivalence categories.

A.A. Lashkhi in [2] gives a lattice theoretical characterization of projective geometries over rings, i.e. for the principal ideal domains.

Definition 1. (Axioms for the projective geometry over rings).

The K-projective geometry is a set G with a binary relation $P \subseteq G \times G$ and a ternary relation $l \subseteq G \times G \times G$ satisfying the axioms

- (1) $l(a,b,a), \forall a,b \in G;$
- (2) $l(a,p,q) \ \& \ l(b,p,q), \overline{P(q,p)} \Rightarrow \exists a_1 \in G, P(a_1,a), l(a_1,b,p);$
- (3) $l(p,a,b), l(p,c,d) \Rightarrow \exists q,a_1,b_1,c_1,d_1, P(a_1,a), P(b_1,b), P(c_1,c), P(d_1,d), l(q,a_1,d_1), l(q,c_1,b_1)$

The elements of G are called the points of the geometry. The points a,b are called dependent if $P(a,b)$; the points a,b,c are called collinear if $l(a,b,c)$.

Definition 2. A subspace of a geometry G is a subset $E \subseteq G$ with the property $b, c \in E, \overline{P(b,c)} \ \& \ l(a, b, c) \Rightarrow a \in E$.

Remark. With the restriction of the relation l to the set E , E is also a projective geometry. For any subset $A \subseteq G$ there exists the smallest subspace containing A ; it will be denoted by $\mathfrak{R}(A)$.

Definition 3. One says that a subset A of a K-projective geometry G is independent if $a \in A$ implies to $a \notin \mathfrak{R}(A \setminus a)$. Subset A generates G if $\mathfrak{R}(A) = G$. A basis of G is a subset $B \subseteq G$ which is independent and generates G .

This standard application of Zorn's lemma can be proved.

Proposition 1. Every K-projective geometry admits the basis. Let l be an independent subset and A the generating subset of G . Then there exists an injective map $\varphi: l \rightarrow A$. Therefore any two basis of G are equivalent.

Definition 4. Let G be K-projective geometry. The rank $R(E)$ of a subspace $E \subseteq G$ is the cardinal number of basis B of E . The dimension of E is defined as:

$$D(E) := R(E) - 1$$

Thus one has

- (1) $d(E) = -1$ if $f(E) = \emptyset$;
- (2) $d(E) = 0$ if $f(E)$ is singleton.

The subspaces of dimension 1 are called lines and those of dimension 2 are called planes.

Proposition 2. Let $\mathfrak{S}(G)$ denote the set of all subspaces of G , ordered by set inclusion. Then $\mathfrak{S}(G)$ is a complete modular lattice.

The fact that $x < y$ and $R(y \setminus x) = 1$ for $x, y \in G$ we will denote by $x < y$.

Let L be a modular lattice $0 \in L$. Define a unique height function $h: L \rightarrow \mathbb{N} \cup \infty$ satisfying the following properties:

- (1) $h(0) = 0$;
- (2) $x \leq y \Rightarrow h(x) \leq h(y)$;
- (3) $x < y \Rightarrow h(y) = h(x) + 1$;
- (4) $x \leq y, h(x) = h(y) \Rightarrow [0, x] \cong [0, y]$;
- (5) $h(x \vee y) + h(x \wedge y) = h(x) + h(y)$.

Remark. For $\mathfrak{S}(G)$ the rank yields the map $h: \mathfrak{S}(G) \rightarrow \mathbb{N} \cup \infty$ with these five properties; for a finite-dimensional subspace $E \leq G$ one has $h(E) = R(E)$ otherwise $h(E) = \infty$.

Let $\aleph(L) \leq L$ with the condition

$$(*) \quad x \in \aleph(L) \Leftrightarrow h(x) = 1.$$

By $PG(L)$ we denote the set of all elements of $\aleph(L)$ with the relation

$$(**) \quad \text{for } a, b, c \in \aleph(L)$$

$$l_{\perp}(a, b, c) \Leftrightarrow h(a \vee b \vee c) \leq 2.$$

Proposition 5. The set $PG(L)$ is a K -projective geometry. Moreover, one has $l_{\perp}(a, b, c)$ if $b = c$ or $a \leq b \vee c$.

Theorem 1. Let G be a K -projective geometry. Then the K -projective geometry $PG(\aleph(L))$ can be identified with G .

Definition 5. The lattice L will be called K -projective if it is complete, modular, upper continuous and

$$L = \mathfrak{R}(\aleph(L)).$$

Theorem 2. Let L be a modular lattice with 0 . Then L is isomorphic to the lattice $\mathfrak{S}(\aleph(L))$ if and only if L is K -projective.

Georgian Technical University

REFERENCES

1. C.A.Faure, A.Frolicher. *Geom. Dedicata*, 47, 1993, 25-40.
2. A.A.Lashkhi. *The Results of Sci. and Tech., Probl. Geom., VINITI*, 1, 1995, 168-211.



Member of the Academy T.Burchuladze, R.Rukhadze, Yu.Bezhuashvili

On the Fundamental Solutions of the System of Equations for Oscillation of Hemitropic Micropolar for Two-Dimensional Case

Presented November 30, 1998

ABSTRACT. The matrix of fundamental (singular) solutions of a homogeneous system of equations for oscillation of hemitropic micropolar medium in two-dimensional Euclidean space R^2 is effectively constructed.

Key words: hemitropic, micropolar, two-dimensional, oscillation, fundamental matrix.

A system of homogeneous differential equations of stationary oscillation for hemitropic micropolar medium for two-dimensional case has the form [1,2]

$$\left\{ \begin{aligned}
 &(\mu + \alpha)\Delta u_1 + (\lambda + \mu - \alpha)\frac{\partial}{\partial x_1} \operatorname{div} u + (\nu + \eta)\Delta w_1 + \\
 &+ (\delta + \nu - \eta)\frac{\partial}{\partial x_1} \operatorname{div} \omega + 2\alpha\frac{\partial \omega_3}{\partial x_2} + \rho\sigma^2 u_1 = 0, \\
 &(\mu + \alpha)\Delta u_2 + (\lambda + \mu - \alpha)\frac{\partial}{\partial x_2} \operatorname{div} u + (\nu + \eta)\Delta w_2 + \\
 &+ (\delta + \nu - \eta)\frac{\partial}{\partial x_2} \operatorname{div} \omega - 2\alpha\frac{\partial \omega_3}{\partial x_1} + \rho\sigma^2 u_2 = 0, \\
 &(\mu + \alpha)\Delta u_3 + (\nu + \eta)\Delta \omega_3 + 2\alpha\left(\frac{\partial \omega_2}{\partial x_1} - \frac{\partial \omega_1}{\partial x_2}\right) + \rho\sigma^2 u_3 = 0, \\
 &(\nu + \beta)\Delta \omega_1 + (\varepsilon + \nu - \beta)\frac{\partial}{\partial x_1} \operatorname{div} \omega + (\nu + \eta)\Delta u_1 + \\
 &+ (\delta + \nu - \eta)\frac{\partial}{\partial x_1} \operatorname{div} u + 4\eta\frac{\partial \omega_3}{\partial x_2} + 2\alpha\frac{\partial u_3}{\partial x_2} + (I\sigma^2 - 4\alpha)\omega_1 = 0, \\
 &(\nu + \beta)\Delta \omega_2 + (\varepsilon + \nu - \beta)\frac{\partial}{\partial x_2} \operatorname{div} \omega + (\nu + \eta)\Delta u_2 + \\
 &+ (\delta + \nu - \eta)\frac{\partial}{\partial x_2} \operatorname{div} u - 4\eta\frac{\partial \omega_3}{\partial x_1} - 2\alpha\frac{\partial u_3}{\partial x_1} + (I\sigma^2 - 4\alpha)\omega_2 = 0, \\
 &(\nu + \beta)\Delta \omega_3 + (\nu + \eta)\Delta u_3 + 4\eta\left(\frac{\partial \omega_2}{\partial x_1} - \frac{\partial \omega_1}{\partial x_2}\right) + \\
 &+ 2\alpha\left(\frac{\partial u_2}{\partial x_1} - \frac{\partial u_1}{\partial x_2}\right) + (I\sigma^2 - 4\alpha)\omega_3 = 0,
 \end{aligned} \right. \tag{1}$$

where Δ is a two-dimensional Laplace operator, $u(x) = (u_1, u_2, u_3)$ is a displacement vector, $\omega(x) = (\omega_1, \omega_2, \omega_3)$ is a rotation vector, $x = (x_1, x_2)$ is a point in R^2 , ρ is the density medium, I is inertia momentum, σ is oscillation frequency; $\lambda, \mu, \alpha, \varepsilon, \nu, \beta, \nu, \eta, \delta$ are elasticity constants satisfying the conditions: $\mu > 0, \alpha > 0, 3\lambda + 2\mu > 0, \mu\nu - \nu^2 > 0, \alpha\beta - \eta^2 > 0, (3\lambda + 2\mu)(3\varepsilon + 2\nu) - (3\delta + 2\nu)^2 > 0$.

The system (1) can be rewritten in the form:

$$\begin{cases} M^{(1)}(\partial x)u(x) + M^{(2)}(\partial x)\omega(x) = 0, \\ M^{(3)}(\partial x)u(x) + M^{(4)}(\partial x)\omega(x) = 0, \end{cases} \quad (2)$$

where $M^{(k)}(\partial x) = \|M_{ij}^{(k)}(\partial x)\|_{3 \times 3}$ is a matrix differential operators of dimension 3×3 , whose elements according to (1) can be easily written.

The solution of system (2) will be sought in the form

$$\begin{cases} u(x) = M^{(4)}(\partial x)\tilde{X}(x) - M^{(2)}(\partial x)\tilde{Y}(x), \\ \omega(x) = -M^{(3)}(\partial x)\tilde{X}(x) + M^{(1)}(\partial x)\tilde{Y}(x), \end{cases} \quad (3)$$

where \tilde{X} and \tilde{Y} are unknown three-dimensional vector-functions. Substituting (3) in (2) to determine \tilde{X} and \tilde{Y} , we obtain

$$D(\partial x)\tilde{X}(x) = 0, \quad D(\partial x)\tilde{Y}(x) = 0, \quad (4)$$

where $D(\partial x) = M^{(1)}(\partial x)M^{(4)}(\partial x) - M^{(2)}(\partial x)M^{(3)}(\partial x)$.

Calculations give us: $D(\partial x) = \|D_{ij}(\partial x)\|_{3 \times 3}$, where

$$D_{ij} = d_1(\Delta + \lambda_3^2)(\Delta + \lambda_4^2)\delta_{ij} + (d_0 - d_1)(\Delta + \lambda_6^2) \frac{\partial^2}{\partial x_i \partial x_j}, \quad i, j = 1, 2;$$

$$D_{ij} = -d_1 d_2 (\Delta + \lambda_5^2) \sum_{k=1}^2 \varepsilon_{ijk} \frac{\partial}{\partial x_k}, \quad i = 3, \quad j = 1, 2 \quad \text{or} \quad j = 3, \quad i = 1, 2;$$

$$D_{33} = d_1(\Delta + \lambda_3^2)(\Delta + \lambda_4^2).$$

Here δ_{ij} is a Kronecker symbol, ε_{ijk} is a Levi-Civita symbol, $d_0 = (\lambda + 2\mu)(\varepsilon + 2\nu) - (\delta + 2\nu)^2$, $d_1 = (\mu + \alpha)(\nu + \beta) - (\nu + \eta)^2$, $d_2 = 4(\mu\eta - \alpha\nu)d_1^{-1}$, $\lambda_3^2 + \lambda_4^2 = [(\mu + \alpha)I\sigma^2 - 4\alpha\mu + \rho\sigma^2(\nu + \beta)]d_1^{-1}$, $\lambda_3^2\lambda_4^2 = [\rho\sigma^2(I\sigma^2 - 4\alpha)]d_1^{-1}$, $\lambda_5^2 = \rho\sigma^2\eta(\mu\eta - \alpha\nu)^{-1}$, $\lambda_6^2 = [(I\sigma^2 - 4\alpha)(\lambda + \mu) - I\sigma^2\alpha + \rho\sigma^2(\varepsilon + \nu - \beta)](d_0 - d_1)^{-1}$.

Denote by D^* adjoint matrix to matrix D and represent \tilde{X} and \tilde{Y} in the form

$$\tilde{X}(x) = D^*(\partial x)X(x), \quad \tilde{Y}(x) = D^*(\partial x)Y(x), \quad (5)$$

where X and Y are unknown three-dimensional vector-functions. To determine X and Y , from (4) we obtain

$$\det DX = 0, \quad \det DY = 0, \quad (6)$$

here $\det D = d_1^2 d_0 \prod_{i=1}^6 (\Delta + k_i^2)$, where $k_i^2 (i = \overline{1,6})$ satisfy the conditions:

$$\begin{aligned} k_1^2 + k_2^2 &= [(\lambda + 2\mu)(I\sigma^2 - 4\alpha) + \rho\sigma^2(\varepsilon + 2\nu)]d_0^{-1}, & k_1^2 k_2^2 &= \rho\sigma^2(I\sigma^2 - 4\alpha)d_0^{-1}; \\ k_3^2 + k_4^2 + k_5^2 + k_6^2 &= 2(\lambda_3^2 + \lambda_4^2) + d_2^2, & k_3^2 k_4^2 k_5^2 k_6^2 &= \lambda_3^4 \lambda_4^4; \\ k_3^2 k_4^2 + k_5^2 k_6^2 + (k_3^2 + k_4^2)(k_5^2 + k_6^2) &= (\lambda_3^2 + \lambda_4^2)^2 + 2\lambda_3^2 \lambda_4^2 + 2d_2^2 \lambda_3^2, \\ (k_3^2 + k_4^2)k_5^2 k_6^2 + (k_5^2 + k_6^2)k_3^2 k_4^2 &= 2(\lambda_3^2 + \lambda_4^2)\lambda_3^2 \lambda_4^2 + d_2^2 \lambda_5^4. \end{aligned}$$

Consider the equality

$$\prod_{i=1}^6 (\Delta + k_i^2) X_0(x) = 0, \tag{7}$$

where $X_0(x)$ is an unknown scalar function.

It follows from (3) and (5) that we must construct such a solution of equation (7) which partial tenth order derivatives have the singularity of the kind $\ln|x|$. It is easily seen that the desired solution will be

$$X_0(x) = \frac{1}{2\pi i d_1^2 d_0} \sum_{l=1}^6 \prod_{j=1}^5 \frac{1}{k_{l+j}^2 - k_l^2} \frac{\pi i}{2} H_0^{(1)}(k_l |x|), \tag{8}$$

$$k_{6+j}^2 = k_j^2, \quad j = \overline{1,5}; \quad \sum_{l=1}^6 \prod_{j=1}^5 \frac{k_l^{2m}}{k_{l+j}^2 - k_l^2} = \delta_{2m,10}, \quad m = \overline{0,5};$$

where $H_0^{(1)}$ is Hankel function of the first kind and of the zero order.

According to (5), (3) can be rewritten in the form

$$\begin{cases} u(x) = M^{(4)}(\partial x) D^* (\partial x) X(x) - M^{(2)}(\partial x) D^* (\partial x) Y(x), \\ \omega(x) = -M^{(3)}(\partial x) D^* (\partial x) X(x) + M^{(1)}(\partial x) D^* (\partial x) Y(x). \end{cases} \tag{9}$$

Introduce a six-component vector $v = (u, \omega) = (u_1, u_2, u_3, \omega_1, \omega_2, \omega_3) = (v_1, v_2, v_3, v_4, v_5, v_6)$. Let $\delta^k = (\delta_{k1}, \delta_{k2}, \delta_{k3})$, $k = \overline{1,3}$. If in (9) we take $X \equiv X^k = X_0 \delta^k$, $k = \overline{1,3}$; $Y = (0, 0, 0)$ and then $Y \equiv Y^k = X_0 \delta^k$, $k = \overline{1,3}$; $X = (0, 0, 0)$, then we get six solutions of system (2), which we denote by $v^k = (u^k, \omega^k)$, $k = \overline{1,6}$.

Consider a quadratic matrix of dimension 6×6 : $\Gamma(x, \sigma) = \|\Gamma_{mn}(x, \sigma)\|_{6 \times 6}$, where $\Gamma_{mn} = v_n^m$, $m, n = \overline{1,6}$. By definition, each column of the matrix $\Gamma(x, \sigma)$, taken as a vector, is the solution of system (2) at all points of the space R^2 , except at the beginning of the coordinates. Taking into consideration the expression for the operators $M^{(1)} D^*$, $M^{(2)} D^*$, $M^{(4)} D^*$, we can introduce the matrix $\Gamma(x, \sigma)$ in the following form

$$\Gamma(x, \sigma) = \begin{pmatrix} \Gamma^{(1)}(x, \sigma) & \Gamma^{(2)}(x, \sigma) \\ \Gamma^{(3)}(x, \sigma) & \Gamma^{(4)}(x, \sigma) \end{pmatrix},$$

where $\Gamma^{(p)}(x, \sigma) = \left\| \Gamma_{mn}^{(p)}(x, \sigma) \right\|_{3 \times 3}$, $p = \overline{1, 4}$;

$$\begin{aligned} 2\pi\Gamma_{mn}^{(1)} &= \Gamma_{33}^{(1)}\delta_{mn} + \frac{\varepsilon + 2\nu}{d_0} \sum_{l=1}^6 \prod_{j=1}^5 \frac{\lambda_8^2 - k_l^2}{k_{l+j}^2 - k_l^2} \left[d_2^2 (\lambda_5^2 - k_l^2)^2 - \frac{d_0 - d_1}{d_1} (\lambda_3^2 - k_l^2) \times \right. \\ &\quad \left. \times (\lambda_4^2 - k_l^2)(\lambda_6^2 - k_l^2) \right] \frac{\partial^2}{\partial x_m \partial x_n} \frac{\pi i}{2} H_0^{(1)}(k_l | x) + \sum_{l=3}^6 \prod_{j=1}^5 \frac{(k_1^2 - k_l^2)(k_2^2 - k_l^2)}{k_{l+j}^2 - k_l^2} \times \\ &\quad \times \left[\frac{\varepsilon + \nu - \beta}{d_1} (\lambda_3^2 - k_l^2)(\lambda_4^2 - k_l^2) - \frac{4\eta d_2}{d_1} (\lambda_5^2 - k_l^2) \right] \frac{\partial^2}{\partial x_m \partial x_n} \frac{\pi i}{2} H_0^{(1)}(k_l | x), \quad m, n = \overline{1, 2}; \\ 2\pi\Gamma_{mn}^{(1)} &= \sum_{l=3}^6 \prod_{j=1}^5 \frac{(k_1^2 - k_l^2)(k_2^2 - k_l^2)}{k_{l+j}^2 - k_l^2} \left[\frac{(\nu + \beta)d_2}{d_1} (\lambda_2^2 - k_l^2)(\lambda_5^2 - k_l^2) - \frac{4\eta}{d_1} (\lambda_3^2 - k_l^2) \times \right. \\ &\quad \left. \times (\lambda_4^2 - k_l^2) \right] \sum_{q=1}^2 \varepsilon_{mnq} \frac{\partial}{\partial x_q} \frac{\pi i}{2} H_0^{(1)}(k_l | x), \quad m = 3, n = \overline{1, 2} \text{ or } n = 3, m = \overline{1, 2}; \\ 2\pi\Gamma_{33}^{(1)} &= \sum_{l=3}^6 \prod_{j=1}^5 \frac{(k_1^2 - k_l^2)(k_2^2 - k_l^2)}{k_{l+j}^2 - k_l^2} \left[\frac{\nu + \beta}{d_1} (\lambda_2^2 - k_l^2)(\lambda_3^2 - k_l^2)(\lambda_4 - k_l^2) + \right. \\ &\quad \left. + \frac{4\eta d_2}{d_1} (\lambda_5^2 - k_l^2)(-k_l^2) \right] \frac{\pi i}{2} H_0^{(1)}(k_l | x). \end{aligned}$$

The analogous forms have the other components of $\Gamma(x, \sigma)$ matrix and analogous matrix in R^3 is constructed in [3].

Georgian Academy of Sciences
 A. Razmadze Mathematical Institute

REFERENCES

1. E.V.Kuvshinski, E.L.Aero. FTT, 5, 5, 1963, 2592-2598 (Russian).
2. I.P.Nowacki, W.Nowacki. Bull. Polon. Acad. Sci., Ser., Sci. Techn., 25, 151, (297) 1997, 1-14
3. T.Burchuladze, R.Rukhadze, Yu.Bezhuashvili. Bull. Georg. Acad. Sci., 159, 1, 1999, 32-36.

G.Karumidze, G.Giorgadze, D.Goshadze, E. Kordzaia, T.Tsitlidze

On One Parametric Method for Mathematical Programming Problems Solving

Presented by Member of the Academy M. Salukvadze, August 10, 1998

ABSTRACT. This paper presents a parametric method for mathematical programming problems. The minimization problem has been transformed into the solution of inequalities set by this method.

Key words: mathematical programming, parameter, inequality set, minimization.

The actuality of optimization problem solving caused intensive studies in programming theories. The present day level of computer sciences made it possible to realize effectively the numeric methods for these problems by means of modern programming languages. In this article we present the minimization method for $f: R^n \rightarrow R^1$ function on $D \subset R^n$ set, where D is $g_l(x) \leq 0, l = 1, \dots, m$ manifold of inequality system solutions and $g_l: R^n \rightarrow R^1$ are given functions.

For one of the large classes of such type problems solution it is characteristic to transform the constrained nonlinear programming problems into equivalent unconstrained extremum problems. These problems can be effectively solved by a standard method.

To solve the stated problem we shall consider the family of functions dependent on

the real λ parameter [1,2]:
$$\varphi_\lambda(x) = \frac{1}{2}[f(x) - \lambda]^2 \text{sg}[f(x) - \lambda] + \frac{1}{2} \sum_{l=1}^m g_l^2(x) \text{sg}[g_l(x)],$$

where $\text{sg}(t)$ function is identically equal to 1 for positive t and to 0 in the opposite case.

We shall show that mathematical programming problem can be reduced to find such λ parameter and x vector for which condition $\varphi_\lambda(x) = 0$ is satisfied. In particular the following theorem is valid.

Theorem. Suppose there exists a pair of (x^0, λ^0) when $Q_\lambda(x) = \{x \in R^n : \varphi_\lambda(x) \leq \varphi_{\lambda^0}(x)\}$ set is compact and $f(x), g_l(x) l = 1, \dots, m$ are continuous functions, then there exists such value λ of λ parameter, when the set of $\varphi_\lambda(x)$ function minimum points on R^n coincides with the set of $f(x)$ function minimum points on D .

Proof. Note the point sets of $\varphi_\lambda(x)$ and $f(x)$ functions minimums are denoted accordingly by M_φ and M_f . From the conditions of the theorem and from the definition of $\varphi_\lambda(x)$ function it follows:

- 1) $\varphi_\lambda(x) \geq 0$ for any $(\lambda, x) \in R^1 \times R^n$ pair, 2) $\min_{(\lambda, x) \in R^1 \times R^n} \varphi_\lambda(x) = 0$, 3) for every fixed λ

the following equality is right:

$$\{x \in R^n : \varphi_\lambda(x) \equiv 0\} = \{x \in R^n : g_l(x) \leq 0, f(x) - \lambda \leq 0, l = 1, \dots, m\}.$$

Let $x \in M_f$ and $\lambda = f(x)$ then according to 2) $\min_{x \in R^n} \varphi_{\lambda}(x) = 0$. This means that $x \in M_{\varphi}$ and therefore the inclusion is right $M_f \subset M_{\varphi}$. Now suppose on the contrary: $x \in M_{\varphi}$, there will exist such $\check{\lambda}$, that $\varphi_{\check{\lambda}}(x) = 0$. Thus $\check{\lambda} = \lambda$. From this statement and 3) condition we receive $x \in M_f$. The theorem is proved.

Remark. In fact we have shown that λ parameter indicated in the theorem is the minimum on D of minimized function $f(x)$.

For finding of the optimal pair $(\lambda, x) \in R^1 \times R^n$ the following problem must be solved: to find such minimal λ , for which the equation $\varphi_{\lambda}(x) = 0$ is executed. Searching of the pair may be realized with the following procedure: minimizing of the $\varphi_{\lambda}(x)$ function for arbitrary fixed λ parameter. If the minimum of this function is equal to 0 we must repeat the $\varphi_{\lambda}(x)$ function family minimization for decreasing values of λ parameter, until we

found such value $\check{\lambda}$ that satisfies the conditions:

$$1) \min_{x \in R^n} \varphi_{\check{\lambda}}(x) = 0, \quad 2) \min_{x \in R^n} \varphi_{\check{\lambda} - \varepsilon}(x) > 0 \text{ for any lowest } \varepsilon > 0.$$

If $\varphi_{\check{\lambda}}(x) > 0$, the minimization procedure must be repeated for the increasing λ parameter values, until we find such value $\check{\lambda}$ that satisfies the conditions:

$$1) \min_{x \in R^n} \varphi_{\check{\lambda}}(x) > 0, \quad 2) \min_{x \in R^n} \varphi_{\check{\lambda} + \varepsilon}(x) = 0.$$

Note that minimization of $\varphi_{\lambda}(x)$ function can be realized by any existing method.

The preceding algorithm was realized on the personal computer. It was verified on the testing examples. Here we show one of them [3]:

$$\text{To minimize } f(x) = (x_1 - 2)^2 + (x_2 - 1)^2 \text{ subject to } g_1(x) = -x_1^2 + x_2^2 \geq 0; \quad g_2(x) = -x_1^2 - x_2^2 + 2 \geq 0.$$

We have taken for initial point $x^{(0)} = (2.2)$ vector and initial value of λ we have defined with equality $\lambda^0 = f(x^0)$. We have received the solutions: minimum point is vector $(1.001566, 1.001554)$ and the minimum is 1.001574 with precise 10^{-3} .

The convergence of $\varphi_{\lambda}(x)$ function minimizing algorithms, based on the minimum searching parallel methods, will be considered in future publications.

Georgian Academy of Sciences
 Institute of Cybernetics

REFERENCES

1. G.V.Karumidze. In: Metodika statističeskoj optimizacii. 1968, Riga (Russian).
2. G.V.Karumidze. Izvestia AN SSR, Tehničeskaja Kibernetika, 6, 1969 (Russian).
3. D.M.Himmelblau. Prikladnoe nelineinoe programirovanie, M., 1975 (Russian).

L. Kadagishvili

Recognition of Images by Quadtree Method

Presented by Member of the Academy I. Prangishvili, June 8, 1998

ABSTRACT. The coding of images recognition by quadtree deals with the transfer of unconscious informative parameters to machine language that makes possible to use the mentioned algorithm, as a system of recognition. The algorithm is significant, because all the information presented in numerical codes in the form of matrices can be input for recognition.

Key words: quadtrees, algorithm, recognition of images, system of recognition.

The given algorithm of images recognition is constructed on the basis of unconscious informative parameters revealed during apprehension. This method of evristic programming is based on polishing of artificial parameters with algorithm of the so-called quadtrees [1].

Nowadays this direction is developed very intensively. Various versions of quadtrees are given in the literature [2,3]. We have chosen one of these versions with a certain modification. This version of quadtrees gives us the chance to divide the given region into measured parts. Let us describe the diagram of quadtree construction. The square with the size $2^n \times 2^n$, i. e. consisted of 2^{2n} piccells (cell), divided into four branches with dimensions $2^{n-1} \times 2^{n-2}$. The branches are numbered, that means they have their addresses. Later each of branches is separated again into four squares with dimensions $2^{n-2} \times 2^{n-2}$. Their addresses are two sorted numbers: 00, 01, 02, 03, 10, 11, 12, 13, 20, 21, 22, 23, 30, 31, 32, 33. The division of each square and their numbering accordingly, will be continued up to separate piccells. By the rules of address's appropriation for each of square follows that addresses of quadtree piccells $2^n \times 2^n$ will be n -sorted numbers.

Let R be the region, which boundares will be searched r_x . The area r_x is smaller than that of the R . The R is the rectangle with dimensions $M \times N$, where M and N are quantities of piccells (cells) on the horizontal and vertical line accordingly.

Each of piccells with coordinates (i, j) have its intensity d_{ij} . That is why the maximum of intensities: $M^* = (i, j)$, $i = \overline{1M}$, $j = \overline{1N}$ correlates with the area R .

Let us construct on R the union of every possible real square with dimensions $2^n \times 2^n$: $R^* = \bigcup_{k=1}^L r_k$, where $L = (M - 2^n + 1) \times (N - 2^n + 1)$, $\min(M, N) > 2^n$. The matrix of intensities, that correlates with square r_k , will be designated as M_k^* .

The aim of the given paper is to work out the algorithm, that will be appropriate to each of regions, i.e. the square $r_k < R^*$ code, from some matrix's elements $M_k^* = (a_{i,j}^k) \subset M^*$, $i, j = \overline{1, 2^n}$ with an employment of quadtree. The $a_{i,j}^k$ is the (i, j) piccells intensity of k -kind quadtree (region).

Let us assume $n = 3$ and each of squares r_k with $2^3 \times 2^3$ dimensions is presented as quadtree. Let us denote the diagram of quadtree $2^3 \times 2^3$ as Q_0 . The determination, mentioned above will have such form (Fig. 1).

Inside every piccell (i, j) its address $A_{i,j}$ is recorded. For example, piccell (3,5) has an address $A_{3,5} = 213$. Piccells address according to the determination, will be obtained by the process of square r_k division. But it is easier to check that any piccell address can be obtained by summation of its coordinates too, if we record them in the binar form. For the recording of horizontal coordinates, symbols 0 and 1 and vertical coordinates 0 and 2 are used. For example, coordinates of piccell (3, 5) in the binary form will be (011, 201), by their summation the address will be obtained $A_{3,5} = 213$. Let us transform elements of

each matrix $M_k^*(a_{i,j}^k)$, $i, j = \overline{1, 2^n}$ during the utilization of quadtree piccells. Matrix conforms to the square (region) r_k in such a way

$$q_{i,j}^k = A_{i,j} \cdot a_{i,j}^k. \quad (1)$$

Then instead of matrix M_k^* every r_k will be conformed with the value

$$Q_k = (q_{i,j}^k), \quad i, j = \overline{1, 2^n}$$

Each square r_k is represented as Q_{ko} quadtree that is obtained by putting the quadtree diagram Q_0 on the square r_k . In the quadtree Q_{ko} piccell is written down an address with coordinates (i, j) , from Q_{ko} diagram and intensity r_k from the square Q_0^* which product is an element of matrix Q_k . The quadtree is illustrated in Fig. 2. The $\forall Q_{ko}$ consists of 4 branches Q_{ko}^l , $l = \overline{1, 4}$, i. e. squares with dimensions $2^2 \times 2^2$ (Fig. 3). The $\forall Q_{ko}^2$ on its part

A_{11}^k	A_{12}^k	A_{13}^k	A_{14}^k	A_{15}^k	A_{16}^k	A_{17}^k	A_{18}^k
a_{11}^k	a_{12}^k	a_{13}^k	a_{14}^k	a_{15}^k	a_{16}^k	a_{17}^k	a_{18}^k
A_{21}^k	A_{22}^k	A_{23}^k	A_{24}^k	A_{25}^k	A_{26}^k	A_{27}^k	A_{28}^k
a_{21}^k	a_{22}^k	a_{23}^k	a_{24}^k	a_{25}^k	a_{26}^k	a_{27}^k	a_{28}^k
A_{31}^k	A_{32}^k	A_{33}^k	A_{34}^k	A_{35}^k	A_{36}^k	A_{37}^k	A_{38}^k
a_{31}^k	a_{32}^k	a_{33}^k	a_{34}^k	a_{35}^k	a_{36}^k	a_{37}^k	a_{38}^k
A_{41}^k	A_{42}^k	A_{43}^k	A_{44}^k	A_{45}^k	A_{46}^k	A_{47}^k	A_{48}^k
a_{41}^k	a_{42}^k	a_{43}^k	a_{44}^k	a_{45}^k	a_{46}^k	a_{47}^k	a_{48}^k
A_{51}^k	A_{52}^k	A_{53}^k	A_{54}^k	A_{55}^k	A_{56}^k	A_{57}^k	A_{58}^k
a_{51}^k	a_{52}^k	a_{53}^k	a_{54}^k	a_{55}^k	a_{56}^k	a_{57}^k	a_{58}^k
A_{61}^k	A_{62}^k	A_{63}^k	A_{64}^k	A_{65}^k	A_{66}^k	A_{67}^k	A_{68}^k
a_{61}^k	a_{62}^k	a_{63}^k	a_{64}^k	a_{65}^k	a_{66}^k	a_{67}^k	a_{68}^k
A_{71}^k	A_{72}^k	A_{73}^k	A_{74}^k	A_{75}^k	A_{76}^k	A_{77}^k	A_{78}^k
a_{71}^k	a_{72}^k	a_{73}^k	a_{74}^k	a_{75}^k	a_{76}^k	a_{77}^k	a_{78}^k
A_{81}^k	A_{82}^k	A_{83}^k	A_{84}^k	A_{85}^k	A_{86}^k	A_{87}^k	A_{88}^k
a_{81}^k	a_{82}^k	a_{83}^k	a_{84}^k	a_{85}^k	a_{86}^k	a_{87}^k	a_{88}^k

Fig. 2.

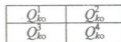


Fig. 3.

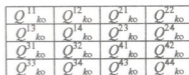


Fig. 4.

is divided into branches $Q_{ko}, t = \overline{1,4}$, i. e. into squares with dimensions 2×2 (Fig. 4). The

result of Q_{ko}^t division are squares with dimensions $2^0 \times 2^0 = 1 \times 1$, i. e. separate piccells.

They are quadtree leaves. Any branch can be used as a leaf, if it consists of equal piccells, i. e. if elements of matrix $m_k^* = (a_{ij}^k)$, and corresponding piccells, are equal. The principle of quadtree's construction gives us the possibility to perform stepwise codation.

Let us describe an algorithm of codes to regions $r_k \subset R$ stepwise.

1. As a code of every piccell (i.e. leaf with address A_{ij}), we'll assume $A_{ij} \cdot a_{ij}^k = q_{ij}^k \subset Q_k^*$.

2. Code Q_{ko}^t . If A_{ij} is an address of the square Q_{ko}^t of the first cell, the Q_{kit}^* matrix (i.e.

matrix of intensities, which conforms to the square Q_{ko}^t) will be expressed as:

$$Q_{kit}^* = \begin{pmatrix} A_{i,j} \cdot a_{i,j}^k & A_{i,j+1} \cdot a_{i,j+1}^k \\ A_{i+1,j} \cdot a_{i+1,j}^k & A_{i+1,j+1} \cdot a_{i+1,j+1}^k \end{pmatrix}.$$

Let's determine the rule of code appropriation for the square Q_{ko}^{2t} in the following way:

if Q_{ko}^t is a leaf, i.e. $a_{ij}^k = a_{ij+1}^k = a_{i+1,j}^k = a_{i+1,j+1}^k$, (2)

then $C(Q_{ko}^t) = A_{i,j} \cdot a_{i+1,j}^k = q_{i+1,j}^k$.

Otherwise $C(Q_{ko}^t) = A_{i,j} \cdot a_{i,j}^k + A_{i,j+1} \cdot a_{i,j+1}^k + A_{i+1,j} \cdot a_{i+1,j}^k + A_{i+1,j+1} \cdot a_{i+1,j+1}^k =$
 $= q_{i,j}^k + q_{i,j+1}^k + q_{i+1,j}^k + q_{i+1,j+1}^k$, (3)

where $C(Q_{ko}^t)$ denotes the code Q_{ko}^t . It is sometimes reasonable to skip the examination of condition (2) and estimate code $\forall Q_{ko}^t$ by the formula (3). It depends on the region, exactly on intensities of neighboring piccells.

3. Code Q_{ko}^t . $C(Q_{ko}^t) = \sum_{t=1}^4 (Q_{ko}^t)$. (4)

On this step the algorithm square Q_{ko} correlates with vector $(C(Q_{ko}^1), C(Q_{ko}^2), C(Q_{ko}^3), C(Q_{ko}^4))$.

4. Code Q_{ko} . $C(Q_{ko}) = \frac{1}{4} \sum_{t=1}^4 C(Q_{ko}^t)$. (5)

5. Code r_k . The code of region r_k is an artificially created sign, which characterizes the given region. The algorithm will be constructed so as to appropriate to all areas their own code, different from other codes of any region, if their corresponding intensive matrices are different.

Thus, the offered algorithm is the algorithm of education. The education will be

produced on the basis of Q_k^* , $k = \overline{1, 2}$ matrices elements. The name of these matrices will be the image of educational matrices. For the education every region r_k is presented only with one image. That is why the algorithm increases the quantity of images artificially and algorithm changes in such a way. If we shall turn the square r_k on 90° , then quadtree Q_k transforms in quadtree Q_{k1} . In this way the intensity a_{ij}^k that corresponds to piccell (i, j) of quadtree Q_{k1} , i.e. $a_{x'}^k$, where $x = 2^n + 1 - (j)$ and the formula (1) for the determination of matrix Q_k^* element q_{ij}^k will have the form:

$$q_{ij}^k = A_{ij} \cdot a_{xi}^k. \quad (6)$$

The turn of the square r_k on 180° to it conforms quadtree and element q_{ij}^k of correlated matrix Q_k^* will be determined as:

$$q_{ij}^k = A_{ij} \cdot a_{yx}^k \quad (7)$$

where $y = 2n + 1 - i$.

And finally, after the turn of the square r_k on 270° we'll obtain quadtree Q_{k3} with corresponding matrix Q_k^* which element will be:

$$q_{ij}^k = A_{ij} \cdot a_{ij}^k. \quad (8)$$

Formulae (2) - (5) give us the possibility to determine codes of squares Q_{k1} , Q_{k2} and Q_{k3} .

In this case (6), (7), (8) formulae will be used and correspondingly the squares Q_{k0} , Q_{k1} , Q_{k2} , Q_{k3} give the image of r_k region. The code r_k must be their integral code.

The expressions $C(Q_{k0})$, $C(Q_{k1})$, $C(Q_{k2})$, $C(Q_{k3})$ will be obtained by averaging:

$$C(r_k) = \frac{1}{4} \sum_{s=0}^3 C(Q_{ks}).$$

Thus, the offered algorithm appropriates to every region $r_k \subset R$ the code $C(r_k)$.

After the coordination of algorithm a data base will be created and knowledge base in order to recognize the explored regions. The codes $C(r_k)$ and coordinates (x_k, y_k) , $k = \overline{1, r}$ will be put down in the basis of information.

The r_k region coordinates will be considered coordinates of that left cell of square R . Formulae (1) - (5) will be put down in the basis of knowledge.

The examples show that if matrices m_α^* and m_β^* that correspond to the r_α and r_β are different only by one element then codes $C(r_\alpha)$ and $C(r_\beta)$ will be different.

The given informative system can do an important scope of demands. This system does not limit the quantity of cards that can be written into the information basis.

The proposed algorithm as the system of recognition is important for its utilization because all the information that can be represented in numerical codes as matrices may be written down in it for recognition.

Georgian Academy of Sciences
 Institute of Cybernetics

REFERENCES

1. L. kadagishvili. Aghkmis sighrme da mankanuri programireba, Tbilisi, 1993 (Georgian).
2. A.Klinger. Patterns and search statistics. Optimizing Methods in Static's. New York, Acad. Press, 1977.
3. H.Sanet, A.Rosenfield et al. A Geographic Information System using Quadrees, GB; Pattern Recognition, 1984, 17, N 6, 647-656.



O.Tavdishvili, T.Sulaberidze

Statistical Approach to Image Segmentation

Presented by Member of the Academy I. Prangishvili, May 17, 1999

ABSTRACT. The paper describes an algorithm for a non-parametric segmentation of image in multidimensional feature space and determines a procedure for such a segmentation. The procedure is based on Parzen statistical estimation of the probability density function. A strict definition of cluster and the segment corresponding to it is given.

Key words: cluster, segment, connected unity.

Real scene image can be described with vector-function $Z = f(x,y) = (f^{(1)}(x,y), \dots, f^{(k)}(x,y))$ of characteristic features, where each $f^{(i)}(x,y)$ component is a numerical value of i characteristic feature at plane point (x,y) .

We consider the case, when a digital image of real scene is represented as matrix

$$A = \left\| a_{ij} \right\|_{i=1, \overline{N}}^{j=1, \overline{M}},$$

where each a_{ij} is a k -dimensional point (data vector) $a_{ij} = (a_{ij}^{(1)}, \dots, a_{ij}^{(k)})$ and

$a_{ij}^{(l)} = f^{(l)}(x_i, y_j)$, $l = \overline{1, k}$. It is implied, that the coordinates are ordered by increasing:

$$x_1 < x_2 < \dots < x_N, \quad y_1 < y_2 < \dots < y_M$$

The final aim of segmentation is a partition of the real scene picture $z = f(x,y)$ into disjoint, uniform parts, based on data set clustering and then matrix A segmentation. Clusters are formed as the uniform groups, while segments are maximal connected disjoint unities, as a result of mapping back extracted clusters to the matrix A .

Definition 1. The unity B of matrix A ($B \subset A$) is called a connected unity, if for arbitrary couple $a_{ij}, a_{i+s, j+t} \in B$ (s, t - integers) we can find in B such elements, one of the indices of which at least should run non-decreasing sequence from i till $i + s$, if $s > 0$ (accordingly, from $i + s$ till i , if $s < 0$), or from j till $j + t$, if $t > 0$ (accordingly, from $j + t$ till j , if $t < 0$).

In order to solve the segmentation task, it is necessary to introduce some metric for estimating closeness of contiguous elements in matrix A . Let us assume, that it is Euclidean metric $\rho(\dots)$ in k -dimensional Euclidean space.

For each element a_{ij} , $i = \overline{1, N-1}$, $j = \overline{1, M-1}$ of matrix A let determine the so-called "window" of size 2×2 . Move it, beginning with a_{11} , along the rows from left to right, and calculate for each a_{ij} in its "window" six distances in the following order:

$$\rho(a_{ij}; a_{i+1, j}), \quad \rho(a_{ij}; a_{i+1, j+1}), \quad \rho(a_{ij}; a_{i+1, j+1}),$$

$$\rho(a_{i+1,j}; a_{i,j+1}), \rho(a_{i+1,j}; a_{i+1,j+1}), \rho(a_{i,j+1}; a_{i+1,j+1}), \quad i = \overline{1, N-1}, j = \overline{1, M-1} \quad (1).$$

Introduce respective notations according to sequence (1):

$$\xi_1 = \rho(a_{11}; a_{12}), \xi_2 = \rho(a_{11}; a_{22}), \xi_3 = \rho(a_{11}; a_{21}) \text{ and etc.}$$

Therefore, while computing distances ξ_q in each given "window" we have to ignore distances, which were already computed in previous "windows". As a result, we will receive a sequence of non-negative numbers $\{\xi_q\}$, $q = \overline{1, n}$, $n = 4(N-1)(M-1) + N + M - 2$

Let's assume, that $\{\xi_q\}$, $q = \overline{1, n}$ is a sample size n of such a parent population, which has theoretical density function $\varphi(x)$. Let's take the Parzen estimation in order to estimate it

$$\hat{\varphi}_n(x) = \frac{1}{n \cdot h} \sum_{q=1}^n k\left(\frac{x - \xi_q}{h}\right),$$

where $h = h(n) > 0$ and $h(n) \rightarrow 0$, $nh(n) \rightarrow \infty$, when $n \rightarrow \infty$; $k(x)$ is a Borel function integrable with respect to Lebesgue measure, while sequence $\{\hat{\varphi}_n(x)\}$ converges to $\varphi(x)$ uniformly with respect to x , with probability 1, when $\varphi(x)$ and $k(x)$ satisfy specific additional conditions [1].

We consider the case, when $k(x) = 1 - |x|$, if $|x| \leq 1$ and $k(x) = 0$, if $|x| > 1$ (in general, definite idea the best selected $k(x)$ function can be possible with the well-known statistical methods). For such $k(x)$ we will have piecewise linear function $\hat{\varphi}_n(x)$. According to the above mentioned, we may assume, that the computations given below will be true with probability 1.

The presented segmentation method is based on extraction of uniform disjoint groups - clusters from the sequence $\{\xi_q\}$, $q = \overline{1, n}$. These clusters form around the points of local maxima, i.e. modes $M_1 < M_2 < \dots < M_p$ of the function $\hat{\varphi}_n(x)$, as the centers of the clusters. In particular, for each mode M_i , $i = \overline{1, p}$ determines the so-called domain of a cluster [2], which is the interval $[m_i, m_{i+1})$, $i = \overline{1, p}$, while m_i and m_{i+1} are the points of local minima of the function $\hat{\varphi}_n(x)$ for which $m_i \leq M_i < m_{i+1}$. Therefore, $m_1 = \min\{\xi_q - h, \xi_q, \xi_q + h\}$ and $m_{p+1} = \max\{\xi_q - h, \xi_q, \xi_q + h\}$, $q = \overline{1, n}$. Ordering the sequence $\{\xi_q - h, \xi_q, \xi_q + h\}$ by increasing, we will receive sequence $\eta_1 < \eta_2 < \dots < \eta_r$, $r \leq 3n$, where each η_j , $j = \overline{1, r}$ has its own multiplicity in $\{\xi_q - h, \xi_q, \xi_q + h\}$, $q = \overline{1, n}$. Thus, since $\hat{\varphi}_n(x)$ is a piecewise linear function, in order to find the modes M_i and points of minima m_i it will be necessary to compute only the meanings of $\hat{\varphi}_n(\eta_j)$, $j = \overline{1, r}$. If the points of local maxima fill in the whole interval $[\eta_p, \eta_{j+1}]$, as the meaning of mode, we can take the middle point of this interval, while if the points of maxima fill in several intervals in succession, then the meaning of mode will be the middle point of the very last

interval on the right. Analogously, the points of local minima can fill one or several intervals in succession. At the former case, in the capacity of meanings of the m_i we can take middle point of the intervals of the minima, while in the latter case, middle point of the union of intervals of the minima. So, we will have the domains of the clusters: $[m_1, m_2), [m_2, m_3), \dots, [m_p, \eta_r]$. Only a part of the sequence $\{\xi_q\}$, $q = \overline{1, n}$ will get into every domain $[m_i, m_{i+1})$, let's say ξ_i, \dots, ξ_{i_j} . Create new sequence $\{|\xi_{i_j} - M_i|\}$, $j = \overline{1, l}$ and compute for it the Parzen estimation of the density function again and let's call the maximal of its modes the radius of the sameness R_i of cluster.

Definition 2. The unity of those elements of the sequence $\{\xi_q\}$, $q = \overline{1, n}$ which belong to domain $[m_i, m_{i+1})$ and satisfy the condition of uniformity

$$|\xi_q - M_i| \leq R_i, \quad i = \overline{1, p}; \quad q = \overline{1, n} \quad (2)$$

is called cluster K_i with center M_i and radius R_i , $i = \overline{1, p}$. The so-called isolated elements a_{ij} in matrix A correspond to the other elements of the sequence $\{\xi_q\}$, which belong to the domain $[m_i, m_{i+1})$ and do not satisfy condition (2).

Coming out of the rule of constructing of the sequence $\{\xi_q\}$, $q = \overline{1, n}$ each cluster K_i of the sequence $\{\xi_q\}$ uniquely determines specific group of elements in matrix A , which can be conditionally called "matrix" cluster A_i in matrix A .

Definition 3. A maximal connected unity of elements of the "matrix" cluster A_i is called a segment.

The connected unity S extracted in "matrix" cluster A_i is maximal, if supplement of another arbitrary element from A_i into S dissolve condition of connectivity. Starting from this definition, every A_i can be divided into some segments S_t^i , $t = \overline{1, T_i}$, $i = \overline{1, p}$.

Naturally, we have to perform the process of segments extraction in the same order, as modes $M_1 < M_2 < \dots < M_p$ are ordered. For this, let's move in matrix A "window" of size 2×2 in the same way as before and we find for adjacent elements (1) distances between which belong to cluster K_1 , i.e. we determine "matrix" cluster A_1 . A maximal connected unities of the elements will be extracted into segments S_t^1 , $t = \overline{1, T_1}$ in A_1 .

Next segments S_t^2 , $t = \overline{1, T_2}$ will be created in the "matrix" cluster A_2 , which correspond to cluster K_2 (therefore elements segmented in previous step will not take part in extraction of segments S_t^2) and etc. The process of segmentation of the matrix A will be completed.

The algorithm has been tested on computer.

Georgian Academy of Sciences
 Institute of Cybernetics

REFERENCES

1. E. Nadaraya. Non-parametric Estimation of Density Function and Regression Curve. Tbilisi, 1983 (Russian).
2. O. Tavdshvili. A Method of Segmentation of a Set of Measurements Based on Parzen Statistical Estimation. Moscow, 1988 (Russian).
3. "მეცნიერება", ტ. 160, №2, 1999

N.Archvadze, E.Dekanosidze, J.Vakhtangadze, M.Nizharadze, N.Papunashvili,
M.Pkhovelishvili, M.Tsuladze

System of Tutorial Courses Building

Presented by Member of the Academy V.Chavchanidze, December 21, 1998

ABSTRACT. One problem of tutorial system referring to the construction of current educational courses of particular purpose and structure is considered. Tutorial system is proposed to be a combination of subsystems of building and functioning.

Key words: programming, representation of knowledge, tutorial systems.

The tutorial system [1] is aimed to create concrete educational courses and to help the learner to get quick and exhaustive information on the studied subject, to do proper exercises to confirm the knowledge, to check and evaluate the level of apprehension. One of the subsystems of tutorial system must be the system of the tutorial courses building the essential principles of which are formulated below. As for the other parts of tutorial system, they are not described thoroughly.

The author of the course is implied to prepare a tutorial text, the structure of which will be specified later in advance. The building of tutorial course subsystem will be organized to enter this text into the computer and to process it. As a result a tutorial course will be obtained. Thus, tutorial course is a computer program, ready to be performed and to play the role of a teacher.

The structure of a textbook is meant to be a file of knowledge portions, i.e. the lessons. Each portion consists of five different parts: basic, pro-precedent, transfer new material, illustrative and training. Dropping out of any part (except of new material transfer) is admissible. The portion and its parts should be titled and/or walkthrough number.

The basic part is the one, where the elements of precedent portions are reminded. These elements are necessary in recent portion for formulation of new material.

The pro-precedent part also serves for preparation and improvement of apprehension of a new material in current portion. Clear separation of analogies, coincidences and differences serving to increase the effectiveness of learning is desirable.

The part of a new material transfer serves to present fresh knowledge of portion. The texts, including the purpose of a given topic, determination of new notions and introduction of appropriate terminology, are presented. So, this part consists of theoretical theses to be studied in connection with the next topic.

The fourth is an illustrative part which allows the author to illustrate the process performing some typical exercises by using of theoretical theses presented in the precedent part. The detailed scheme of resolution is accompanied by the author's comments, presented not only textually but also as formulas, graphs, tables, etc. The author helps the learner to be skilful to use theoretical knowledge.

The fifth, training part has a great deal of assignment. It serves to firm the knowledge and check up the knowledge adoption level. It consists of questions and exercises com-

posed by the author. Each question essentially deals with some problems taken from the third part but each example represents the one which doesn't take part in any other part of the course. These examples require a special approach in the building subsystem.

The functioning of building system arrives down to processing the sequence of portions prepared by the author. On processing a portion the building system receives a part of educational course depending on the purpose of this part of portion.

During functioning of educational system the building system must provide the display of the texts (drafts, drawings, graphs, tables) onto the screen and the sound-track in case of necessity. It is the simplest way of processing the portions. The same is implied for the other parts of the portion, but for the fourth and fifth parts the building subsystem must perform different kind of job. The fourth, illustrative part implies that each complete text is considered to be an example. It implies to formulate an example and to show the process of solving it. The latter may be presented as the so-called cliché. Cliché may be represented as a sequence of texts displayed onto the screen. There must be two kinds of texts differently represented on the screen: a permanent one and the one that is to be filled. The author of the textbook preliminarily prepares an information given by the cliché, which is transformed by the building system in the following way: the recent permanent part is delivered to the tutorial course unchanged, as for the current fillable text, it is filled up by the author with some information of predetermined destination.

The building system works similarly during the process of transformation of the fifth part of knowledge portion into the tutorial course, but it can not process the fillable part of the cliché, because this one must be filled up by the student during functioning of the tutorial course. It is expedient to organize the performance of filling up the cliché not within the building system but separately, and to make application to it in two different ways: a) when the author fills it during an activity of the building system, b) when the student fills it during an activity of the tutorial course's subsystem.

Along with the cliché the so-called menu is used to answer the questions. It implies the existence of a subsystem of compiling a menu and a subsystem of a choice within the menu. The building system uses them to obtain the fourth portion of tutorial course (while the author compiles the menu) and the fifth portion (while the student selects some topic from menu during functioning of the tutorial course).

In case when the tutorial course is built up for the programming languages and the exercises are the programs or its parts the existence of two more subsystems is necessary for the syntax and the semantic analysis of the programs. Building system uses them in the fourth part of the portion to analyze the program (or its fragment) presented by the author and in the fifth part to analyze the program (or fragment) presented by the student.

Later these results of analyses will be compared to determine the equivalence between them. This work will be done by a subsystem of semantic equivalence determination.

During functioning of the tutorial course the knowledge level of a student in presented knowledge portion is checked up and if there exists any gap the student is returned back to the portion already studied.

Georgian Academy of Sciences
 N. Muskhelishvili Institute of Computing Mathematics

REFERENCES

1. L.V.Zaitseva et al. Razrabotka i primeneniye avtomat obuchayushich sistem na baze EVM. Riga, 1989 (Russian).

T. Ebralidze, N. Ebralidze

The Self-Excited Oscillation Hydraulic System (The Hydraulic Motor)

Presented by Member of the Academy V. Chavchanidze, June 29, 1998

ABSTRACT. The article studies self-excited oscillations of a new hydraulic system. The system characterized by all indications of non-linear system is established. The oscillation form, almost sinusoidal oscillation period and conditions of obtaining such oscillations are determined.

Key words: hydraulic motor

The work aims to study the self-excited oscillations [1] in a new hydraulic system [2,3]. This system represents a hydraulic motor. It converts the energy of constant liquid flow into the energy of piston oscillation giving liquid flow pulsation at the output.

The motor operation may be compared with hydraulic ram action [4], although as we'll see below there are fundamental differences between them.

In hydraulic ram the drain plug of liquid flow insures blockage of the flow by means of the flow movement along its direction and creates a hydraulic impact [5]. As to the systems [2,3], the hydraulic impact appears by the opposite action of piston drain to liquid flow caused by the opposite flow of liquid. In Fig. 1 the motor [2] is depicted by the bold lines. It consists of chamber-3 and piston-4 located in it. The chamber is a cylinder, ending on both sides with the truncated cones. The cylinder shaped branch pipes are attached on the chamber 1,2. The piston is a chamber shaped also with the difference that it has untruncated cones on the ends. There is a slot between the chamber and piston cylinder parts. Piston cone vertex for the cone cavity serves as a plug. The length difference between chamber and piston is not less than that of doubled height of piston cone vertex.

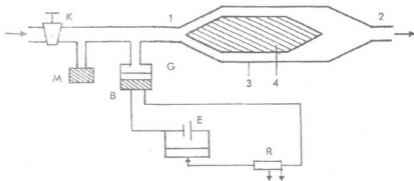


Fig. 1 Experimental device diagram. The arrows show the flow direction, (K) denotes a tap, (M) a manometer, (G) a diaphragm, (B) a microphone, (E) a power source, (R) a rheostat. 1, 2 are branch pipes, 3 a chamber, 4 a piston.

In the motor [3] the chamber and piston have shape of trapesium obtained by [2] chamber and piston perpendicular axial cross-section. The motor operates in the constant liquid flow. The flow gets into the chamber with pipe 1, passes through the wall clearance between piston and chamber and gets out with pipe 2.

In the state given in the Figure the force acted from the liquid flow on the piston cone vertex is less than that of acted on piston end from the liquid flow (the pipe cross-section area at piston cone vertex is less than that of at the end of corresponding piston vertex).

Therefore the piston moves opposite to the flow. The closer is the cone surface to the chamber the more is the force. It continues until piston vertex will decrease liquid flow rate into the chamber. As the force acting on the piston opposite to the flow depends on flow rate it is obvious that with the decrease of flow rate the force will also decrease.

We suppose that the piston stops in some certain position and it saves a certain flow in chamber.

Obviously it would be true if there is no following circumstances. After the reduction of the flow rate in the branch pipe incomplete hydraulic impact appears [5]. The pressure will increase rapidly above the static pressure. In a short period the resultant forces acting on piston will change the direction. It will act now to the flow direction giving to the piston certain kinetic energy.

The operation of this motor has been monitored by the experimental device (Fig. 1).

Water has been conducted from the left to the right into the motor as it is shown by arrows (Fig. 1). In the chamber the value of flow rate was regulated by K-tap. In branch pipe 1 liquid pressure oscillation was recorded by M-manometer. Liquid pressure oscillation was converted into electric oscillation by B-microphone. The microphone was isolated from liquid by G-diaphragm. There was an air between G-diaphragm and microphone diaphragm under the atmosphere pressure. The microphone B together with rheostat C was switched on in direct current E circuit fed by D. C. source.

The voltage drop obtained on rheostat C was delivered to the recorder KCTI-4-input. Water was given onto K-tap from the town water pipe-line approximately under 4-5 atm pressure.

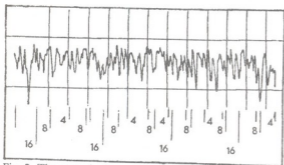


Fig. 2. The record of pressure oscillation diagram made by recorder during high flow rate.

When increasing the flow the piston will move opposite to the flow limiting the flow into the chamber. The increasing of liquid will be marked. Manometer arrow drops are observed (Fig. 2). The inversive action is also observed (see the extreme right section of Fig. 3).

During the oscillations the pressure was about 0.8 atm. As it is shown from the right part of the figure, almost sinusoidal oscillations were formed. Its frequency was approximately 2 Hz.

The oscillation form may be kept for a certain interval of flow changing. If we shall increase the flow going out of this interval, the motor will stop oscillating process. At that time the piston falls out of the active zone. The extreme left area of the Fig. 3 points to this condition.

It was established by the experiment that self-excited oscillations may be kept during

the flow increasing. For this we need to increase the resistance force temporarily effecting on piston. While changing the flow we lifted the output neck 2.

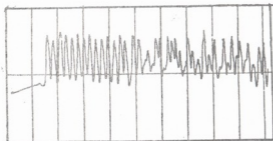


Fig. 3. The record of pressure oscillation diagram made by recorder during low flow rate.

The specially chosen shape of motor chamber and piston makes the feedback possible. In the motor the liquid flow creates the opposite force to the flow effected on piston, causing the hydraulic impact.

The value of incomplete hydraulic impact depends upon flow speed and tap closing duration. In our case the tap stopping duration depends upon force directed opposite to flow, i. e., in our case the force of hydraulic impact depends upon flow rate in as obvious as nonobvious ways. That is why as oscillation amplitude will depend upon the value of hydraulic impact. We suppose that selfregulation will occur inside the system. Really, in the case of great flow high oscillation amplitude is observed (Fig. 2).

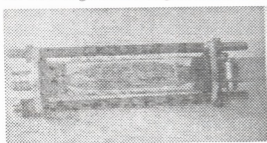


Fig. 4.

The above mentioned points out oscillation [2].

Thus, the new self-excited oscillation hydraulic system is worked out. It has all indications that are characterized for non-linear systems. In certain conditions the system can make almost sinusoidal oscillation, the frequency of which does not depend upon flow rate. The self-excited oscillation amplitude value depends upon flow rate.

The motor in this case oscillates even with increased flow. If we return the motor in horizontal location little by little, the oscillations will be kept. In Fig. 2 4, 8 and 16 times increased period pulsations is shown.

As it was established by the experiment the oscillating motion under constant flow is characterized by all features of self-excited oscillation.

As it follows after the comparing of Figs. 2 and 3, the oscillation maximal frequency created inside the system does not depend on flow value. It will depend upon geometric parameters value of chamber and piston and piston masses.

Conversion of turbulent (chaotic) oscillation from the almost sinusoidal oscillation takes place according the non-linear system regularities [6]. that non-linearity plays the main role in system

Georgian Academy of Sciences
 Institute of Cybernetics

REFERENCES

1. A.A.Andreev, A.A.Vitt, S.Z.Khaikin. Teoria kolebanii, M., 1981 (Russian).
2. T.D.Ebralidze. 001690 Official bull. of the industr. property, Ge, 11(20), (Russian).
3. Idem. Ibidem, 001691, (Russian).
4. M.S.Feigenbaum. Los Alamos Science, 1,1,1980, 427.
5. A.A.Kharkhevich. Self-excited oscillations M., 1954 (Russian).
6. N.E.Zhukovsky. O gidravlicheskom udare v vodoprovodnykh trubakh, M., 1948 (Russian).

A.Bichinashvili, M.Zviadadze, T.Mkhatrishvili, V.Achelashvili, I.Bendiashvili

The Formation of the Thermosensitive Equipment on the Basis of γ -Mn Alloy

Presented by Member of the Academy R. Salukvadze, November 12, 1998

ABSTRACT. The following work outlines the opportunity of usage of γ -Mn alloy in the thermal automatics. It is mentioned that the manganese consistence, deformation, thermal treatment within the γ -Mn alloy are the main factors increasing the thermosensitiveness of this material. The alloyage of the γ -Mn binar alloys increases the degree of form restoration and thermosensitiveness respectively.

Key words: thermosensitiveness, form memory, γ -Mn alloy.

The formation of thermosensitive equipment within the martensite alloys is mainly based on the effect of form memory. This effect is studied in a number of works [1-3]. The authors of those works consider that the main factors of creation of the form memory effect are: the transformation of martensite type and the regulation of the inner tensions created as a result of form deformation. The first factor provides the reflection of the process, while the second one directs this process in one direction.

The γ -Mn alloys differ from the other form memory alloys by the factor that the martensite transformation is carried out as a result of magnetic transformation. For this reason the form memory within these alloys may be carried out by changing not only the temperature but the magnetic field as well.

The degree of form memory and the increase of the thermosensitiveness, respectively, are not thoroughly studied. Thus the purpose of this work is to determine the main units that promote the increase of the thermosensitiveness of these materials.

We have studied the binar alloys Mn-Cu (Mn 60-85%), Mn-Fe (Mn 70-90%), Mn-Ni (Mn 60-90%) as well as alloyaged binar alloys 70% Mn - 25% Cu - 5% Pb, 70% Mn, - 25% Cu - 5%Sn, 70% Mn- 25% Cu - 5% Ni and 70% Mn - 25% Cu - 5% Fe. The homogenization of the alloys took place at 850^oC during 100 hours, after which they were steeled in the water. The loosening took place at 400^oC during 5, 10, 20, 40 hours. The unit of preliminary plastic deformation was 0.6%, 1.2%, 1.9%, 2.4 %, 3.2% and 3.9%.

At a high temperature (250-300^oC) corresponding to cubic phase, we gave the oval form to the sample and straighten it at the room temperature. As a result of heating the sample restored its original form, while the cooling caused the straightening of the form.

The experiments prove that the degree of restoration of deformation is high within the loosen alloys than within the steeled alloys. This might be caused by increasing the steadiness of the alloys connected with the creation of zone structure. It is evident that the tensions created during the form restoration undergo less relaxation.

The work studied the change of restored deformation in the intervals of 20-200^oC



during the various preliminary plastic deformation on 79.6% Mn alloy, that was loosen at 400°C during 10 hours. Figure 1 shows that the maximum comes on 2.5% of preliminary plastic deformation. This fact, as mentioned above, may be caused by increasing the steadiness.

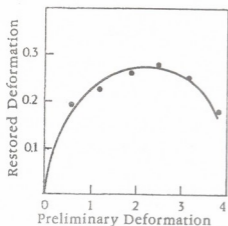


Fig. 1.

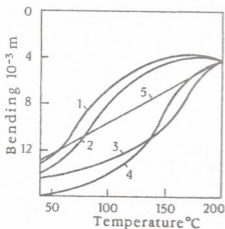


Fig. 2.

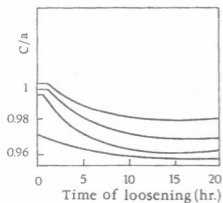


Fig. 3.

The influence of thermal treatment on the specific bending unit during one and the same preliminary plastic deformation (2.5%) has also been studied. The investigation was carried out at 68.9% Mn and 79.6 Mn alloys, that were loosen at 400°C during 5, 10, 20 and 40 hours. As seen from Fig. 2 by increasing the time of loosening the restored deformation is increasing as well. This might be caused by increasing the importance of the thermoflexible martensite within the whole volume of the sample. At the same time this is connected with the tetragonal degree and steadiness. These units are increasing by increasing the time of loosening. The Fig. 2 shows that γ -Mn binar alloys at treated maximum thermosensitiveness greatly exceed thermobimetal with high thermosensitiveness by the specific bending. Namely, such thermobimetals as TB2013 (Fig. 2 bend 5). This privilege might be referred to the negative temperature interval.

The Fig. 3 shows the tetragonal change (c/a) caused by looseness at 400°C during 5, 10, 20 hours within 59.2% Mn, 67.9% Mn, 78.5% Mn, 86.4% Mn alloys. As seen from the Figure, by increasing the time of loosening (c/a) the tetragonal degree increases and reduces (1-c/a). The increase of the latter causes the increase of thermosensitiveness. The looseness for γ -Mn alloys is important, unlike the other form memory alloys, as within the other alloys the small time of loosening reduces the degree of form restoration. The same Fig. 3 shows that c/a changes by the temperature. Such change is characteristic for antiferromagnetic alloys. For this reason the bend of deformation restoration is of the same type. It should be mentioned that c/a change refers to the negative temperature.

The interval of maximum change of the restored deformation depends on the temperature of martensite transformation, because with the increase of tetragonal degree the temperature of transformation increases

as well. Thus we have investigated the dependence of the temperature of martensite transformation from the manganese concentration both within steeled and loosen alloys

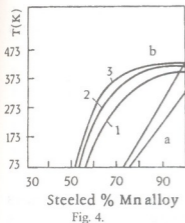


Fig. 4.

(Fig. 4). The Fig. shows that within the steeled Mn-Cu alloys the martensite transformation is carried out during 70%Mn and more concentrated intervals, while within the loosen alloys this interval begins with 50%Mn, i.e. the concentration interval increases as a result of the loosening, where the form restoration takes place. Besides, as seen from the Fig., by increasing the time of loosening the two-phase area (FCC \rightarrow FCT) reduces and hysteresis reduces respectively that indicates to the increase of the importance of the thermoflexible transaction at the whole volume of the sample. The latter increases the degree of form restoration. It should be also mentioned that with the

increase of the time of loosening the temperature of FCC \rightarrow FCT transformation increases as well, i.e. we may change the time of loosening the interval of temperature where the maximum form restoration takes place in the areas of positive as well as of negative temperatures[4].

We have investigated Mn-Cu alloys which were alloyaged in Pb, Sn, Ni, Fe metals. According to the investigations the alloyage increases the tetragonal degree and restored deformation.

Thus, the degree of the form restoration of γ -Mn and thermosensitiveness respectively depends on: the concentration of manganese, preliminary deformation, thermal treatment and alloyage.

Georgian Technical University

REFERENCES

1. V.N.Khachin, V.N.Itin. Splyny s pamiaty. M., 1984.
2. V.N.Khachin. Pamiat formy. M. 1984.
3. A.S.Tikhonova et al. Primeneniye efecta pamiati formy v sovremennom mashinostroyenii. M., 1981.
4. E.Z.Vintaikin, V.A.Udoverko, D.F.Litvin, V.B.Dmitriev, A.I.Bichinashvli. Avtorskoje svidetelstvo na izobretenie. No610403. 1978.

S. Gotoshia, L. Gotoshia

Laser Raman Spectroscopy of A^3B^5 Amorphous Binary and Ternary Semiconductors Synthesized by Ion Implantation

Presented by Corr. Member of the Academy T. Sanadze, December 21, 1998

ABSTRACT. Thin films of A^3B^5 binary and ternary amorphous semiconductors synthesized by proper ion implantation in targets have been identified by laser Raman spectroscopy. The analysis of phonon density of state of proper compounds has been obtained on the basis of RS.

Key words: laser Raman spectroscopy, amorphous binary and ternary semiconductors.

As it is known at Raman scattering in crystal compounds optical phonon is absorbed or illuminated at about $k \approx 0$. When crystal structure is crushed and the periodicity is lost due to the disappearing of far order then $k=0$ selection rule loses its sense and in the first order the phonons with big k participate. Such state is originated in amorphous semiconductors, when all the vibrational modes are allowed and take part in Raman scattering process. Thus, we conclude that in amorphous semiconductors the first order Raman spectra reflect the general form of distribution of one-phonon density of vibrational state. Vibrational density of state of amorphous compounds in the first approximation seems to express the extended variant of the proper crystal lattice vibrational density of state and A^3B^5 group semiconductor Raman spectra as well as IV group have the whole spectrum characteristic structure rather than the narrow bands, which correspond to the zero wave vector phonons being active in Raman scattering. According to [1], phonon density of state $\rho(\omega)$ for amorphous semiconductors is computed using the Stox scattering intensity formula:

$$I(\omega) \sim \omega^{-1} [n(\omega, T) + 1] \rho(\omega), \quad (1)$$

where $n(\omega, T)$ is Bose-Einstein distribution function. Scattering probability for all phonons is implied to be the same.

The RS in amorphous semiconductors Si, Ge and A^3B^5 compounds has been studied in [2, 3]. In these works the amorphous semiconducting films were obtained by different methods. It was established that despite different methods of synthesis the RS obtained from these films characterize amorphous phase.

The purpose of the present work is to identify by laser Raman spectroscopy method GaP and GaAs amorphous binary and ternary compounds synthesized by ion implantation on one hand and to study RS peculiarities in these films, on the other hand. It is worth to notice that some compounds, for example GaPA1, have been first synthesized by ion implantation method and studied by laser Raman spectroscopy by us [4].

To receive amorphous films we were dealing with ion implantation of monocrystalline GaP and GaAs targets by Ar, B, N, Ph, Al, As ions. The target surfaces were of two

kinds: (111) and (001) orientations. Ion energies varied from 40 to 110 keV and because of this we dealt with amorphous films of various thickness in different depths from the crystalline surface. Implantation was fulfilled with different doses at room temperature as well as at high temperature 400°C . For Raman spectra recording home made Raman spectrometer constructed on the basis of double monochromator DFC-12 was used. Argon laser emission wavelengths 5145A, 4480A and helium-cadmium laser emission wavelength 4416A were used for spectra excitation by us. The mentioned emission wavelengths (energies) were chosen so that we should be able to conduct probing in different depths of target surfaces implanted with various energies.

The study of Raman spectra of surfaces implanted with different doses showed that with dose increase in RS gradually decreases the intensity of LO and TO phonons, their halfwidths increase, peaks small shift towards low frequencies occurs and nearly after critical dose Raman spectrum loses its sharp peak structure and turns into shapeless wide band. The halfwidth of this band is about 70cm^{-1} for GaP and 40cm^{-1} for GaAs. Fixation of this wide bands in Raman spectrum shows nucleation of an amorphous phase. It should be noted that amorphous phase nucleation is influenced by implanted ion mass, energy and temperature of target. The orientation of target is of certain importance too.

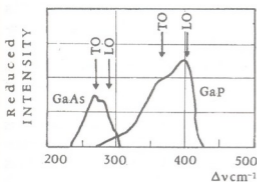


Fig. 1. Reduced Raman spectra of α -GaP and α -GaAs obtained by ion implantation.

the formula (1) have been computed. Reduced Raman spectra received by this method are shown in Fig. 1. Positions for TO and LO phonons corresponding to crystalline GaP and GaAs respectively are indicated with arrow in the same Fig. 1. When comparing these reduced spectra with theoretical calculations given in references, one will be assured that in certain approximation they correspond to the crystal lattice phonon density of state curves which are expanded by a certain coefficient.

To synthesize amorphous ternary compound GaPAs by ion implantation we have implanted GaAs surface with (111) orientation by 40 keV energy phosphorous ions. The implantation occurred at the room temperature as well as at high 400°C temperature.

Figure 2 shows Raman spectrum which reflects the picture created by phosphorous ion implanta-

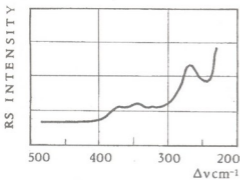


Fig. 2. Raman spectra of α -GaAsP synthesized by phosphorous ion implantation of GaAs.

tion in GaAs. The implantation occurred at the room temperature and the implantation dosage was 10^{17} ion/cm². Two wide bands at about 275cm⁻¹ and 375 cm⁻¹ proximity are distinctly seen in the Raman spectrum. These bands are sharply shifted from α -GaAs and α -GaP characteristic spectra in Fig. 1. Thus the Raman spectra in Fig. 2 characterizes a new compound α -GaPAs, where the band at about 275 cm⁻¹ corresponds to Ga-As pair vibration; the band at about 375 cm⁻¹ shows Ga-P pair vibration. Using (1) we have

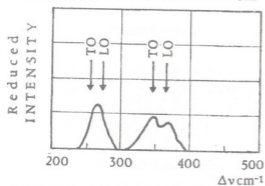


Fig. 3. Reduced Raman spectrum of α -GaAsP.

calculated the reduced spectrum of α -GaPAs from the mentioned spectrum which is shown in Fig. 3 and reflects the vibrational density of state of this compound. The RS show that even during the high temperature 400°C synthesis amorphous ternary compound α -GaPAs is obtained. However because of its characteristic spectral bands being slightly narrower and more intensive we can conclude that in this case radiation defects are probably smaller.

When implanting GaP with 70 keV energetic arsenic ion with 10^{17} ion/cm² dose, identification of ternary compound GaPAs had not been managed, neither ternary compound GaPN had been identified when implanting nitrogen ion in GaP with 10^{17} ion/cm² dose.

To synthesize ternary amorphous semiconductor GaAlAs we have implanted GaAs surface with (001) orientation by 100 keV energetic aluminium ions with the dose of 2.8×10^{16} ion/cm². Target's implantation done at 400°C temperature.

Figure 4 shows RS which reflects Al implantation of GaAs surface. Comparison this spectrum with standard GaAs Raman spectra (Fig. 1) shows clearly that after implantation at about 275cm⁻¹ frequency area wide spectral band is created, which characterizes Ga-As pair vibration in amorphous phase; created in 360cm⁻¹ frequency interval weak spectral band characterizes Al-As pair vibration in amorphous phase i. e. at GaAs surface after implantation ternary amorphous phase GaAlAs is synthesized. It is also seen from the discussed RS that at 284cm⁻¹ frequency a little sharp peak is created which is shifted from the L0 phonon of crystalline GaAs by 6cm⁻¹ and this peak corresponds to the crystalline

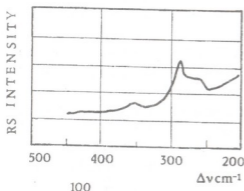


Fig. 4. Raman spectrum of α -GaAlAs synthesized by aluminium ion implantation of GaAs.

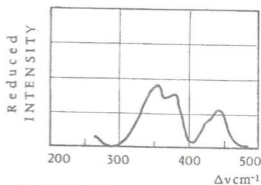


Fig. 5. Reduced Raman spectrum of α -GaAlP synthesized by aluminium ion implantation of GaP.

phase of GaAlAs. Thus during implantation under the above mentioned conditions amorphous ternary compound is originated which includes a small part of the crystalline phase.

To synthesize GaPAl in (001) and (111) oriented GaP we have introduced by ion implantation aluminium ions with doses 2.8×10^{16} ; 2.5×10^{17} ion/cm² with 100 and 110 keV energies respectively and 60 keV energy with 8.7×10^{16} ion/cm² dose. Implantation took place at 400°C.

In all the three cases at the GaP surface single phased ternary compound GaAlP is created in the amorphous state. This is proved by two wide spectral bands in RS: one in the 450cm⁻¹ region which corresponds to Al-P pair vibration and the second, which is in the 400-350cm⁻¹ region and reflects the Ga-P pair vibration. Using (1) we have calculated the reduced spectrum which is shown in Fig. 5. It gives a-GaAlP vibrational density of state.

Georgian Academy of Sciences

R. Agladze Institute of Electrochemistry and Inorganic Chemistry

REFERENCES

1. R. Shuker, R.V. Gammon. Phys. Rev. Lett. 25, 1970, 22.
2. J.E. Smith, Jr. M.H. Brodsky, et al. Phys. Rev. Lett. 26, 1971, 642.
3. M. Wihl, M. Cardona et al. Solids, 8-10, 1972, 172.
4. S.V. Gotoshia. Tezisy dokl. XIX vsesoiuz. sezda po spektroskopii. Tomsk, 1983, 145.



V. Jakeli, Z. Kachlishvili, E. Khizanishvili

Electrothermal Ionization Mechanism and Impurity Breakdown

Presented by Corr. Member of the Academy T. Sanadze, June 8, 1998

ABSTRACT. The existence of the electrothermal (ET) mechanism of ionization of neutral centers is shown. The corresponding ionization coefficient is calculated and the conditions under which this mechanism can be predominant in the process of ionization are established.

Key words: ionization, breakdown, electrothermal mechanism.

The investigation shows that the ET mechanism leads to the increase of free carriers in the prebreakdown condition and to the decrease of the breakdown electric field which results in better agreement with experiment.

As is well-known, the nonequilibrium charge carrier concentration is often determined by various combined ionization mechanisms such as photothermal, thermofield ionization [1-3].

The nonequilibrium concentration of hot charge carriers is determined mainly by impact ionization of neutral impurity atoms when the lifetime of hot charge carriers is controlled by the unlike centre trapping.

In [4] it was shown that under certain conditions inelastic scattering of hot electrons by neutral impurity atoms with the 2p level excitation can be the main channel in energy dissipation and makes a certain contribution to the breakdown process [5]. This fact perfectly explains the well-known experimental dependence of the breakdown electric field on the neutral impurity atom concentration [4], but so far its strong temperature dependence has not been explained. There is also no satisfactory explanation of the dependence of the electrical conductivity on the electric field strength under the prebreakdown condition.

In our work a new combined ionization mechanism of neutral impurity atoms is proposed, i.e. under inelastic scattering of hot electrons by neutral impurity atoms the atoms are excited and the electrons can travel from this excited state into the conductivity band due to phonon absorption. We call this mechanism electrothermal (ET). As far as is known, this ionization mechanism has not been previously considered. In the work the conditions are established under which this mechanism is essentially responsible for the process of neutral impurity ionization. The calculations are made in the electron temperature (T_e) approximation.

With allowance for the ET ionization mechanism breakdown electric fields and electrical conductivity in prebreakdown fields are calculated. A good agreement with experiment suggests that the ET ionization mechanism is actually realized and becomes more effective with the lattice temperature increase compared to the impact ionization mechanism.

It is known the Born method is unsatisfactory in a number of cases.

According to the calculations [6], if the hot electron energy is high or if the lattice temperature (T) is well above 100K (400 K) for Ge(Si), the cross section normalization is not important. Since we use lower temperatures, the normalized excitation and ionization cross sections should be used in A_{ET} and A_T calculations [6]. In [7] it is shown that the probability of thermal ionization of an excited state of the Coulomb impurity centre is independent of the way this electron has been trapped by this level and the corresponding probability is found. Taking all this into account, we obtain the following expressions for A_{ET} and A_I :

$$A_{ET} = \left(\frac{8\pi k T_e}{m} \right)^{1/2} \cdot C a_B^2 \left(\frac{R_y}{k T_B} \right) \left(\frac{T_2}{T_1} \right)^{3/2} \frac{Q(\alpha_0, \alpha_1)}{2l_0 + 1} \times$$

$$\times \left(1 + \frac{T_2}{T} \right) \exp\left(-\frac{T_2}{T} \right) \int_{T_B/T_e}^{\infty} \frac{\left(1 + \frac{T_B}{T_e x} \right)^{1/2} x \cdot \exp(-x) dx}{\frac{T_e}{T_B} x + \varphi - 1}, \quad (1)$$

$$A_I = \left(\frac{8\pi k T_e}{m} \right)^{1/2} C' a_B^2 \int_{T_1/T_e}^{\infty} \left(1 - \frac{T_1}{T_e \cdot x} \right)^{3/2} \frac{x \cdot \exp(-x) dx}{\frac{T_e}{T_1} x + \varphi' - 1}. \quad (2)$$

Here R_y is the Rydberg unity, T_1 is the ionization temperature of the ground impurity centre state, T_2 is the ionization temperature of the excited state, $T_B = T_1 - T_2$ is the excitation temperature, $Q(\alpha_0, \alpha_1)$ is the angular factor which depends on quantum numbers of angular moments of α_0 and α_1 states, l_0 is the orbital quantum number. The parameters C , C' , φ and φ' are given in [6].

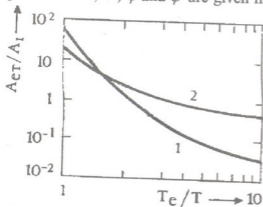


Fig. Dependence of A_{ET}/A_I on T_e/T for different T (for n -Ge). 1 - $T = 4.2$ K, 2 - $T = 10$ K.

In Figure the plots of A_{ET}/A_I ratio versus electron temperature T_e/T (for Ge) are given. Curve 1 is constructed at $T = 4.2$ K and curve 2 - at $T = 10$ K. The comparison of curves 1 and 2 shows that the higher is T , the wider the T_e region, where the ET mechanism is predominant compared to the impact one.

Considering the n -type semiconductor with shallow donor (N_D) and acceptor (N_A) impurities and analyzing the stationary solution of the recombination kinetic equation with allowance for the ET mechanism we obtain the impurity breakdown condition:

$$(A_I + A_{ET})(N_D - N_A) - A_T - B_T N_A = 0, \quad (3)$$

which coincides with the well-known breakdown condition at $A_{ET} = 0$. In this case the

impurity breakdown is still a stationary process. Here A_T is the thermal ionization coefficient.

From (3) it is clear that the allowance for ET ionization mechanism leads to the decrease in the breakdown electric field. The higher is T , the smaller E_{br} . This agrees well with experiment [8]. For example, for $T = 4,2$ K (10 K) E_{br} decreases by 1V/cm (7V/cm). Besides, the analysis of (3) suggests that the ET mechanism is responsible for the increase in the free carrier concentration in the prebreakdown state as well as for the decrease in T_e at which n is saturated. As a result, the discrepancy between the existing theory [4] and experiment [8] for j in the current-voltage characteristics in the prebreakdown condition is removed.

Tbilisi I. Javakhishvili State University

REFERENCES

1. L.V.Berman, T.I.Domashveva, A.G.Tukov. FTP, 7, 1973, 1882 (Russian).
2. V.Karpus, V.I.Perel. ZETF, pisma, 91, 1986, 2319 (Russian).
3. C.V.Kruchkov, G.A.Siroedov. FTP, 25, 1991, 655 (Russian).
4. Z.A.Kachlishvili. Phys. Stat. Sol. (b), 48, 1971, 65.
5. V.A.Sablukov, S.V.Poliakov, O.A.Riabushkin. FTP, 30, 1996, 1251 (Russian).
6. A.A.Veinstein, I.I.Sobelman, E.A.Jukov. Atoms Excitation and Spectral Lines Widening, M., 1979, 320 (Russian).
7. V.I.Abakumov, I.I.Iassievich. ZETF, Pisma. 71, 1976, 657 (Russian).
8. E.I.Zavaritskaia. Trudy FIAN, M., 37, 1966, 41 (Russian).

N.Margiani, T.Medoidze, J.Nakaidze, T.Nakaidze, G.Nakashidze, G.Tsintsadze

Fabrication and Investigation of the High-Temperature Superconducting Wires and Electromagnetic Solenoids

Presented by Member of the Academy R. Salukvadze, June 9, 1998

ABSTRACT. The technological principles of moulding of the high-temperature superconducting cylindrical non-hollow and tubular hollow as well as the planar band wires are described. Energetic and critical parameters of the obtained wires have been studied. The planar spirals and laboratory working models of the single-layer multiturn (having 12-15 turns) electromagnetic solenoids were fabricated on the basis of the obtained wires.

Key words: superconducting ceramics, superconducting wire, energy storage, critical parameters.

Since the discovery of high-temperature superconducting materials [1], the fabrication and investigation of superconducting elements, based on these materials and having certain geometrical shape and size, is one of the important problems. Among these elements the high-temperature superconducting wires are of considerable interest because the potential of their application appears very promising both in power transmission lines without losses ($R=0$) and in the various electromagnetic solenoids i. e. key elements of the high capacity ($W=10^8-10^{13}$ Joule) energy storages [2-6].

In this paper, we report on the technology of fabrication of the cylindrical and planar band wires, as well as the planar spirals and electromagnetic solenoids on the basis of Y-Ba-Cu-O-type high-temperature ceramics. The Y-Ba-Cu-O-type ceramic material was prepared from the mixture of Y_2O_3 , BaO and CuO by conventional solid state reaction [7,8]. In order to achieve and preserve a desired geometrical shape of the prepared material, the powder mixed with the liquid organic plasticizer and homogeneous suspension of the paste-like consistence was obtained.

Figure 1 shows a schematic view of the experimental set-up used to mould the superconducting wires.

Determined amount of paste-like mass, with certain consistence, was mounted in the high-precision packer mould 10. The high-precision packer 6 and punch 9 were put on the top of the mould. The upper

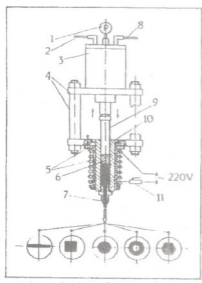


Fig. 1. Schematic view of the experimental set-up used to mould the superconducting wires. (1) manometer, (2) oil pipe for return of piston rod, (3) hydraulic press, (4) carcass, (5) heater, (6) high-precision packer, (7) tip, (8) oil pipe, (9) punch, (10) case.

end of the punch was adjoined to the piston of the hydraulic press. On the bottom of the tip 7 a bolt with the through section of desirable size and form, ensuring the geometrical form and size of the section of wire was mounted.

Electrical heater 5 heats the paste-like mass and simultaneously regulates its viscosity. When the mass is heated up to desired temperature, hydraulic press 3 should be switched on automatically. The lower end of the piston presses the punch 9 and the wire of desired section and size is extruded from the lower end of the tip.

The just moulded wire is elastic and therefore, could be easily wound before drying. The moulded wires were dried at room temperature, then put in the drying cabinet at 150-160°C for several hours. Dried wires together with the corundum ceramics were placed into the muffle furnace and annealed at 940°C in neutral and then in oxygen-rich atmosphere.

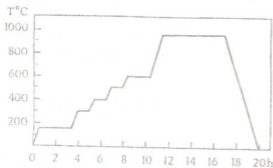


Fig. 2. Temperature regime of annealing of the wires.

Temperature regime of the annealing is presented graphically in Fig.2. Heating and subsequent cooling rates equaled 5°C·min⁻¹. In the 150-600°C temperature range the wires were annealed in neutral atmosphere (gaseous nitrogen) and in the 600-950°C range under oxygen-rich atmosphere.

By means of the above mentioned wires there were fabricated: superconducting planar spirals having 6-7 turns (Fig.3); cylindrical wires wound (12-15 turns) on the ceramic corundum coils (Fig.4) and laboratory working models of the electromagnetic solenoids (Fig. 5), with one layer of 15 turns.



Fig. 3. General view of the planar spiral. (1) superconducting wire, (2) ceramic support.

To determine the critical current density J_c , as well as the onset and the bulk of the superconducting transition, four contacts of metallic gold were thermally deposited onto the each sample.

Temperature dependences of resistances of the above mentioned three wires are shown in Fig. 6. It is seen, that all prepared samples exhibit the onset of the superconducting transition in the range of 93-94K, whereas the bulk of the transitions ($R=0$) for these samples was observed at different temperatures. For example, the bulk of the superconducting transition ($T_c = 92K$) is higher and transition width ($\Delta T_c = 1-2K$) is narrower for tubular samples than that for planar band ($T_c = 91K$ and $\Delta T_c = 3K$, respectively) and cylindrical non-hollow ones ($T_c = 90K$ and $\Delta T_c = 4K$, respectively).

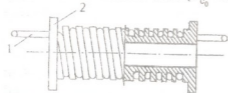


Fig.4. General view and sectional view of the solenoid. (1) superconducting wire, (2) ceramic coil (10 turns, winding pitch 3 mm).



Fig.5. Laboratory working model of the superconducting inductive solenoid.

It should be noted that due to the existence of inner and outer open surfaces the process of burning out of the plasticizer is more easily realized for the tubular samples. As it

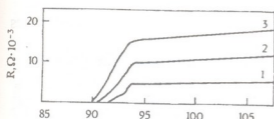


Fig. 6. Temperature dependences of resistances of the superconducting wires. (1) cylindrical tubular wire, (2) planar band wire, (3) non-hollow cylindrical wire.

field increases, a sharp decrease of critical current density is gradually decreased.

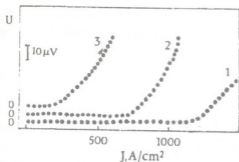


Fig. 7. Voltamperic characteristics of the superconducting wires at 77K. (1) cylindrical tubular wire, (2) planar band wire, (3) non-hollow cylindrical wire.

It was established, that the advantage of the tubular wires as compared with the band and cylindrical wires is in the fact that the tubular wires are characterized by the high value of critical current density ($J_c \geq 1000 \text{ A}\cdot\text{cm}^{-2}$) and narrow width of the superconducting transition ($\Delta T_c \sim 1+2\text{K}$).

Thus, the physico-technological processes of the fabrication of superconducting wires, planar spirals and electromagnetic solenoids are discussed and preliminary results of investigation of the energetic and critical parameters of three different superconducting wires are presented.

It has been shown that superconducting wires of Y-Ba-Cu-O system are characterized by the critical parameters: $T_c = 92\text{K}$, $\Delta T_c = 1+2\text{K}$, $J_c = 10^3 \text{ A}\cdot\text{cm}^{-2}$ ($H=0$). The wires with a maximum length of 6m have been obtained. On the basis of the superconducting wires the laboratory working models of electromagnetic solenoid coils have been fabricated.

Georgian Academy of Sciences
Institute of Cybernetics

should be expected, critical current density of the tubular samples $J_c = 10^3 \text{ A}\cdot\text{cm}^{-2}$ is essentially higher than that of band-like samples $J_c = 5 \cdot 10^2 \text{ A}\cdot\text{cm}^{-2}$ as well as cylindrical non-hollow samples $J_c = 10^2 \text{ A}\cdot\text{cm}^{-2}$ (Fig. 7). Voltamperic characteristics of the tubular samples at 77K for small magnetic fields having different values are shown in Fig. 8. It can be seen that as the value of magnetic

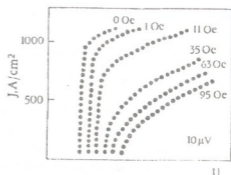


Fig. 8. Voltamperic characteristics of the cylindrical tubular wire for different values of magnetic field.

REFERENCES

1. J.G.Bednorz, K.A.Muller. *Z. Phys.* 1986, B64, 189.
2. Y.Yamada, N.Fukushima, S.Nakaiama et al. *Jap. J. Appl. Phys.* 26, 5, 1987, 865.
3. S.Jin, R.C.Sherwood, R.B.Dover et al. *Appl. Phys. Lett.* 51, 3, 203, 1987.
4. G.A.Whitlow, N.C.Jyer, A.T.Male et al. *IEE Trans. Magnet.* 25, 2, 1988, 2317.
5. J.T.Lue, J.H.King, H.H.Yen et al. *Modern Phys. Lett.* 2, 2, 1988, 589.
6. B.P.Mikhailov, A.R.Kadirbaev et al. *Sverkhprovodimost: fizika, khimia, tekhnika*, 3, 8, 1990 (Russian).
7. O.Fukunada, Y.Ishizawa, T.Tanaka. *J. Ceram. Soc. Jpn.* 95, 6, 1987, 663.
8. H.Bohr, C.S.Jacobsen, K.E.Nielsen et al. *J. Cryst. Growth.* 84, 2, 1987, 332.



M.Dzhibladze, Z.Melikishvili, V.Bykov, Corr. Member of the Academy T.Sanadze

The Interaction of Photon Clusters with Matter

Presented April 5, 1999

ABSTRACT. Analyzing the results obtained with high-power laser radiation, we revealed that the process of multiquantum absorption of atoms could be explained by interaction of photon cluster with matter. We expect that laser radiation consists of multiquantum spikes, the intensity of which is described by small numbers law. Experimental results are described in the supposition that multiphoton spikes can be simultaneously absorbed by atoms.

Key words: photon cluster, multiphoton spikes.

From the point of modern experiments with strong and superstrong fields of laser radiation [1] the problem of simultaneous interaction of number of photons with quantum system becomes rather actual. It turns out, that successfully used nonstationary perturbation theory does not allow to describe satisfactorily a number of new effects observed in the process of interaction of quantum object with high intensity laser radiation [2].

Of special interest is the effect of above-threshold ionization (ATI) of atoms in the field of high intensity laser radiation [3,4]. Under the conditions of the multiphoton ionization process, increasing the radiation intensity, a lot of additional peaks appear in the energy spectrum of electrons. This points that atom can absorb more light energy than it is enough for ionization [1]. Moreover, there are peaks which are observed at the distance of one quantum of light energy. That is, each following peak corresponds to the absorption of the additional quantum of energy. A surprising distribution of maxima in the energy spectrum of electrons is observed. It was found, that for high intensities of laser radiation the energy distribution of electrons looks like Maxwellian or Poisson distribution. This points to the possibility of such process when the absorption of more quanta is more favorable than less. This rigidly excludes the quantum-mechanical treatment of multiphoton process. Indeed, if for relatively low light intensities the perturbation theory can still be used for calculation of probabilities of finding electron in the Above-Threshold maximum, then for high intensities the perturbation theory is not valid.

It must be also noted that the series of experiments showed the appearance of the same distribution in the above-threshold peaks of the energy spectrum of electrons while performing photoelectric effect [5] and anomalistically high order harmonics when interacting of high intensity laser radiation with atom were observed [6].

The light consisting of many chaotic spikes of intensity represents the complicated interference picture. The amplitude of these spikes changes not only with spatial coordinate change but also in time (Fig.1). It will be expected, that different clots of multiquantum spikes of light consist of various number of quanta and simultaneously can be absorbed by atom according to spatial location.

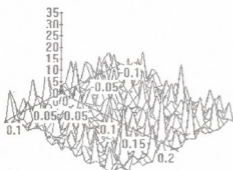


Fig. 1.

It is expected, that different spikes of field intensity represent the superposition of several photons in a random way with the same direction of electric field vector and while interacting with atom the energy of this superposition is absorbed simultaneously as whole. Thus, different spikes, which simultaneously can be absorbed by atom, may consist of various numbers of photons. Electric fields of these spikes are synchronized in a random way according to spatial location at the fixed moment of

time and their energy is defined by summarizing the energies of quanta.

We can also suppose that by increasing the laser radiation intensity the relative number of multiquantum spikes increase, which leads to the significant changes in their quantity distribution.

It is necessary to expect, that the amplitude of multiquantum spikes grows nonlinear with increasing the intensity of laser radiation. The spikes of intensity in a stochastic field of light can be presented as a photon cluster consisting of n quanta. Thus, laser field can be represented as clusters chaotically distributed in space and time with energies many times exceeding the energy of one quantum.

Special interest represents the case of the ultra high intensities of a laser radiation. In this case, in cluster representation, it is necessary to expect, that the number of high quantum clusters can be more, than with smaller energy. If the absorption of all photons happens simultaneously, the probability of n -quantum process will be determined by number of n -quantum clusters (spikes of intensity of a field) in a laser radiation.

It is obvious, that alongside with one-photon characteristics the multiphoton characteristics of a field should exist, which should dominate in the case of high intensities and more adequately describe both strong field of radiation and processes of interaction of such fields with matter. Therefore, studies of a radiation multiphoton character need another approach. With this purpose, first of all, we shall consider photon collective, in which the photons are similar to the particles of ideal gas. This example will further serve as a starting point for the analysis of multiphoton structure of light.

Let's consider stationary process of distribution of a monochromatic radiation in space. It means, that the spatial distribution of number of photons in space elements does not depend on time. Let's designate occupied volume by a radiation through V and number of photons in this volume through N . Let's select from a general system a small subsystem consisting from n of photons ($n \ll N$). The selection of subsystem is based on that circumstance, that for a relativistic particle the linear size of localization is determined by the de Broglie wavelength, which for the photon corresponds to the wavelength of radiation λ . Therefore minimum volume of subsystem can be defined as λ^3 . As our system is homogeneous, the probability of detection of any photon in a chosen subsystem is equal λ^3/V . The probability of simultaneous detection of n photons in the same subsystem is equal accordingly $(\lambda^3/V)^n$.

For our consideration $\lambda^3 \ll V, n \ll N$ the probability of detection of n photons in λ^3 volume equals:

$$P_n = \frac{\langle n \rangle^n}{n!} e^{-\langle n \rangle}.$$

Thus, ideal gas of photons enables to introduce classical representation of a photon cluster. In the quantum picture, the represented photon cluster can be treated as Bose condensate with de Broglie wavelength given by λ/n , where λ is the wavelength of constituent photons [7].

While considering the process of interaction of high power laser pulse with atom within the frameworks of the given model, we should receive energy spectrum of photoelectrons. The character of this spectrum will be defined by statistics of the Poisson and also by the potential of ionization of atom as for the invariance of parameters of laser pulse for different atoms we shall have different number of photons in interaction.

Now we shall consider concrete examples. Let's allow, that the probabilities of ionization of atom while absorbing n_0 - and $(n_0 + s)$ of photon clusters (n_0 - minimum number of photons necessary for ionization) are equal. Then in each elementary volume λ^3 the energy spectrum of ejected photoelectrons must be described according to the Poisson distribution, that leads to the generalization of the Einstein formula for the photoelectric effect

$$E_{kin} = (n_0 + s)h\omega - E_b.$$

In this expression s is the number of the above threshold photons; E_b -energy of ionization of atom. In the considered case the energy spectrum of photoelectrons will carry a discrete equidistant character with energy distance $h\omega$ and Poisson distribution of amplitudes. It is necessary to mention once again that the character of envelope of energy spectrum highly depends on the energy of ionization of atom E_b and average number of photons $\langle n \rangle$ in λ^3 volume (Fig.2). Such dependence of number of electrons on energy experimentally was observed in [3,4]. In Fig.2 the experimental outcomes obtained in [4] are also indicated. It is visible, that the possible situations are not reached with only those being indicated in the Figures.

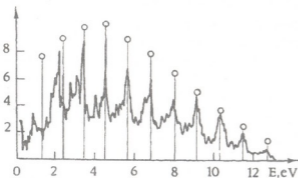


Fig.2

Thus, it is necessary to expect, that in strong light field of a laser radiation, due to superposition of many photons, chaotically distributed in space and in time optical clusters (spikes of intensity of a light field) appear, containing a multiple quantum, which can be simultaneously absorbed by atom in each elementary act of interaction of a radiation with matter. The distribution function of number of optical clusters according to their energies has a maximum, which displaces to high intensity spikes while increasing laser radiation power.

The represented mechanism of radiation interaction with atom should be valid in case of lower intensities of light field. Therefore, in the case of two- or three-photon processes it is necessary to expect nonlinear interaction caused by cluster character of a field. In this

connection it is necessary to conduct experimental researches of multiphoton absorption in various materials. It is necessary to expect, that having new submission about interaction of radiation with atom it is possible to explain nonlinear growth of probability of multi-quantum processes when increasing the intensity of a laser field.

The work is carried out under financial support of International Scientific and Technical Center (ISTC).

Tbilisi I. Javakishvili State University

REFERENCES

1. N.B. Delone, V.P. Krainov. Multiphoton Processes in Atoms. Springer-Verlag, 1994, 318.
2. M.V. Fedorov. Electron in Strong Light Field. Moscow, 1991, 224 (Russian).
3. P. Agostini, F. Fabre, G. Mainfray et al. Phys. Rev. Lett. **42**, 1979, 1127.
4. G. Petite, P. Agostini, F. Yergeau. J. Opt. Soc. Am. B. **4**, 1987, 765.
5. Gy. Farkas, Cs. Toth. Above Threshold Multiphoton Photoelectric Effect of Metal Surfaces. Scientific Report, Budapest, 1990, N1783/9.
6. X.F. Li, A.L. Huillier, M. Ferray, L.A. Lompre, G. Mainfray et al. Phys. Rev. Lett. **42**, 1979, 1127.
7. J. Jacobson, G. Bjork, I. Chuang, Y. Yamamoto. Phys. Rev. Lett. **74**, 1995, 4835.

M. Elizbarashvili, N. Kekelidze, M. Metskhvarishvili, Y. Metskhvarishvili

Investigation of the Internal Conversion Electrons spectrum for the ^{154}Gd 123.07 keV γ -Transition

Presented by Member of the Academy N. Amaglobeli, July 27, 1999

ABSTRACT. The conversion spectrum for the ^{154}Gd 123,07 keV γ -transition was investigated. It was found out that K, L_I, L_{II}, L_{III} conversion lines have various half-width for this transition. On the basis of comparison of the experimental and theoretical internal conversion coefficients it was established that experiment is in good agreement with theory on the L_{II} and L_{III} subshell. The differences on the L_I subshell are observed.

Key words: β - spectrometer, radioactive source, conversion spectrum, subshell.

Investigation of the internal conversion electron spectrum for γ -transitions of the radioactive nuclei allows not only to establish multipole of γ -transition exactly, but to determine the amount of mixture in case of mixed γ -transition. If the γ -transition is without mixture, as for example in case of $2^+ \rightarrow 0^+$, then it is of scientific interest to determine the relative and absolute internal conversion coefficients for this γ -transition on the L_I, L_{II}, L_{III} -subshells and to compare them with corresponding theoretical tables for their verification [1,2], as well as the study of K, L_I, L_{II}, L_{III} - conversion lines form. Such investigations are desired, but it's impossible for every γ -transition of radioactive nuclei, because it is necessary to fulfill a number of conditions. The spectrometer must have high resolution and it must not exceed several one hundredth percent. Thickness of radioactive source must not influence on the widths of the conversion lines; studied γ -transition must be intensive, its conversion coefficient must be higher. For such investigation ^{154}Gd 123.07 keV γ -transition, which takes place between first excited state and ground state with quantum characteristic $2^+ \rightarrow 0^+$ was chosen [3].

Investigation of the internal conversion electron spectrum for the ^{154}Gd 123.07 keV energy γ -transition was measured by magnetic prism β -spectrometer with (0.02-0.04) % resolution [4-6].

Radioactive source of $10 \times 1 \text{ mm}^2$ sizes was obtained by electrolytical method. Electrolyze was carried out in the ethyl alcohol on the europium chlorid solution, including the radioactive ^{152}Eu and ^{154}Eu isotopes. Radioactive sources of various thickness were made. From them were chosen such thickness sources, which didn't influence on the resolution of the spectrometer in the limited area of energy.

Figure 1 shows conversion spectrum of the ^{154}Gd 123.07 keV energy γ -transition measured on the spectrometer with 0.04% resolution. As it is shown in the Fig. 1, the L_{II} -line of the ^{154}Gd is close to the L_{III} -line of the ^{152}Sm for 121.78 keV energy γ -transition and this line is more intensive than ^{154}Gd L_{II} -line. In order to separate these conversion

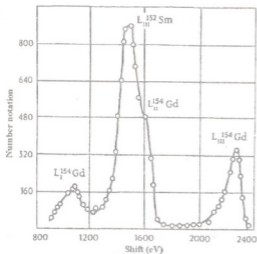


Fig. 1.

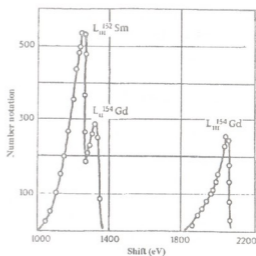


Fig. 2.

lines, this region of spectrum was taken off on the spectrometer with 0.02 % resolution. The results of measurements are given in Fig. 2. As it is seen in the Figure the above mentioned lines were not completely separated by the spectrometer. Their final separation was carried out graphically. Investigation of the K, L₁, L₁₁, L₁₁₁ conversion lines for the ¹⁵⁴Gd 123.07 keV energy γ -transition has shown that these lines have not the same half-width. When the spectrometer resolution is 0.04% L₁ conversion line has the minimal half-width with 80 eV. The half-widths of the other conversion lines increase in the following succession: L₁₁₁, L₁₁, K are 105, 110 and 132 eV respectively.

The L₁-conversion line has 40 eV half-width when the resolution of the spectrometer is 0.02% and half-width of L₁₁₁, L₁₁, K conversion lines are 65, 70, 92 eV respectively. As it is demonstrated in Table 1 when the resolution of the spectrometer are 0.04% and 0.02%, the half-width of the L₁-line in percent in both cases are close to the theoretical resolution of the spectrometer. From this follows that for establishing of the enlargement of the L₁-conversion line it is necessary to investigate the half-width of this conversion line by the spectrometer with the resolution higher than 0.02%. K, L₁₁, L₁₁₁ conversion lines enlargement may be explained by the influence of the K-shell and L₁₁, L₁₁₁ subshells natural widths of ¹⁵⁴Gd atom on the respective conversion lines half-widths.

Table 1

Half-widths of K-, L₁-, L₁₁-, L₁₁₁- conversion lines for the ¹⁵⁴Gd 123.07 keV γ -transition

Nucleus	E _{γ} , keV	Half-widths of conversion Lines	Conversion lines			
			K	L ₁	L ₁₁	L ₁₁₁
¹⁵⁴ Gd	123.07	%	0.095	0.039	0.053	0.051
		eV	132	80	110	105
		%	0.066	0.020	0.034	0.032
		eV	92	40	70	65

The relations of theoretical and experimental significance for internal conversion coefficients of the K-, L-, L₁-, L₁₁-, L₁₁₁- shells and subshells of ¹⁵⁴Gd 123.07 keV energy γ -transition are given in Table 2. The theoretical significance is calculated on the basis of

[1,2]. As it is shown in the Table the relations of the experimental significance of the conversion coefficients on the L_{111} and L_{11} subshells coincide well with analogical theoretical relations within the experimental and theoretical calculation errors but experimental relations on the L_{111} and L_1 subshells considerably differ from the theoretical relations.

Table 2
Experimental and theoretical ratios of the internal conversion coefficients on L_1 , L_{11} , L_{111} subshells for ^{154}Gd 123.07 keV γ -transition

Nucleus E_γ , keV	* ICC ratio	Experiment	Theory [1]			Theory [2]	Multipole
			E1	E2	E3	E2	
^{154}Gd 123.07	α_K / α_L	1.51 ± 0.03	—	1.65	—	1.70	E2
	$\alpha_{L_{111}} / \alpha_{L_{11}}$	2.46 ± 0.06	0.24	2.75	1.67	2.82	
	$\alpha_{L_{111}} / \alpha_{L_{11}}$	0.92 ± 0.03	1.21	0.96	1.31	0.98	

*-Internal conversion coefficient

On the basis of the relations of the conversion coefficients for the ^{154}Gd 123.07 keV energy γ -transition on the K- and L-shells and L_1 -, L_{11} -, L_{111} -subshells given experimentally the absolute significance of conversion coefficients on the L_1 -, L_{11} -, L_{111} - subshells was determined by us. Analogical theoretical significance was calculated from [1,2]. The results are given in Table 3.

Table 3
Experimental and theoretical significance of internal conversion coefficients of L_1 -, L_{11} -, L_{111} - subshells for ^{154}Gd 123.07 keV γ - transition.

Nucleus E_γ keV	Absolute signific. of ICC	Experiment	Theory [1]			Theory [2]	Multipolarity
			E1	E2	E3	E2	
^{154}Gd 123.07	α_{L_1}	0.071 ± 0.002	$1.52 \cdot 10^{-2}$	0.063	0.262	0.062	E2
	$\alpha_{L_{11}}$	0.190 ± 0.006	$2.76 \cdot 10^{-3}$	0.181	4.20	0.182	
	$\alpha_{L_{111}}$	0.181 ± 0.006	$3.22 \cdot 10^{-3}$	0.173	4.61	0.176	

As it is shown in this Table significance of experimental conversion coefficients on L_{11} and L_{111} -shells is in good agreement with the analogous theoretical significances. The difference of the experimental and theoretical absolute significance of the conversion coefficients on the L_1 -subshell rather exceeds the area of experimental and theoretical calculation errors.

Tbilisi I. Javakhishvili State University

REFERENCES

1. *I.M.Band, M.B.Trzaskovskaia*. Tablitsy koefisientov vnutrennei conversii gamma-luchej na K-, L-, M-obolochkakh $10 \leq Z \leq 104$ L, IIAF AN SSSR, 1978.
2. *P.S.Hager, E.Seltzer*. Nucl. Data. A. 1968. 4, 1.
3. *C.M.Lederer, V.S.Shirley*. Table of Isotopes. 7th ed., 1978.
4. *J.R.Metskhvarishvili, M.R.Metskhvarishvili*. Tesisy dokladov 45 mezhdunarod. Soveshanii po iadernoi spectroscop. i struct. atomnogo iadra, S-PT 1995, 72.
5. *N.Kekelidze, M.Metskhvarishvili et al.* Tesisy dokladov 45 mezhdunarod. Soveshanii po iadernoi spectroscop. i struct. atomnogo iadra, S-PT 1996, 34.
6. *V.M.Kelman, V.A.Romanov et al.* Nucl. Phys. 2, 1956/1957, 395-407.

J.Mebonia, M.Abusaini, P.Saralidze, K.Sulakadze, G.Skhirtladze

Mechanism of Nucleon-Deuteron Elastic Scattering

Presented by Corr. Member of the Academy A. Khelashvili, December 30, 1998

ABSTRACT. Nucleon-deuteron elastic scattering is investigated using unitary method, taking into account only single scattering. The comparatively simple offered approach gives the ability to explain wide range of experimental data, which make possible to use it for more complex nuclear processes.

Key words: impulse approximation, unitarity, three-body problem, cut-off, off-shell-energy.

Three-body processes in the field of nonrelativistic scattering are important for obtaining valuable information on the basic nuclear problems. Here basic principle difficulties associated with many-particle problems arise. We mean both writing the correct equations and solving them. The discovery of Faddeev integral equations [1] contributed not only to high progress of three-body theory, but also gave the possibility to find more consecutive approach to complex processes. However the application of Faddeev equations for three-body problem is connected with some technical difficulties. Therefore, various approximate variants are used. The unitary schemes of investigation were suggested [2-4]. However they did not find wide application because of the calculating difficulties. The method of summation of the cut-off iterated series of Vatson-Faddeev [5] also turned out to be uneffective.

The two quite different unitary approaches for three-body processes were suggested by one of the authors (Mebonia): three-body impulse approximation with cut-off (TIAC) [6] and three-body unitary impulse approximation (TUIA) [7]. Starting point of both approaches is consecutive account of the mechanism of single scattering. Realization of such purpose has been performed in different ways. In TUIA the method of unitarity of the amplitude on the basis of the approximated solutions of Faddeev equation in K-matrix formalism has been found.

It should be noted, that while performing the rigid conditions of eikonal approximation and congelment of the particles of the nucleus-target, differential cross section of elastic scattering, which has been calculated by TUIA, coincides with the known formula of Glauber-Sitenko [8,9].

In TIAC it is proved, that in specific cases in order to solve Faddeev equations in T-matrix formalism one can be restricted by the members of the first order. However, these solutions will correspond to real single scattering only in the case, if the incident particle (e.g. 1) simultaneously does not "brush against" both particles of bond state (e.g. 2,3). This can be achieved using the cut-off of Fourier-transform of radial function of bond state $\phi(r): G(q) \rightarrow G(q, R)$, where

$$G(q, R) = \sqrt{2/\pi} \int_R^{\infty} r^2 dr \varphi(r) \frac{\sin(qr)}{qr}. \quad (1)$$

The cut-off radius R must be not less than Debroill wavelength λ of the relative motion of the particle 1 and (2,3), it is easily connected with the quantity of the corresponding impulse $\vec{\omega}$ (Fig.1):

$$R = \frac{C}{|\vec{\omega}|}, \quad (2)$$

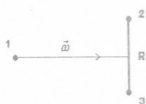


Fig.1.

where C is the constant, defining the performance of inequality $\lambda \leq R$. Then the amplitude of the three-body scattering by TIAC is written as follows:

$$M_{fi} = \hat{A} \langle \Phi_f | \sum_{j=2,3} t_j | \Phi_i \rangle, \quad (3)$$

where t_j is the two-particle matrix of scattering of l and n particles ($jl n = 123, 231, 312$), Φ_p, Φ_f - asymptotic functions in initial and final states, \hat{A} - operator of antisymmetrization on identical particles.

Natural question arises. How does the cut-off (1) lead to the unitarity of the amplitude of single scattering? It was shown by Nakamura [10], that if the amplitude of the three-body scattering is expanded by partial two-particle amplitudes, then the three-body unitarity would be broken by the amplitudes, which correspond to low orbital moments. Therefore, it has been suggested to carry out the cut-off in orbital space by introducing specific parameters of cut-off. However, if we adopt quantitative semiclassical judgement, then the orbital moment might be connected with impulse and radius-vector $L \sim Rk$. Therefore, the cut-off in orbital space for fixed energy must be equivalent to cut-off in x -space. Hence, TIAC may be considered as the intuitive alternative of more grounded theoretically TUIA. Nevertheless, it was found to be quite effective for various three-body processes [11-13]. Later the practical equivalence of two approaches for nucleon-deuteron scattering was proved [14].

The purpose of the present paper is to show the ability of TIAC in the case of investigation of elastic scattering of nucleons on deuteron $d(N,N)d$.

Elastic scattering $d(N,N)d$. With the discovery of Faddeev equations Nd elastic scattering came to be studied first of all [15-17]. The problem can be solved in closed form for any realistic nucleon-nucleon potentials. These potentials, allowing to obtain the same results for physical two-nucleon amplitudes, in general can be brought to various off-shell amplitudes. Therefore, the solution of Faddeev equations with high accuracy for various energies, requiring to involve various partial off-shell amplitudes, and comparing theoretical and experimental results may show additional advantage of individual NN potentials. In this respect, besides differential cross section the so-called polarizing asymmetry (analyzing power) gives useful information.

There is another possibility, connected with the investigation of Nd scattering. Here we can thoroughly examine various approximate methods of three-body solutions with

further generalization for more complicated processes. This induced us to use TIAC, the simplest of unitary schemes, for investigation of Nd elastic scattering.

According to formula (3) the differential cross section of Nd elastic scattering in mass center system is defined as follows:

$$\frac{d\sigma}{d\Omega} = (2\pi)^4 \frac{2m^2}{27} \sum_{spins} |M|^2, \quad (4)$$

$$M = \hat{A} \sum_{j=2,3} \int d\vec{q} \Psi_d^*(\vec{p}) t_j(\vec{\xi}, \vec{\eta}; \varepsilon) \Psi_d(\vec{p}_0), \quad (5)$$

$$\begin{aligned} \vec{p} &= -\frac{\vec{k}}{2} - \vec{q}, \quad \vec{p}_0 = -\frac{\vec{k}_0}{2} - \vec{q}, \\ \vec{\xi} &= \vec{k} + \frac{\vec{q}}{2}, \quad \vec{\eta} = \vec{k}_0 - \frac{\vec{q}}{2}, \\ \varepsilon &= \frac{3}{4m} (\vec{k}^2 - \vec{q}^2) - Q, \end{aligned} \quad (6)$$

where Ψ_d is overall wave function of deuteron; m – mass of nucleon; Q – binding energy of deuteron; $\vec{k}_o(\vec{k})$ – impulse of incident nucleon before (after) scattering. The summation clear in (4) occurs by spin projections of nucleon and deuteron before and after scattering; in explicit form they, appear after partial expansion of Ψ_d and t_j also as $G(p_0)$ and $G(p_0, R)$.

We use unit system, where $\hbar = c = 1$. In the detailed calculations the two-body off-shell T-matrix and the radial part of deuteron wave function have been constructed using inlocal and separable potentials Mongan [18].

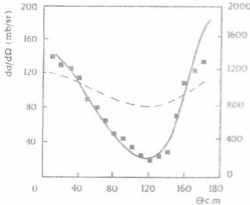


Fig. 2. Dependence of differential cross section of elastic scattering $d(N,N)d$ of scattering angle $\theta_{c.m}$ in system of centre mass at energy of incident neutrons $E_n=12$ meV in lab. system; where the solid curve and left scale correspond to calculation with cut-off, dashed curve and right scale-analogous to calculation without cut-off. Experimental data (left scale) were taken from [19].

In Figs. 2-4 are shown the results of our calculations: dependence of differential cross section of Nd elastic scattering on scattering angle $\theta_{c.m}$ with corresponding experimental data for three various energies in lab. system: 12, 16.5, and 22.7 meV. The solid curve and left scale correspond to calculation by TIAC, the dashed curve and right scale analogous to calculation without cut-off. Experimental data (left scale) were taken from [19,20]. In our calculation we have taken into account various two-nucleonic states: $^1S_0, ^1P_1, ^1D_2, ^3S_1 + ^3D_1, ^3P_0, ^3P_1, ^3P_2 + ^3F_2, ^3D_2$. However, as far as we examine relatively low energies, in final results the main contribution was carried by S-phases.

It is easy to note, that the impulse approximation without cut-off, which is usually identi-

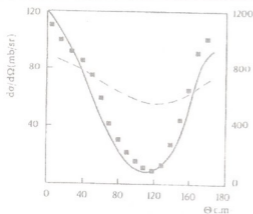


Fig. 3. The same as Fig. 2, but for energy $E_n = 16.5$ meV. Experimental data were taken from [19].

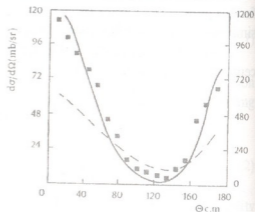


Fig. 4. The same as Fig. 2, but for energy $E_n = 22.7$ meV. Experimental data were taken from [20].

fied by the mechanism of the single scattering, is quite different from the experiment both by form and magnitude of differential cross section.

Even such simple method of unitarity of amplitude, which represents the cut-off of wave function of bond state, significantly improves the agreement of the theory and experiment. However, the quantitative discrepancy still remains. But these discrepancies are expected, since we are examining an approximate method to solve the problem. It should be noted, that the precise Faddeev calculations give good description of *Nd* elastic scattering.

The analysis of the obtained results indicates not only the ability of TIAC to be used for three-body problem, but also the generalization to be used for more complex nuclear processes.

Tbilisi I. Javakhishvili State University

REFERENCES

1. L.D.Faddeev. JEF, 39, 1960, 1459.
2. R.T.Cahill. Nucl.phys. A194, 1972, 599.
3. K.L.Kowalski. Phys. Rev. D5, 1972, 395.
4. T.Sasakawa. Nucl.phys. A203, 1973, 496.
5. J.M.Wallac. Phys. Rev. c7, 1973, 10.
6. J.V.Mebonia. Phys.Lett, B 48, 1974, 196.
7. T.J.Kvaratskhelia, J.V.Mebonia. Phys.Lett., B 90, 1980, 17.
8. R.J.Glauber. Lect. theor. phys. 1, 1959, 315.
9. A.G.Sitenko. UFI, 4, 1959, 152.
10. H.Nakamura. Nucl.phys. A208, 1973, 207.
11. T.J.Kvaratskhelia, J.V.Mebonia. J. Nucl.phys., 10, 1984, 1677.
12. O.L.Bartata, J.V.Mebonia. Phys. Atomic nucl. 33, 1981, 1987.
13. V.SH.Djinia, T.Kvaratskhelia, J.Mebonia. Nucl.phys., 58, 1995, 30.
14. T.J.Kvaratskhelia, J.V.Mebonia. Report, AS, GSSR, 136, 1989, 53.
15. M.Sawada et.al. Phys. Rev., C 27, 1983, 1932.
16. P.Doleschall. Nucl. Phys., A 220, 1974, 491.
17. W.Kluge, R.Schlufier, W.Ebenhoh. Nucl.Phys. A 228, 1974, 29.
18. Th.Mongan. Phys. Rev., 178, 1968, 1957.
19. G.Rauprich et al. Few- Body System, 5, 1988, 67.
20. H.Witala, W.Glockle. Nucl.phys., A528, 1991, 48.



Z. Kereselidze, I. Gabisonia

On the Specificity of a Large Scale Electric Field Modelling on the Boundary of the Dayside of the Earth's Magnetosphere

Presented by Corr. Member of the Academy T. Chelidze, July 27, 1998

ABSTRACT. Dayside of the magnetosphere is represented as a sphere whose centre coincides with the Earth. In the spherical system of coordinates we estimated the difference of electric potentials in any equatorial or meridian sections of the magnetosphere. The obtained values are in good agreement with the energy spectrum of the solar wind particles near the boundary of magnetosphere.

Key words: magnetosphere, large scale electric field, kinematics, MHD flow, electric potential, energy spectrum.

As a rule, in modelling of a large scale plasmatic flow near the magnetosphere, there arise difficulties connected with mathematical solvability of the system of MHD equations. To avoid these difficulties a technique of splitting of the general problem into two parts is used, when the parameters of flow in the transitional area are determined in the gas-dynamic approximation, and then according to the known hydrodynamic picture the equation of induction of magnetic field is solved. Following such operation it is relatively easy to assess the intensity of the electro-magnetic parameters of flow of the magnetosphere boundary.

The first gas-dynamic model of flow around the magnetosphere was suggested by Spreiter and Alksne [1], who obtained the characteristic values of the main parameters of flow and magnetic field in the transitional area using the numerical method. Despite this solution, as well as others that followed it, was not selfconsistent, it appeared very useful, as it proves the validity of applying the gas-dynamic approximation to the problem under consideration. Moreover, it became obvious that it is reasonable to limit oneself to the kinematic approximation, i.e. to consider the flow as given from some analytical model, more or less consistent with the numerical gas-dynamic model. In numerous works of this kind the boundary layer of the magnetosphere was not considered at all and the structure of the magnetic field near the boundary of the magnetosphere was determined by the equation of freezing-in of the interplanetary magnetic field.

It may be assumed that the application of kinematic approximation to the problem of flow around the magnetosphere would be more justified if the authors accounted, at least qualitatively, for the peculiarities of MHD flow around the magnetosphere, which were brought to light during topological consideration of the given problem [2-4].

The mentioned shortcoming may be improved to a marked degree if the model kinematic problem of the flow around the ideal magnetized body is approached correctly and as fully as possible to account for the specificity of flow around the magnetosphere. For

this purpose the model of the stagnant zone in the transitional area (magnetosheath) of the magnetosphere may turn to be quite useful [5].

Let us represent the day-side of the magnetosphere as a sphere whose centre coincides with the Earth. In the spherical system of coordinates Z, θ, φ force lines of the Earth magnetic field are directed along θ (Fig.1). We shall consider the case when the solar wind velocity and the tension of the IMF freezing-in it are parallel

$$\vec{V}_0 = \beta \vec{h}_0, \quad (1)$$

where V_0 is the velocity of solar wind, h_0 is the tension of IMF, β the proportionality factor.

From the theory of flow around the sphere by real liquid it is known that in the hydrodynamic approximation the picture of flow around is symmetrical, owing to which the velocity of flow near the sphere depends only on the radial coordinate and the central angle [6].

Directly on the sphere surface the value of the liquid velocity is determined by the arc ψ (Fig. 1):

$$V_{\perp} = V_0 \cos \psi, \quad V_{\parallel} = V_0 \cdot \sin \psi, \quad (2)$$

where V_{\perp} is the radial to the spherical surface of the velocity component, V_{\parallel} collinear to the surface, which according to the aim of our problem should be connected with the components V_{θ} and V_{φ} .

In order to relate the central angle Ψ with the spherical coordinates let us consider the spherical triangle ΔOMN , from which according to the theory of cosines $\cos \psi = \cos \varphi \cos \theta$ [7]. Thus (2) can be represented as follows:

$$V_{\perp} = V_0 \cos \varphi \cos \theta, \quad V_{\parallel} = V_0 (1 - \cos^2 \varphi \cos^2 \theta)^{\frac{1}{2}}. \quad (3)$$

As for the components V_{θ} and V_{φ} , in order to determine them we shall introduce $\angle \alpha$ between V_{\parallel} and the spherical meridian

$$V_{\theta} = V_{\parallel} \cos \alpha, \quad V_{\varphi} = V_{\parallel} \sin \alpha. \quad (4)$$

If we use the expression (4) and return to the spherical triangle ΔOMN , from which $\cos \alpha = \operatorname{tg} \theta \operatorname{ctg} \varphi$, after simple transformation we shall get

$$V_{\theta} = V_0 \sin \theta \cdot \cos \varphi, \quad V_{\varphi} = V_0 \sin \varphi. \quad (5)$$

In order to have clear idea of the structure of the larger scale electric field near the boundary of the magnetosphere it is necessary to assess the efficiency of the IMF component perpendicular to the boundary of the magnetosphere. The simplest assumption is that on the surface of the magnetosphere $h_{\theta} = h_{\varphi} = 0$, while h_{\perp} , as well as V_{\perp} , is determined by the angles θ and φ

$$h_{\perp} = h_0 \cos \varphi \cdot \cos \theta \quad (6)$$

As we are restricted by the approximation of the ideal electric conductivity of the solar wind the thickness of the magnetic boundary layer of the Earth must be considered as equal to zero. According to the model of the stagnant zone in the magnetosheath, for the maintenance of the magnetospheric processes on the stationary level, the surface of the magnetosphere should be penetrable for plasma. Proceeding from the energetic considerations the coefficient of porosity of the magnetosphere boundary $a = 0.01$. This means that the velocity of the penetrability is approximately two orders of magnitude lower than the velocity of plasma on the surface and is directed into the magnetosphere [5].

To determine the structure of the large-scale electric field on the surface of the magnetosphere let us use the condition of freezing-in

$$\vec{E} = -\frac{1}{c}[\vec{V}\vec{H}], \quad (7)$$

where C is light velocity.

As it may be assumed in the spherical system of coordinate, there exists only θ component of the magnetic field of the Earth. With the assumption of the single component character of IMF and introduction of the electric potential

$$\vec{E} = -\frac{\partial \phi}{\partial z} \vec{i}_r + \frac{1}{r} \frac{\partial \phi}{\partial \theta} \vec{i}_{\theta} - \frac{1}{r \cos \theta} \frac{\partial \phi}{\partial \varphi} \vec{i}_{\varphi} \quad (8)$$

for the surface difference of potentials in the meridional and equatorial sections of the magnetosphere we shall have

$$\begin{aligned} \Delta \phi_{\theta} &= -\frac{1}{c} \int_{\theta_1}^{\theta_2} V_{\varphi} h_r R_0 d\theta, \\ \Delta \phi_{\varphi} &= \frac{1}{c} \int_{\varphi_1}^{\varphi_2} (V_r H_{\theta} - V_{\theta} h_r) R_0 \cos \theta d\varphi, \end{aligned} \quad (9)$$

where R_0 is the distance between the Earth's centre and the front point of the magnetosphere. If we take into consideration (5) and (6), and also the penetrability surface, for the constant plasma velocity and characteristic value of IMF we shall obtain the following expressions:

$$\begin{aligned} \Delta \phi_{\theta} &= \frac{1}{c} V_0 h_0 R_0 \sin \varphi \cos \varphi (\sin \theta_1 - \sin \theta_2), \\ \Delta \phi_{\varphi} &= \frac{1}{c} a V_0 H_{\theta} R_E \cos^2 \theta (\sin \varphi_2 - \sin \varphi_1) - \\ &\quad - \frac{1}{c} V_0 h_0 R_0 \sin \theta \cos^2 \theta \left[\frac{\varphi_2 - \varphi_1}{2} + \frac{1}{4} (\sin 2\varphi_2 - \sin 2\varphi_1) \right]. \end{aligned} \quad (10)$$

As for $\Delta\phi_2$, according to our model, the thickness of the magnetopause is equal to zero, it makes sense to determine only the intensity E_z .

Thus, with the help of (10) we can rather easily assess the difference of electric potentials in any equatorial or meridional sections of the magnetosphere.

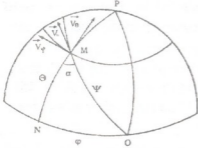


Fig.

It should be noted that for $\Delta\phi_\theta$ the maximal value is attained at $\varphi = \pm \frac{\pi}{4}$, and for $\Delta\phi_\varphi$ at $\theta \approx \pm \frac{\pi}{6}$. As for the central meridian, it is equipotential, like boundary meridians ($\varphi = \pm \frac{\pi}{2}$), which corresponds to the morning-evening section of the magnetosphere.

For the numerical assessment we shall use the following values of the solar wind parameters IMF and the Earth's magnetic field, which are characteristic of the quiet magnetosphere conditions

$$V_0 = 3,6 \cdot 10^7 \text{ cm} \cdot \text{s}^{-1}, \quad H_\theta = 3 \cdot 10^{-4} \text{ G},$$

$$h_0 = -3 \cdot 10^{-5} \text{ G}, \quad R_0 \approx 11R_E = 7 \cdot 10^9 \text{ cm}, \quad a = 0,01.$$

As a result, between any point of the magnetosphere and the peripheral area on the central parallel $\varphi(0, \frac{\pi}{2})$ we shall have $\Delta\phi_\theta^e = 25 \text{ CGSE kV}$, and for the parallel and

meridian which correspond to $\varphi = \pm \frac{\pi}{4}$ and $\theta = \pm \frac{\pi}{6}$,

$$\Delta\phi_\varphi^{\max} \approx 125 \text{ CGSE} = 37,5 \text{ kV}, \quad \Delta\phi_\theta^{\max} \approx 84,5 \text{ CGSE} = 25,4 \text{ kV}.$$

We should note that for the present set of the magnetosphere parameters and the solar wind the maximal value of tension of the normal component of the electric field $E_r^{\max} \approx$

$\approx 10^{-3} \text{ mV} \cdot \text{m}^{-1}$, to which corresponds $\varphi = \pm \frac{\pi}{2}$. The values of $\Delta\phi_\theta$, $\Delta\phi_\varphi$, E_r , that we have

obtained are in good agreement with the energy spectrum of the solar wind particles near the boundary of the dayside of magnetosphere [8].

Georgian Academy of Sciences
 M.Nodia Institute of Geophysics

REFERENCES

1. J.H.Spreiter, A.L.Summers, L.Y.Alsksne. Planet. Space Sci., 14, 1966, 223.
2. V.G. Pivovarov. In: Matematicheskie modeli blizhnego kosmosa. Novosibirsk., 1977, 288 (Russian).
3. N.V.Erkaev, A.B.Mezentsev. magnitosfernie issledovania, 9, 1987, 17 (Russian).
4. M.I.Pudovkin, V.S. Semenov Ann. Geophys., 33, 4, 1977, 429.
5. Z.A. Kereselidze. MGD efekti konechnoi elektricheskoi provodimosti solnechnogo vetra vblizi magnitosphere. Tbilisi, 1986, 122 (Russian).
6. L.G.Loitsiansky. Mexanika zhidkosti i gaza. Moskva, 1959, 764 (Russian).
7. I.N. Bronshtein, K.A.Semendiaev.Spravochnik po matematike. Moskva, 1955 (Russian).
8. V.A.Sergeev, N.V.Tsiganenko. Magnitosfera Zemli. Moskva, 1980. 192 (Russian).



Z.Khvedelidze, A.Topchishvili

Calculations of Radiation Balance in View of a Landscape Peculiarity

Presented by Member of the Academy B.Balavádze, November 9, 1998

ABSTRACT. The dependence of the radiation balance and its components on the surface albedo for Georgian territory has been studied. Concurrence of experimental data with theoretical calculations (difference ~6%) is shown.

Key words: radiation, albedo.

Essential changes of the radiation balance depending on albedo of different types of surface are studied for Tbilisi latitude in the near surface layer of the Earth [1-3].

Albedo r is a ratio of radiation flow reflected by a surface to the radiation falling to the surface, shown in percents or decimal fraction. Radiation balance R of the Earth's surface or near-Earth space consists of the absorbed direct Sun radiation $(1-r)I'$, dispersed radiation $(1-r)I$ and effective radiation of the Earth's surface B^* :

$$R = (1 - r)(I' + I) - B^* \quad (1)$$

Dependence of directed and reflected radiation flow on clouds amount n is described by the following formula:

$$(I' + I)^* = (I' + I)(1 - (1 - k)n), \quad (2)$$

where k is a coefficient, expressing cloud types and varying within $0 < k < 1$.

The influence of cloudness quantity on effective radiation is taken into account using empiric formula [1,4]:

$$B^* = B(1 - (C_L N_L + C_H N_H)), \quad (3)$$

where C_L, C_H are empiric coefficients, $C_L = 0.9$ and $C_H = 0.25$, N_L, N_H are cloudness quantity of the upper and lower layers, correspondingly.

In the case of unclouded sky effective radiation of the Earth's surface is the difference between own radiation of the Earth's surface B_0 and the part, absorbed by the Earth:

$$B = B_0 - \delta B_A, \quad (4)$$

where δ is a relative coefficient of absorption, varying within the limits $0.85 < \delta < 0.99$ with average value $\delta = 0.95$.

On the basis of Kirghopf rule for the flow of radiation of the Earth's surface we have

$$B_0 = \delta \sigma T_0^4, \quad (5)$$

where T_0 is the Earth's surface temperature, $\sigma = 5.67 \cdot 10^{-8} \text{ BT/M}^2\text{K}^4$ is Stefan-Boltzmann's coefficient.

For calculation of contrary radiation of the atmosphere B_A we will use Brent's formula:

$$B_A = \sigma T_1^4 (a_1 + b_1 \sqrt{e}), \quad (6)$$

where T_1 is air temperature in the altitude z , $a_1 = 0.526$ and $b_1 = 0.065$ dimensionless coefficients of the contrary radiation δB_A .

Substituting (6) and (5) in (4) we get:

$$B = \delta\sigma T_0^4 - \delta\sigma T_1^4 (a_1 + b_1 \sqrt{e}) = \delta\sigma (T_0^4 - T_1^4 (a_1 + b_1 \sqrt{e})). \quad (7)$$

Let us consider this problem on the example of Georgia, the territory of which is a complex physico-geographical district, where the processes in the atmosphere in the near-earth surface $H = 50-100 \text{ m}$ change essentially, depending on the landscape local.

For radiation balance the investigation on the territory of Georgia meteorological data granted by database of meteorostation of Tbilisi State University for 1987 have been used [5]. The calculations were done using specially developed software, modern computer technologies for the mid months of the seasons (January, April, June and October).

Results are shown in Figs. 1-3. As we can see from these Figs., the less albedo is the sharper short-wave component of radiation balance increases, and with the latter the radiation balance increases too (top lines in the charts correspond to $r = 0.05$ for dark grounds, $r = 0.15$ for wet grey grounds and coniferous forests, $r = 0.25$ for dry loam and grey grounds, $r = 0.4$ for dry light sandy soil, $r = 0.5$ for polluted snow).

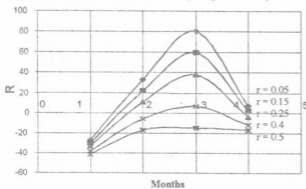


Fig. 1.

one maximum and one minimum) are not observed, this can be explained by influence of distribution of temperature and humidity by altitude on the atmosphere radiation. Yearly changes of the effective radiation under presence of clouds are more complex than in no-clouds case, but general tendency of increasing effective radiation during summer months in comparison with winter ones is observed in the cloudcase, too.

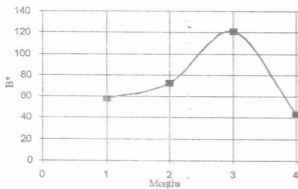


Fig. 2.

(wet grey grounds and coniferous forests, Fig. 6).

The present work enables us to make the following conclusions:

1. The computed values of R coincide well with the observed ones (6%);

The influence of effective radiation B^* causes the decrease of radiation balance R . Yearly changes of effective radiation are shown in Fig 2. Effective radiation is always more than 0, because of long-wave radiation, by which the Earth loses energy. As a rule, maximal values of B^* are observed during summer months, when temperature of the Earth's surface reaches maximum.

Though, simple yearly changes (with one maximum and one minimum) are not observed, this can be explained by influence of distribution of temperature and humidity by altitude on the atmosphere radiation. Yearly changes of the effective radiation under presence of clouds are more complex than in no-clouds case, but general tendency of increasing effective radiation during summer months in comparison with winter ones is observed in the cloudcase, too.

Seasonal changes of radiation balance R and its short-wave part R_k dependent on albedo r are given in Figs. 4, 5. The most clearly expressed changes of R and R_k are observed with minimum value of albedo. With albedo increasing till $r=0.5$ radiation balance is approximately the same for all the year seasons (crossing lines in Fig. 4).

The best coincidence with observed values of variables R_k , R and B^* for Tbilisi [6] was obtained for $r=0.15$ and $k=0.85$

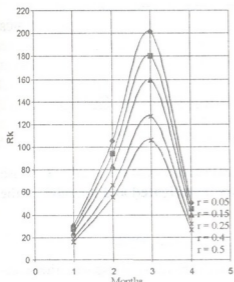


Fig. 3.

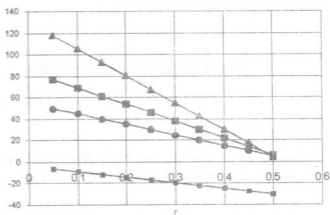


Fig. 4.

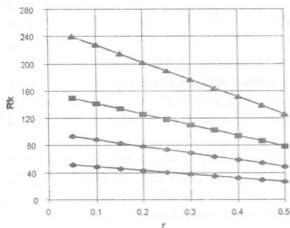


Fig. 5.

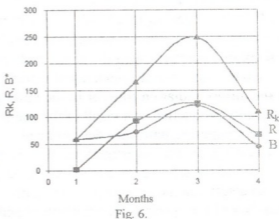


Fig. 6.

2. The best coincidence is obtained for $r=0.09$ and $k=0.85$;

3. Similar results were obtained for short-wave B^* and long-wave R_k parts of radiation balance.

Tbilisi I. Javakhishvili State University

REFERENCES

1. L.T. Matveev. Kurs obshchei meteorologii. Leningrad, 1984 (Russian).
2. Z.V. Khvedelidze. Wave motion in lower layers of the throposphere and polution problems. TGU, 1991, 205 (Russian).
3. Liou Ki Nan. Basis of radiation processes in the atmosphere. L., 1984, 376.
4. A. H. Hrgian. Fizika atmosfery. M., 1986, 101 (Russian).
4. Meteostation TGU, Metheorological Bulletin, 1987.

I. Shengelia

A Model of the Spectral Diffuse Radiation Field for Georgia

Presented by Member of the Academy G. Svanidze, September 2, 1998

ABSTRACT. Patterns of the spatial and temporal variation of the spectral diffuse radiation for Georgia in the clear sky conditions are investigated and a model of the spectral diffuse radiation field is constructed.

Key words: extinction coefficient, single scattering, optical depth

As a result of scattering of the solar radiation flux in the Earth's atmosphere, the short-wave radiation reaching the Earth's surface contains along with the direct sun radiation, the diffuse radiation too. Hence in the study of regime of the total short-wave radiation reaching the Earth's surface, together with the direct radiation, study of the diffuse radiation is also necessary. Since our aim is investigation of diffuse radiation in the clear sky conditions, we will confine ourselves with the single scattering of radiation in the atmosphere.

Up to date, several fundamental works have been devoted to the creation of a theory of the diffuse radiation transfer in the atmosphere; research in this direction has become especially productive as a result of the use of the approximate calculation methods based on the computing hardware development.

Relying on the investigations of K. Shifrin, O. Avaste and others [1-3] we have constructed the scheme for calculation of the spectral diffuse radiation for the clear sky [4, 5]. To determine the extinction coefficients of aerosols in this scheme a method of determination of the spectral optical depth of aerosols has been utilized [6,7].

Using the latter method, for the first time in Georgia values of the diffuse monochromatic radiation fluxes have been calculated at 107 points in the (0.2-4.0) μm interval of the spectrum for several months of actinometric observation times at 90 meteorological stations. Furthermore based on these calculation values of the ultraviolet, visible, infrared and integral diffuse radiation have been determined.

Spectral composition of the diffuse radiation reaching the Earth's surface is entirely different from the spectral composition of the solar flux energy at the upper boundary of the atmosphere. For example, maximal intensity in the latter is the range of (0.46-0.48) μm . Whereas by the molecular scattering maximum of radiation is significantly shifted towards short waves (0.34-0.37 μm). Moreover it has a secondary maximum too (0.43 - 0.44 μm). Diffuse radiation energy distribution spectrum is closely related to the sizes of the scattering particles. Their growth results in shifting of the maximum of the diffuse radiation towards long waves and for large particles is acquired at 0.70 μm .

For various sun altitudes pattern of the spectral distribution of the diffuse radiation is practically unchanging (Fig. 1); this pattern is also similar for typically characteristic meteorological stations of Georgia. Hence in the present work we have illustrated it by presenting Sokhumi only.

As it is known, quantity of the diffuse radiation in the clear sky condition is determined, together with other factors (atmosphere transparency, albedo of the underlying surface) by the sun altitude. The growth of the latter increases the diffuse radiation flux, intensely in the beginning, and with smaller amplitude at small zenith angles. This dependence is clearly observed from the graphs of the daily change of the diffuse radiation (Fig. 2), produced by averaging of corresponding values of radiation at typically characteristic stations in Georgia (on the graphs, by vertical intervals the values of mean square deviations are given).

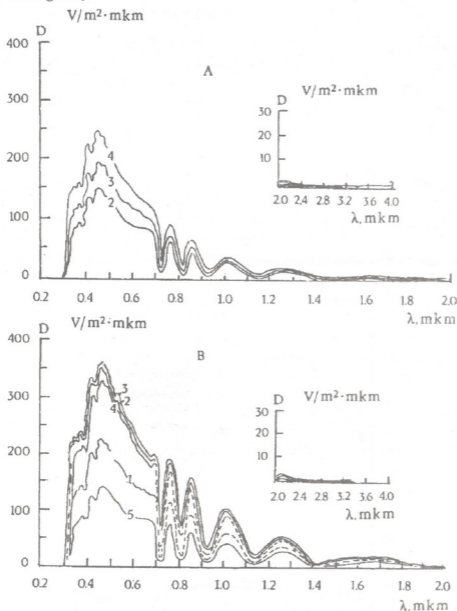


Fig. 1. Spectral distribution of diffuse radiation for Sokhumi.

As seen from Fig. 3, diffuse radiation has a maximum twice in the year (April and July). General background of its distribution is much larger in the warm period of the year. It undergoes small reduction in June and reaches absolute minimum in December.

Let us note that for some meteorological stations it is reached in November.

Based on the interpolation and extrapolation of the discrete values of radiation computed by us, maps of possible monthly sums of ultraviolet, visible, infrared and integral radiation have been built for January and July (Fig. 4).

As seen from Fig. 4, possible monthly sums of diffuse radiation in January and July on the territory of Georgia are highest on plains of Shida Kartli and in the South and

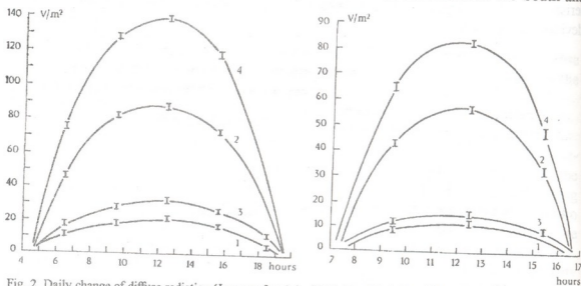


Fig. 2. Daily change of diffuse radiation (January, June) 1 - UV (ultraviolet), 2 - visible, 3 - IR (infrared), 4 - integral.

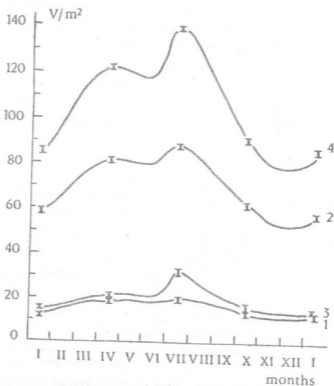


Fig. 3. Annual change of the diffuse radiation (12 hr 30 min) 1 - UV, 2 - visible, 3 - IR, 4 - integral.

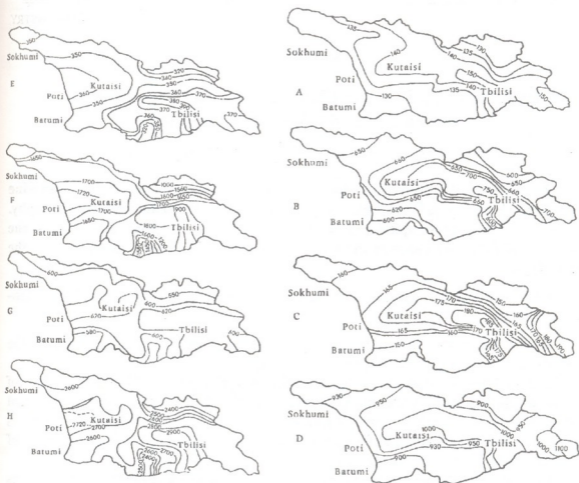


Fig. 4. Possible monthly sums of diffuse radiation (kw/m^2) A -UV, January; B - visible, January; C - IR, January; D-int., January; E-UV, July; F - visible, July; G - IR, July; H - int., July.

South-East direction from Tbilisi mainly along the Mtkvari valley. With growth of the altitude above ground level its values decrease whereas the general background of the diffuse radiation is higher in Eastern Georgia compared with its western part.

Georgian Academy of Sciences
 Institute of Hydrometeorology

REFERENCES

1. K.S.Shifrin, *I.A.Minin*. Proc. GGO, **68**, 1957 (Russian).
2. K.S.Shifrin, *O.Avaste*. Investigations in the atmosphere physics, Institute of the Atmosphere Physics of the Acad. Sci. Est. SSR, **2**, 1960 (Russian).
3. *O.Avaste, H.Moldau, K.S.Shifrin*. Investigations in the atmosphere physics, Institute of the Atmosphere Physics of the Acad. Sci. Est. SSR, **3**, 1962 (Russian).
4. *I.A.Shengelia*. Bull. Acad. Sci. GSSR, **130**, 1, 1988.
5. *I.A.Shengelia*. Cand. thesis (Russian).
6. *K.A.Tavartkiladze*. Meteorology and hydrology, **4**, 1985 (Russian).
7. *K.A.Tavartkiladze, E.V.Sajaia*. Bull. Acad. Sci. GSSR, **124**, 3, 1986.



Sh. Shatirishvili

High Performance Liquid Chromatography for Determination of Phenol Carboxylic Acids in Wine Materials

Presented by Member of the Academy T. Andronikashvili, September 28, 1998

ABSTRACT. We determined the composition of phenol carboxylic acids in wine materials of "Kakheti" and "Rkatsiteli" using high performance chromatography. Calculation of both samples main components change is given according to the duration of thermal treatment and temperature regime, in order to compare with the final typical wine.

Key words: phenol carboxylic acids, wine materials, high performance liquid chromatography.

Despite rather low content the phenol carboxylic acids play significant role in the formation of taste and aromatic properties of drinks.

The methods of phenol carboxylic acids determination given in [1, 2] are a subject of rather scrupulous study, including Georgian wines [3, 4]. The above stated papers deal with the results of analysis during concentration of heavy fractions of wine materials aiming to increase the volume of a number of compounds up to the limits of sensitivity of detector blocks of liquid chromatographs.

In our case for the concentration of heavy fractions the evaporation in the vacuum was performed as well as gas extraction by helium at 40-50⁰C of easily volatile components. The volume of initial mixture decreased about 20-times. To the obtained 0.5-0.6 g concentrate was added methanol standard solution of 0.025 cinnamonic acid of 0.2725 mg/ml concentration and then 20 μ l of the sample was injected to a dosator with a loop. The experiment was performed on a liquid chromatograph of "Watters" firm with a double unit block of gradient control system needed for gradient elution.

Detection occurred by the "Spectro 8800" detector which gives the possibility to select detectors wave length. Calculation of the obtained results was performed on the computer - integrator "Carlo Erba". The previous studies have shown [3, 4] that detection is performed better at 280 nm. One of the major factors making influence on the separation of phenol carboxylic acids is the composition of liquid phase and the regime of detection. The systems of solvents for the complex mixtures of natural origin known earlier appeared less efficient than the gradient regimes with two systems of solvents offered in the mentioned papers [3, 4]. Taking into account the above stated, the separation was carried out utilizing two systems of solvents, A and B systems, which was changed by isocratic gradient regime:

A : H₂O-ACOH(980:20) - 0.02 MNaOAC

B : H₂O - ACOH -iPrOH- MEOH (815:25:20:140) 0.02MNaOAC

The samples of wine materials "Kakheti" and "Rkatsiteli" were examined. After

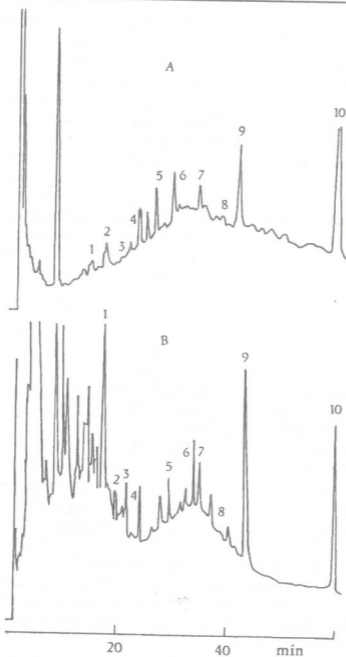


Fig. Chromatogram of phenol carboxylic acids in wines "Kakheti", A- 50°C, in case of thermal treatment for 25 days; B - ready, 2 years old wine; (1) H -hydroxybenzoic acid; (2) vanillic acid; (3) jasmine acid; (4) caffeic acid; (5) vanillin; (6) P-cumaric acid; (7) M-cumaric acid; (8) ferulic acid, (9) sinapic acid; (10) cinnamic acid.

removal of light components by helium flow and 5-fold concentration to 10 ml of specimen standard solution of cinnamonic acid was added. 20 μ l sample was injected to chromatograph by means of a dosator with a loop. The standard column of 250x4.6 mm was packed with 40 μ m size grains of spherosorb S5-ODS sorbent. Elution regime: for the initial 6 min we injected 90% A - 10% B mixture, then, for 19 min gradient detection -

4.7% B/min was carried out until it reached 100%. Finally we performed isocratic detection for 35 min. The regime program was provided by microprocessors. Changes of mixture equaled to 1.5 ml/min. Identification was made by tracer technique, but as the number of existing phenol carboxylic acids was rather low, identification of a number of compounds, was achieved by the use of relative retention volumes according to [5].

A chromatogram of wine material "Kakheti" is illustrated in Figure 1 which shows that separation power of the column for the chosen regime is rather high. The total number of recorded peaks reaches 20. Although, a great number of peaks, the nature of which is unknown to us at present is marked in the left section of chromatograms. In the middle part greater part of peaks are identified. When using cinnamonic acid as a standard, calculation of changes of major components of both samples of semifinished products was conducted for their comparison with typical wine (see Table).

Table
Composition of phenol carboxylic acids in wines "Rkatsiteli" and "Kakheti"

Wine material Substance	"Rkatsiteli"		"Kakheti"	
	Treated at 50°C, for 25 days	2 years	Treated at 50°C, for 25 days	2 years
1. Hydroxybenzoic acid	12.6	24.0	16.1	32.2
2. Vanillic acid	14.3	17.8	9.6	14.2
3. Jasmine acid	4.0	5.0	3.2	6.8
4. Caffeic acid	2.0	5.8	9.6	34.4
5. Vanillin	10.3	13.4	15.3	17.6
6. P-cumaric acid	5.6	12.1	11.2	14.0
7. M-cumaric acid	7.2	23.0	5.2	9.8
8. Ferulic acid	11.3	16.0	8.3	19.3
9. Sinapic acid	7.6	8.2	17.6	35.2
10. Cinnamic acid	standard		standard	

The obtained data show, that in the studied wines phenol carboxylic acid concentration is rather high. Similar to other studied cases, here, too, composition of phenol carboxylic acids at the initial stage of ageing of wine material is rather high already. High content of caffeic acid and vanillin in the wine "Kakheti" is worth to notice, which is often disregarded during wine-tasting.

Georgian State Agrarian University

REFERENCES

1. J. Sh. Shatirishvili. Chromatography in Ecology. Tbilisi, 1986, 112, (Russian).
2. J. Sh. Shatirishvili. Chromatography of Georgian Wines. Tbilisi, 1988, 172 (Russian).
3. J. Sh. Shatirishvili. J. of Chromatography, Amsterdam, 364, 1986, 183.
4. J. Sh. Shatirishvili, R. M. Tsikoridze. Bull. Acad. Sci. GSSR, 192, 1986, 305(Russian).
5. A. Waterhouse, J. Towey. J. Arg. and Food Chem., 42, 9, 1994, 1971-1974.

R.Revia, G.Makharadze, G.Supatashvili

Preconcentration of Fulvic Acid from Aqueous Media Using Nonionic Surfactants

Presented by Corr. Member of the Academy D.Ugrekheldidze, September 14, 1998

ABSTRACT. The cloud-point extraction technique was used to concentrate river water fulvic acid. Triton X-100 was utilized in this work as nonionic surfactant. The results of study of the water sample acidity, temperature, equilibration time and surfactant concentration effect on the extraction efficiency are presented. Optimal scheme of concentration of fulvic acid by Triton X-100 is suggested. The recovery of fulvic acid achieved under optimized conditions was 82 %.

Key words: fulvic acid, Triton X-100, cloud-point extraction.

Isolation and concentration of humic substances from natural waters is one of the problematic questions of analytical chemistry. Currently, the sorption methods are widely used for these purposes (XAD-2, XAD-8, DEAE-cellulose, activated carbon), which are time-consuming and associated with difficulties [1-3]. Besides, during the last decade nonionic surfactants have been successfully used for concentration of different substances from aqueous solutions [4-7]. The basis of their use is unique property of their aqueous micellar solutions to undergo a phase separation upon alteration of the conditions (e.g. change of temperature or pressure, electrolytes adding, etc.). Any hydrophobic substances originally presented in solution binded to the micellar aggregates will be extracted and concentrated in the surfactant-rich phase [8]. This concentration method is technically easy to realize, economic, less laborious and fast. By extraction completeness it doesn't yield other traditional methods.

The aim of this work was the investigation of the principal possibility of using the nonionic surfactants (on example of Triton X-100) for preconcentration of fulvic acid (FA) from aqueous media. The FA standard sample was isolated from water of the river Mtkvari (Georgia) by adsorption-chromatographic method [9].

The scheme of the concentration of FA by Triton X-100 was as follows: to FA model solution ($T=30$ mkg/ml) was added Triton X-100 and stirred up, aliquot part of solution (10 ml) was taken in test tube and placed in thermostated water bath. To set the optimal conditions of the concentration we study the effect of sample acidity, temperature, equilibration time and surfactant concentration on extraction efficiency.

To control FA in separated phases we use both photoelectrocolorimetry (for aqueous phase analysis) and HPLC (for surfactant-rich phase analysis).

Photoelectrocolorimetric measurements (KFK-20, Russia) were performed on wave length 364 nm in quartz cuvette of 1 cm thickness. Chromatographic analysis was carried out on microcolumn liquid chromatograph "Milichrom-1" (Russia) with UV-detector

($l=230$ nm). The separation of FA was performed on stainless steel column (100×2 mm i.d.) which was packed with Separon- C_{18} (Lachema, Brno, Czech Republic). Particle diameter was $5 \mu\text{m}$. The eluent was a mixture of 1-propanol and 15 mM tetrabutylammonium hydroxide in 0.05 M Na_2HPO_4 (25:75). Mobile phase flow-rate was $50 \mu\text{l}/\text{min}$. The acidity of the mobile phase was adjusted with phosphoric acid to 4.0. It should be noted that in given chromatographic conditions Triton X-100 doesn't prevent FA determination.

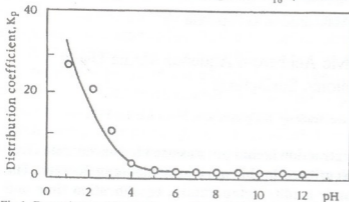


Fig.1. Dependence of distribution coefficient of FA on pH of the solution. Conditions: temperature - 80°C ; thermostatic time - 5 min; centrifuge time - 5 min; $C_{\text{Triton X-100}}$ - 3% (wt.).

The obtained data show that the distribution of FA between separated phases significantly depends on the acidity of a solution (Fig.1). The distribution coefficient increased as the pH of the solution (pH 12.0-1.0) decreased. In our opinion it is caused by the fact that at low pH of the solution FA exists in molecular form, which unlike ion form binds more strongly to micellar aggregates of nonionic surfactants. So, the less FA dissociated, the higher the recovery is.

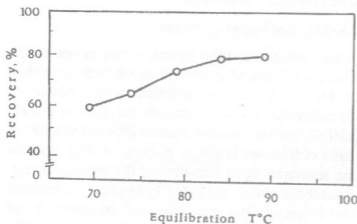


Fig.2. Dependence of the extraction efficiency of FA on the temperature. Conditions: pH 1.0; thermostatic time - 5 min; centrifuge time - 10 min; $C_{\text{Triton X-100}}$ - 3%(wt.).

The effect of temperature in the range from 70°C up to 90°C on the extraction efficiency of FA was studied. As it is seen from the obtained data (Fig.2) the recovery increases with temperature increase. The carried out experiments demonstrate that the mentioned effect is not caused by FA molecules degradation at high temperature.

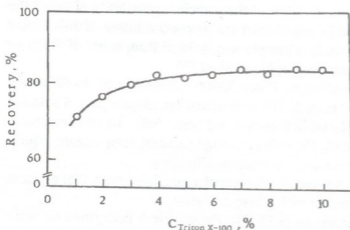


Fig.3. Variation of the extraction efficiency of FA as a function of the surfactant concentration (wt.%). Conditions: pH 1.0; temperature - 85°C ; thermostatic time - 10 min; centrifuge time - 10 min.

It should be noted that increase of temperature was accompanied by a reduction of the volume of surfactant-rich phase. This

is caused by the following: in aqueous solutions nonionic surfactants are present in a hydrated state. As the temperature is increased dehydration occurs [10]. The higher the temperature the more is dehydration degree. As a result the surfactant-rich phase contains less water and consequently the volume of this phase is smaller. Thus we can conclude that temperature increase promotes both extraction and concentration efficiency increase.

The effect of surfactant concentration on FA recovery was also investigated. The concentration of Triton X-100 was increased from 1% to 10%. The results obtained show that an increase of surfactant concentration causes an increase of recovery for FA (Fig. 3). As for the time of equilibration 10 min is enough to achieve the extraction maximum (Fig. 4).

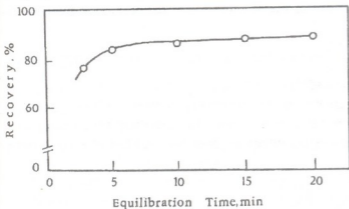


Fig.4. Dependence of the extraction efficiency of FA on the thermostatic time. Conditions: pH 1.0; temperature - 85°C; centrifuge time - 10 min; C_{Triton X-100} - 3% (wt.).

Triton X-100 is added to 10 ml water sample, stirred and placed in thermostated (85°C) water bath for 10 min; then it is centrifuged (3000 rpm), aliquot of surfactant-rich phase is collected by microsyringe and analysed by HPLC. The extraction degree of FA achieved at given conditions was 82%, the preconcentration factor was 13.5.

Thus it can be concluded that nonionic surfactants can be used for concentration of FA from aqueous media with the aim of their further chromatographic determination.

Tbilisi I.Javakhishvili State University.

REFERENCES

1. G.R.Aiken. In: Humic Substances and their Role in the Environment, F.H.Frimmel and R.F.Christman (ed.), Chichester, 1988, 15-28.
2. R.L.Malcolm. In: Humic Substances in the Aquatic and Terrestrial Environment, B.Allard, H.Boren, A. Grimvall (ed.), Lecture Notes in Earth Sciences, 33, 1991, 9-36.
3. M.H.Sorouradin, M.Hiraide, Y.S.Kim, H.Kawaguchi. Anal. Chim. Acta, **281**, 1993, 191.
4. R.P.Frankewich, W.L.Hinze. Anal. Chem., **66**, 1994, 944.
5. B.Moreno Cordero, J.L.Pérez Pavón, C.Garcia Pinto, M.E.Fernandez Laespada. Talanta, **40**, 1993, 1703.
6. C.Garcia Pinto, J.L.Pérez Pavón, B.Moreno Cordero. Anal. Chem., **67**, 1995, 2606.
7. T.Saitoh, W.L.Hinze. Anal. Chem., **63**, 1991, 2520.
8. W.L.Hinze, E.Pramauro. Crit. Rev. Anal. Chem., **24**, 1993, 133.
9. G.M.Varshal, T.K.Velyukhanova et al. Gidrokhimicheskie materialy, **59**, 1973, 143 (Russian).
10. I.A.Gritskova, R.M.Panich, S.S.Voiutski. Uspekhi Khimii (Russian Chemical Review), **11**, 1965, 1989.



I. Chikvaidze, Sh. Samsoniya, T. Narindoshvili

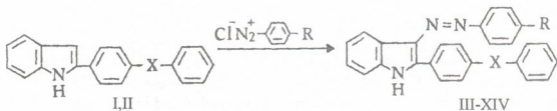
Azocoupling Reactions of 2-(diphenylmethane-4-yl)indole and 2-(diphenylethane-4-yl)indole

Presented by Corr. Member of the Academy D. Ugrekhelidze, September 28, 1998

ABSTRACT. The azocoupling reactions of some arylindoles have been carried out. Electronic absorption spectra data of the obtained azoproducts have been studied.

Key words: arylindoles, azocoupling reactions, electronic absorption spectra data.

The azocoupling reactions of the indoles: 2-(diphenylmethane-4-yl)indole (I) and 2-(diphenylethane-4-yl)indole (II), reported by us earlier [1], with phenyldiazonium, p-chlorophenyldiazonium, p-nitrophenyldiazonium, p-sulfamidophenyldiazonium, p-methoxycarbonylphenyldiazonium, p-oxycarbonylphenyldiazonium chlorides have been studied at pH 6-7.



(III, IX) R = H; (IV, X) R = Cl; (V, XI) R = NO₂;
 (VI, XII) R = SO₂NH₂; (VII, XIII) R = COOCH₃; (VIII, XIV) R = COOH;
 (I, III-VIII) X = CH₂; (II, IX-XIV) X = CH₂-CH₂.

In diluted solutions the reaction completes in 30 min to give the azocoupling products (III-XIV) in high yields (85%-95%). In the concentrated solutions the partial precipitation of the initial arylindoles takes place, due to which further course of the reactions is complicated and yields of the azoproducts are significantly decreased.

In each case β -substitution takes place in pyrrol ring of the I and II arylindoles giving the corresponding arylazoproducts (III-XIV) coloured from orange to dark red. The long wave absorption maxima in electronic absorption spectra of 3-phenylazo-2-(diphenylmethane-4-yl)indole (III) and 3-phenylazo-2-(diphenylethane-4-yl)indole (IX) appear at 406 nm and 400 nm respectively (Table 1). The hypsochromical shift of these maxima to 375 nm and 380 nm takes place in the spectra of compounds (IV, X), which could be explained by the total positive electronic influence of the chlorine atom [2]. The mentioned maxima are bathochromically displaced in the spectra of the compounds (V-VIII) and (XI-XIV) to 416.6 nm, 426 nm, 416.6 nm, 465 nm respectively. The shift value increases according to the rising of electron-withdrawing capacity of the substituents.

Experiment. Control over reaction course and compounds purity as well as determination of R_f data were fulfilled on the Silufol plates UR-254.

Table 1
 The physico-chemical characteristics of the compounds (III-XIV)

Compound	M.p. °C	Yield, %	R _f ^a	IR spectral data ν , cm ⁻¹	UV spectral data λ_{max} , nm(lge)
N	1	2	3	4	5
III	132-133	95	0.59 ^a	3455 (NH); 1460 (N=N)	209 (4.43); 253 (4.27); 300 (4.35); 406 (4.26)
IV	82-83	95	0.61 ^b	3420 (NH); 1425 (N=N)	211 (4.56); 254 (4.40); 302 (4.50); 375 (4.44)
V	249-250	95	0.54 ^b	3345 (NH); 1420 (N=N); 1330 (NO ₂)	209 (4.34); 289 (4.24); 465 (4.21)
VI	171-172	90	0.75 ^c	3325 (NH); 1450 (N=N); 1360 (NO ₂)	210 (4.57); 254 (4.44); 299 (4.56); 416.6 (4.52)
VII	190-191	85	0.55 ^b	3340 (NH); 1700 (CO); 1420 (N=N)	211 (4.49); 250 (4.31); 308 (4.41); 426 (4.13)
VIII	241-242	89	0.71 ^d	3400 (NH); 1680 (CO); 1410 (N=N)	211 (4.51); 255 (4.31); 303 (4.40); 416.6 (4.35)
IX	131-132	95	0.58 ^e	3400 (NH); 1455 (N=N)	208 (4.67); 250 (4.48); 298 (4.57); 400 (4.39)
X	124-125	95	0.71 ^a	3460 (NH); 1430 (N=N)	209 (4.58); 252 (4.39); 300 (4.44); 380 (4.36)
XI	261-262	95	0.74 ^e	3360 (NH); 1420 (N=N); 1320 (NO ₂)	207 (4.43); 286 (4.21); 465 (4.14)
XII	200-201	90	0.74 ^c	3300 (NH); 1430 (N=N); 1370 (SO ₂)	210 (4.54); 252 (4.36); 303 (4.41); 416.6 (4.35)
XIII	180-181	89	0.51 ^b	3330 (NH); 1690 (CO); 1410 (N=N)	210 (4.73); 254 (4.58); 303 (4.64); 426 (4.60)
XIV	248-249	85	0.78 ^c	3450 (NH); 1670 (CO); 1420 (N=N)	210 (4.54); 252 (4.36); 303 (4.41); 416.6 (4.36)

*Eluent for R_f: a - hexane-ether, 3:2; b - benzene-ether, 1:1; d - benzene-ether, 1:3; e - benzene-hexane, 1:3.

 Table 2
 Elemental analysis data of the compounds (III-XIV)

Compound	Found, %			Formula	Calculated, %		
	C	H	N		C	H	N
N	1			2	3		
III	83.10	5.50	10.81	C ₂₇ H ₂₁ N ₃	83.70	5.45	10.85
IV	76.10	4.76	9.89	C ₂₇ H ₂₀ N ₃ Cl	76.80	4.74	9.96
V	74.90	4.60	13.10	C ₂₇ H ₂₀ N ₄ O ₂	75.00	4.62	12.96
VI	69.48	4.80	11.97	C ₂₇ H ₂₂ N ₄ SO ₂	69.53	4.74	12.01
VII	77.90	5.38	9.41	C ₂₉ H ₂₃ N ₃ O ₂	78.20	5.16	9.43
VIII	78.00	4.84	9.80	C ₂₈ H ₂₁ N ₃ O ₂	77.96	4.87	9.74
IX	83.81	5.68	10.39	C ₂₈ H ₂₃ N ₃	83.79	5.70	10.47
X	77.20	5.01	9.59	C ₂₈ H ₂₂ N ₃ Cl	77.15	5.05	9.64
XI	75.12	4.97	10.72	C ₂₈ H ₂₂ N ₄ O ₂	75.33	4.93	10.76
XII	69.90	5.01	9.95	C ₂₈ H ₂₄ N ₄ SO ₂	70.00	5.00	10.00
XIII	78.61	5.25	9.21	C ₃₀ H ₂₅ N ₃ O ₂	78.43	5.44	9.15
XIV	78.40	5.11	8.12	C ₂₉ H ₂₃ N ₃ O ₂	78.20	5.16	8.09

IR spectra were obtained in petrolatum oil in UR-20, UV spectra were recorded in absolute ethanol solution on the spectrophotometer "Specord".

General procedure for the synthesis of 3-arylazoderivatives of 2-(dipenylmethane-4-yl)indole and 2-(diphenylethane-4-yl)indole (III-IX). To the solution of 1 mmol indole derivative (I, II) in 160 ml of isopropanol and 60 ml of dioxane, the diazosolution obtained from 4mmol aniline derivative and adjusted to pH6 with aqueous solution of sodium acetate (CH_3COONa) was added. Reaction mixture was stirred at 0°C for 30 min, diluted with 600 ml of cold water and allowed to stand for 10-12 hours. The isolated precipitation was filtered, washed off with water and dried to give products. (Tables 1, 2)

Tbilisi I. Javakhishvili State University

REFERENCES

1. T.Narindoshvili, I.Chikvaidze, Sh. Samsoniya. Bull. Georg. Acad. Sci., 157, 1, 1998, 64-66.
2. P.Gordon, P.Gregory. Organicheskaya khimia krasitelei. M, 1987, 135-175 (Russian).

M. Trapidze, E. Chkhaidze, Sh. Samsoniya

Conversion of 2,7-naphthylendihydrazine

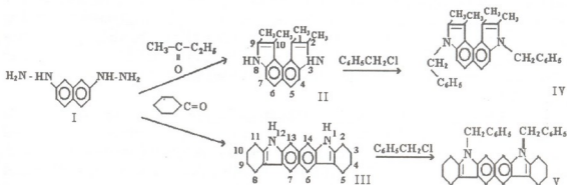
Presented by Corr. Member of the Academy L. Khananashvili, June 22, 1998

ABSTRACT. By the converting of 2,7-naphthylendihydrazine corresponding tetramethylsubstituted indolo[4,5-e]indole and octahydrocarbazo[3,4-d]carbazole were obtained. The reactions of their *N, N*-benzylation were studied.

Key words: naphthylendihydrazine, indoloindole, carbazolocarbazole, indolization, benzylation.

Arylated products of multinuclear, condensed systems are interesting as compounds, which have potential anticancer activity. Previously *N, N*-dibenzylproducts of unsubstituted indoloindoles were synthesized [1,2]. In the present work alkylsubstituted derivative of indolo[4,5-e]indole was synthesized and the reaction of its benzylation was studied.

On the basis of 2,7-naphthylendihydrazine by its simultaneous condensation and indolization with methylethyl ketone and cyclohexanone in acetic acid without isolation of intermediate dihydrazones alkylsubstituted indolo[4,5-e]indole and octahydrocarbazo[3,4-d]carbazole were prepared according to the scheme:



By boiling 2,7-dioxinaphthalene in hydrazine hydrate 2,7-naphthylendihydrazine (I) was obtained [3]. As a result of interaction of 2,7-naphthylendihydrazine and methylethyl ketone 1,2,9,10-tetramethyl-3H,8H-indolo[4,5-e]indole (II) was obtained with 20 % yield of chromatographically pure product. The I.R. spectrum revealed a ring NH group at 3400 cm^{-1} .

A cyclization of 2,7-naphthylendihydrazine with cyclohexanone in icy acetic acid and concentrated sulphuric acid was described in work [4]. Condensation and cyclization by boiling in acetic acid for 1h was made by us. Obtained compound coincides with previously described corresponding 1H, 12H - 2,3,4,5,8,9,10,11-octahydrocarbazo[3,4-d]carbazole (III) by chromatographical control.

The reactions of benzylation of (II) and (III) compounds were made under condition

of interphase catalysis using tetrabutyl ammonium bromide as catalyst by boiling in benzene solution. After the purification on column *N,N*-dibenzyl 1,2,9,10 - tetramethyl indolo[4,5-*e*]indole (IV) and *N,N*-dibenzyl carbazolo[3,4-*d*]carbazole (V) were obtained. In I.R.spectra the absorption band of NH bond at 3400 cm^{-1} region had been disappeared. The control in the course of reaction, purity of compounds and calculation of Rf were carried out by thin-layer chromatography on "silufol UV-254" plates. I.R. spectra were recorded on "UR-20" (in white paraffin oil). Mixture of silica gel with size of grain 40/100 : 100/250 - (1:1) was used.

1,2,9,10 - tetramethyl - 3H, 8H - indolo[4,5-*e*]indole (II). To the solution of 0.94g (5.1 mmole) 2,7-naphthilendihydrazine in acetic acid 1 ml (11 mmole) of methylethyl ketone was added and was stirred in acetic acid for 1h. The reaction mixture was poured into the water, filtered, washed out with water till neutral reaction and dried. The yield was 1.2g (79%). The product, containing several spots, was purified on column. Eluent benzene. The yield of isolated compound was 0.1g (20%). m.p. 285-286°C, Rf 0.58 (benzene: ether (1:1)), I.R.spectrum cm^{-1} : 3400 (NH).

1H,12H - 2,3,4,5,8,9,10,11-octahydrocarbazolo[3,4-*d*]carbazole (III). To the solution of 0.9g (5 mmole) 2,7-naphthilendihydrazine in acetic acid 1.55 ml (15 mmole) of cyclohexanon was added and was stirred in acetic acid for 1h. The reaction mixture was poured into the water, filtered, washed out with water till neutral reaction and dried. The yield was 0.9g (60%), I.R.spectrum cm^{-1} : 3390 (NH), according to the literary data 3350 [4].

***N,N*-dibenzyl - 1,2,9,10 - tetramethyl-indolo[4,5-*e*]indole [IV].** To the solution of 0.1g (0.4 mmole) (II) compound in benzene 50% solution of KOH, 1.1ml (1.8 mmole) of benzyl chloride and catalyst - tetrabutyl ammonium bromide were added. The mixture was stirred for 8h, extracted by ether, washed out with water till neutral reaction, dried on Na_2SO_4 and purified on column. Eluente heptane: ether (1:4). The yield of chromatographically pure compound was 0.2g (26%), m.p. 270-271°C, Rf 0.28 (heptane: ether (1:4)). In I.R.spectrum the absorption band of NH bond at 3400 cm^{-1} region had been disappeared.

***N,N*-dibenzyl - 2,3,4,5,8,9,10,11 - octahydrocarbazolo[3,4-*d*]carbazole (V).** To the solution of 0.2g (0.6 mmole) (III) compound in benzene 50% solution of KOH, 22 ml (3.6 mmole) of benzyl chloride and catalyst - tetrabutyl ammonium bromide were added. The mixture was stirred for 10h, extracted by ether, washed out with water till neutral reaction, dried on Na_2SO_4 and purified on column. Eluente heptane: ether (1:4). The yield was 0.4g (42%), m.p. 255-256°C, Rf 0.64 (heptane: ether (1:4)). In I.R.spectrum the absorption band of NH bond at 3400 cm^{-1} region had been disappeared.

The data of elemental analysis of synthesized compounds coincide with theoretical ones.

Tbilisi I.Javakhishvili State University.

REFERENCES

1. *N.A.Esakiya, M.V.Trapaidze, Sh.A.Samsoniya.* Tezisy dokl. I Vsesoiuz-Konf. "Chimia, Biochimia i farmakologia proizvodnikh indola", 1986, 182 (Russian).
2. *Sh.A.Samsoniya, N.A.Esakiya, N.N.Suvorov.* Khim. Geterotsikl.Soedin., 4, 1991, 464-467 (Russian).
3. *A.M.Kolesnikov, F.A.Mikhailenko.* Zhurnal Organich.Soedin., 18, 1982, 441 (Russian).
4. *D.O.Kajrishvili, S.V.Dolidze et al.* Khim. Geterotsikl.Soedin., 3, 1990, 346-348 (Russian).

G. Chakhtauri, M. Gverdsiteli, N. Tssetsadze, E. Gelashvili

Graph "Asymmetric Star" and its Application for Algebraic-Chemical Study of Reactions of Coordination Compounds

Presented by Member of the Academy K. Japaridze, May 18, 1998.

ABSTRACT. Graph "symmetric star" and "asymmetric star" can be used for description of coordination compounds. It was proved that the determinant of pseudocontiguity matrix of "asymmetric star" is equal to zero.

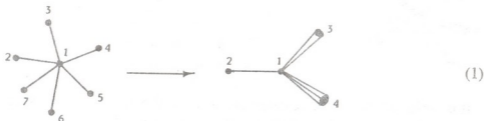
Key words: graph "asymmetric star", determinant, zero.

One of the interesting chemical processes are the reactions of substitution of two or more monodentate ligands with polydentate ligands in coordination compounds [1]. Suppose that from six monodentate ligands one remains, two are substituted by bidentate ligand and three are substituted by tridentate ligand. In algebraic chemistry such processes can be modelled by graph "symmetric star" and "asymmetric star" [2, 3].

Graph "symmetric star" is algebraic construction which consists of one vertex with degree n ($n \geq 1$) and some vertexes with degrees equal to 1.

Graph "asymmetric star" is algebraic construction which consists of one vertex with degree S_n and some vertexes with degrees equal to: 1, 2, 3, ..., n ; thus S_n is the sum of arithmetic progression.

The model register of the above-mentioned chemical process has a form:

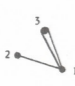


For algebraic-chemical investigation of this process the invariant of the graphs "symmetric star" and "asymmetric star" must be ascertained. Previously it was proved, that the determinant of pseudocontiguity matrix of "symmetric graph star" is equal to zero [4]. Below we shall prove this theorem in the case of "asymmetric star".


Theorem. The determinant of pseudocontiguity matrix of "asymmetric star" is equal to zero. Pseudocontiguity matrix is the matrix, which diagonal elements are the degrees of vertexes, nondiagonal elements are the multiplicities of edges.

$$\det \begin{pmatrix} S_n & 1 & 2 & 3 & \dots & n \\ 1 & 1 & 0 & 0 & \dots & 0 \\ 2 & 0 & 2 & 0 & \dots & 0 \\ \dots & \dots & \dots & \dots & \dots & \dots \\ n & 0 & 0 & 0 & \dots & n \end{pmatrix} = 0. \tag{2}$$

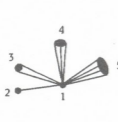
Proof. Let's consider some "asymmetric stars" and determinants of corresponding pseudocontiguity matrices:



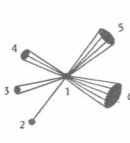
$$\Delta(3) = \begin{pmatrix} 3 & 1 & 2 \\ 1 & 1 & 0 \\ 2 & 0 & 2 \end{pmatrix};$$



$$\Delta(4) = \begin{pmatrix} 6 & 1 & 2 & 3 \\ 1 & 1 & 0 & 0 \\ 2 & 0 & 2 & 0 \\ 3 & 0 & 0 & 3 \end{pmatrix};$$



$$\Delta(5) = \begin{pmatrix} 10 & 1 & 2 & 3 & 4 \\ 1 & 1 & 0 & 0 & 0 \\ 2 & 0 & 2 & 0 & 0 \\ 3 & 0 & 0 & 3 & 0 \\ 4 & 0 & 0 & 0 & 4 \end{pmatrix};$$



$$\Delta(6) = \begin{pmatrix} 15 & 1 & 2 & 3 & 4 & 5 \\ 1 & 1 & 0 & 0 & 0 & 0 \\ 2 & 0 & 2 & 0 & 0 & 0 \\ 3 & 0 & 0 & 3 & 0 & 0 \\ 4 & 0 & 0 & 0 & 4 & 0 \\ 5 & 0 & 0 & 0 & 0 & 5 \end{pmatrix};$$

It is noticeable that in these determinants a_{11} is the sum of arithmetic progression: 1, 2, 3, ..., (n-1). For example for $\Delta(5)$ $a_{11}=10=1+2+3+4$ (so, for $\Delta(5)$ a_{11} is S_4 . Thus, $\Delta(n+1)$ is equal to (2).

Let's consider the determinants:

$$\Delta_1(3) = \begin{pmatrix} 1 & 1 & 0 \\ 2 & 0 & 2 \\ 3 & 0 & 0 \end{pmatrix}; \quad \Delta_1(4) = \begin{pmatrix} 1 & 1 & 0 & 0 \\ 2 & 0 & 2 & 0 \\ 3 & 0 & 0 & 3 \\ 4 & 0 & 0 & 0 \end{pmatrix}; \quad \Delta_1(5) = \begin{pmatrix} 1 & 1 & 0 & 0 & 0 \\ 2 & 0 & 2 & 0 & 0 \\ 3 & 0 & 0 & 3 & 0 \\ 4 & 0 & 0 & 0 & 4 \\ 5 & 0 & 0 & 0 & 0 \end{pmatrix};$$

$$\Delta_1(6) = \begin{vmatrix} 1 & 1 & 0 & 0 & 0 & 0 \\ 2 & 0 & 2 & 0 & 0 & 0 \\ 3 & 0 & 0 & 3 & 0 & 0 \\ 4 & 0 & 0 & 0 & 4 & 0 \\ 5 & 0 & 0 & 0 & 0 & 5 \\ 6 & 0 & 0 & 0 & 0 & 0 \end{vmatrix}$$

Decompose these determinants by last column:

$$\Delta_1(3) = (-2) \times (-3) = 2 \times 3 = 3! \quad \Delta_1(4) = (-3) \times 8 = -24 = -4!;$$

$$\Delta_1(5) = 5!; \quad \Delta_1(6) = -6!.$$

Let's prove that for every n:

$$9n \Delta_1(n) = -n!, \text{ if } n \text{ is even;}$$

$$\Delta_1(n) = n!, \text{ if } n \text{ is odd.}$$

Let's consider the structures of determinants obtained by decomposition of $D_1(4)$, $\Delta_1(5)$ and $\Delta_1(6)$ by last column:

$$\Delta_1(4) = \begin{vmatrix} 1 & 1 & 0 & 0 \\ 2 & 0 & 2 & 0 \\ 3 & 0 & 0 & 3 \\ 4 & 0 & 0 & 0 \end{vmatrix} = -3 \begin{vmatrix} 1 & 1 & 0 \\ 2 & 0 & 2 \\ 4 & 0 & 0 \end{vmatrix} = -3 \begin{vmatrix} 1 & 1 & 0 \\ 2 & 0 & 2 \\ 3 & 0 & 0 \end{vmatrix} - 3 \begin{vmatrix} 0 & 1 & 0 \\ 0 & 0 & 2 \\ 1 & 0 & 0 \end{vmatrix};$$

$$\Delta_1(5) = \begin{vmatrix} 1 & 1 & 0 & 0 & 0 \\ 2 & 0 & 2 & 0 & 0 \\ 3 & 0 & 0 & 3 & 0 \\ 4 & 0 & 0 & 0 & 4 \\ 5 & 0 & 0 & 0 & 0 \end{vmatrix} = 4 \cdot 3 \begin{vmatrix} 1 & 1 & 0 \\ 2 & 0 & 2 \\ 3 & 0 & 0 \end{vmatrix} + 4 \cdot 3 \begin{vmatrix} 0 & 1 & 0 \\ 0 & 0 & 2 \\ 2 & 0 & 0 \end{vmatrix};$$

$$\Delta_1(6) = -5 \cdot 4 \cdot 3 \begin{vmatrix} 1 & 1 & 0 \\ 2 & 0 & 2 \\ 3 & 0 & 0 \end{vmatrix} - 5 \cdot 4 \cdot 3 \begin{vmatrix} 0 & 1 & 0 \\ 0 & 0 & 2 \\ 2 & 0 & 0 \end{vmatrix}$$

Designate:

$$\begin{vmatrix} 1 & 1 & 0 \\ 2 & 0 & 2 \\ 3 & 0 & 0 \end{vmatrix} = A; \quad \begin{vmatrix} 0 & 1 & 0 \\ 0 & 0 & 2 \\ 1 & 0 & 0 \end{vmatrix} = B.$$

It is noticeable that $A=6$; $B=2$.

We have obtained that: $\Delta_1(4) = -3 \cdot A - 3(1-B)$;

$$\Delta_1(5) = -4 \cdot 3 \cdot A + 4 \cdot 3(2B);$$

$$\Delta_1(6) = -5 \cdot 4 \cdot 3 \cdot A - 5 \cdot 4 \cdot 3 \cdot (3B);$$

For every n :

if n is even:

$$\Delta_1(n) = -(n-1)(n-2) \dots 3A - (n-1)(n-2) \dots 3(n-3)B;$$

if n is odd:

$$\Delta_1(n) = (n-1)(n-2) \dots 3A + (n-1)(n-2) \dots 3(n-3)B.$$

If we consider, that $A=6$ and $B=2$, it's noticeable that: when n is even $\Delta_1(n) = -n!$, when n is odd $\Delta_1(n) = n!$

Let's consider initial determinant:

$$\begin{aligned} \Delta(4) &= \begin{vmatrix} 3+3 & 1 & 2 & 3 \\ 1+0 & 1 & 0 & 0 \\ 2+0 & 0 & 2 & 0 \\ 3+0 & 0 & 0 & 3 \end{vmatrix} = \begin{vmatrix} 3 & 1 & 2 & 3 \\ 1 & 1 & 0 & 0 \\ 2 & 0 & 2 & 0 \\ 3 & 0 & 0 & 3 \end{vmatrix} + \begin{vmatrix} 3 & 1 & 2 & 3 \\ 0 & 1 & 0 & 0 \\ 0 & 0 & 2 & 0 \\ 0 & 0 & 0 & 3 \end{vmatrix} = \\ &= 3 \cdot \Delta(3) - 3 \begin{vmatrix} 1 & 1 & 0 \\ 2 & 0 & 2 \\ 3 & 0 & 0 \end{vmatrix} + 3 \begin{vmatrix} 1 & 0 & 0 \\ 0 & 2 & 0 \\ 0 & 0 & 3 \end{vmatrix} = 3 \Delta(3) - 3 \Delta_1(3) + 3 \cdot 3! = 3 \cdot \Delta(3) - 3 \cdot 3! + 3 \cdot 3! = 3 \cdot \Delta(3). \end{aligned}$$

Thus for every n :

$$\Delta(n) = (n-1) \Delta(n-1) \tag{3}$$

and as $\Delta(3)=0$; $\Delta(4)=4$, thus $\Delta(n)=0$ for every n .

It was to be proved.

Thus for graphs "symmetric star" and "asymmetric star" when modelling (1) process (and other analogous transformations), invariant can be the zero value of determinant of pseudocontiguity matrices.

Tbilisi I. Javakhishvili State University

REFERENCES

1. F.Basolo, R.Jonston. Chemistry of Coordination Compounds. London, 1966.
2. P.R.Rouvray. Chemical Application of Topology and Graph Theory. Ed. A. T. Balaban, Amsterdam, 1983.
3. G.Gamziani, N.Kobakhidze, M.Gverdsiteli. Topologic Indexes. Tbilisi, 1995.
4. G.Chakhtauri, M.Gverdsiteli, N.Tsetsadze. Bull. Georg. Acad. Sci., 155, 1, 1997.

G. Makharadze, G. Sidamonidze, T. Khoperia, M. Gudavadze, N. Goliadze

The Infrared Spectrum of Humic Acids Isolated from Sediments

Presented by Member of the Academy G. Tsintsadze, June 6, 1998

ABSTRACT. Humic acids isolated from sediments of lake Kvedrula and Indian Ocean were studied by infrared spectroscopy method. Comparison of IR spectra of humic acids isolated from fresh water and ocean water have shown that there are mainly similar absorption bands in both spectra. Hereby, inessential difference in intensities of absorption bands must be noted.

Key words: humic acids, IR-spectrum.

The goal of this work was comparison of humic acids (HA) isolated from sediments of natural waters (Kvedrula lake and Indian Ocean) by IR spectroscopy method. The infrared spectroscopy method is one of the accepted physical methods to study humic acids [1-3]. Using this method information about content of functional groups, interaction of atoms and atom groups upon their vibrations can be obtained.

Humic acids were isolated from sediments of natural waters by method described previously [4-6]. Extraction was carried out by 0.1N sodium hydroxide. Solution was acidified to pH = 2 and for coagulation of HA it was heated for two hours on the water bath. The HA precipitate was separated from fulvic acids by centrifugation and again dissolved in sodium hydroxide for purification. This process was repeated several times. HA was dried under vacuum.

The IR spectra were recorded with a UR-20 infrared spectrophotometer using KBr pellets. Four grams of each sample were taken.

In the spectra of HA isolated from sediments of Kvedrula lake and Indian Ocean mainly similar absorption bands are marked.

In both spectra in the $3500-3200\text{cm}^{-1}$ region broad signal of OH groups stretching vibrations is observed, which may be caused by adsorbed water molecules as well as by alcoholic and phenolic OH groups.

In the spectra of lake and ocean sediments HA absorption bands of asymmetrical and symmetrical stretching vibrations of methyl and methylene groups occur in the 2900cm^{-1} region (Table 1). Absorption bands of aromatic CH_3 , asymmetrical and symmetrical vibrations of methylene $-\text{CH}_2-(\text{OR})$ and $-\text{CH}_2-(\text{OH})$ bonded to different atoms groups are observed at $2945-2935\text{cm}^{-1}$ and $2865-2820\text{cm}^{-1}$. Also it must be noted, that symmetrical vibration bands of the methyl and methylene bonded to carbonyl group in the $2990-2980\text{cm}^{-1}$ region and CH bond of methine group at the 2885cm^{-1} are distinguished in the spectra of ocean HA in contrast to that of lake. In both spectra methylene absorption bands are stronger in intensities than those of methyl.

In the spectra of both samples occur overlapping in the region 1600cm^{-1} of vibrations

characteristic of different group atoms: wide absorption band may be caused by C—C bond, double C=C and C=O bonds. The presence of carbonyl group in this area mainly is due to conjugation, participation in hydrogen bond, influence of adjacent substituting groups and cycles tension [7]. In the spectra of humin acid isolated from Kvedrula lake peak is centered at 1610 cm^{-1} and in the spectra of Indian ocean sample at 1600 cm^{-1} . Shift of the peak in the lake humin acid spectra may be explained by increasing number of aromatic rings what is confirmed also by intensity and quantity of —C—H bond characteristic deformation vibrations at $900\text{--}700\text{ cm}^{-1}$. Both spectra exhibit ledge in the 1600 cm^{-1} region from high frequency field side what is caused by quinone, ketone, aldehyde and may be by esters stretching vibrations. In the same region at 1625 cm^{-1} spectra exhibits absorption band of water molecules. Also there is asymmetric stretching vibrations of carboxylate ion COO^- at $1600\text{--}1580\text{ cm}^{-1}$ region (low frequency field side) placed on the band mentioned above.

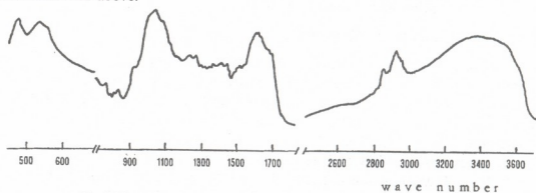


Fig. 1. The IR spectra of humin acid isolated from sediments of Kvedrula lake.

From characteristic bands for polypeptide fragments in the lake humin acids IR spectra just weak absorption band at 1545 cm^{-1} can be pointed out, but this does not except existence of polypeptide components in the studied sample; overlapping of vibrations prevents formation of independent absorption bands characteristic for NH and amide C=O bonds. In the spectra of humin acid isolated from ocean sediments existence of polypeptide fragments may be confirmed by observance of amide-I and amide-I I absorption bands at 1650 cm^{-1} and 1540 cm^{-1} respectively.

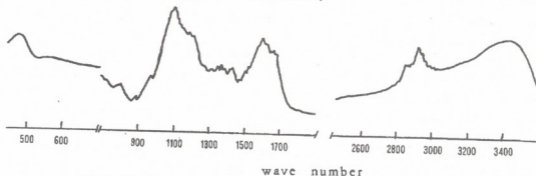


Fig. 2. The IR spectra of humin acid isolated from sediments of Indian Ocean.

In both IR spectra, both shape and intensities of absorption bands at $1495\text{--}1200\text{ cm}^{-1}$ are similar (Table 1).

Table 1

Atom groups and vibrations	Humic acids isolated from sediments of Kvedrula lake, cm ⁻¹	Humic acids isolated from sediments of Indian Ocean, cm ⁻¹
1. OH group participating in hydrogen bond; stretching vibration	3500-3200	3500-3200
2. NH group; stretching vibration	—	—
3. C-H stretching vibration; CH ₃ asymmetric and symmetric;	2955-2950, 2880-2875	2960, 2870
CH ₂ asymmetric and symmetric; CH stretching vibration;	2920, 2850	2920, 2848
CH ₃ aromatic;	—	2885
CH ₂ bonded to different atom groups; stretching vibrations. -CH ₂ -(OR) -CH ₂ -(OH)	2945-2940, 2865-2855	2940, 2855
-CH ₂ -(C=O) -CH ₂ -(C=O)	—	2990-2980
4. quinones, ketones, aldehydes, esters C=O, stretching vibration;	1690, 1578-1665, 1630-1618	1680, 1670, 1638-1618
5. amide I	—	1650
6. aromatic C---C, double C=C, carbonyl C=O, stretching vibration;	1610	1600
7. COO ⁻ asymmetric, stretching vibration;	1600	1595-1585
8. amide II	1545	1540
9. aromatic C---C	1510	1510
10. C-H deformation CH ₃ asymmetric -CH ₂ -(OR) -CH ₂ -(OH)	1480	1480
R-CH ₂ -R	1442	1435
Si-CH ₃	1430, 1420	1420
CH ₃ symmetric	1358	1365
11. COO ⁻ symmetric, stretching vibration;	1400	1390
12. interaction of alcoholic and phenolic C-O stretching vibration and O-H deformation vibration;	1340	1350
13. carboxylic C-O stretching vibration; aromatic acids, esters, phthalates, phenols, ethers;	1296, 1260, 1240, 1230	1270, 1225, 1218
tertiary alcohols;	1155	1210, 1180, 1155, 1135
secondary alcohols, mineral components Si-O	1120	1122, 1112, 1105
primary alcohols, mineral components Si-O	1040	1090
14. polysaccharides	1080	1070
15. ---CH deformation: 1,2-, 1,2,3-, 1,2,4- substituted, hydrogen adjacent two unsubstituted atoms;	920-910	975, 940
hydrogen adjacent three unsubstituted atoms;	835	895
hydrogen adjacent four unsubstituted atoms;	808	808
hydrogen adjacent two unsubstituted atoms;	780	—
16. polysaccharides	750	—
	490	490



The most intensive band in lake sediments humin acid spectrum is observed at 1040 cm^{-1} , but in the spectra of ocean sediments humin acid at 1105 cm^{-1} . This absorption band is formed by O-C-C groups asymmetric stretching vibration of primary alcohols and its esters. High intensity of this band except participation of O-C-C groups may be caused by different mineral components containing Si-O bonds and it is supposed that they are combined to humin acids with chemical bonds.

The $1000\text{-}780\text{ cm}^{-1}$ region exhibits deformation vibrations of aromatic —C-H groups and intensity of this band is high in lake sediments humin acid spectrum. Vibrations at $1080\text{-}1070\text{ cm}^{-1}$ and 490 cm^{-1} confirm the existence of polysaccharides in studied samples.

Thus we can conclude that humin acids isolated from sediments of fresh water and ocean water do not differ from each other.

Tbilisi I. Javakhishvili State University

REFERENCES

1. J.C.Lobartini, K.H.Tan et al. *Geoderma*, **49**, 1991, 241-254.
2. J.A.Leenheer, M.A.Wilson, R.L.Malkolm. *Org. Geochem.*, **11**, 1987, 4, 273-280.
3. Zheng-Di Wang, B.C.Pant, C.H.Langford. *Chemica Acta*, **232**, 1990, 43-49.
4. G.A.Makharadze, G.D.Supatashvili, G.M.Varshal. *Bull. Acad. Sci. GSSR*, **90**, 13, 1978, 625-628 (Russian).
5. G.Makharadze, G.D.Supatashvili, G.M.Varshal. *Hydrochemical materials*, **106**, 1989, 22-30 (Russian).
6. J. Stivenson, J.H.A.Batler. In: *Organic geochemistry*, M., 1974, 389-412 (Russian).
7. R.M.Silverstein, G.C.Bassler, T.C.Morrill. *Spectrometric identification of organic compounds*, M., 1977 (Russian).



R. Kvaratskhelia, E. Kvaratskhelia

Voltammetry of Oxalic Acid at the Solid Electrodes in Aqueous Solutions and Mixed Media

Presented by Corr. Member of the Academy J. Japaridze, June 29, 1998

ABSTRACT. Voltammetry of oxalic acid at the Cu, Cd, Ni, Sn-Cd and Cd-Cu rotating disk electrodes in aqueous solutions and mixtures of water with acetonitrile, ethanol, dimethylformamide and pyridine has been studied. The kinetic parameters of the hydrogen ions discharge process proceeding in the solutions of oxalic acid and second dissociation constants of this acid in aqueous and mixed solutions have been determined.

Key words: oxalic acid, voltammetry, electrode, wave, dissociation constant, organic solvent.

Electrochemical behaviour of dicarboxylic acids has been studied on the whole in polarographic conditions [1]. The data on their voltammetry at the solid electrodes and in mixed media are hardly available.

The measurements were carried out by the methods of voltammetry at the rotating disk electrodes and chronovoltammetry at the stationary electrodes from high-purity Cu, Cd, Ni and alloys Sn-Cd (80% Sn) and Cd-Cu (28% Cu) in the sealed cell with a pure helium atmosphere. Technique of a preparation of the electrodes for the measurements has been described in [2]. The background electrolyte NaClO₄ has been twice recrystallized from a bidistillate and then has been dried for several days at 190°C. Oxalic acid has been also twice recrystallized from a bidistillate. Technique of purification and drying of used organic solvents - acetonitrile, ethanol, dimethylformamide and pyridine has been described in [3]. The saturated calomel electrode has been used as a reference electrode. The measurements have been carried out at 20°C.

Oxalic acid in 0.1M NaClO₄ at all the used electrodes forms well-defined waves; their $E_{1/2}$ values are equal to -0.95V(Cu), -0.74V(Ni), -1.27V(Sn-Cd), -1.43V(Cd-Cu) and -1.50V(Cd). These values are close to the $E_{1/2}$ values for a hydrogen ions discharge process in 0.1M NaClO₄ with 0.001N H₂SO₄; this fact gives us a possibility to attribute these waves to this process (in our conditions the electroreduction of oxalic acid to glyoxylic or glycolic acids described in some works [4] is not observed). In Fig. 1 the voltammograms of H₂C₂O₄ for various electrodes are presented. For all the used electrodes the $i_{lim} = -\sqrt{\omega}$ linear relationship is observed; this fact testifies to proceeding of a process in diffusion regime. In the case of copper electrode the chronovoltammograms with well-defined current peaks have been registered; with the aid of the parameters of these peaks the k_0 rate constants have been calculated. In Table 1 the values of peak

potential E_p , αn (calculated with the aid of Matsuda-Ayabe equation) and rate constant k_0 for the solutions of $H_2C_2O_4$ and H_2SO_4 are presented. The closeness of the parameters presented in the table is an additional evidence of proceeding in both cases of the hydrogen ions discharge process

Table 1

Acid	$-E_p, V$	αn	$k_0, \text{cm/s}$
$H_2C_2O_4$	1.16	0.313	$6.23 \cdot 10^{-9}$
H_2SO_4	1.17	0.340	$1.34 \cdot 10^{-9}$

Electrochemical behaviour of $H_2C_2O_4$ has been also studied in the mixtures of water with acetonitrile, ethanol, dimethylformamide and pyridine. Addition of organic component causes the gradual decrease of the $H_2C_2O_4$ wave height which is more pronounced in the mixtures of water with ethanol and dimethylformamide and comparatively weakly in the water-acetonitrile system. This fact testifies to an important role of the increase of viscosity of the mixtures with the rise of organic component content. The small additions of high-basic pyridine (0.0005-0.001M) cause the sharp decrease of the $H_2C_2O_4$ wave height and a significant shift of $E_{1/2}$ values in the negative direction. When the pyridine content is equal to 0.002-0.1M, the change of the wave height and $E_{1/2}$ values is less noticeable. These facts are accounted for a quantitative proton resolution; in consequence the hydrogen ions are in the form of pyridinium cations, when the pyridine concentration exceeds 0.002M (concentration of $H_2C_2O_4$ is equal to 0,001M).

The results of the study of $H_2C_2O_4$ voltammetry in water and water-organic mixtures give us a possibility to determine the concentration of hydrogen ions and to estimate the dissociation constants of oxalic acid. The latter belongs to a group of dibasic acids which have a comparatively small difference between first and second dissociation constants (in the case of $H_2C_2O_4$ the $(pK_a''-pK_a')$ value is equal to 3 [5]). This fact can be a reason of simultaneous proceeding of both dissociation steps. Our data show that the average value of i_d in 0.1M $NaClO_4$ with 0.001M $H_2C_2O_4$ is equal to $2.537 \cdot 10^{-3} A/cm^2$; the similar value in 0.1M $NaClO_4$ with 0.001N H_2SO_4 is equal to $2.3 \cdot 10^{-3} A/cm^2$ (this value corresponds to 0,001M concentration of hydrogen ions). Hence the hydrogen ions concentration in 0.1M $NaClO_4$ with 0.001M $H_2C_2O_4$ is equal to $1.103 \cdot 10^{-3} M$. This value shows that a dissociation of $H_2C_2O_4$ proceeds not only on first step, but also on second step; the H_3O^+ ions concentration connected with second step is equal to $1.03 \cdot 10^{-4} M$. The $C_2O_4^{2-}$ ions concentration is the same; than the $HC_2O_4^-$ ions content is equal to:

$$[HC_2O_4^-] = 0.001M - [C_2O_4^{2-}] = 8.97 \cdot 10^{-4} M$$

With the aid of the concentration values of these ions second dissociation constant of $H_2C_2O_4$ has been calculated:

$$K_a'' = \frac{[H^+][C_2O_4^{2-}]}{[HC_2O_4^-]} = 1.266 \cdot 10^{-4} \quad (1)$$

($pK_a''=3.90$). Taking into account that $[C_2O_4^{2-}]=[H^+]-C$ and $[HC_2O_4^-]=C-[C_2O_4^{2-}]=2C-[H^+]$ (where C is the total concentration of $H_2C_2O_4$), we obtain an equation which connects second dissociation constant, concentration of hydrogen ions and total concentration of

acid (for the case of dibasic acid with the comparatively close values of first and second dissociation constants when a dissociation on first step is complete):

$$K_a'' = \frac{[H^+]\{[H^+] - C\}}{2C - [H^+]} \quad (2)$$

Equation (2) may be presented as quadratic equation:

$$[H^+]^2 + (K_a'' - C)[H^+] - 2CK_a'' = 0 \quad (3)$$

For an experimental proof of validity of K_a'' value with the aid of equation (3) the $[H^+]$ values for the various concentrations of $H_2C_2O_4$ have been calculated and compared with the corresponding experimental values. One can see from Fig. 2 that the experimental and calculated values are very close.

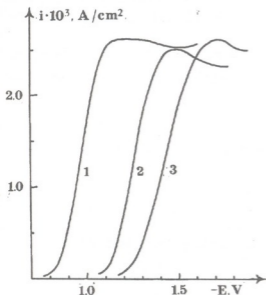


Fig. 1. The voltammograms of oxalic acid at the rotating disc electrodes. 0.1M $NaClO_4$; $10^{-3}M$ $H_2C_2O_4$; 1050 r. p. m. 1 -Cu; 2 -Sn-Cd (80% Sn); 3 -Cd.

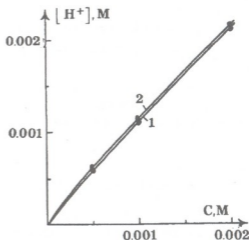


Fig. 2. The dependence of the hydrogen ions concentration in the solutions of oxalic acid on $H_2C_2O_4$ concentration. 0.1M $NaClO_4$; 1050 r. p. m. 1 - values calculated from equation (3); 2 -experimental values.

The values of second dissociation constant of $H_2C_2O_4$ have been also calculated in the used in our work water-organic mixtures (it is necessary to note that these values are hardly available in literature). The values of pK_a are presented in Table 2.

Table 2

C_{org} % (vol.)	pK_a'' of $H_2C_2O_4$		
	acetonitrile	ethanol	dimethylformamide
10	3.66	3.58	3.72
20	3.76	3.59	3.93
30	3.88	3.84	4.25
40	3.79	3.97	4.09
50	3.49	3.65	3.86
60	3.56	3.33	3.45

The data presented in Table 1 show that in the broad interval of the binary mixtures contents the pK_a values do not undergo sharp changes. This fact is connected with a comparatively small difference between a basicity of water and used organic solvents: it is also necessary to note that dielectric permeability of mixtures in the used interval of their contents is sufficiently high.

It has been mentioned above that when pyridine content in the water-pyridine mixture exceeds 0.002M the limiting current values change is not so noticeable. The hydrogen ions concentrations in this region are equal to $1.61 \cdot 10^{-3} M$ (0.005M pyridine), $1.8 \cdot 10^{-3} M$ (0.01-0.05M) and $2 \cdot 10^{-3} M$ (0.1M) when the $H_2C_2O_4$ concentration is equal to 0.001M. The K_a values are equal correspondingly to $2.52 \cdot 10^{-3}$ (pK_a 2.6), $7.2 \cdot 10^{-3}$ (pK_a 2.14); in 0.1M pyridine case acid is completely dissociated. Such rise of second dissociation constant of $H_2C_2O_4$ is connected with a high basicity of pyridine (the values of dielectric permeability in the conditions of the small concentrations of pyridine are not practically changed).

This study is fulfilled within the framework of 1998 Grant of the Georgian Academy of Sciences. Authors are also grateful to E. Shevardnadze Fund for a grant to one of the authors.

Georgian Academy of Sciences

R. Agladze Institute of Inorganic Chemistry and Electrochemistry

REFERENCES

1. *L.Eberson*. In: *Electrochemistry of organic compounds*. Moscow, 1976 (Russian).
2. *R.K.Kvaratskhelia, T.S.Machavariani*. *Elektrokhimiya*, **20**, 3, 1984, 303.
3. *R.K.Kvaratskhelia, M.G.Zhamierashvili, H.R.Kvaratskhelia*. *Elektrokhimiya*, **28**, 12, 1992, 1869.
4. *Catalytic, photochemical and electrolytic reactions*. Moscow, 1960.
5. *O.J.Neiland*. *Organic chemistry*. Moscow, 1990. (Russian).

G. Agladze, G. Gordadze, N. Koiava, N. Nioradze

Experimental Study of Current and Potential Distribution on Bipolar Electrode

Presented by Corr. Member of the Academy J. Japaridze June, 29, 1998

ABSTRACT. The method of simultaneous measurement of current and potential at different sites of bipolar electrode surface consisted of vertically displaced current feeder sectors is offered. It is shown that the correlation of the current and potential distributions of this method is distinguished from those ones established by the other methods. In order to explain this discrepancy some considerations are advanced.

Key words: bipolar electrode, three dimensional electrode, dispersed system.

A transition from the parallel flat electrodes to the dispersed three-dimensional electrodes, where the effective surface area increased and the transport of mass, charge and heat quickens is the actual task of contemporary applied electrochemistry. In theoretical and experimental investigations the most difficult step is to establish macro-kinetic properties of the process occurred on the particles surfaces. Great attention is paid to three-dimensional dispersed system, where both anodic and cathodic potentials are realized on each particle.

To solve the problem step by step, it is expedient to determine current and potential distribution on separate unitary electrode of the electrochemical system, which is influenced by cell geometry, mass and charge transfer, electrical conductivity of the solution and by value of polarizing field. In such systems the indirect way of experimental measurement of current density distribution is possible. In particular, by counting the corresponding current densities of the potentials fixed on the surfaces of bipolar electrodes on the polarization curves plotted in monopolar regime. This method enables redox processes taken place on bipolar electrode surfaces to be partly characterized.

Fig. 1. Arrangement for potential scanning on the surface of bipolar electrode: (1) electrolytical cell; (2, 3) current feeders; (4) tested sample; (5) energy source; (6) reference electrode of Ag/AgCl; (7) Luggine capillary; (8) micro-thread mechanism; (9) high Ohm voltmeter; (10) ampermeter; (11) wires; (12) electric scheme for current measurement.

We have developed an original system of improving the above mentioned method, which allows to measure values of current densities immediately at the potentials fixed on the surface of bipolar electrode. A sample

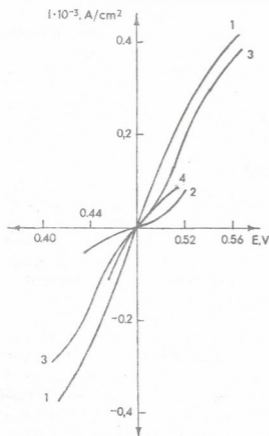


Fig. 2. Relationship between potentials and current densities on platinum electrode in monopolar (1) and bipolar (2, 3, 4) regimes at 2 - 10 mA; (3) 25 mA - ten sheets; (4) 25 mA, five sheets.

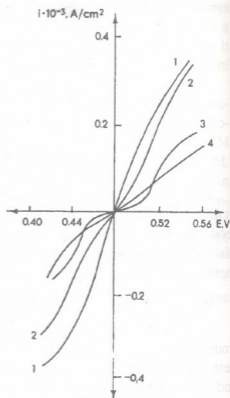


Fig. 3. Relationship between potentials and current densities on platinum electrode in bipolar regime at a polarizing current of 25 mA. (1) central electrode; (2) electrode shifted to the anode feeder on 50 mm; (3) electrode shifted to the cathode feeder on 50 mm; (4) electrode shifted to the cathode feeder on 100 mm.

to be tested consisted of two platinum sheets of 1.9×1.7 mm and it was fixed on the organic glass plate in the intervals of 2 mm. They were connected electrically out the solution composing so the unified bipolar electrode. A special electrical scheme allowed to measure the current on each sheet.

The electrode to be tested was placed in the cell of 200×50 mm parallel to the electric field lines. The 50 mm of length platinum sheets placed in the perchlorvinyl diaphragm used as current feeders, Ag/AgCl as a reference electrode. Results are counted regarding the normal hydrogen electrode. Luggine capillary shifted along the electrode by means of facility for potential scanning. The scheme of the arrangement is given in Fig. 1.

In order to obtain reproducible and accurate experimental results a redox system was used: ferro-ferricyanide in solution of 0.5 molle/l K_2SO_4 . The concentrations in each redox couple were 0.015 molle/l. Measurements were made at temperatures of 20-25°C. The redox potential of the system was measured to control the solution composition. Stationary polarization curves were plotted by means of complex apparatus consisted of potentiostat and Programmator.

In Figure 2 curve 1 E-I relationship of platinum electrode in monopolar regime is shown. Curves 2 and 3 represent potential and current density correlation on the surface of bipolar electrode consisted of ten sheets in the cell at the currents of 10mA(2) and

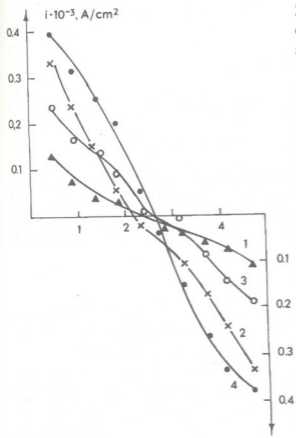


Fig. 4. Current density distribution on whole length of bipolar electrode. 1, 2 - measured by electrical scheme at the currents of 10 mA and 25 mA; 3, 4 - plotted on indirect way by means of polarization curve.

fact, that in monopolar regime the potential defining whole current passes through the electrode, while in case of bipolar mode of work only the part of it. It can be assumed that such nonconformity is caused by strong influence of Ohmic drop on the values of potential measured in bipolar systems, which can not be excepted because of the presence of tangential field.

25 mA(3). On curve 4 the E-I relationship of the test-electrode consisted of five sheets at 25 mA is expressed.

The curves in Fig. 3 are plotted at a current of 25mA when the bipolar electrode of ten sheets is placed in the middle of the cell (curve 2), when the bipolar electrode is placed near the cathode (curve 3), and when it is 50 mm from the centre of cell to the anode (curve 4).

In Figure 4 a current distribution at the whole length of bipolar electrode consisted of ten sheets at the currents of 10 mA (curve 1) and 25 mA (curve 2) are given and also the curves obtained by superposition of E-L relationships of bipolar electrode upon those of monopolar electrodes.

Experimental results indicate that polarizing current, bipolar electrode length and its position in the cell influence relationships which exists between potential and current density measured at the surface of bipolar electrode.

It is established that the corresponding values of current densities for the same potentials are higher in monopolar regime than in bipolar one. It can be explained by the

Georgian Academy of Sciences
R. Agladze Institute of Inorganic Chemistry and Electrochemistry

REFERENCES

1. G.R.Agladze. Electrosyntezy oksislitelei i elektrokhimicheskaia ochistka stochnykh vod.. Tbilisi, 1994, 220 (Russian).

D. Shengelia

Again about the Atsgara Tectonic Wedge

Presented by Member of the Academy I.Gamkrelidze, July 6, 1998

ABSTRACT. As a result of critical consideration of a number of geologic-petrological diagnostic features the Pre-Jurassic age of the Atsgara tectonic wedge (ATW) was established. The granitoids of the ATW attributed to the potassium series and like the Late Hercynian granites of the Dzirula crystalline massif represent the products of melting of sialic crust.

Key words: tectonic wedge, granitoid.

The Atsgara tectonic wedge (ATW), represented mainly by granitoids, has been exposed in Abkhazia, in the gorge of Atsgara river on the Southern Slope of the Greater Caucasus within the Chkhalta-Laila structural zone, in the Liassic sediments.

The Atsgara granitoids initially have been considered as some small intrusives, cutting Liassic and Bajocian formations. Later in 1973 [1] it was established, that the granitoids form an integral narrow (250-400m) body, which stretches for a 15km. At the same time it turned out, that with the granitoids the outcrops of schists, plagiogneises, plagiomigmatites, quartzites and amphibolites are spatially connected, the aggregate of which forms the tectonic wedge of Pre-Jurassic crystalline basement in the Liassic sediments. According to the data of the same authors granitoids and migmatites are transgressively overlain by basal conglomerates of Liassic sediments. In the pebble of conglomerates, along with the predominant quartz, the existence of plagiogranites, plagiogneises, quartz-muscovite-chlorite shales are also noted. It is also mentioned that the granitoids have cataclastic structure, are mylonitized and within them the intensive processes of muscovitization are developed. The age of these processes, determined in muscovites by K-Ar method, corresponds to the Pre-Upper Carboniferous (324 ± 12 and 341 ± 14 Ma).

The Paleozoic age of the ATW rocks is also confirmed by the following investigations [2-4], though on the several geological problems the different opinions was expressed. We believe the ATW not to be similar to the metamorphites and granitoids of Makera series, against A. Okrostsvaridze's opinion, because the results of the recent investigations [5,6] confirm, that the Makera tectonic sheet represents the upper part of the Buulgen series, overthrust from the South to the North - from the Pass subzone to the Elbrus subzone at the Late Hercynian time. According to our observation the schists of the ATW by their composition essentially differ from the metamorphites of the Buulgen series and don't represent its direct, unbroken part, as it has been mapped by O.Khutsishvili. According to the previous consideration the ATW is attributed to the Pre-Jurassic basement of the Greater Caucasus [1-3]. We believe it to be a tectonic wedge of the crystalline basement in the Liassic sediments on the northern margin of the Dzirula subterrane [7].

Based on the investigations of 1977-78 M.Topchishvili and G.Lobzhanidze [8] recently again supported the Bathonian age of the Atsgara granitoids that is determined by the following data: the thermal influence of granitoid massif on the host rocks - their contamination, the existence of granite apophyses and of xenoliths of host liassic rocks in the granitoids; the main, the most major component rock of the Atsgara granitoid body is the Bathonian granite, and microcline and muscovite varieties existing in them represent included Paleozoic formations; the Late Hercynian figures of radiometric measurements of the muscovites of the Atsgara granitoids appear to represent the age of muscovites of the Paleozoic granitoids including the main granitoids of Bathonian age; the presence of anorthoclase in the granitoids, the mineral, characteristic for "neointrusions"; typical granites, as a rule, are found only in the middle part of the outcrop, while on the periphery they are represented by microgranite or granite-porphyre; Liassic basal conglomerates, situated on the ATW and found by the previous investigators [1,4], according to their opinion represent "unrecognized" breccia-conglomerates and can not confirm the transgressive overlapping of the Sinemurian, on the granite-migmatites.

Our interpretation of data differs from the opinion of M.Topchishvili and G.Lobzhanidze and proves the initial opinion[1] of the Pre-Jurassic age of the ATW. We consider, that the opinion of the above mentioned authors about the thermal influence of granitoids on the host rocks are rather general. The neomineralization in the host rocks, caused by the contact-thermal influence of granitoids is not marked at all. The phenomenon of contamination is also mentioned in general terms, but the petro-mineralogical diagnostic of its determination is not given. As for "xenoliths" of wall rocks in granitoids and existence of "apophyses" of granite in the host rocks are concerned, as it was mentioned above [1], that they present the typical tectonic breccias and boudinated bodies, arised from dynamometamorphism. The granitoids of the ATW in the contact zone with the wall rocks are more intensively broken down, milonitized and brecciated, than in the central part (graniteporphyres and microgranites have not been found anywhere) and wall rocks are striped by glide planes. It is not even explicated what the so-called "main-the most general" rocks - the Middle Jurassic granitoids are and what is the difference between them (except for the content of "anorthoclase") and "included" granitoids. As for the presence of anorthoclase in the Atsgara granitoids, it has been proved only by a single result of optical measurement, carried out by G.Zaridze - (001); $-2V 61-66^\circ$ ([9],p.116). But these optical constants don't define a mineral as anorthoclase. The value of $-2V 61-66^\circ$ even according to the previous meaning doesn't eliminate microcline. Along with it the wide spread of only lattice microcline in the granitoids of the ATW is noted in many publications [1,3,etc]. According to R.Manvelidze in the granitoids of the ATW according to the data of the statistic processing of K-spars spread, it is elucidated that the lattice microcline reaches for 60-70% and non-lattice type K-spars $-2V$ as a rule is more than $70-75^\circ$ and only 3 times it had lower significance ($60,67$ and 68°).

Muscovite and microcline are the main rockforming minerals for the Pre-Jurassic granitoids of the Greater Caucasus, but don't play the role in the Jurassic intrusive bodies of the Main Range zone of the Greater Caucasus and its Southern Slope. The presence of the minerals in the Bathonian granitoids of the ATW by means of mechanism of "inclusion" of the Paleozoic granites is not proved by any data.

If one assumes that the Bathonian muscovite "from the Paleozoic granitoids included in the host granitoids" is radiometrically defined, it would be clear that as it is characteristic for K-Ar method, for the Paleozoic granitoids, thermally altered by the Bathonian granitoids we would have the more young Jurassic figures and not the Paleozoic ones.

Besides of the quartz pebbles, which are predominant in the basal conglomerates, located on the schists and migmatites of the ATW, the pebbles of schists, plagiogneises and plagiogranites [1] have been established, but it is not mentioned by authors, who name them "nonidentified" breccia-conglomerates. Attention is drawn to the fact that in the conglomerates there is no material of the Liassic sediments. Presumable age of the conglomerates is Sinemurian [1,4], as the basal beds of the Southern Slope of the Greater Caucasus usually are Sinemurian. It is not excepted that the Paleozoic formations and overlapping directly on them intensively broken down conglomerates co-build the ATW, or may be there is a Late Pliensbachian Transgression on this location.

The granitoids of the ATW and the Liassic magmatites of the Southern Slope of the Greater Caucasus greatly differ in the mineral-petrographic characteristics, which are characterized by pronounced gibrizim (assimilation and contamination) alien to granitoids of the ATW; wide spread and variety of quartz diorites, which transit to granitoids and sometimes of genetically associated intermediate and basic rocks and their xenolithes; transition into the porphyroid, granophyric and micropegmatitic textures, wide spread of hornblende and zonal plagioclase and absence of muscovite; the low degree of regulating of potassium feldspar.

It should be noted that granitoids of the ATW by their composition practically don't differ from the fourth exposure of the Pre-Jurassic basement - the Nenskra (Upper Svaneti) tectonic wedge of muscovite- -microcline granitoids, recently found again within the Chkhaltal-Laila zone, in the contact zone of the western periclinal termination of Dizi series and in the contact zone of Liassic sediments [10].

Thus, the analysis of the geological and petrological data show, that the studied granitoids and associated metamorphites constitute the tectonic wedge of the Pre-Jurassic crystalline basement in the Liassic sediments.

Georgian Academy of Sciences
 A.Janelidze Geological Institute

REFERENCES

1. O.Z.Dudaury, D.N.Ketskhoveli, M.G.Togonidze, D.M.Shengelia. Bull. Acad. Sci. Georg. SSR, 71, 1, 1973 (Russian).
2. Sh.A.Adamia. Trudy Geolog. Inst. AN GSSR, 86, 1984 (Russian).
3. A.V.Okrostsvaridze. Bull. Acad. Sci. Georg. SSR, 133, 2, 1989 (Russian).
4. O.D.Khutsishvili. Doctor thesis, Tbilisi, 1993 (Russian).
5. I.P.Gamkrelidze, D.M.Shengelia, G.L.Chichinaidze. Bull. Acad. Sci. Georg. SSR, 154, 1, 1996.
6. D.M.Shengelia. Trudy Geolog. Inst. AN GSSR, 110, 1998 (Russian).
7. I.P.Gamkrelidze. Bull. Georg. Acad. Sci., 155, 3, 1997.
8. M.Topchishvili, G.Lobzhanidze. Bull. Georg. Acad. Sci., 157, 1, 1998.
9. G.M.Zaridze. Petrography of Magmatic and Metamorphic Rocks of Georgia. Moscow, 1961 (Russian).
10. D.Shengelia, M.Gagnidze, A.Kvitsiani. Bull. Georg. Acad. Sci., 155, 3, 1997.



M.Chelidze

Influence of Electromagnetic Disturbing Force on Dynamic Stability of Vibration

Presented by Member of the Academy R. Adamia, May 25, 1998

ABSTRACT. In the present paper, on the basis of theoretical analysis and solution of differential equation of magnetic flow describing the disturbing electromagnetic force of vibration machine main harmonics causing nonlinear resonance regimes have been revealed.

Key words: differential equation, oscillation system.

Simple design, full absence of rubbing surfaces, and big reliability creates a broad possibility of using electromagnetic vibration machines in different branches of national economy. In spite of multiple work the influence of disturbing force on the stability of these machines is studied insufficiently. Particularly, its role in the process of generating the nonlinear resonance regimes is not clear.

Differential equation system of oscillatory motion of the electromagnetic machines is as follows [1]:

$$\ddot{x} + 2hx + \omega_0^2 x = a\psi^2, \quad (1)$$

$$\dot{\psi} = b \sin \omega t - c(\delta - x)\psi, \quad (2)$$

For highly small or completely absent mechanical oscillation displacement the equation was solved in [1]:

$$\psi = \frac{b\omega}{(c\delta)^2 + \omega^2} e^{-c\delta t} + b \frac{c\delta \sin \omega t - \omega \cos \omega t}{(c\delta)^2 + \omega^2}. \quad (3)$$

The analysis of equation (3) shows that the square-law member $a\psi^2$ of equation (1) does not express correct role in the process of generating of the nonlinear resonances and it is found in the literature in the same form. Certainly, when feeding a magnet only by the direct currents $\omega = 0$ (that is the same $b\sin \omega t = u_0$) tractive magnet force $F = a\psi^2$ is changed square-law. However in case of alternating current ($\omega \neq 0$) in the presence of the inductance of spools the variable δ causes back proportional changing in inductive resistance ωL . Thus tractive force of electromagnet becomes practically independent of δ . For instance, under $\omega = 0$ according to the equation (3) $\psi = u_0/\delta$, but under $\omega \neq 0$ and $\delta = 0$ it takes the following form:

$$\psi = \frac{b}{\omega} - \frac{b}{\omega} \cos \omega t. \quad (4)$$

Equation (4) shows that magnetic flow in a magnet core is sharply limited because of



the presence of inductance of spools in it. Member b/ω exists only in the moment of starting the machine and is referred to fading part of equations (3).

Equation (2) is formed for linear magnetization area. Magnetic resistance in the core is ignored [2] so functional dependency between ψ , δ and x is linear.

On the basis of the aforesaid, for the determination of the influence of air clearance δ on the dynamics of vibration machine it is reasonable to solve equation (2) analytically. For simplification of mathematical calculation on the first stage let us use $a\psi^2$ instead of harmonic disturbance in the form of $a \sin \omega t$. Analytical decision of equation (1) in such case is:

$$x = Ae^{\alpha t} \sin(\omega_0 t + \varphi_0) + A_{(\omega)} \sin(\omega t + \varphi), \quad (5)$$

$$\text{where } \dots A_{(\omega)} = \frac{a}{m\sqrt{(\omega_0^2 - \omega^2)^2 + \alpha^2 \omega^2}}.$$

With the increase of t the first harmonics in (5) tends to zero ($\alpha = -h < 0$). After substituting (5) in (2) with account of the above said, the latter may be solved analytically with respect to ψ

$$\begin{aligned} \psi = & \frac{b}{\omega} - \frac{bc^2(\delta - A_{(\omega)} \sin \varphi)^2 t}{\omega^2} \sin \omega t + \dots \\ & \dots - \frac{b}{\omega} \cos \omega t + \frac{bc(\delta - A_{(\omega)} \sin \varphi)}{\omega^2} \sin \omega t + \dots \end{aligned} \quad (6)$$

In the process of integrating subintegral function was factored in a power series [3]. So the obtained analytical solution (6) is presented in a power row. Members including δ , A and ω are not taken into account in high power because of their smallness

$$\psi = \frac{b}{\omega} - \frac{bc^2(\delta - A_{(\omega)} \sin \varphi)^2 t}{\omega^2} \sin \omega t + \dots, \quad (7)$$

Similarly to the first member of equation (3) the first members of equation (6) now (7) present fading components of disturbing force and exist only on starting the vibrator. The members of equation (7), whose amount is limited are presented as an independent time parameter t in a power series. Consequently, in order to avoid mistakes the process of solving should be broken for $t < \omega t^2 \delta$ or equation (7) should be levelled with zero. Thereafter, transitional process connected with the starting of the machine is considered completed

$$\psi = -\frac{b}{\omega} \cos \omega t + \frac{bc\delta}{\omega^2} \sin \omega t - \frac{bcA_{(\omega)} \sin \varphi}{\omega^2} \sin \omega t + \dots \quad (8)$$

Really, with the increase of t the first member tends to zero in (3). Consequently, oscillatory process is supported only by the second member.

From the equation (8) it follows that the first member $(b/\omega)\cos\omega t$ plays main role in the oscillatory process. For example, for $b = 0.2+0.3$; $c = 300+500$; $\delta = 0.002+0.004$; and $\omega = 314$ corresponding to 50 Hz turn out to be in 200+300 times greater in quantity than



parametric resonance. It is testified by multiple results obtained by mathematical simulating and experimental studies.

For the simplification of calculations without the essential error it is possible to change a differential equation system by one equation, or leave in the right part of (1) only the main member stimulating only one basic resonance

$$\ddot{x} + 2h\dot{x} + \omega_0^2 x = -a \frac{b^2}{\omega^2} \cos^2 \omega t, \quad (11)$$

Finally, it should be noted that in certain regimes in electromagnetic machines, including electric motors and generators, the presence of air clearance in circuits of magnetic flow can cause vibrations as well as parametric resonance with increasing amplitudes of oscillation.

Georgian Academy of Sciences
R. Dvali Institute of Machine Mechanics

REFERENCES

1. *M. Chelidze*. Bull. Georg. Acad. Sci., **156**, 2, 1997, 266-267.
2. *B. I. Kriukov*. Dynamics of vibratory machines, Kiev, 1967, 210 (Russian).
3. *N. S. Piskunov*. Differential and integral calcul, Moscow, 1974, 575, (Russian).
4. *V. L. Biderman*. Theory of mechanical oscillations, Moscow, 1980, 410 (Russian).
5. *V. C. Popov*. Theoretical electrical engineering, Moscow, 1975, 550 (Russian).

V. Kashakashvili

On the Optimal Structure of Georgian Power System

Presented by Member of the Academy V. Chichinadze, February 1, 1999

ABSTRACT. Electric power original cost mostly depends on power system structure, or on the ratio of hydropower output to thermal power output. With the structural index 0.6 for Georgia the change-over of the thermal power plant from imported fuel-firing to captively produced fuel would cut down electric power original cost by 17.1%, whereas the change-over from thermal power plant to nuclear power plant would make 56% electric power original cost reduction.

Key words: power system, electric power, water power plant, thermal power plant.

Since 1987 water power plants (wpp) of Georgia have generated more power than thermo-power plants (thpp). Mean annual output ratio P_{wpp}/P_{thpp} made 60% within 1980-1998. It would be interesting to estimate if there is or will be possibility to achieve such optimal ratio of $P_{wpp}/P_{thpp(npp)}$ for the net cost of generated electric power to be minimal.

With this object in view some work has been done on the Georgian power system model, employing the simplified graphs of electric power plant [1]. The power system output was constant (20 billion kwh) and power output ratios of presently operating water power plants, thermal power plant and nuclear power plant designed for future operation. P_{wpp}/P_{thpp} and P_{wpp}/P_{npp} were variables. The 70% of the total power was generated by reservoir (and 30% by seasonal water power plants. The above proportion was constant all the time. It is to be noted that there have been two alternatives of thermal power plant operation, burning either imported (Fig. (thpp1)) or captively produced fuel (Tkibuli coal suspension) (Fig. (thpp2)).

In view of the above considerations and on the basis of the data given in [1, 2] the following calculations have been performed. 1. Power plant installed capacity N has been determined by annual operating time (1500 h for reservoir power plant, 3500 h for seasonal water power plant and 6000h for thermal and nuclear power plants). 2. Power plant capital investment K has been determined by respective specific capital investment US\$2600/kw for reservoir power station, US \$ 1500/kw for seasonal power plant and US \$ 1500 /kw and US \$ 2250/kw for thermal and nuclear power plants, respectively; 3. Power plant operating costs B have been determined multiplying K by transfer factor (0.07 for thermal power plant, 0.08 for nuclear power plant, 0.045 for reservoir power station and 0.03 for seasonal power plant).

Fuel and transportation expenses thereof have been incorporated in thermal and nuclear power plant total operating costs. The transportation of imported fuel (fuel oil, natural gas), needed for the generation of 1 billion kw·h. electric power in Georgia, has been valued at 36 million \$ US. With the fuel produced captively, the above-mentioned costs are 1.24- and 4.1 fold reduced in case of nuclear fuel.

Table

	Name		$P_{wpp}/P_{thpp(npp)}$			
			1.0	0.9	0.7	0.5
1	Annual output million kw.h	Wpp	20.000	18.000	14.000	10.000
		water storage	14.000	12.600	9.800	7.000
		Seasonal	6.000	5.400	4.200	3.000
		Thpp (1)				
		Thpp (2)		2.000	6.000	10.000
2	Capacity, Mw Annual	Wpp	1106	934	774	552
		water storage	935	840	654	466
		Seasonal	171	154	120	86
		Thpp (1)				
		Thpp (2)	-	33.3	100	166.5
3	Capital investment Million \$ US	Wpp	2686	2411	1880	1339
		Seasonal	2430	2180	1700	1210
		Thpp (1)	256	231	180	129
		Thpp (2)	-	50	150	250
		Npp	-	75	225	375
4	Operating costs Million \$ US	Wpp	128.7	105	81.9	58.4
		water storage	121.0	98.1	76.5	54.5
		Seasonal	7.7	6.9	5.4	3.9
		Thpp (1)	-	3.5	10.5	17.5
		Thpp (2)				
5	Fuel and transportation costs Million \$ US	Wpp	-	-	-	-
		Thpp (1)	-	72	216	360
		Thpp (2)	-	58	174	280
		Npp	-	17.6	52.6	87.7
		6	Total operating costs Million \$ US	Wpp	128.7	105
Thpp (1)	-			75.5	226.5	377.5
Thpp (2)	-			61.5	184.5	297.5
Npp	-			23.6	70.6	117.7
7	Power system annual operating costs Million \$ US			wpp/Thpp (1)	128.7	182.5
		wpp/Thpp (2)	128.7	166.5	266.4	355.9
		wpp/npp	128.7	129.6	152.5	176.1
8	The costs of 1 kw.h. generated in power system, cent/kw.h	wpp/Thpp (1)	0.64	0.92	1.54	2.18
		wpp/Thpp (2)	0.64	0.88	1.33	1.78
		wpp/npp	0.64	0.68	0.76	0.88

The results of calculations are summarized in Table.

A set of curves in the Figure shows dependence of the power cost on the ratio of power outputs of $P_{wpp}/P_{thpp(npp)}$. All these lines extend from the point with the ordinate $P_{wpp}/P_{thpp(npp)}=1$, which is taken only for the case of 20 billion. kw.h hydropower output. Under these circumstances electric power original cost is minimal, comprising 0.64 cents. The intersection of X-axis by the lines extending from the common point determines the cost of power generated by npp or by thpp burning captively produced or imported fuel. For

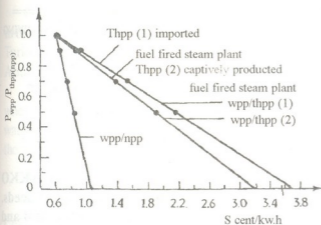


Fig. Electric power original cost vs power system structure diagram

For example, the original cost of power for Georgian power system with the structural index 0.6, which is the annual average for the recent 19 years, is 1.87 cents. Thus, with the same structural index, the change-over from the imported to captively produced fuel will reduce the original cost of electric power generated in power system down to 1.55 cents, the figure being 17.1% of that presently available. At the same time, the change-over from thermal power plant to nuclear power plant will reduce the original cost of electric power generated in power system down to 0.82 cents, the figure being 56% of that presently available.

In view of the above analysis it can be concluded that thermal power plant burning imported fuel is unprofitable and unacceptable for Georgian power system to generate base electric power.

Change-over the thermal power plant for captively produced fuel or building nuclear power would outperform imported fuel building power-plant by a factor of 1.21 and 2.25 respectively.

In our opinion base electric power generation at water power plant (for instance, base power plant operating on flow partially transferred from river Tergi to river Aragvi) or the coupling of water storage plant with reservoir power plant [2] to be the best solution of the problem, coming in line with the strategy of hydropower priority utilization in Georgia. It should be noted that a number of countries utilize only the power generated of water power plants are a good case in point. For example, Norway, whose population is lesser than ours, in 1993 generated power of 120 billion kwh, that surpasses our corresponding index by 11.8. If the power generated in Norway by the hydropower stations in the mentioned year made 99.6%, in Georgia its share was only 69%.

Georgian Technical University

REFERENCES

1. V. Kashakashvili. *Energia*, 3, 1998 (Georgian).
2. V. Kashakashvili. *Energia*, 3, 1999 (Georgian).

these cases electric power original cost is maximal, comprising respectively 1.1; 2.9 and 3.7 cents. The analysis of the cost of curves presented in Fig. shows that a steep fall can be observed in the original cost of electric power generated in power system with the rise of hydropower generation specific share. The larger the latter, the smaller is the drop. With constant power system structural index, the smaller its value, the steeper is the fall of electric power original cost from wpp/thpp (Fig.) to wpp/npw.

N. Lomtadze

Biological Peculiarities of Seeds Germination of Japanese Medlar Turkish Varieties in Humid Subtropical Zone of Georgia

Presented by Corr. Member of the Academy P. Naskidashvili, January 29, 1999

ABSTRACT. The following Turkish varieties of Japanese medlar: Armut, AKKO XIII and Taza were described biomorphologically. Germinating capacity of seeds, growth dynamics and biometric indices of seedlings have been studied at the first and second years of vegetation in humid subtropical zone of Georgia.

Key words: *Eriobotria japonica* Lindl., germinating capacity, biometric indices, humid subtropical zone.

Japanese medlar *Eriobotria japonica* L. is a fruit-bearing valuable subtropical culture. Its native land is South-Eastern Asia, namely China, where it grows wildly in eastern coastal provinces of Sichuan and Chekiang [1].

According to Vilmoren, Chinese origin of the Japanese medlar is proved by the fact that this culture has another name - Loukwat (it is a South Chinese pronunciation) which in English was transformed as Lokuat.

Japanese medlar is widely spread in Himalai and North India both in culture and wildly. It is cultivated in nearly all subtropical regions including the Black Sea coast of Georgia [2].

Medlar is divided into two main genealogical branches: Chinese and Japanese groups. Fruits of Chinese group are thick, pearshaped, orange, white, have fleshy pulp and ripen comparatively late. Fruit of Japanese group is smaller, round, yellow, it has less fleshy pulp, and ripens early [2].

According to Francesco de Rosa (1913), medlar was first brought to Europe from Japan in 1784 by the French. This plant was first brought to Turkey from Algeria and Lebanon 150-200 years ago, and in the Black Sea coast of Georgia it first appeared in early 70s of the last century. It is supposed that medlar was brought to Russia from Japan by A.Krasnov and I.Klingen's expedition [3].

Humid subtropical zone of Georgia (Adjarian and Abkhazian seaside) can be considered as the main spreading region for Japanese medlar, where it grows and gives much crop.

Japanese medlar deserves attention not only as a fruit-bearing plant, but also as an ornamental plant. With its fragrant flowers, long, leather-like leaves and nicely branched crown it creates wonderful background and is therefore used for town, plantation roads and avenue greenery. From this aspect its spreading area is almost unrestricted.

In the dry subtropical conditions of the Mediterranean coast of Antalya the Japanese medlar blooms and gives fruits comparatively early than in the Black Sea humid subtropical zone. Particularly it blooms in Antalya in September-November and gives fruits from April till May, but in our country it blooms in October-December and gives fruits in May-June. This is caused by differences in soil and climatic conditions [4].

Our aim was to study germinating and biometric indices of seeds of Turkish varieties in the changed new surroundings and conditions. For this purpose seeds of the following Turkish varieties had been introduced in and planted at the Batumi Botanical Gardens: Armut, AKKO, Taza.

AKKO XIII, Gold nuggets, Hafif Cukurgobek - seeds were planted in 4-5 cm depth beds where soil temperature was 20-30°C and air temperature 25-30°C. In normal nursing and watering conditions they began growing after 25-27 days. Germinating ability according to the varieties ranged between 8.2-9.0%, variability - between 5.2-7.5% (Table 1).

Table 1

Seeds of Medlar Turkish varieties

As it is shown in Table 1, among Turkish varieties of medlar the variety Hafif Cukurgobek is characterized by the highest germinating ability, and the variety AKKO

Name of variety	Date of planting	Number of seeds	Duration of germination (days)	Number of germinated seeds	Variability, %
Armut	20.07	150	338	136	9.0+5.4
AKKO	20.07	145	40	120	8.2+5.2
Taza	20.07	105	44	92	8.7+7.5

XIII - by low ability. Duration of germination ranges between 38-44 days.

Dynamics of germination and biometric indices of Turkish varieties of the first and second years of vegetation have also been studied.

The average height of the above-land part of the seedlings received at the end of the first vegetation period ranges between 25.1-30.0 cm, the crown diameter ranges between 8.4-10.5 cm, the number of side branches is 2-3, the crown diameter at the root is 1.0-1.2 cm, the number of the leaves is 7-10. Size of the leaves is changeable and varies between 7x2.5 cm - 10x3.1 cm (Table 2).

Table 2

Biometric indices of seedlings at early stage

Name of variety	Number of measured plants	Average length of the above-land part		Diameter of the stem		Number of side branches		Diameter of trunk at the root		Number of the leaves		Size of the leaves (length x width)	
		1year old	2years old	1year old	2years old	1year old	2years old	1year old	2years old	1year old	2years old	1year old	2years old
Armut	136	30.0	90.0	10.5	25.4	3	5	1.2	4.0	10	18	10x3.1	30x5
AKKO	120	28.0	85.7	9.7	23.5	2	4	1.1	3.8	8	15	9x2.8	28x4
Taza	92	25.1	78.2	8.4	18.2	2	3	1.0	3.5	7	11	7x2.5	26x4

At the end of the second vegetation period medlar seedlings have 3-5 side branches and their height reaches from 78.2 cm to 90.4 cm, number of the leaves is 11-18, size from - 26x4 cm to 30x5 cm. Diameter of the crown reaches from 18.2 cm to 25.4 cm (Table 2).

Armut is an early variety, in Antalya climatic conditions it ripens at the beginning of April. Fruit is round oval shaped, of medium size, reddish-orange, tasty and sweetish. It is of medium transportability, steady against diseases. A 15-20 year old tree-plant gives

1000-1200 kg crop. Taza is of medium season, it ripens at the end of April and at the beginning of May. The fruit is pear-shaped, thick, dark reddish-orange, very tasty and sweet. It is characterized by good transportation ability and steadiness against diseases. A 15-20 year old plant gives 1300-1400 kg crop. AKKO is a late variety, it ripens at the end of May. The fruit is round, apple-shaped, yellowish-orange, of medium size, tasty and sweetish, transportable and steady. A 15-20 years old tree-plant gives 1200-1300 kg crop [4].

Thus, after studying Turkish varieties of Japanese medlar - Armut, AKKO XIII, and Taza it had been established that they are characterized by high germinating indices in our humid subtropical conditions. Peculiarities of appearing, growth and development of the seed greatly depend on climatic and soil conditions as well as on the size of the seed, namely, seedlings produced from thin seeds are weak and lag behind in growth. Differences noticed in the intensity of growth between the breeds give possibility of underdeveloped form selection.

From our observations we can conclude that Turkish varieties of Japanese medlar are well adjusted to humid subtropical conditions of Georgia and characterized by high growth rate which gives basis for their introduction.

Georgian Academy of Sciences
Batumi Botanical Gardens

REFERENCES

1. G. Gutiev. Subtropicheskie plodovie rastenia. M., 1958, 224 (Russian).
2. A. Dragavtsev. Mushmula vostochnaya. Plodovodstvo v Kitae. M., 1966, 166-170 (Russian).
3. Francesco de Rosa. Il Nespolo del Gjappone. Napoly, 1913, 323 (Italian).
4. T. C. Tarim orman ve Koyisleri bakanligi. Narenciye arastirma enstitüsü mudürlüğü. Yenidunya yetistiriciligi. Senes Demir. Antalya, 1987, 31 (Turkish).



I. Grigolia, A. Tsitsvidze

Some Peculiarities of Pine Growth, Development and Cultivation in Eastern Georgia

Presented by Corr. Member of the Academy G.Nakhutsrishvili, March 8, 1999

ABSTRACT. It was revealed that water deficiency is the main limiting factor for growth and development of pine species introduced in Eastern Georgia. Specimens of three pine species are numerous here. Five species propagate by fallen seeds.

Key words: introduced pines, water deficiency, seed-bearing, propagation, adaptation, drought.

Pine (*Pinus L.*) represents one of the oldest genera of gymnosperms. The Jurassic [1] or earlier period [2] is believed to be a time of its origin. About 100 species of this genus have been preserved up to now. They are spread in northern hemisphere and one species reaches the equator [3]. Three species of pine naturally grow in Georgia.

Introduction of pine in Georgia has been going on since the end of XIX century. At present 37 species of pine are introduced in Adjarian Black Sea coast (Batumi Botanical Gardens). Subtropical pines such as *Pinus patula P.montezumae* (Mexico), *P.canariensis* (Canary Islands), *P.roxburgii* (Himalayas), *P.palustris* (Northern America) etc., grow well here. All of them flourish here and aren't limited in growth. Lots of them propagate also by fallen seeds (*P.pinaster*, *P.taeda*, *P.rigida*, *P.strobus*, *P.griffithii*, *P.thunbergii*, etc.).

In 1996-1998 we have studied peculiarities of growth, development and spreading of pine species introduced in Eastern Georgia (Borjomi, Tbilisi, Telavi). The aim of research was to determine the level of pine adaptation in conditions of Eastern Georgia and to reveal drought tolerant species.

The following indices were determined: plant height, number of individuals and phenology. Plurality was established according to the plant number. Particularly, number of individuals on the studied territory less than 10 was considered to be little and marked off as "+". If number of individuals varied among 10 and 100, it was considered as medium and marked off as "(+)", Number of individuals prevailing 100 was regarded to be plural and marked as "(++)".

In phenological observations special attention was paid to the generative phase of pine individuals, particularly to the ability for seed-bearing and seed germination. Seed-bearing individuals were designated by the symbol "++", while the individuals able for seed germination in natural conditions by the symbol "+++".

Due to the differences of vital factors the number of species introduced in Eastern Georgia (20 species, Table) is less than in Adjaria. During the period under study the absolute minimum temperature in Tbilisi attained to -9.3°C, annual amount of precipitations - to 380-560 mm, which is insufficient for woody plants. The most acute water

deficiency was registered from May till the October, when humidity factor was less than 2, and during July-August this index dropped to 0.2-0.5.

It is known that at the humidity factor below the 1.5 the plant isn't supplied with water. At the humidity factor less than 1 water deficiency is well-defined [4]. In addition, in the course of vegetation the relative atmospheric humidity sharply decreases and very often equals 15-10%, aggravating water deficit of plants.

Table
Pine growth and development in Eastern Georgia

	Species	Borjomi		Tbilisi		Telavi		Generative development
		Maximum height, m	Plurality	Maximum height, m	Plurality	Maximum height, m	Plurality	
1	<i>Pinus kochiana</i>	23.0	⊕	18.0	⊕	18.0	⊕	+++
2	<i>P. griffithii</i>	20.0	+	22.0	+	26.0	+	+++
3	<i>P. cembra</i>	-	-	-	-	10.0	+	++
4	<i>P. pallasiana</i>	22.0	⊕	20.0	⊕	23.0	⊕	+++
5	<i>P. pinea</i>	16.0	+	15.0	⊕	20.0	+	++
6	<i>P. sabiniana</i>	-	-	18.0	+	17.0	+	++
7	<i>P. sylvestris</i>	23.0	+	15.0	+	18.0	+	+++
8	<i>P. strobus</i>	18.0	+	8.0	+	21.0	+	++
9	<i>P. pityusa</i>	20.0	+	30.0	⊕	21.0	+	++
10	<i>P. eldarica</i>	15.0	⊕	8.0	⊕	14.0	⊕	+++
11	<i>P. coulteri</i>	-	-	9.0	+	3.0	+	++
12	<i>P. radiata</i>	-	-	10.0	+	-	-	++
13	<i>P. rigida</i>	-	-	3.0	+	-	-	-
14	<i>P. taeda</i>	-	-	4.0	+	5.0	+	++
15	<i>P. armandii</i>	-	-	4.5	+	-	-	++
16	<i>P. pinaster</i>	20.0	+	20.0	⊕	15.0	⊕	++
17	<i>P. thunbergii</i>	-	-	-	-	8.0	+	++
18	<i>P. mugo</i>	-	-	3.0	+	2.0	+	++
19	<i>P. halepensis</i>	-	-	18.0	+	-	-	+++
20	<i>P. bungeana</i>	-	-	10	+	-	-	++

Plurality
+ low < 10
⊕ medium
⊕ plural > 100

Generative renewal
++ seed bearing
+++ species able for seed germination in nature

The following pine species: *P.kochiana*, *P.eldarica* and *P.pallasiana* (Crimean species) are widely used in decorative gardening and forest plantations of Eastern Georgia. The first two species also grow naturally in Georgia. All of them are well adapted to edaphic and climatic conditions of Eastern Georgia, which makes possible their further cultivation. Though in 1996-1997 in Tbilisi environs and especially in Tbilisi Botanical Gardens rather great number of Crimea pine *P.pallasiana* and several specimens of *P.kochiana* had dried-up in the age of 60-100. This might be caused by the water deficiency, since the mentioned period was characterized by rather heavy drought and watering was significantly humpered.

Relatively high adaptation ability is characteristic of two-needled pines except *P. pinaster* and *P. thunbergii* requiring high humidity of the atmosphere and soil. Water deficiency is the main factor limiting their growth in Eastern Georgia. The former of the two above mentioned species is relatively widely used in Tbilisi greenery, despite the fact that its representatives often dry-up in the age of 40-50. *P. bungeana* grows better than other three-needled pines (*P. sabiniana*, *P. coutleri*, *P. radiata*, *P. taeda*). About the same adaptation ability is characteristic of *P. sabiniana* and *P. coutleri* pines. Though *P. sabiniana* reveals the signs of early aging in the age of 40-50 (one specimen has even dried) and the second species (*P. coutleri*) is marked by extremely low growth rate. As regard to five-needled pines: *P. griffithii*, *P. strobus*, *P. armandii*, the first grows and develops relatively well. In Tsinandali the height of its specimens prevails 20-25 m and diameter reaches 90-100 cm. In Tbilisi the specimens of the same species (*P. griffithii*) attain to 20-22 m height, propagate by fallen seeds but require the regular watering during vegetational period. Presumably the water deficiency has caused the drying-up of several unwatered pine-trees in Tbilisi Botanical Gardens during the droughty period of 1996-97 years. *P. griffithii* sharply differs from other pine species by its decorative importance and further cultivation seems to be possible. As for *P. strobus*, morphologically close to *P. griffithii*, it suits badly to East Georgian conditions due to which its wide spreading is unpromising. This is the only species of *Pinus* genus resistant to shading but is unadapted to direct sun radiation and soil dryness in lowland. It may be cultivated only on the territories where annual precipitations make 800-1000 mm and relative atmospheric humidity during vegetational period doesn't fall below 70%. *P. armandii* is almost unadapted to climatic conditions of Eastern Georgia and, especially, of Tbilisi. This species was repeatedly tested but high atmospheric temperature and water deficiency caused its drying-up.

Specimens of *P. kochiana*, *P. pallasiana* and *P. eldarica* pines are often found at the Tbilisi Botanical Gardens, Likani and Tsinandali parks. In medium quantity are found representatives of *P. pinea*, *P. pityusa* and *P. pinaster* at the Tbilisi Botanical Gardens and specimens of *P. pinaster* in Tsinandali park.

P. kochiana, *P. griffithii*, *P. pallasiana*, *P. sylvestris*, *P. eldarica* and *P. halepensis* are found to be well propagated by seeds, while the others (*P. cembra*, *P. pinea*, *P. sabiniana*, *P. strobus*, *P. pityusa*, *P. coulteri*, *P. radiata*, *P. taeda*, *P. armandii*, *P. pinaster*, *P. thunbergii*, *P. mugo* and *P. bungeana*) have not such ability.

Thus, based on the study of pine plantations in parks of Eastern Georgia one may conclude that the following pine species are adapted to the ecological conditions of this region best of all (*P. kochiana*, *P. griffithii*, *P. pallasiana*, *P. sylvestris*, *P. eldarica*, *P. halepensis*) being expressed in high reproductive ability of their seeds.

Georgian Academy of Sciences
 Tbilisi Central Botanical Gardens

REFERENCES:

1. K. L. Alvin. Mem. Inst. Roy. Sci. Natur. Belg. 146, 1982, 1-39.
2. C. N. Miller. Amer. J. Bot. 70, 5, 2, 1983, 75.
3. G. M. Kozubov, E. N. Muratova. Sovremennye golosemnyye. Leningrad, 1986 (Russian).
4. G. T. Selyaninov. Perspektivy subtropicheskogo khozyaistva SSSR v svyazi s prirodnyimi usloviyami. Leningrad, 1961 (Russian).



M. Iashvili, N. Melia, L. Gbedava, L. Zhgenti

On Ultrastructural Study of Somatic and Generative Cells in Some Subnival Belt Plants of Kazbegi

Presented by Corr. Member of the Academy G. Nakhutsrishvili, August 10, 1998

ABSTRACT. Ultrastructure of the embryo sac (before and after fertilization), nucellar cells, pollen grain and anther wall layers in the following subnival belt (3100 m.a.s.l.) plants of the Central Caucasus: *Saxifraga flagellaris* Wild, *Potentilla gelida* C.A.May, *Cerastium polymorphum* Wild. and *Veronica telephiiifolia* Vahl. have been investigated. The complex of ultrastructural indexes ensures adaptability of plants to the severe alpine climate conditions due to the manoeuvring metabolism.

Key words: *Cerastium polymorphum*, *Potentilla gelida*, *Saxifraga flagellaris*, *Veronica telephiiifolia*.

Subnival belt of the Central Caucasus despite its poor floral constitutions is characterized by high variety of vital forms [1]. Investigating some plants of this region, adapted to the extreme conditions, we have studied embryo sac (before and after fertilization), nucellar tissue, pollen grain and anther wall layer cells ultrastructural organization in the following subnival belt plants of the Central Caucasus (3100 m.a.s.l.): *Saxifraga flagellaris* Wild. (*saxifragaceae*), *Potentilla gelida* C.A May (*Rosaceae*), *Cerastium polymorphum* Rupr. (*Caryophyllaceae*) and *Veronica telephiiifolia* Vahl. (*Scrophulariaceae*).

Material was fixed in 3% glutaraldehyde with postfixation in 2% osmium tetroxide, embedded in mixture of Epon-812 and Araldit-M. The sections were cut on LKB-III ultratome and examined with EM-200 electron microscope.

The investigation of the embryo sacs has shown, that the development of the female sexual sphere of the plants is limited. In major cases megagametophyte is not formed at all, or its development is depressed on different stages. In spite of this, the certain amount of normal, capable for fertilization embryo sacs are formed, the percentages of which is very small in *Potentilla gelida* 5-10%, in others it varies from 39 to 56 %.

The comparative analysis of the ultrastructural data has revealed some distinguishes, as well as some similarities among the same components of different plant embryo sacs. That permits to speak about their common features. The egg nucleus has condensed chromatin in all plants and contains large nucleolus, where granular component is well developed. The egg cytoplasm is saturated with organelles. Mitochondria are polymorphous in *Veronica telephiiifolia*, great number of active dictyosomes occur near the egg nucleus. Long membrane of rough endoplasmic reticulum (RER) and microbodies are generally seen in the egg of *Cerastium polymorphum* and *Saxifraga flagellaris*. Lipid bodies are numerous in *Cerastium polymorphum*. Hypersecrete Golgi bodies placing about the polar nuclei, zone of ergastoplasm, microbodies, great amount of mono and

polysomes, circular bodies, osmiophilic contents in vacuoles, large starch grains - are generally seen in central cell cytoplasm of all plants.

The embryo sacs structural peculiarities were noticed especially in the constructions of their surrounding walls and cell walls of egg apparatus (Fig.1).

Significant reorganization occurs in the fertilized embryo sac, particularly in the cell wall system inside the embryo sacs and covering envelopes. Extension of all membrane systems (Fig.2), plasmalemma and outer membranes invaginations, great concentration of starch and lipid bodies in the endosperm cells, are all found within embryo sacs after fertilization.



Fig. 1. Egg apparatus cells walls of *Veronica telephifolia* (embryo sac before fertilization).



Fig. 2. Embryo sac wall of *Veronica telephifolia* (after fertilization).

Nucellar tissue is well developed in all the experimental plants, (Fig.4) except *Veronica telephifolia*, which has integumentary tapetum around the embryo sac.(Fig.3). Somatic cells showed the organelle saturation, varying configuration of mitochondria and plastids, well developed Golgi bodies and ER, abundance of ribosomes, formation of the structured vacuoles, myeline like bodies and dense inclusions. It should be noted some peculiarities of investigated plants: *Cerastium polymorphum* is characterized by more developed plastidome, *Saxifraga flagellaris* - chondriome, *Potentilla gelida* and *Veronica telephifolia* - both of these systems. Minimal amount of the osmiophilic inclusions occurs in *Veronica telephifolia*.



Fig. 3. Integumentary tapetum of *Veronica telephifolia*.

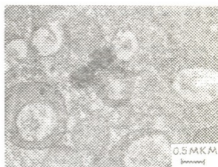


Fig. 4. Nucellar cell of *Saxifraga flagellaris*

The development of the male sphere is normal and goes on without any considerable divergence from the typical ones. The numerous organelles, particularly mitochondria, lamellar bodies and reserve compounds, frequent plastid invaginations, extension of the perinuclear membrane area, dictyosomes with large associated vesicles, have been noticed

at all stages of the pollen development. Mitochondria concentration observing near the nucleus of microspore, may be interpreted as the evidence of producing and accumulating of energy by mitochondria, necessary for the microspore division, as well as another their possible function as a result of the influence of extreme alpine conditions [2]. Our observations revealed also the occurrence of plastids in generative cell of *Potentilla gelida* (Fig. 5). There is not the same opinion in literature about the presence of plastids in generative cell. Some authors deny this fact [3], others admit it [4]. It is reasonable to assume, that the occurrence of plastids in generative cell may represent species feature, although the dependence on growing conditions must not be excepted completely.

In the anther wall cells at the stage of mature pollen grain very active plastidome, chondriome and RER are seen (Fig. 6).



Fig. 5. Vegetative and generative cells of the pollen grain in *Potentilla gelida*.



Fig. 6. Anther fibrous layer cell of *Cerastium polymorphum*.

Considering our complex investigation data, it should be pointed out, that ultrastructure of the somatic cells is richer than of sexual ones. Both types of the cells (sexual and somatic) are characterized by well developed various membrane system, including myelin-like bodies which may be both the indicator of the cell's synthetic activity [5] and the manifestation of the adaptive mechanism and cell's non-specific reactions upon outer influence [6,7]. In our opinion, neither of the structural elements may be determinative in the adaptation processes. The complex of ultrastructural indexes ensures adaptability of plants to the severe alpine climate conditions due to the manoeuvring metabolism.

Georgian Academy of Sciences
 N. Ketskaveli Institute of Botany

REFERENCES

1. G. S. Nakhutsrishvili, Z. G. Gamtsemlidze. Zhizn rastenii v ekstremalnikh usloviakh visokogorii, L., 1984 (Russian).
2. E. A. Miroslavov, S. Bubolo. Bot. J. 11, 65, 1980 (Russian).
3. J. Heslop Harrison. J. Cell Sci., 3, 1968.
4. P. Ronald. Amer. J. Bot. 64, 1977.
5. E. L. Kordium. Cytology, 35, 10, 1993.
6. E. B. Matienko, V. P. Mashanski, B. G. Matienko. Bot. Journ. 62, 2, 1977 (Russian).
7. R. M. Crawford. Trans. Bot. Soc. Edinburgh, 44, 1982.



Member of the Academy T. Oniani, N. Darchia, I. Gvilia, N. Lortkipanidze,
L. Maisuradze, L. Oniani, M. Eliava, V. Moliadze

The Effect of Food Deprivation on the Sleep-Wakefulness Cycle in Rodents

Presented October 12, 1998

ABSTRACT. The effect of food deprivation on the sleep-wakefulness (S/W) cycle was studied by 24h polygraphic recording in rodents (rat, guinea pig). It has been demonstrated that food motivation cannot exert a specific influence on the need for sleep and the S/W cycle deranged by hunger recovers to its normal pattern still during food deprivation.

Key words: food deprivation, sleep-wakefulness cycle, guinea pig, rat.

The interaction of the two biologically such important motivations as sleep and hunger has not been finally clarified. It has been reported that there is a definite correlation between the amount of consumed food and sleep duration. It has also been supposed that the two types of behavior may have one or several common modulators [1]. Siegel's findings indicating the existence of correlation between food amount and paradoxical sleep (PS) are also noteworthy [2]. Hunger induced changes in the structure of the S/W cycle have been studied by Jacobs and McGinty [3] on a rat model. It has been shown that rat's S/W cycle is rather stable in relation to food deprivation. Namely, initial reduction of PS amount is followed by the recovery of a normal ratio of the S/W phases. In the experiments of these authors only very prolonged hunger (11 days) resulted in the death of animals.

In order to clarify the interrelation and interaction of sleep and food motivations, we have studied the effect of hunger on the S/W cycle in two different representatives of rodents, rat and guinea pig.

Methods. Experiments were carried out on adult adapted rats and guinea pigs. Surgery for the implantation of electrodes was performed under nembutal anaesthesia (40-60 mg/kg). The coordinates for stereotaxic localization of the electrode tips were chosen from the atlas of Bureš [4] for rats and Voitenko, Marlinski [5] for guinea pigs. Electrodes were chronically implanted in the motor and suprahypocampal areas of the cerebral cortex. Oculomyogram was recorded via constantan electrode implanted in the oculomotor muscle. Apart from polygraphic recordings of the 24h S/W cycles, permanent visual observations were made on the animals behavior.

After the establishment of the stable background S/W cycle total food deprivation was begun. It lasted 6 days and nights for rats and 5 for pigs. Animals were given water *ad libitum*. After the cessation of food deprivation, recording of the cycle continued until the recovery of a stable background level.

The changes in the S/W cycle structure resulting from food deprivation were compared with the respective background level and were treated statistically. Validity of difference in mean values was determined by Student's T-criterion.

Results and Discussion. The S/W cycle of rats appears more or less stable to 6-day total food deprivation, although some hunger induced changes are in evidence. In particular, on the 2nd and 3rd day after food deprivation the amount of wakefulness (W) increases at the expense of a decrease in the amount of slow wave and PS (Fig. 1). Fluctuation of phase ratio is insignificant in the following days, while on the 6th day after deprivation the amount of W reincreases. In spite of reduction of sleep phases there was no total reduction of PS. Shortly after the cessation of food deprivation the normal structure of S/W recovered (Fig. 1,6) on the background of which there occurred a marked rebound of PS. It should be noted that the changes described above appeared more pronounced in the rats which as shown by visual observations, were more emotional.

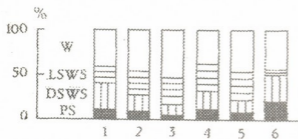


Fig. 1. Hunger effect on the ratio of the S/W cycle in rats. Column 1 - background; the following 4 columns - the S/W cycle structure on the 1st, 2nd, 3rd, 4th day after food deprivation; column 6 - structure of the S/W cycle after cessation of the 6-day food deprivation. Designations: W - wakefulness, LSWS - light slow wave sleep, DSWS - deep slow wave sleep, PS - paradoxical sleep.

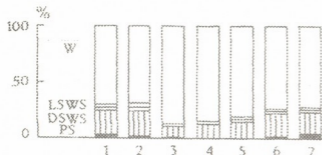


Fig. 2. Hunger effect on the ratio of the S/W cycle in guinea pigs. Column 1 - background; the following 5 columns - structure of the S/W cycle during 5 days of food deprivation consecutively; column 7 - structure of the S/W cycle after cessation of food deprivation. Designations are the same as in Fig. 1.

The changes arising in the S/W cycle structure after food deprivation may be explained as follows: hunger results in the enhancement of emotional tension of the body that *per se* activates the central mechanisms of W. While this latter causes inhibition of sleep mechanisms on the reciprocal principle which is followed by reduction of amount of slow sleep and consequently of PS. Thus, in spite of the existence of the demand for sleep, its development is hindered because of enhanced excitability of the W system. This is suggested by the fact that in relatively calm animals the ratio of phases in the S/W cycle remained more stable during hunger.

In view of emotionality dependent stability of the S/W cycle in relation to food deprivation, we determined to study the effect of hunger in such a phobic representative of rodents as is a guinea pig. The result is that the S/W cycle of guinea pigs is far more susceptible to hunger effect. Indeed it appeared that on the 2nd and 3rd day after food deprivation there occurred a sharp decrease in slow sleep amount and a total reduction of PS (Fig. 2). On the 4th day

of the experiment stabilization of the S/W cycle starts, while on the 5th virtually recovers the structure specific for the S/W cycle of this animal. After the cessation of food deprivation

vation (6th day) against the background of a normal structure of S/W there is a rebound of PS. Taking into account that the S/W cycle of guinea pigs by itself is less structured and characterized by frequent arousals [6] it becomes evident that hunger induced enhancement of emotionality and anxiety can effectively activate the W system. Because of this there would actually occur sleep deprivation and accumulation of quota of slow sleep required for triggering PS would be impeded. During sleep deprivation, on the other hand, accumulation of internal needs for sleep occurs. As soon as this need attains the critical level, the internal mechanisms of sleep become so activated that they are able to inhibit the W system even on the background of its increased excitability, leading to the recovery of the S/W cycle to its normal pattern.

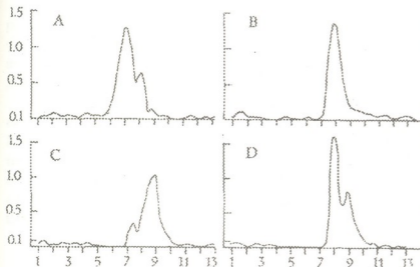


Fig.3. Hunger induced amplitude-frequency change of the hippocampal theta rhythm during PS in rats. On the axis of abscissa frequency in Hz, on the axis of ordinate relative amplitude. A - background, B - 3 days after the start of food deprivation, C - after 6 days, D - 12h after cessation of food deprivation.

amplitude gets augmented from 230 to 340 μ V (Fig.4). These changes in the hippocampal electrical activity persist during 24h after offset of food deprivation.

Hunger induced activation of the W system and an increase in the hippocampal theta rhythm intensity, on the one hand and PS rebound after offset of food deprivation, on the other, are in terms of the postulate about the availability of biological needs during PS (emotional stage of PS) and imitation of their satisfaction (nonemotional stage) [7] and indicate that PS must be involved in the regulation of levels of motivation processes during wakefulness subsequent to sleep. Moreover, the fact that such a principal biological need as the need for food is, cannot exert a considerable influence on the S/W cycle of rodents and its

Hunger induced activation of the W system and enhancement of excitability are suggested also by frequency analysis of electrohippocampograms during PS. In particular, in rats hippocampal theta rhythm, as compared to the background level (7Hz), is characterized by a higher (8-9 Hz) index (Fig.3). As regards the guinea pigs, the frequency increases negligibly, while the ampli-

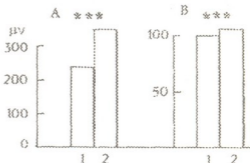


Fig.4. Hunger effect on the amplitude of hippocampal theta rhythm (A) and frequency (B) during PS in guinea pigs. Column 1 - background level, column 2 - 5th day of deprivation. Amplitude is shown in μ V *** - $p < 0.001$.

normal pattern recovers still against hunger, suggests that food motivation cannot exert a specific influence on the need for sleep in general and for PS in particular.

The changes recorded in structure of the S/W cycle during enhanced food motivation should be due to the transition of the excitability triggering link of the W system to a high level resulting in a considerable suppression of the appetitive phase of sleep as one of the major forms of instinctive behavior. Consequently the appearance of the consummative phase of sleep is delayed. Thus the system of sleep fails to inhibit effectively the W system and it takes a definite time for the central mechanisms of sleep system to start optimal work via gradual accumulation of internal needs.

Georgian Academy of Sciences
I. Beritashvili Institute of Physiology

REFERENCES

1. *J. Danguir, S. Nicolaidis.* *Physiol. Behav.*, **22**, 4, 1979, 735-740.
2. *J. Siegel.* *Physiol. Behav.*, **15**, 1975, 399-403.
3. *B. Jacobs, D. McGinty.* *Exp. Neural.*, **30**, 2, 1971, 212-222.
4. *J. Bures, M. Petran, J. Zachar.* *Electrophysiol. Methods in Biol. Research*, Prague, 1967.
5. *L. Vojtenko, V. Marlinski.* *Nejrofiziologia*, **1**, 1, 1993, 52-76 (Russian).
6. *T. Oniani, N. Darchia, I. Gvilia, M. Eliava.* *Bull. Georg. Acad. Sci.*, **156**, 1, 1997, 113-117.
7. *T. Oniani.* The integrative function of the limbic system, Tbilisi, 1980, 132-149, (Russian).



G. Mikadze, M. Melikishvili, Member of the Academy M. Zaalishvili

The Tropomyosin Molecule Domain Potentiating Actomyosin Contraction

Presented June 15, 1998

ABSTRACT. The investigation of the influence of rabbit skeletal muscle tropomyosin and rabbit antibodies against the chicken gizzard muscle tropomyosin on the contractile properties of rabbit skeletal muscle actomyosin has shown that antigene and antibodies act identically- they both potentiate contraction, that means that they must have sites of similar construction.

Considering this fact and literary data about the antigene sites of rabbit skeletal muscle, chicken breast, cardiac and gizzard muscles tropomyosins we supposed the localization of domain of tropomyosin molecule which is responsible over the potentiation of actomyosin contraction. It corresponds to fragment of tropomyosin molecule which can be obtained by cleavaging the tropomyosin molecule using the cyanogenbromide - CNBr-1 and contains the part of tropomyosin molecule from 11 to 126 amino acid residues inclusively.

Key words: tropomyosin, actomyosin, antibodies, antigenes.

Tropomyosin is the necessary component of muscle contractile system. In striated and cardiac muscle tropomyosin with troponin create the system which "switches on" and "off" the actin-myosin interaction depending on the Ca^{2+} ions concentration [1]. The physiological role of tropomyosin in this process is inhibitory [2]. On the other hand, besides the regulation of actin-myosin interaction tropomyosin also potentiates the contractive process of actomyosin of striated and smooth muscles [3].

The present article studies the domains of tropomyosin molecule which might cause potentiation while actin-myosin interaction.

Myosin has been obtained according to Perry [4], actin - according to the modified method of Spudich [5] - from rabbit striated muscles. Tropomyosin has been obtained from chicken gizzard muscle according to the method for obtaining of protein M [6], which then happened to be tropomyosin [7]. The obtaining of actomyosin film fibres and measuring of their contractile ability has been carried out according to Zaalishvili and Mikadze [8]. The antibodies against chicken gizzard muscle has been produced in rabbit.

In the article of Ierne there was mentioned an interesting fact that antibodies produced by rabbit organism as the result of bringing the antigene in it, might themselves resemble these antigenes alien to them [9]. This fact was somehow confirmed in our experiments.

We obtained antibodies against chicken gizzard muscle tropomyosin produced in rabbits. The study of these antibodies influence on the contractile properties of rabbit

skeletal muscle actomyosin showed that they acted like the antigens (tropomyosin) - that is they potentiated actomyosin contraction (Figure). From those observations it obviously follows that antibodies and antigens must have the sites of similar construction. It allows to suppose about the localization of the tropomyosin domain responsible for the potentiation of contraction.

The molecule of tropomyosin consists of two α -helical subunits. These subunits differ from each other by electrophoretic mobility and are called α and β tropomyosins. Tropomyosin exists in the form of homo- and heterodimers. The subunit construction reflects the type of the muscle it is isolated from [10]. The cardiac and chicken breast muscles tropomyosin include only α -chains and they are called α -tropomyosin [11].

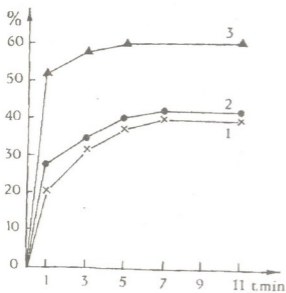


Fig. The influence of antibodies against chicken gizzard muscle tropomyosin on the film fibres contractivity (%) of rabbit skeletal muscle reconstructed actomyosin (myosin/actin 4:1):

1 - actomyosin + serum of normal rabbit; 2 - actomyosin; 3 - actomyosin + serum of antitropomyosin.

The consistence of the area 0.05M KCl, 10^{-4} M $MgCl_2$, 0.02M veronal-potassium buffer pH 7.5; $5 \cdot 10^{-3}$ M ATP.

and vice versa. Considering that CNBrB2 is the antigene site of tropomyosin and our observations that rabbit antitropomyosin produced against chicken gizzard muscle potentiates contractile properties of rabbit skeletal muscle actomyosin, the tropomyosin site localized in the CNBrB1 area is supposed to be the domain responsible for the activation of actomyosin contraction.

To such supposition we came by indirect way. To prove such supposition directly it is necessary to study the influence of tropomyosin fragments CNBrB1 and CNBrB2 in the actomyosin contraction.

The chicken skeletal muscle α -tropomyosin fragments CNBrB1 and CNBrB2 correspond to rabbit skeletal muscle α -tropomyosin sites from 11 to 126 residues inclusively

The cleavage of chicken breast muscle tropomyosin by cyanogenbromide results in CNBrB1 and CNBrB2 fragments. Antigene sites are mainly situated in CNBrB1; and CNBrB2 includes the tropomyosin binding sites. In the presence of tropomyosin CNBrB2 activates the actomyosin ATPase. It is important that the immunodiffusion in agar gel showed that the skeletal muscle CNBrB1 produces precipitation line with cardiac muscle tropomyosin antyserum and this line is identical with that one produced by CNBrB1 with chicken gizzard muscle tropomyosin [12]. From the above mentioned it comes that tropomyosin fragment - CNBrB1 and chicken cardiac and gizzard muscles tropomyosin include nonspecific antigene sites. Previously it has been shown that tropomyosin potentiating influence on actomyosin contractile properties doesn't manifest tissue and species specificity [13], chicken and rabbit gizzard muscle tropomyosins potentiate the contraction of skeletal muscle actomyosin

and 142-280 residues respectively [14].

In CNBrB2-fragment there is Cys-190 area that is the important component of tropomyosin structure. The cross-link between Cys-190-s of neighbouring subunits causes the deformation of molecule, it changes its conformation in the way that causes the weakening of tropomyosin binding with F-actin [15], the covalent binding of pirinmaleimide with Cys-190 causes the lost of polymerization ability in cardiac tropomyosin [16]. But we have shown [17] that neither cross-linking of subunits by Cys-190, nor the blocking of cysteins by iodacetamide exterminated the potentiating influence of tropomyosin on the actomyosin contractile ability.

Even such effect of changings in Cys-190 area exists on tropomyosin potentiation of actomyosin contraction somehow confirms the supposition that active domain causing the potentiating acting of tropomyosin must be localized in the area that corresponds to CNBrB1 including site from 11 to 126 residues.

Georgian Academy of Sciences
 Institute of Molecular Biology and
 Biological Physics

REFERENCES

1. S. Ebashi, M. Endo, I. Ohtsuki. *Quart. Rev. Biophys.* **2**, 4, 1969, 351-384.
2. T. Wakabayashi, H. E. Huxley, L. A. Amos, A. Klug. *J. Mol. Biol.*, **93**, 4, 1975, 477-497.
3. G. V. Mikadze, M. Melikishvili, T. Surguladze, M. Zaalishvili. *Bull. Acad. Sci. Georg. SSR*, **15**, 4, 1989, 205-210.
4. S. Perry. *Methods in Enzymology*, **23**, 1955, 583-588.
5. J. A. Spudich, S. Watt. *J. Biol. Chem.* **246**, 1971, 4866-4871.
6. G. V. Mikadze, N. Gognadze, M. Zaalishvili. *Bull. Acad. Sci. Georg. SSR*, **1**, 1, 1975, 104-106 (Russian).
7. G. V. Mikadze, M. Melikishvili, M. G. Dolidze, M. Zaalishvili. *Bull. Acad. Sci. Georg. SSR*, **14**, 3, 1988, 211-216.
8. M. Zaalishvili, G. Mikadze. *Biokhimiya*, **24**, 4, 1959, 612-624.
9. N. Lerne, R. A. Cazenave, G. Roland. *EMBO J.* **1**, 1982, 263.
10. P. Cummins, S. Perry. *Biochem. J.* **133**, 1973, 765-777.
11. E. Kardami, M. Y. Fuzman. *FEBS Letters*, **163**, 1983, 250-256.
12. J. Hayashi, T. Hirabayashi, Y. Watanabe. *Biochem. and Biophys. Res. Comm.*, **81**, 4, 1978, 1260-1267.
13. G. V. Mikadze, G. V. Tsitlanadze, M. Zaalishvili. *Krovoobraschenie. Acad. Sci. Armenia*, **12**, 3, 1979, 8-11.
14. D. Stone, L. B. Smillie. *J. Biol. Chem.*, **253**, 1978, 1137-1148.
15. T.p. Walsh, A. Wegner. *Biochem. Biophys. Acta*, **626**, 1980, 79.
16. P. Graceffa, S. S. Lehrer. *J. Biol. Chem.* **255**, 1980, 11296.
17. G. Mikadze, M. Melikishvili, M. Zaalishvili. *Bull. Georg. Acad. Sci.* **160**, 1, 1999, 150-153.

I. Pagava, G. Grigorashvili

Study of Biological Value of a Protein Concentrate from Grape Pomace

Presented by Corr. Member of the Academy D. Ugrehelidze, December 14, 1998

ABSTRACT. Using chemical and biological methods (experiments on rats), the biological value of proteinaceous concentrate has been evaluated. The relative biological value of proteinaceous concentrate of grape pomace is 83.4%.

Key words: grape pomace, amino acid, chemical score, biological value.

Remainders of grape industrial processing, which are the secondary sources of protein resources, make up 15-20% of raw material [1]. Preparations containing 75-85% of protein [2] can be produced from the main remainders of wine-making, i. e. yeast slush (amount of remainder 10%), grape pomace (5%), and grape stone (3%), by the presented technology. Non-traditionality of origin and experimental nature of protein separation from the mentioned sources conditions their wide medicobiologic evaluation.

In the present work we determine biological value of protein concentration from grape pomace. Separation of protein preparation from grape pomace was conducted at Sagarejo wine factory. By the generally accepted methods [3] the chemical composition of separated protein preparation was determined.

The method of amino acid score [4] and experiments on animals was used to estimate biological value of protein concentration. Biological investigations were carried out on 20 white male rats with initial body weight 55g, divided into two groups: experimental and control, 10 rats in each. The experiment was performed with one-level (10%) content of protein in food. Besides, we calculated the following coefficients: protein efficiency (PER), protein pure utilization (NPU_{tr}), biological value (BV_{tr}) and consumption [5]. Determination

Table 1

Amino acid	Standard scale		Slush protein concentrate	
	a	s	a	s
isoleucine	4.0	100	4.1	103
leucine	7.0	100	7.1	101
lysine	5.5	100	7.0	127
methionine	3.5	100	2.4	70
cystine				
phenylalanine+	6.0	100	8.5	141
tyrosine				
threonine	4.0	100	4.4	110
tryptophane	1.0	100	0.8	80.0
valine	5.0	100	5.6	112

note: a - amino acid content; s - amino acid score.

of chemical composition showed that protein content in grape pomace preparation is 80% and it makes possible to consider it as protein concentrate [6].

Separated protein preparation is limited with sulphurcontaining (methionin - cystine), tiniphtopan and isoleucine (Table 1).

Amino acid score of grape pomace protein preparation is determined by the relative value of the sulphurcontaining amino acids and it makes 70%.

Table 2 presents the indicators of biological value of the studied protein preparation obtained after the experiment on rats.

Table 2

Protein preparation	PER %	BVtr %	NPUtr %	Consumption %
grape pomace	2.0 ±0.1	69.5 ±03.2	58.4 ±03.2	85.0±1.7
casein	2.63 ±0.26	82.2 ±03.1	65.1 ±06.3	92.3 ±1.9

As the Table shows the indicators of standard protein - casein are higher, than those of experimental protein preparation. Hence we calculated the biological value of protein preparation with reference to casein, which made for PrE, BV and consumption accordingly 76.0; 84.5 and 89.7%. Biological value calculated as average mean of mentioned coefficients sum divided by per cents with reference to control (casein) for pomace protein concentrate makes 83.4% [7].

Georgian Scientific-Research Institute of Sanitary and Hygiene

REFERENCES

1. N. N. Razuvayev. Kompleksnaya pererabotka vtorichnykh produktov vinodelia. M., 1975 (Russian).
2. I. I. Moniava, E. I. Lekiashevili. Otkrytia, 5, 1975, 6. (Russian).
3. A. I. Burstein. Metody issvedovaniia pishchevykh produktov. Kiev, 1973 (Russian).
4. A. A. Pokrovski. Voprosy pitania, 3, 1975, 25-30 (Russian).
5. V. G. Visotski, T. A. Iatsishina, E. M. Mamaeva. Voprosy pitania, 6, 1977, 3-9 (Russian).
6. V. G. Visotski, T. A. Iatsishina, T. V. Rimarenko. Med. Ref. Zhurnal, 6, 1976, 24-30 (Russian).
7. K. S. Petrovski, B. P. Sukhanov, S. V. Rogozhin. Voprosy pitania, 3, 1978, 48-53. (Russian).

B. Arziani

On Some Regularities of Phenol-Peptide Conjugates Formation

Presented by Member of the Academy G. Kvesitadze, August 3, 1998

ABSTRACT. The mechanism of phenol-peptide conjugates formation has been studied. Phenol, incubated with low-molecular total fraction in the presence of enzymatic preparations, forms phenol-peptide conjugates. By the method of selective inhibition it was found, that the synthesis of the indicated compounds is accomplished by metalloenzymes with copper and iron active sites. To localize the process of detoxication the distribution of $1\text{-}^{14}\text{C}$ phenol radioactive carbon in cellular organelles has been studied. It was stated that intact plastids possess phenol-peptide conjugates forming ability.

Key words: simple phenols, low-molecular peptides, conjugation, metalloenzymes, intact plastids.

It's known that main way of simple monoatomic phenols detoxication in plants is their conjugation with low-molecular peptides [1]. The goal of the experiment was to study the above mentioned conjugation mechanism. The experiments carried out at the laboratories demonstrate that the synthesis of phenol-peptide conjugates is realized by means of enzymatic systems. Peptide fraction, extracted from pea roots and purified from amino acids was incubated with $1\text{-}^{14}\text{C}$ phenol (concentration $5 \times 10^{-4}\text{M/l}$).

The results of the analysis show that under the given conditions the synthesis of phenol-peptide conjugates is not accomplished. In further experiments together with the peptide fraction and phenol, total protein preparation extracted from the same plant roots was applied. After three hours of incubation protein was precipitated from the researched mixture by means of ethanol. The analysis of sediment and supernatant showed that the part of phenol didn't undergo the changes, the part was bound with peptides and the other one made protein-quinone complex (Table 1).

In order to set up the nature of the enzymes catalyzing monoatomic phenols conjugation with peptides of selective inhibition method was applied. The influence of sodium P-chloromercury benzoate, α , α^1 - dipyridyl and sodium N-diethyldithiocarbamate upon the process of phenol-peptide conjugates formation, which was catalyzed by the total protein preparation isolated from pea roots, has been studied.

Table 1

Distribution of radioactive carbons of $1\text{-}^{14}\text{C}$ phenol in fractions *in vitro*
 (phenol radioactivity 7.4×10^5 Bq/g; concentration $5 \times 10^{-4}\text{M}$ per 1 g of protein;
 exposition -3hr; 25°C).

Radioactivity 10^3 imp/min per 1 g of protein		
protein-quinone complex	peptide conjugates	untransformed phenol
67.1 \pm 5.4	32.6	2473 \pm 232.1

As the research data showed sodium P-chloromercury benzoate (concentration 10^{-4} M/l) effects phenol peptide conjugates synthesis insignificantly. Hence, it could be supposed that the researched enzyme doesn't contain sulfhydryl group in active site.

Sodium N-diethylthiocarbamate (concentration 10^{-4} M/l) affects protein-quinone complex synthesis insignificantly, but suppresses the process of phenol-peptide conjugates formation. Proceeding from this it could be assumed, that metalloenzyme with copper in active site, catalyzes the phenol-peptide conjugates synthesis. Sodium-N-diethylthiocarbamate seems to affect the enzymes accomplishing the synthesis of phenol-peptide conjugates selectively. At the same time phenoloxidases activity and the protein-quinone complexes formation are insignificantly suppressed.

The α, α^1 -Dipyridil (concentration 10^{-4} M/l) analogous to sodium N-diethylthiocarbamate suppresses the phenol-peptide conjugates synthesis. The synthesis of protein-quinone complex is also suppressed. As it is known, peroxidase reveals both peroxidase and oxidase activities [2-4]. At first sight, it could be supposed that phenol conjugation is preceded by its hydroxylation, but the data of the carried out experiments applying sodium N-diethylthiocarbamate disproves this version.

Proceeding from the above-mentioned it can be concluded, that the enzymes catalyzing phenol-peptide conjugation, are metalloenzymes with iron and copper atoms in active sites.

To state the location of the detoxication processes, distribution of $1-^{14}\text{C}$ phenol radioactive carbon in pea cellular organelles has been studied. According to the experimental data (Table 2), after 72 h of exposition radioactive carbon inserts in every fraction of a cell, though another picture is observed in cases of leaf and root. Radioactivity in roots is mainly found in soluble fractions and plastids, and in leaves it is found in soluble fraction and mitochondria.

Table 2

Distribution of $1-^{14}\text{C}$ phenol radioactive carbon in pea cellular organelles (absorption from roots, radioactivity - 7.4×10^5 Bq/g, concentration - 250 mg/l; exposition - 72 h; 20-25°C).

Part of plant	Radioactivity 10^3 imp/min per 1g of raw biomass				
	nuclei and cellular membranes	plastids	mitochondria	ribosomes	supernatant
leaf	0.1 ± 0.0023	0.16 ± 0.018	0.38 ± 0.01	0.12 ± 0.03	1.49 ± 0.13
root	0.74 ± 0.07	1.51 ± 0.1	0.78 ± 0.03	0.23 ± 0.03	8.71 ± 0.32

It should be mentioned, that the accumulation of radioactivity in plastids indicates the significance of organelles participation in the process of detoxication. If the localization of phenoloxidases [5-7] and corresponding substrates-phenols [8, 9] in chloroplasts are taken into account then it will be supposed that phenol oxidative transformations are proceeded just in the plastids.

As it is evidenced from the experiments (Table 3) most of radioactive phenol incubated with intact plastids isolated from pea roots and leaves is oxidized into diphenols and then corresponding quinones, which are bound irreversibly producing the protein-quinone complex.

As it has been mentioned, the main pathway of monoatomic phenols detoxication is their conjugation with the cell low-molecular peptides. The influence of introduced into plant phenols on the biosynthesis of low-molecular peptides has been studied (Table 4). Experiments were carried out on pea seedlings. Their incubation was accomplished on the corresponding phenol solutions. After 48 h of exposition free peptides fraction was iso-

lated from treated and untreated plant roots. Isolation of α -amino acids from peptides was accomplished by the modified method of Ligand chromatography [10].

Table 3
Distribution of $1\text{-}^{14}\text{C}$ -phenol radioactive carbon in fractions of pea intact plastids.
(phenol concentration $2 \times 10^{-4}\text{M}$ per 1g of protein, exposition 2h; 25°C)
from total radioactivity

Part of a plant	Total radioactivity 10^3 imp/min per 1g of raw biomass	% from total radioactivity		
		protein-quinon complex	peptide conjugates	untransformed phenol
leaf	1.23 ± 14	51.7	5.7	42.6
root	5.28 ± 0.63	63.4	22.9	13.7

Table 4
Influence of exogenous simple phenols on low-molecular peptide content in pea seedlings
(phenol absorption through roots, concentration 250 mg/l, exposition 48 hr, $20\text{-}25^{\circ}\text{C}$).

phenol	kind of treatment	optical density of copper-peptide complex solution
phenol	treated	$5.2 \cdot 10^{-2} \pm 1.1 \cdot 10^{-2}$
	untreated	$4.4 \cdot 10^{-2} \pm 0.8 \cdot 10^{-2}$
O-nitrophenol	treated	$9.2 \cdot 10^{-2} \pm 0.8 \cdot 10^{-2}$
	untreated	$4.7 \cdot 10^{-2} \pm 1.1 \cdot 10^{-2}$
2,4 - dinitrophenol	treated	$5.4 \cdot 10^{-2} \pm 1.1 \cdot 10^{-2}$
	untreated	$4.0 \cdot 10^{-2} \pm 0.8 \cdot 10^{-2}$
hydroquinone	treated	$8.9 \cdot 10^{-2} \pm 0.7 \cdot 10^{-2}$
	untreated	$4.2 \cdot 10^{-2} \pm 0.8 \cdot 10^{-2}$

As the experimental data showed, introduction of exogenous simple phenols into pea seedlings causes definite reaction of a plant, which is expressed in stimulation of peptide biosynthesis.

Georgian Academy of Sciences
S. Durmishidze Institute of Plant
Biochemistry

REFERENCES

1. D. Ugrekhelidze, B. Arziani, T. Mitaishvili. *Physiologia Rastenii*, **30**, 1, 1983, 102-107.
2. T. Ivanova, B. Rubin. *Biokhimiya*, **27**, 4, 1962, 622-630.
3. L. Ramazanova, F. Miftakhudinova, V. Alekseeva. *Biokhimiya* **36**, 1, 1971, 67-71.
4. I. Yamazaki, K. Yokoto, R. Nakajama. *Oxidases and Related Redox Systems*. **1**, New-York-London-Sydney, 1965, 485-494.
5. M. Bokuchava, T. Shalamberidze, G. Soboleva. *DAN SSSR*, **192**, 6, 1970, 1374-1375.
6. G. Pruidze. *Moambe Sakart. SSR Metsn. Acad.*, **66**, 3, 1972, 677-680.
7. R. W. Parish. The Intracellular Location of Phenoloxidases and Peroxidase in Starma of Spinach Beet / *Beta vulgaris* L. / *Z. Pflanzenphysiol.*, **66**, 2, 1972, 176-183.
8. V. Kefely, R. Turetskaya. *DAN SSSR*, **170**, 2, 1966, 472-475.
9. M. Zaprometov, S. Kolonkova. *DAN SSSR*, **176**, 2, 1967, 470-473.
10. T. Telegina, T. Pavlovskaya. In: *Metody Sovremennoi Biochimii* (eds.: V. Kretovich, K. Sholts) 1975, 61-63.



I. Abdushelishvili, V. Phiriashvili, B. Arziani, V. Ugrekhelidze

Influence of Copper on the Hydroxylation of Exogenous Benzoic Acid in Pea Seedlings

Presented by Member of the Academy G. Kvesitadze, August 3, 1998

ABSTRACT. Transformation of 1^{14}C -benzoic acid in sterile pea seedlings grown in nutrient solution with (40 mg ion/l) copper has been studied. The formation of labelled p-hydroxybenzoic acid in its free and conjugated form is found to be higher in plants, grown in copper-containing medium. Enzyme preparation obtained from plants grown in copper-containing medium shows high diphenoloxidase (substrate – pyrocatechol) and monophenoloxidase (substrate p-cresol) activities. It is suggested, that the primary hydroxylation of exogenous compounds in higher plants is catalyzed mainly by copper-containing enzymes.

Key words: plant, exogenous compound, hydroxylation, phenoloxidase.

There are data, which point to the important role of copper in detoxication mechanism in high plants. In particular, it is shown that Cu^{+2} when entering in pea seedlings increases a velocity of detoxication of monoatomic phenols [1]; in plants of American Black Nightshade *Solanum americanum* treated with $\text{Cu}(\text{OH})_2$ toxic influence of herbicide paraquat upon these plants decreases [2]; the study of hydroxylation of benzene by the total enzyme preparation of leaves shows that the prosthetic group of the enzyme catalyzing this process contains copper [3]. The aim of the given work is to study the influence of copper on the hydroxylation process of exogenous benzoic acid in pea seedlings.

Experiments were carried out with the sterile pea seedlings (*Pisum sativum*), growing in Knop's medium. The 7-day old seedlings from the nutrient medium were fed with copper as a citrate complex (40 mg ion/l) for five days. Control plants were fed with natrium citrate, instead of copper citrate. After exposition in citrate medium, nutrient solutions both of experimental and control plants were replaced first by distilled water three times (exposure time in water 1 hr), and after that by 1 millimolar solution of radiochemically pure 1^{14}C -benzoic acid (specific radioactivity 8.8 MBq/mmmole; exposure time in benzoic acid solution 72 hr). Finally roots of experimental and control plants were washed, frozen with liquid nitrogen, crushed, and the low-molecular weight compounds extracted with 70% ethanol; the insoluble biomass was hydrolyzed and in hydrolyzate the ^{14}C -labelled compounds were studied. In the same experiments the effect of copper on diphenoloxidase activity (substrate – pyrocatechol), monophenoloxidase activity (substrate – p-cresol), and activity of benzoic acid oxidizing system have been studied in pea roots by means of Warburg manometric method. The hydroxybenzoic acids were identified and quantitatively determined both in hydrolyzed and non-hydrolyzed fractions by means of known method [4], combined with autoradiography. The radioactivity was deter-

mined by an LKB RackBeta II liquid scintillation counter in Bray's hydrophilic system [5]. The protein was determined according to Lowry method.

The obtained results show that plants grown in copper-containing medium (experimental plants) transform benzoic acid more actively, than plants grown in the medium without copper (control plants). To that indicate the data in Table 1, where is shown that the radioactivity of fractions of biopolymers (insoluble in 70% ethanol) and of low-molecular weight substances (soluble in 70% ethanol) is much higher in experimental plants. It should be noted that the labelled carbon of ^{14}C -benzoic acid, taken up from the solutions of identical radioactivity and concentration, is incorporated mainly into low-molecular weight compounds in both experimental and control plants (Table 1).

Table 1

Distribution of labelled carbon atoms of ^{14}C -benzoic acid among the metabolites in pea roots (the average results of 3 parallel experiments)

Plants	Radioactivity of fraction, 10^3 cpm/g dry wt, (%)		
	biopolymers	low-molecular weight compounds	diazo conjugation compounds
Grown in copper-containing medium	0.8 (0.9)	69.3 (81.2)	15.3 (17.9)
Grown in medium without copper	0.5 (1.1)	38.1 (83.7)	6.5 (15.2)

Two ways of transformation of exogenous benzoic acid in plants are known: on the one hand via carboxylic group it conjugates with asparaginic acid [6], asparagine and glucose [7], low-molecular weight peptides [8]. On the other hand, benzoic acid undergoes hydroxylation [9], and formed hydroxybenzoic acids are subjected to decarboxylation [10,11]. These products of hydroxylation and decarboxylation are present in plant tissues mainly as conjugates [8, 12], and after the biomass hydrolysis they are set free, however the part of these products are found in plant tissues in a free state too. Such hydroxylation products of benzoic acid, hydroxybenzoic acids presented in plant tissues in free state or get free by hydrolysis, and their decarboxylation product – phenol, conjugated with diazotized p-nitroaniline forms corresponding diazo conjugation compounds. The radioactivity of summary fraction of such diazo conjugation compounds of non-hydrolyzed biomass, got in our experimental conditions, is given in Table 1. This datum shows the total radioactivity of free (non-conjugated) hydroxylation products of benzoic acid, presented in plant tissues. According to this, in plants grown in copper-containing medium, such products are formed 2.5 times more, than in control plants.

As it was noted, the exogenous benzoic acid and its transformation products exist in plants mainly in conjugated form with cell compounds. Big part of these products is represented by conjugates of benzoic acid, and relatively, minor part by the conjugates of hydroxybenzoic acids and products of their farther decarboxilation [7, 9, 11]. We determined the correlation between hydroxylated and non-hydroxylated transformation products of labelled benzoic acid in fraction of low-molecular weight compounds in roots, after acidic hydrolysis of the latter. The results are presented in Table 2, which show, that after 72 hr exposure of roots in copper-containing medium the amount of hydroxylation products of benzoic acid in root biomass increases to a considerable extent.

We are searching for such hydroxylated compounds in both hydrolyzed and non-hydrolyzed summary fractions. The analysis of summary fraction of low-molecular weight compounds has shown the low content of p-hydroxybenzoic acid in non-hydrolyzed fraction in plants grown only in copper-containing medium. In corresponding hydrolyzed fractions this acid was found in roots of both experimental and control plants, although in experimental plants its content was much higher (approximately 4.7 times). It must be noted that in roots of plants grown in copper-containing medium, in hydrolyzed summary fraction of low-molecular compounds, the labelled salicylic acid was found in small amounts.

Table 2

The correlation between hydroxylated and non-hydroxylated transformation products of ^{14}C -benzoic acid in fraction of low-molecular weight compounds in roots, after acidic hydrolysis (the average results of 3 parallel experiments).

Plants	Radioactivity of fraction, 10^3 in cpm/g dry wt. (%)		
	low-mol. wt. compounds	non-hydroxylated compounds	diazo conjugation compounds
grown in copper-containing medium	69.3 (100)	28.2 (40.7)	41.1 (59.3)
grown in medium without copper	38.1 (100)	20.4 (53.5)	17.7 (46.5)

Among copper-containing plant enzymes the phenoloxidase system as carrier of hydroxylase function at the first place comes into notice. Number of data points that by this system is realized the primary hydroxylation of exogenous compounds into plant cell [3]. We have measured absorption of oxygen in the process of oxidation of benzoic acid, pyrocatechol and p-cresol by total enzyme preparation received from roots of experimental and control plants. Absorption of oxygen in process of oxidation of pyrocatechol by total enzyme preparation received from roots of control plants (so-called diphenoloxidase activity), was accepted for 100%; an oxygen absorbed by oxidation of p-cresol accordingly shows the monophenoloxidase activity of enzyme preparation. The results in Table 3 show that in the enzyme preparation, received from plants grown in copper-containing medium, diphenoloxidase activity is particularly high, accordingly the monophenoloxidase activity is high as well. In accordance with this, benzoic acid is oxidized more actively by

Table 3

Absorption of oxygen in the process of substrate oxidation by total enzyme preparation received from pea roots (concentration of: enzyme preparation - 20 mg/ml, substrate - 0,1M, phosphate buffer 1/15M, pH 6.5; exposure time 3 hr; volume of oxygen absorbed by oxidation of pyrocatechol is accepted for 100% (the average results of 4 parallel experiments).

Total enzyme preparation from roots	Absorbed oxygen, %		
	pyrocatechol	p-cresol	benzoic acid
grown in medium with copper	210	47	32
grown in medium without copper	100	25	10

enzyme preparation, received from plants grown in copper-containing medium.

It must be noted that such stimulation of oxidizing enzymes by copper ions, is described for catalase, peroxidase, and IAA-oxidase [13,14].

Thus, we can conclude that in plants grown in nutrient solution containing surplus, but no toxic amounts of copper ions, hydroxylation of benzoic acid is stimulated. In such plants also phenoloxidase system is accordingly active. These results confirm the consideration that primary hydroxylation of exogenous compounds in higher plants is catalyzed mainly by copper-containing enzymes.

Georgian Academy of Sciences

S. Durmishidze Institute of Plant Biochemistry

REFERENCES

1. D. Ugrekhelidze, T. Peikrishvili, V. Piriashvili. Metabolism of biosphere chemical pollutants in plants. Tbilisi, 1979, 57-63.
2. T. A. Bewick, S. R. Kostewicz et al. Weed Sci., **38**, 1990, 634.
3. D. Ugrekhelidze, F. Korte, G. Kvesitadze. Ecotoxicol. Environ. Safety, **37**, 1997, 24.
4. J. B. Harborne. Phytochemical Methods. London, 1973, 34-41.
5. E. Rapkin. Sample Preparation for Liquid Scintillation Counting. Plaisir, France, 1970.
6. W. A. Andreae, N. E. Good. Plant Physiol., **32**, 1957, 566.
7. H. D. Klambt. Nature, **196**, 1962, 491.
8. T. Mitaishvili, S. Durmishidze, D. Ugrekhelidze, D. Chrikishvili. Dokl. Akad. Nauk SSSR, **242**, 1978, 457.
9. S. Z. El-Basyouni, D. Chen, R. K. Ibrahim, A. C. Neish, G. H. N. Towers. Phytochemistry, **3**, 1964, 485.
10. S. Berlin, W. Barz, H. Harms, K. Haidler. FEBS Letters, **16**, 1971, 141.
11. T. Mitaishvili, S. Durmishidze, D. Ugrekhelidze, D. Chrikishvili. Dokl. Akad. Nauk SSSR, **247**, 1979, 247.
12. G. Cooper-Driver, J. J. Corner-Zamodist, T. Swain. Z. Naturforsch., **27b**, 1972, 913.
13. S. Mukherji, B. Das Gupta. Physiol. Plant., **27**, 1972, 126.
14. A. J. Coombes, N. W. Lepp, D. A. Phipps. Z. Pflanzenphysiol., **80**, 1976, 236.



N. Moseshvili, Corr. Member of the Academy N. Aleksidze

Distribution of Soluble Proteins with Lectin Activity in Different Organs of *Mentha pulegium* and Biological Characteristics

Presented May 3, 1999

ABSTRACT. Soluble proteins with lectin activity have been revealed in *Mentha pulegium*. Their quantitative distribution in different parts of the plant was established according to the season. Two lectins sensitive to D-galacturonic acid and D-trehalose are found to be mainly present in *Mentha pulegium*. Both of these lectins display their maximum activity on nontrypsin treated rabbit erythrocytes, which indicates to the specific dependence of erythrocytes membrane in relation to glyco-protein-glycolipid structures.

Key words: lectin activity, proteins, *Mentha pulegium*.

In recent years, biologically active substances of vegetable origin, particularly, lectins have been under intensive study [1-3]. In present paper we have studied lectins of *Mentha pulegium* which is a widespread plant in Georgia, with anti-insect properties. The over-ground parts of *Mentha pulegium* grown in natural conditions were the object of our research.

After reduction of different parts of the plant to fragments homogenization and proteins extraction was performed in buffer solution of 40 mM K⁺-phosphate, which was prepared on 0.9% NaCl solution and contained 0.5 mM phenylmethylsulfonyl fluoride (PMSF) and 0.5 mM β-mercaptoethanol (pH 5.0). Incubation was performed at room temperature for an hour. To remove polyphenols 5% Polyclar AT was used. Their desalinization was carried out by ammonium sulphate in 20%, 40%, 60%, 80% and 0-80% saturation conditions. The obtained solutions were centrifuged at 20000g for 20 min, at 0-4°C; precipitation was solved in buffer solution: on 40 mM K⁺-phosphate was prepared 0.9% NaCl solution (pH 7.0) (PBS) and dialyzed in the same buffer solution. Protein fractions were kept at +4°C before using.

Hemagglutination test was carried out in PBS in U-bottomed microtest plates using trypsin and nontrypsin treated rabbit erythrocytes. In the first bottom of the plate 100 ml of protein solution was placed and titrated. Titrated solution was added to 50 ml of 2% erythrocytes suspension [4]. The hemagglutination titer was estimated visually after 2 h incubation at room temperature. Lectins sensitivity to sugar was established by hapten-inhibitor technique. For this to 0.6 M of twofold dilutions of sugar 50 ml of protein with lectin activity was added, incubated for 40 min at room temperature. Then added 50 ml of 2% suspension of trypsin-treated rabbit erythrocytes and determined agglutination visually.

Retention of lectin activity was estimated by that minimum concentration (mM) of sugar which caused complete inhibition of hemagglutination activity. Protein concentration was determined according to Lowry et al. [5]. Hemagglutination activity of proteins

with lectin activity was determined by the minimum concentration of protein (mg/ml) which still causes hemagglutination and lectins content was estimated by the following formula: protein concentration/hemagglutination activity. The obtained data are processed statistically [6]. To obtain protein fractions with maximum lectin activity in the first series of test various extraction solutions have been tested [7]. For this the effect of *Mentha pulegium* freez-thawing on proteins extraction with lectin activity was studied first of all.

Table 1

The effect of freez-thawing on proteins extraction with lectin activity from *Mentha pulegium*.

Extraction conditions	Fraction nonprecipitated by ammonium sulphate		Protein fraction precipitated by ammonium sulphate	
	Protein concentration	Hemagglutination activity	Protein concentration mg/ml	Hemagglutination activity
Without freez-thawing	3.5±0.3	0.037±0.003	2.0±0.5	0.0026±0.0005
In conditions of freez-thawing	3.3±0.4	0.035±0.004	2.7±0.5	0.0018±0.0004

Table 1 shows that freez-thawing doesn't affect the quality of proteins extraction with lectin activity. It should be noted that there is a tendency to increase lectin activity by freez-thawing action but it is not statistically significant ($p < 0.05$). In parallel, the affect of picked plant storing length on lectin activity (Table 2) was studied.

Table 2

Dependence of hemmagglutination activity of proteins with lectin activity extracted from *Mentha pulegium* on storing length of plant

Storing time	Protein concentration mg/ml	Hemagglutination activity mg/ml
0 day	3.5±0.3	0.037±0.003
10 day	2.2±0.5	—

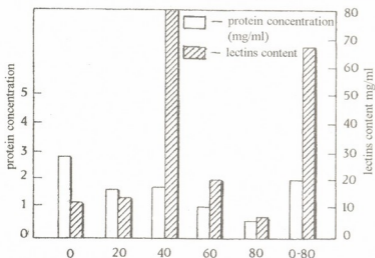


Fig. Lectins activity extracted from *Mentha pulegium* in conditions of ammonium sulphate desalinization

a) proteins concentration

b) lectins content in hemagglutination k- units (protein concentration/hemagglutination activity)

Table 2 demonstrates that lectin activity is not practically observed after plant picking and to storing at room temperature for 10 days. That's why in further series of tests we used raw material of freshly picked plant.

In the further series of experiments proteins with lectin activity have been studied in protein fractions obtained in saturation conditions of ammonium sulphate step by step desalinated 20%, 40%, 60%, 80% and 0-80%.

Figure illustrates that proteins fraction which was de-

salinated by ammonium sulphate in conditions of 40% saturation is distinguished by lectins high content. Lectins content in that fraction as compared to the initial one was increased eight times.

Significant differences of lectins distribution in different organs of the plant were marked (Table 3).

Table 3
Distribution of proteins with lectin activity extracted from *Mentha pulegium*
in different organs of the plant

Plant organ	Protein concentration mg/ml	Hemagglutination activity mg/ml	Lectins content
Stem	1.1±0.5	0.18±0.08	6.1±0.3
Torus	0.9±0.1	0.30±0.03	3.0±0.2
Leaf	1.8±0.6	0.30±0.10	6.0±0.4
Greenless part of flower	1.2±0.5	0.05±0.02	24.0±0.5

It has been established that in lectins distribution significant changes are marked according to plant organs. Comparatively high content of lectins was observed in greenless parts of the flower. This index as compared to the overground parts (leaves, stem, torus) appeared about four times as much. According to Hapten-inhibitory qualitative difference was marked just in lectins which was experimentally proved by using of carbohydrates. As haptens D-trehalose-dihydrate, raffinose and D-galacturonic acid were used [7]. Minimum concentration of sugar is indicated (mM) which causes complete inhibition of hemagglutination activity. It should be noted that hapten of extracted lectins from greenless parts of plant was not established, whereas preparations made of leaves and stems revealed specificity in relation to D-galacturonic acid and D-trehalose, and preparation obtained from torus only in relation to D-galacturonic acid. Therefore it is supposed that at least three lectins with hemagglutination activity exist in *Mentha pulegium*.

Table 4
Specificity to sugars of proteins with lectin activity from *Mentha pulegium*

Plant organ	D-galacturonic acid (mM)	D-trehalose dehydrate (mM)	Raffinose (mM)
Leaf	25	25	>100
Stem	25	25	>100
Torus	25	--	--
Greenless part of flower	--	--	--

According to literary data in some plants lectins dependence on season of the year was marked. It was noted that leaf lectins (ML I and ML III) of *Viscum Album* L. presented in the largest amount in winter months and the smallest – in summer months. A proposition was made on lectins participation in adaptation mechanisms to the environmental conditions [8]. That's why we have studied lectin activity of *Mentha pulegium* specially in different periods of the year (Table 5).

Proteins content with lectin activity in *Mentha pulegium* in spring and early summer is maximum and in July and August-September its content is gradually decreasing: in July 8 times and in September 16 times. At the same time when there is noted slight

Table 5
 Hemagglutination activity of protein fractions extracted from *Mentha pulegium*
 in different periods of the year

Month	Protein concentration mg/ml	Hemagglutination activity mg/ml	Lectins content in hemagglutination unity
Beginning of May	4.4±0.5	0.046±0.005	95.7±0.5
Beginning of June	3.5±0.4	0.036±0.003	97.2±0.4
Beginning of July	3.4±0.5	0.28±0.04	12.1±0.3
August-September	2.3±0.3	2.38±0.05	6.1±0.4

ability of trypsinized erythrocytes agglutination of fractions with lectin activity of *Mentha pulegium*, agglutination ability of nontrypsin-treated erythrocytes of the same fraction is well expressed (Table 6). It indicates that proteins with lectin activity extracted from *Mentha pulegium* better interact with glycolipids /glycoproteins of nontrypsin-treated rabbit erythrocytes membranes and far better with glycoproteins of erythrocytes membranes [9]. It was also found that erythrocytes agglutination by *Mentha pulegium* proteins with lectin activity takes place in none of human being's blood group (O,A,B, AB).

Table 6
 Hemagglutination ability of proteins with lectin activity of *Mentha pulegium*

2% suspension of rabbit erythrocytes	Protein concentration mg/ml	Titer T	Hemagglutination activity
Trypsinized	2.3±0.3	4	95.7±0.5
Nontrypsinized	2.3±0.3	16	97.2±0.4

The aim of our further investigation is the establishment of the possible function of D-trehalose and D-galacturonic acid sensitive lectins. Such quantitative changes conditioned by environment and plant age probably point to specific role of lectins in the plant. It is also testified by the fact that lectin activity of the mentioned protein fraction is well revealed at the trypsinized and nontrypsinized rabbit erythrocytes agglutination.

Tbilisi I.Javakhishvili State University

REFERENCES

1. N. Aleksidze. Ekologiuri biokhimiis sapudzvebi. Tbilisi, 1999 (Georgian).
2. W. J. Peumans, E. J. M. Van Damme. Lectins: Biology, Biochemistry, Clinical Biochemistry. **10**, 1994, 128-141.
3. J. E. Huesing et al., Phytochemistry, **30**, 1991, 3565.
4. W. J. Peumans et al., Planta, **160**, 1984, 220-228.
5. O. H. Lowry et al., J. Biol. Chem., **193**, 1, 1951, 265-275.
6. A. Afifi, S. Eizen. Statisticheskii analiz. M., 1982 (Russian).
7. N. Moseshvili et al., Bull. Acad. Sci. Geor. **156**, 3, 1996.
8. D. K. Hincha et al., 17th Intern. Lektin. Muting. Germany. September 24-27, 1997.
9. H. Lis, N. Sharon. Biol. an intern. Series of monographs and textbooks. The lectins. Acad. Press. INC, 1986.



A. Gujabadze, T. Macharashvili, N. Gabashvili

Ecologo-Physiologic Groups of Bacteria Formed on the Coatings of Certain Materials

Presented by Member of the Academy N. Aleksidze, April 27, 1999

ABSTRACT. The specific bacterial composition of coverings of different materials, exposed on the open and closed areas was studied in the region of Colchida Scientific - Research Center of Georgia (Ozurgeti region, vil. Shekviteli). It appeared that on the open area most of them (88 strains) were gramm-positive baccilli and cocci of the families of *Arthrobacter*, *Corynebacterium*, *Rhodococcus*, *Bacillus*, *Micrococcus* and *Staphilococcus*. At the same time, specific composition of coverings of materials on the closed stands was presented by equal amount of gramm-positive and gramm-negative bacilli probably connected with comparatively higher stability of gramm-positive bacteria to the external environmental factors.

Key words: ecology, bacteria, subtropics.

Along with the known physical factors (such as humidity, temperature, UV radiation) causing damages of different materials, the microorganisms, including bacteria play important role. Therefore, determination of species composition of bacteria characteristic for coverings of the surfaces of different materials as well as the establishment of the dominant complexes of the studied microorganisms under the conditions of humid subtropics are of special interest.

The study deals with the coverings of various industrial materials, which were exposed to the special stands at atmospheric zones of the region of Colchida Scientific Research Center of climatic investigations: No 1 (50 m from the seashore), No 2 (400 m from the seashore) and No 3 (500 m from the seashore in the thickets of high vegetation. Material for the present study was scrubbed off from the surface of material covering and was placed in sterile vessels with physiological solution or liquid feeding media (for thio-bacteria and ferric-bacteria). The obtained bacteria were sown on different selective media in order to determine physiologic groups being present in the studied population [1].

The presence of ammonifiers in the coverings was determined by sowing the samples in 1% peptone water. Their development was estimated according to the dimness of media, formation of flakes, residue and the film on the surface as well as according to the isolation of ammoniu and hydrogen sulfide [2]. Oligonitrophilic bacteria were determined by means of sowing of samples by the palette-knife on the surface of thick nutrient media of Ashby [3]. For the exposure of nitrogen fixing bacteria the colonies grown on the Ashby medium (without nitrogen source) were subjected to passes minimum three times. The presence of nitrifying bacteria was evaluated according to lucid zones around the colonies at their growing on the hungry agar with $MgNH_4PO_4 \cdot 6H_2O$.

For determining the presence of ferric-bacteria the thick medium of Vinogradsky (for *Leptothrix*) and liquid medium of Kalinenko for heterotrophic bacteria, able to utilize the iron were used. Alongside with it the thio- and sulfate-reducing bacteria were revealed according to the method described in [1], while the presence of spore bacteria were determined by means of sowing on meat-peptone agar with maize extract.

As a result of the experiments certain regulations of development of bacteria, inherent to the composition of coverings of various industrial materials were determined. Thus, for example, the characteristic index for the above-stated coverings is the presence of bacteria, taking part in the circulation of nitrogen. As seen from the *Table, the most rich variety of bacteria is observed in the coverings of materials*, exposed on the open stands of the atmospheric area No 1 (50 m from the seashore). In the coverings of materials such as glass-plastic, foam plastic, epoxy resin, the ammonifying, nitrogen-fixing, oligonitrophilic bacteria were observed as well as the heterotrophic ferric-bacteria of the species *Siderocapsa*.

The study of the coverings of materials exposed on the open stands, placed within 400 m from the seashore has shown that diversity of physiologic groups of bacteria was decreased to the minimum. The data (glass plastic, caprone, epoxy resin, foam plastic) only ammonifying nitrogen-fixing and oligonitrophilic bacteria were found. Investigation of bacterial microflora of coverings of materials, exposed in the closed stands showed that it consists also of the ammonifying, nitrogen-fixing and oligonitrophilic bacteria.

Specific composition of bacteria of coverings of the materials under humid subtropics is as follows: spore-forming (22 strains): *Bacillus macerans* (9 strains), *B. polymixa* (7 strains), *B. cereus* (6 strains), nonspore forming gramm-positive bacilli and cocci: *Arthobacter sp.* (28 strains), *Corinebacterium sp.* (17 strains), *Rhodococcus sp.* (10 strains), *Micrococcus luteus* (6 strains) and *Staphylococcus aureus* (1 strains) and non-sporeforming gramm-negative bacilli: *Pseudomonas sp.* (5 stains), *Ervinia sp.* (5 strains), *Flavobacterium sp.* (2 strains) as well as non-identified bacteria (10 strains).

For the specific composition of bacteria of coverings of materials, exposed on open areas, mainly gramm-positive non-sporous bacilli are inherent. At the same time specific composition of material coverings on the closed stands is represented by equal quantity of gramm-positive and gramm-negative bacilli. Such distribution should be connected with

Table

Physiological groups of bacteria detected in material coverings, exposed on open stands of the atmosphere areas No 1 (50 m from the seashore) and No 2 (400 m from the seashore)

Physiological groups of bacteria	50 m from the seashore				400m from the seashore			
	Glass-plastic	Caprone	Epoxy resin	Foam plastic	Glass-plastic	Caprone	Epoxy resin	Foam plastic
Ammonifying	+*	+	+	-	+	+	+	+
Nitrifying	+	-*	+	-	-	-	-	-
Nitrogen-fixing	+	-	+	+	+	+	+	+
Oligonitrophilic	+	-	+	+	+	+	+	+
Thionic	-	-	-	-	-	-	-	-
Sulfate-reducing	-	-	-	-	-	-	-	-
Heterotrophic ferric bacteria	-	-	+	+	-	-	-	-

*+ - presence; - - absence.

the higher stability of gramm-positive bacteria compared with the gramm-negative, ones to the external factors of environment (UV-irradiation, temperature, drying, etc.).

Along with the above-stated the bacteria which are characteristic for soil, water and high vegetation are dominating in the bacterial microflora of material coverings under conditions of humid subtropics and they are the most stable to the factors of external environment due to their biological properties. Namely they do play the principal role in the processes of transformation of carbon- and nitrogen-containing compounds of the biosphere, decomposing the compounds hardly attainable to many other microorganisms (hydrocarbons, synthetic compounds - herbicides, plastic masses, etc.).

Tbilisi I. Javakhishvili State University

REFERENCES

1. *V. I. Romanenko, S. I. Kuznetsov.* Ecology of Microorganisms of Fresh Water Reservoirs., Leningrad, 1974, 194 (Russian).
2. *Methods of General Bacteriology.* V. 1., Moscow, 1988, 536 (Russian).
3. *A. G. Rodina.* Methods of Water Microbiology. Practical Handbook., L.-M., 1965, 362 (Russian).

D. Pataraya, L. Basilashvili, M. Bagalishvili, M. Kikvidze, M. Betsiashvili,
Corr. Member of the Academy N. Nutsubidze

Influence of Nodule Bacteria and Different Microorganisms on Soybean Growth

Presented June 22, 1998

ABSTRACT. The influence of nitrogen fixing microorganisms and actinomycetes on various sorts of soybean plant has been studied. It was revealed, that nodule bacteria mixed cultures of *Azospirillum* and *Actinomycetes* in comparison with monocultures affected the growth of soybean sorts and protein content better.

Key words: nodule bacterium, azospirillum, actinomycete, mixed and monocultures, soybean, growth.

It should be mentioned, that only procaryotic organisms have the ability of molecular nitrogen fixation. Nitrogen fixation is proceeded by freely populated in soil microorganisms and bacteria, which simbiotically coexist with higher plants. Freely populated and symbiotic nitrogen fixing microorganisms transfer inert molecular nitrogen into coupled form and finally into protein. Nowadays protein problem is very important and actual for the mankind. Beans, particularly soybean and kidney-bean, have the major role in problem solving, lately the data showed, that nitrogen fixation was more intensively carried out by microorganisms in mixed cultures [1]. The analogous results were received in case of coexistence of soybean nodule bacteria with other microorganisms [2].

In nature, various populations of microorganisms are tightly connected, accomplishing metabolism. The advantage of mixed cultures over monocultures is: 1) ability to transform heterogeneous substrates; 2) mineralization of complex organic compounds; 3) ability of organic substrates biotransformation; 4) resistance to toxic substrates including heavy metals; 5) high productivity; 6) resistance to environmental changes; 7) ability to exchange genetic information among various species [3].

The goal of the work was to study the influence of nodule bacteria and other microorganisms on various sorts of soybean, namely on "Adreula 6" and "Kartuli 7".

The following strains of nodule bacteria characteristic for various sorts of soybean, isolated from different regions of Georgia by M. Zgenti, the coworker of the Ketskhoveli Institute of Botany were selected for investigation:

Bradyrhizobium japonicum strain 02, Tkibuli 1966, soybean sort "Imeruli";

Bradyrhizobium japonicum strain 57, Zugdidi, Darchelli village - soybean sort - "Guruli";

Bradyrhizobium japonicum 29, Tskhaltubo - soybean sort - "Imeruli", 1972;

Bradyrhizobium japonicum 46 - Tkibuli ; soybean sort "Imeruli".

Also, the strains isolated from different soils of Georgia were chosen for investigations: *Azospirillum brasilense* Γ - 3, *Actinomyces fridiae* 110, *Geodermatophilus obscurus* 11.

At the first stage soybean "Kartuli 7" was observed. The influence of mono- and mixed cultures on these plant has been studied. The above indicated sorts were grown under sterile conditions. Seeds were treated with 0.1% HgCl₂ solution for 15-20 min and then placed on sterile nutrient medium in Erlenmayer flasks. Each variant of experiments was repeated three times:

1. Control;
2. *Bradyrhizobium japonicum* 57;
3. *Bradyrhizobium japonicum* 02;
4. *Bradyrhizobium japonicum* 57 + *Bradyrhizobium japonicum* 02;
5. *Bradyrhizobium japonicum* 57 + *Azospirillum brasilense* Γ-3;
6. *Bradyrhizobium japonicum* 02 + *Azospirillum brasilense* Γ-3;
7. *Bradyrhizobium japonicum* 57 + *Actinomyces fradiae* 110;
8. *Bradyrhizobium japonicum* 57 + *Geodermatophilus obscurus* 2nD;
9. *Bradyrhizobium japonicum* 02 + *Bacterium* sp. 57;
10. *Bradyrhizobium japonicum* 02 + *Geodermatophilus obscurus* D 11.

Plant growth and development was observed for a month. It was revealed, that intensive growth, expressed in cultivation of branched roots having many nodules, was characteristic to soybean treated with N8, 9, 10 mixed cultures. Under the influence of N 5, 6, 7 associations, even development was observed. Infection with monocultures caused the decrease of plant growth.

Hence, on the basis of obtained data, three associations could be used for field experiments: *Bradyrhizobium japonicum* 57 + *Geodermatophilus obscurus* 2nD; *Bradyrhizobium japonicum* 02 + *Bacterium* sp. 57; *Bradyrhizobium japonicum* 02 + *Geodermatophilus*

Table

Influence of inoculation on soybean ("Adreula-6")

Variants of experiments	Plant height, cm		Plant biomass g		Protein content mg/per lg fresh weight	
	Upper part	Root	Fresh weight	Dry weight	Root	Leaf
Control	23.4	17.9	4.0	1.1	2.25	5.85
<i>Azospirillum brasilense</i> Γ-3	24.2	18.3	4.0	1.2	-	-
<i>Bradyrhizobium japonicum</i> 46	24.8	17.9	7.9	1.2	2.6	6.6
<i>Bradyrhizobium japonicum</i> 29	25.0	18.1	8.1	1.3	2.5	5.55
<i>Bradyrhizobium japonicum</i> 46 + <i>Azospirillum brasilense</i> Γ-3	29.3	20.4	9.8	1.6	2.7	8.6
<i>Bradyrhizobium japonicum</i> 29 + <i>Azospirillum brasilense</i> Γ-3	28.9	20.2	9.5	1.6	2.6	7.0

obscurus D 11. They stimulate the growth of soybean yield.

To confirm the received data, different sorts of soybean and nodule bacteria strains were selected for the further investigations. Experiments were carried out on soybean "Adreula 6". Before sowing, the surface of the seeds was sterilized in HgCl_2 mixture for 15-20 min. Seeds inoculation was carried out with the following monocultures: *Bradyrhizobium japonicum* 46, *Bradyrhizobium japonicum* 29, *Azospirillum brasilense* Γ -3, and mixed cultures: *Bradyrhizobium japonicum* 46 + *Azospirillum brasilense* Γ -3 and *Bradyrhizobium japonicum* 29+ *Azospirillum brasilense* Γ -3. Seeds were retained in bacterial suspension containing 10^6 cells per 1 ml; for control uninoculated seeds were selected. The plants grew in flasks under sterile conditions in laboratories. The experiments proceeded under natural light. At first plants grew in water, then in Knop's mixture. The length of the upper part of a plant and roots of 14 days old seedlings was measured. Protein content in 14 days old seedlings was measured by Lowry [4]. In case of inoculation of soybean seeds, stimulation of plant growth, in comparison with control plant was observed. The upper part and roots of the plant grew well (Table 1).

According to the Table, the better effect was received in case of inoculation by association of *Bradyrhizobium japonicum* 46 + *Azospirillum brasilense* Γ -3. Analogously, plants inoculated by strains of *Bradyrhizobium japonicum* 29 + *Azospirillum brasilense* Γ -3 grew better. In case of inoculation by separate strains special effect of plant growth wasn't observed.

According to protein content the most effective was inoculation of plant by *Bradyrhizobium japonicum* 46 + *Azospirillum brasilense* Γ -3 association. Protein content in leaf was equal to 8.6 mg, in roots to - 2.7 mg.

Our experiments exposed the positive influence of *Bradyrhizobium japonicum* 46 and *Bradyrhizobium japonicum* 29 on growth of soybean - "Adreula 6", on biomass and protein content. Mixed cultures of *Bradyrhizobium japonicum* 46 and *Bradyrhizobium japonicum* 29 with *Azospirillum brasilense* Γ -3 affect the plant far better, than mono cultures. In order to increase the yield of "Kartuli 7" the following mixed cultures could be used: *Bradyrhizobium japonicum* 57 + *Geodermatophilus obscurus* 2nD; *Bradyrhizobium japonicum* 02 + *Bacterium sp.* 57; *Bradyrhizobium japonicum* 02 + *Geodermatophilus obscurus* D11.

Georgian Academy of Sciences
 S. Durmishidze Institute of Plant Biochemistry

REFERENCES

1. D. Pataraya, V. Avetiani, N. Nutsbidze. *Matsne of Georg. Acad. of Sci., Ser. Biology.* **16**, 6, 1990, 410-413 (Georgian).
2. N. N. Andreeva, K. Mandkhan, et al. *Fiziologiya rastenii*, **38**, 5, 1991, 897-903 (Russian).
3. M. M. Utarov. *Izvestia AN SSSR, ser. Biol.* **1**, 1982, 93-100 (Russian).
4. O. H. Lowry et al. *Biol. Chem.* **193**, 1, 1951, 261-275.

N. Tsilosani

The Use of a Biological Object, Bacteriophage in Trassing

Presented by Member of the Academy T. Chanishvili, June 7, 1999

ABSTRACT. The ways to model the epidemic process of spreading the infection agents causing intestinal diseases are considered. The data on improving selective methods for biological trasser-bacteriophages are presented. It has been shown, that standard nonspecific bacteriophages may be tested on their fitness for trassing by plating them on the mixture of permissive and nonpermissive bacterial strains. The method is expected to be convenient in terms of its simplicity.

Key words: trasser-bacteriophages, permissive bacterial cultures, phage-resistant mutant.

The purpose of the present paper is to work out a simple method that makes it possible to identify the bacteriophages. The following activities are to be conducted: 1. selection of non-specific clones of phages with high reproductive capacity and with high resistance to environmental factors; 2. determination of the ways for their revealing and cultivating that would facilitate trasser selection and introduction in practice. It seems to be very economical as well.

Bacteriophages of *E.coli* were isolated from standard laboratory strains CR-63 and k-12 (λ) cultures (26 phages), from polyvalent medicine, intestiphage 6 and high-specific phage, M17 being obtained from the colibacterium strain by means of exposing to ultraviolet rays.

13 phages have been cloned and classified into two main groups according to the negative colonies. 3 phages were selected for further studies, in particular FC-1 (from the 1st group), FC-2 (2nd group) and high-specific phage FM-17 (as a control). The latter we had obtained from colibacterium strain and used in trassing.

Investigations of the above mentioned bacteriophages have shown that the phage FC-1 in serological terms is close to DDIV and DDV group phages and belongs to Syphovirides according to Akerman Classification system. As to phage FC-2, it appears to be close to T pair (DDVI phages) and belongs to the group of Myovirides. The bacteriophage FM-17 has nothing in common with the above mentioned group in terms of serological relationship. The main taxonomic characteristics of the mentioned bacteriophages are given in Table 1.

It is clear from Table 1 that the investigated bacteriophages differ from each other by the following features: the capacity to form negative colonies; the morphology of nucleocapsides and the serological relationship. Besides, the studied phages are to be dependent on the influence of lime chloride, ultraviolet rays, high temperature and salt concentrations.

To create a favourable method for bacteriophage identification, phages were plated on permissive and nonpermissive bacterial cultures and on their mixture. The following

Table 1
 General taxonomic characteristics of FC-1, FC-2 and FM-17 bacteriophages

	Morphology of negative colonies	Morphology of nucleocapsides	Serological group	Phases of host-cell relationship		Resistance				
				of maximum adsorption	average harvest per cell	to the high temperature		to the UV rays (compared with Tunit)	chloro-us lime mg/l	NaCl high concentration
						low limit	high limit			
FC-1	Diameter 3.0-4.0 mm with clear centre and incomplete lysis	Syphoviride	I-related to the DDIV and DDV phages	84	140-150	58 °C - 90.6 %	68 °C - 0.3 %	4.5	0.45	15 - 17 %
FC-2	Diameter 3.0-4.0 mm with clear center and complete lysis	Myoviride	II-related to T pair phages	74	90-100	58 °C - 96.6 %	74 °C - 0.5 %	1	0.6	20 % and more
FM-17	Diameter 2-3 mm clear colonies	Sporoviride	Specific	80	190-200	58 °C - 91 %	68 °C - 0.35 %	2.55	0.3	15 - 17 %

cultures were taken as permissive cultures: standard *E.coli*, K12(λ) and *E.coli* M17 and their mutants resistant to phages, *E.coli* K12 (λ) / FC-1, *E.coli* K12 (λ) / FC-2, *E.coli* M17 / FC-17 obtained by indirect selection according to Lederberg's method [8].

Plating efficiency indices of selected bacteriophages on permissive, nonpermissive and mixed bacterial cultures, are given in Table 2.

Within the phage-resistant mutants the tested phages do not reproduce (or their reproduction is very limited), while the efficiency of phage plating on the mixed cultures containing both the permissive and non-permissive strains seems to be in close proximity to the values obtained on the initial strains (Table 2). Only negative colonies have different morphology: they are clear on the initial cultures, but turbid on the mixed cultures. In addition, the mutants do not express capacity of cross-resistance. It indicates the specificity of the method applied for the identification of the trasser-bacteriophages.

For recent years sanitary condition of the Black Sea has been significantly deteriorated resulting in seawater pollution in the resort regions. Seawater has been contaminated with various infectious viruses, pathogenic bacteria and the bacteria, pathogenicity of which depends on environmental conditions.

Modelling of infectious material spreading was conducted in 1989-1990 in the resort zones of the Black Sea (Kobuleti, Gagra and the regions neighbouring Pitsunda).

200 ml of each sample containing the trasser-bacteriophages ($2-5 \times 10^{11}$ infectious unit per ml) were poured into the seawater at different distances from the seacoast, in particular, the sample with phage FC-1 was tested in Kobuleti near the mouth of the Natanebi river. The phages FM-17 were poured into water at 500 m distance from the Pitsunda seashore, and the phage FC-2 samples - in Gagra near the collector-cleaner in 20 m distance from the shore.

The water samples were taken for analysis from different places (at 200, 450, 600 m and 15 km distances from the shore) at the fixed time (1,2,8,12 and 22 h later from starting the experiment) from various depths - 0.5; 2.5; 5.0; 10 and 20 m from a water surface.

In Kobuleti the phage FC-1 was found on the water surface after 1 h at a distance of 200 m, 2h later it moved to the depth (5-10 m) far from the seashore (640 m). After 8h they were found in low quantities only at the place they had been poured.

The spread of FC-2 trasser was observed only in surface layers moving away from and towards the seashore. 8 h later only a small quantity of phages was observed at 500-700 m distance from the sea-front, both in surface layers and at 2.5-5 m depth as well.

In Gagra the presence of FC-2 trassers has been observed at a rather long distance (15 km) on the water surface and at 10 m depths for a quite long period of time (22 h). Distribution of trassers mostly depends on wind and underwater currents. We suppose that the sewage pouring from the collector-cleaner in Gagra could affect the phages causing them to move away from the shore. Viability of the phage can be explained by the relatively high resistance of the phage FC-2 to environmental conditions. Above all, it should be mentioned, that rather large amount of free phages has been observed in the water, pouring from the collector, and the method applied allowed us to reveal the trassers via turbid negative colonies registration.

The data obtained permit us to suggest that any of phages, even the nonspecific bacteriophages, which are easy to select, multiply and concentrate, are fit for trassing.

Table 2

The plating efficiency indices of bacteriophages.

Bacterial strains	Bacteriophages, morphology of negative colonies		
	FC-1	FC-2	FM-17
1	2	3	4
<i>E.coli</i> K-12 λ	$2 \cdot 10^9$	$3 \cdot 10^9$	0
<i>E.coli</i> K-12 λ / FC-1 <i>E.coli</i> K-12 λ +	0	$3 \cdot 10^9$	0
K-12 λ / FC-1	$5 \cdot 10^9$	$3 \cdot 10^9$	0
<i>E.coli</i> K-12 λ / FC-2 <i>E.coli</i> K-12 λ +	$1 \cdot 10^9$	0	0
K-12 λ / FC-2	$4 \cdot 10^9$	$2.7 \cdot 10^9$	0
<i>E.coli</i> M-17	$8 \cdot 10^8$	$8.2 \cdot 10^8$	$3 \cdot 10^9$
<i>E.coli</i> M-17 / FM-17 <i>E.coli</i> K-17 +	$8 \cdot 10^8$	$8.2 \cdot 10^9$	0
M-17 / FM-2	$8 \cdot 10^8$	$8.2 \cdot 10^8$	$3 \cdot 10^9$

Furthermore, the method provides recognition of the trasser-phages from the variety of free phages.

The method is available and economic. Special qualification is not needed for preparing and applying the trassers in practice. It can be used also for studying the process of self-cleaning dynamics of reservoirs and the work efficiency of purificatory devices as well.

Georgian Academy of Sciences

G. Eliava Institute of Bacteriophage, Microbiology
and Virology.

REFERENCES

1. *I. Chkonia et al.* Materials of the conference "Hydrological problems of Georgia" Tbilisi, 1977, 40-43 (Georgian).
2. *I. Chkonia, M. Darsavelidze, N. Chanishvili.* *Ibidem*, 43-45 (Georgian).
3. *M. N. Melnik, V. A. Shatilo, O. V. Shimansky et al.* *Kiev. Zdorovie*, **12**, 1980, 106-109 (Russian).
4. *L. B. Khazenson.* *J. Microbiology.*, **16**, 1975, 101-104 (Russian).
5. *T. G. Chanishvili.* *Proceedings of Tbilisi SRIVS.* **6.1967** (Russian).
6. *P. G. Chumalo, V. S. Kitel.* *Journal of Microbiology*, **2**, 1972, 143-144 (Russian).
7. *H. W. Ackermann, B. Laurent.* *Atlas of Virus Diagrams.* 1995.
8. *J. Lederberg, E. M. Lederberg.* *J. Bacteriol.*, **63**, 1952, 399.

N. Goginashvili

The Increase of Insectine Effectiveness by Weakening Insects Chitinous Barriers

Presented by Member of the Academy G. Gigauri, June 22, 1998

ABSTRACT. Bacterial formulation - Insectine mixed with sublethal doses of Dymiline has been tested on the main leaf-gnawing pest of forest - *Ocneria dispar* L. It appears that the application of Dymiline in advance weakens the pest and then Bt, in this case Insectine, reaches maximal effect in biological control. Substantial decrease of Insectine concentration does not change the results.

Key words: Insectine, Dymiline, chitin, chitinous barrier.

Fast increase of populations of leaf-gnawing insects decreases forest productivity, destroys the integrity of biocenosis and causes great damage. An important and ecologically proved method of biological control consists in the application of biopreparations made on the basis of *Bacillus thuringiensis* (Bt) [1]. It should be noted, that the treatment doesn't always reach the maximal effect. One reason is the low susceptibility of larvae to infection, which is caused by different factors. In insect organism the increase of susceptibility is achievable by using various immunodepressants [2].

The main constituent of cuticle and peritrophical membranes is chitin, protecting the whole organism of the insect. It is possible to infect artificially chitinous barriers and to weaken them by Dymiline prepared on the base of Diphtorbenzuron and thus increase effective action of the bacterial formulation (Bt) [3, 4].

The specifics of Dymiline effect (blocking the last stage of chitin synthesis, going only in *Arthropoda*) inclines that it is practically harmless to warm-blooded and other kind animals living in water and land biocenoses. In soil it would be decomposed in 3-7 days [5, 6].

The reconnoitring investigations were carried out at the Manavi Forestry (Sagarejo, East Georgia) on a population of *Ocneria dispar* L., attacking mainly oak and hornbeam trees. Per 100 ha 5 sample trees were taken.

Insectine, prepared on the basis of Bt was used against this pest with titre 200 active units(au) per 1g, unmixed as well as mixed with Dymiline sublethal doses. The spraying was being conducted by the OBT type tractor sprayer. Dosage of Insectine was 2.5kg/ha, of Dymiline - 0.01kg/ha.

The larvae were in II-IV instars. Colonization density was determined before and 15 days after spraying in order to calculate the effectiveness.

At first oak stand was sprayed with 0.01% aqueous solution of Dymiline and then after 3-7 days interval treated by Insectine (0.1%; 0.002%).

The control plot was in 8-10 km distance from the treated one.

At the Manavi Forestry (Sagarejo), where oak trees are dominant, the *Ocneria dispar* population was broken out. The population density was 30-35 larvae (m/anteroposterior). The oak trees were sprayed with Insectine, Insectine and Dymiline mixture, and unmixed Dymiline. The results are shown in Table 1.

Table 1

Insectine Activity to *Ocneria dispar* Larvae

Test variation	Consumption rate kg/ha	Initial (population) number	Mortality %	Technical effectiveness %
Insectine	2.5	758	87.1	85.9
Insectine Dymiline ⁺	1.5 + 0.01	657	90	89.1
Insectine Dymiline ⁺	2.5 + 0.01	815	97	96.7
Dymiline	0.1	710	69	66.3
Control	-	600	8	-

As shown from the results the decrease of Insectine concentration didn't diminish the control effect, when Dymiline was added. Larvae revealed certain susceptibility to unmixed Dymiline as well.

Thus, the insect immunodepression by Dymiline low doses added to Bt working suspension gave positive and rather consistent results, but inhibitor's ability to weaken chitin during joint action of both preparations is thoroughly incomplete. It would be preferable to treat insect organism with Dymiline in advance.

For this, the spraying was started with Dymiline and followed after 3-7 days by the spraying with Bacterial formulation - Insectine. The results are given in Table 2.

Table 2

Effects of Dymiline and Insectine against *Ocneria dispar*.

Intervals between Dymiline and Insectine spraying	Mortality of pests % after spraying with Bt. days after spraying				
	3	5	7	9	12
Insectine concentration 0.1%					
3	10	22	54	86	89
5	31	50	64	92	100
7	28	45	73	100	100
Insectine concentration 0.002%					
3	9	27	42	58	91
5	24	44	66	90	100
7	25	40	85	100	100
K	-	-	2	6	9

As shown from Table 2, when treatment with Dymiline was conducted in advance: 5-7 days earlier than with bacterial preparation Insectine - entomocidal activity of low and high concentrations of Insectine was 100%. Such method appeared to be more effective

than treatment with Dymiline and Insectine mixture. In experiment sharp decrease of Insectine concentration did not change the result.

The conclusion can be made that pretreatment of pest with Dymiline weakens the pest, and afterwards the spraying with bacterial formulation Insectine gives the maximal effect of biological control.

Georgian Academy of Sciences

V. Gulisashvili Institute of Mountain Forestry

REFERENCES

1. *I. Waizer*. Microbiologicheskie metody bor'by s vrednymi nosekomymi. M. 1972 (Russian).
2. *I. P. Canivet, L. Nef, Ph. Lebrun*. Zeitschrift für Angewandte Entomologie. 1978.
3. Abstracting Journal, ser. "Biology". M., 1981 (Russian).
4. Okhrana i zashchita lesa. M., 1982 (Russian).
5. Instruktsiya po primeneniyu biopreparatov dlya zashchity rastenii protiv massovykh khvoe-listogryzushchikh vrediteli. M., 1990 (Russian).
6. *Ph. C. Kuteev, L. I. Lyashenko, E. A. Kleptova*. Preparations for forest protection. zashchita rastenii. M., 1985. (Russian).
7. *J. M. Franz*. Anz. für Schadl., 5, S. 1968, 65-71.

N. Jimsheleishvili, N. Bagaturia, Corr. Member of the Academy I. Eliava

Two Species of Dorylaimida (Nematoda) New for Georgian Fauna

Presented February 23, 1999

ABSTRACT. Two new species of the number of dorylaimida nematodes for Georgian fauna are described. Their sizes are given and compared with the first description.

Key words: nematoda, dorylaimida, spear.

During 1997-1998 soil nematodes were studied in various regions of Georgia. One of them was studied in Imereti (Western Georgia), while the other - in Tbilisi environs (Eastern Georgia).

Isolated nematodes were fixed in formalin and placed in glycerin. Two species new for the Georgian fauna were discovered in soil samples. Below the redescription of these species is given.

Eudorylaimus subdigitalis Tjepkema, Ferris et Ferris, 1971 [1].

Measurements:

Indiana (USA) specimens:

2♀ L=1.15-1.40 mm; a=20.5-27.3; b=3.30-2.73; c=26.7-40.0; v=56.5-60.9%.

Imereti specimens:

15♀ L=0.7-1.2 mm; a=16-24; b=2.4-4.0; c=18.0-36.6; v=55.0-64.7%.

Body is straight when relaxed. Labial region of width is equal to 1/7 of body diameter at the base of oesophagus. Lips moderately separated from each other and strongly set off from the body. Lips angular, papillae protruding moderately. Amphids funnel shaped about 8.4 mkm wide. Cuticle faintly annulated, the thickness at mid-body about 2-2.5 mkm, at tail a little more. Cuticle is divided into thin outer layer and thicker inner one. Lateral chord not visible.

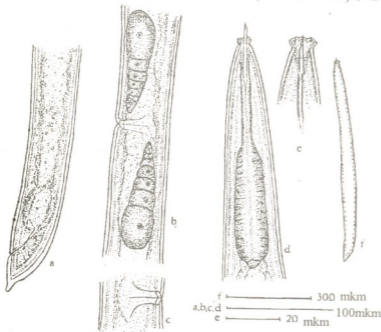


Fig. 1. *Eudorylaimus subdigitalis*: (a) tail region; (b) ovaries; (c) vulval region; (d) anterior part of body; (e) labial region; (f) common view.

Spear moderately strong, its length 12.2 mkm, odontophor 26.2 mkm, with well developed walls. Guiding ring very weak. Oesophagus enlarged at its middle very sharply. Cardia conical-flattened, about 8-10 mkm long. Rectum equals to length of tail, prerectum is slightly longer than rectum.

Tail dorsally convex, with narrow-rounded subdigitate tip. Tail length equals to the anal diameter or slightly more; tail tip is equal to 0.2 of total length of tail.

Gonade paarig, outstretched, reflexed by the vulva. The reflexed part of gonads equals to 40% of its total length. Vulval labia bearing triangular sclerotized pieces. No eggs

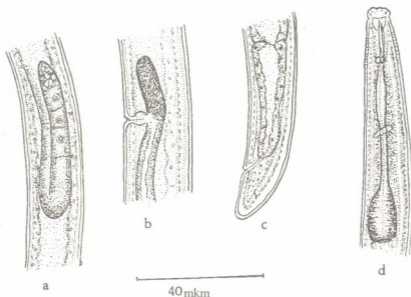


Fig. 2. *Tylencholaimellus eskei*: (a) ovary; (b) anterior uterine sac; (c) tail region; (d) anterior part of body.

observed.

The Imereti region population of *E. subdigitalis* differs from Indiana population by some features: 1. Body slightly shorter; 2. Odontophor well visible; 3. Enlargement of oesophagus sharper; 4. Prerectum slightly shorter.

Habitate: Western Georgia, Imereti region, vineyard soil near Sachkhere, 31 May, 1997.

Tylencholaimellus eskei Siddiqi et Khan, 1964 [2].

Measurements:

Uttar Pradesh (India) specimens:

L=0.53-0.6 mm; a=25-29; b=4.5; c=24-28; v=33-37%; spear+odontophor=17 mkm.

Tbilisi specimens:

♂ L=0.6 mm; a=23; b=5.1; c=26; v=38%; spear+extension=19 mkm.

Body ventrally arcuate when killed by heat. Head bearing distinct labial papille, which do not modify the head contour, offset by slight depression. Body cuticle in two layers; outer layer smooth, inner - faintly striated; inner layer of cuticle on the tail is visibly thickened. Amphids stirrup-shaped, 0.5 of head width. Spear typical for genus. Odontophor bearing large, rounded basal knobs. Complete length of spear is 19 mkm. No sclerotized framework in vestibulum, no labial disc.

Anterior oesophageal tube slender, having a little swollen behind the spear; basal

enlargened part equal to nearly 1/5 of total length of oesophagus, gland nuclei is not visible. Nerve ring by the middle of neck. Oesophagal-intestinal valve short.

Gonade mono-opistodelphic, reflexed to the oviduct. Anterior uterine sac about one body width long. Vaginal wall is weakly cuticularized. Prerectum length is equal to 2.5 anal body diameter, rectum is slightly shorter than anal diameter.

Male is not found.

Habitat: Eastern Georgia, environs of Tbilisi, Khudadovi forest soil, 11 June, 1998.

The specimen from Tbilisi differs from Indian population by some features: 1. Anterior uterine sac contains spindle-shape sperms; 2. Prerectum distinctly definite; 3. The total length of spear a little longer.

The investigation was held by the grant of the Georgian Academy of Sciences.

Georgian Academy of Sciences
Institute of Zoology

REFERENCES

1. J. P. Tjepkema, V. R. Ferris, J. M. Ferris. Res. Bull. Purdue Univ., 882, 1971, 1-52.
2. M. R. Siddiqi, E. Khan. Nematologica, 10, 1, 1964, 105-107.

Corr. Member of the Academy B. Kurashvili

To the Problem of Localization of Echinococcus Larval Stage in Animal and Human Organisms

Presented May 14, 1999

ABSTRACT. The dog, wolf and jackal are definitive hosts of sexually mature forms of the echinococcus pathogene, while humans, domestic and wild hoofed animals are intermediate hosts of its larval, bladder stage. The place of localization of sexually mature forms is the intestine of carnivora, while of the larval stage almost all organs and tissues of the intermediate host except the alimentary tract. Found mainly in liver and lungs.

Key words: Echinococcus, *Echinococcus granulosus*, larval stage, oncosphere, foetus scoloxes.

The dog, wolf, jackal are definitive hosts of a sexually mature form of the echinococcus pathogene, while humans, domestic and wild hoofed animals are intermediate hosts of its larval, bladder stage.

Their localization places are also different: the intestine of carnivora for the sexually mature forms; and almost all internal organs and tissues (except the alimentary tract) of intermediate hosts for the larval, bladder stage.

The development cycle of the echinococcus tape-worm-*Ech. granulosus* is peculiar. Mature proglodits full of ripe eggs are secreted with the definitive host faeces. When out of the organism, the proglottid disintegrates, the eggs get free contaminating the soil, water, grass, vegetables and the animal itself. As soon as the egg gets into the mouth and stomach of the intermediate host by different ways, it gets rid of its coat releasing a foetus which has 6 hooks and displays strong ability for moving. It is called oncosphere (Fig. 1.). It makes its way towards the gut, gets into the blood or lymph system and later is transferred by the blood flow into this or that organ. And what is more, the oncosphere gets into and stops in the portal blood system which explains the localization of echinococcus in the liver.



Fig. 1. Oncosphere of the Echinococcus tape-worm (according to Scriabin and Shults, 1937)

The oncosphere can also be transferred by blood into the lungs and other organs. It is explained by the small size of the foetus and its strong mobility enabling it to go through the liver capillaries and veins and also by the big diametre of capillaries.

According to Scriabin and Shults [1] there are both ways of helminth migration:



Fig. 2. Foetus scolex of the lung echinococcus in men (according to Kurashvili, 1964)

1. Hematogenic migration - moving through a portal circle of blood circulation and 2. Lymphogenic migration - through the Lymphatic ways. As for the echinococcus foetus, its migration occurs by the both mentioned ways.

The spleen, kidneys and heart echinococcus was described too as well as the pleura, diaphragm, lymphatic glands, uterus, urinary bladder, gall bladder, bones (thigh-bone, humerus and ribs). Cases of localization as a result of trauma were registered. When a man with the liver echinococcus suffered a fall the echinococcus bladder burst and the foetus scolexes (Fig. 2) got into the lungs and developed there [2].

Intermediate hosts (humans, animals) are infected with echinococcus through dogs, rarely wolves. As noted above the eggs get out with the dog's excrements. The dog often licks his anus crushing the ripe proglottid, and transfers the eggs onto its hair scattering them. Some people love to care and kiss their dogs letting the echinococcus easily get into their organism. In the stock-raising regions wolves also take part in the spreading of echinococcus.

When out of the organisms of dogs and wolves the eggs get scattered on the grass from where they get into intermediate hosts.

If the definitive hosts - dogs, wolves, jackals happen to eat the intermediate host's organ infected with echinococcus then in their intestine from each foetus scolex the echinococcus tape-worm is developed. About 3 months are necessary for the development of a sexually mature form.

The oncosphere undergoes migration, it becomes free of its coat in the stomach of intermediate host making its way to the wall width of the upper part of the rectum finding itself in the portal vein branching. As soon as it is in the liver the echinococcus foetus gets fastened here more often than in any other organ. The front and middle connecting tissue of the liver and the lobe itself represent a common place of localization. According to the majority of authors, the portal circle of blood circulation is the main way of migration of the echinococcus foetus into the liver.

In order to study the spreading of echinococcus in man the author used the archive material of the Georgian Central Clinics and of the Surgical Clinics of the Transcaucasian Railway Hospital. The literary data on this problem were also used of Acad. Gr. Mukhadze [3], Professors: M. Chachava, E. Pipia, V. Giorgadze, O. Chumberidze, T. Burjanadze etc. [4-7]. Also the map on the geographical distribution of echinococcus in men compiled by

M. Chachava and doctor T. Siria was used. The material applies to the 1910-1948 data, numbering 905 cases. The analysis of the above mentioned material enables us to show a certain regularity in the spreading of echinococcus in humans. The lung echinococcosis is observed more often in the mountain zone as compared with lowlands, where the liver echinococcosis dominates. This phenomenon can be explained by the barrier function being stronger in the mountain zone which makes the oncosphere stop here.

Georgian Academy of Sciences
Institute of Zoology

REFERENCES

1. *K. I. Skrjabin, R. S. Shults.* *Gelmintozny krupnogo rogatogo skota i ego molodnyaka*, M., 1937.
2. *B. Kurashvili.* *Echinococcosis and Alveococcosis of Animals and Humans in Georgia and their Control*, Tbilisi, 1964, (Georgian).
3. *Gr. Mukhadze, M. Chachava.* *Transactions of the Institute of Experimental and Clinical Surgery and Hematology*, II, 1948 (Georgian).
4. *E. Pipia, M. Chachava et. al.* *Transactions of the Institute of Experimental and Clinical Surgery and Hematology*, v. 11, 1949 (Georgian).
5. *M. Chachava.* *Transactions of the Institute of Experimental and Clinical Surgery*, v. VIII, 1959 (Georgian).
6. *B. Kurashvili.* *Proc. of Scien. Session of Helminthologist of Transcaucasian Republics*. Tbilisi, 1963 (Russian).
7. *K. I. Skrjabin, V. N. Ozerskaya.* *Works of Moscow Zooveterinary Inst.*, 11, 1935.

A. Mamardashvili

On the Problem of Metabolic Correlation between Nucleus and Cytoplasm in Neutrophils of Alcoholic Patients

Presented by Member of the Academy T.Chanishvili, February 22, 1999

ABSTRACT. The obtained structural data on neutrophils of alcoholic patients indicate to the existence of discoordination in metabolism between nucleus and cytoplasm.

Key words: neutrophil, metabolism, alcoholism.

The aim of present paper is a detailed study of nuclei and vacuolar system of cytoplasm in neutrophils of alcoholic patients using the method of electron microscope. For this about 4-5 ml of blood was taken from the vein into silicate test tube, centrifuged at 3000 g. The obtained leukocytic film was cut into small parts, which were fixed in 1% solution of osmium on buffer (C-collodin), desiccated and poured into epon. The material was cut on microtome OMU₂ (Austria), taken into special nets, contrasted additionally and then was looked through in electron microscope of "Tesla" type (Czech). In general 10 cases have been studied, males aged 30-40. All of them were suffered from alcoholism during 3-4 years. Control was the blood of practically sound individuals - donors from the station of blood transfusion (5 cases). The control group was consisted from practically non-drinking males aged 40-55.

Our observations showed that attention should be paid to redistribution of hetero- and euchromatin from the side of neutrophils of patients with alcoholism. Large amounts of heterochromatin are marked and it is mainly presented along the edge of nucleus segments. In the central part of nucleus segments the sections containing euchromatin are clearly defined. Nuclear sections occupied by euchromatin are rather light, well contoured and located mainly through the center of segments. The central part is occupied by euchromatin. Thus, around the sections with euchromatin heterochromic sections of different thickness are located.

As to the perinuclear halo its size is large and it is not uniform. It is particularly large in the place where heterochromatin thickness is small. According to the data of a number of scientists [1] perinuclear halo is connected with endoplasmic reticulum. A great number of vacuoles is marked on preparations. Vacuoles are mainly dislocated along cytoplasm edge and near the edge of cell nucleus which seems to be rough and twisted from the side of vacuoles. Vacuoles also represent a part of endoplasmic net, its widened reservoirs and therefore an intensive protein synthesis can take place here [2].

In its turn, vacuolar system must be connected with nuclear membrane i.e. with perinuclear halo and took an active part in a number of vital processes. Thus the existence of vacuoles changes the processes of cytoplasm hydration, value of hydrostatic pressure [3]. The change of value of hydrostatic pressure can lead to the suppression of a number of

physical and physiological processes, to the change of cell stroma, to the regulation of metabolism, to the shifts in diffusion processes [4]. The change of vacuolar system area can change steroids and phospholipids metabolism, which is very important for membrane formation.

Vacuolar system plays an important role in the circulation of substances [5]. It is vacuolar system that takes an active part in such significant functional processes as permeability, circulation, synthesis, accumulation and so on. An increase of vacuolar system area makes it possible formation of ionic gradients and electrostatic potentials on intracellular membranes that makes possible to transmit electrostatic potentials from the surface membrane into deeper layers of cytoplasm. It is with the help of vacuoles that the nucleus can be strongly dislocated to the side of cell edge. Membrane of the nucleus becomes clearly contoured: osmophilia of its leaves is uniform and intensive; chromatin is redistributed, heterochromatin dominates and nucleus edge becomes twisted.

All above mentioned indicates that metabolism between nucleus and cytoplasm of a patient with alcoholism is changed. From the side of cytoplasm a great number of vacuoles of different size and form is marked. That leads to energetic potential disorder on the one hand and, on the other hand, to the breaking of ties between nucleus and cytoplasm.

It is known that main constituent part of a nucleus is chromatin containing DNA and correspondingly genetic information of a cell and organism. On our material chromatin as compared to controls (donor blood) is in a condensed non-active state (heterochromatin dominates). It is not involved in transcription, and RNA synthesis takes place in a little degree. High percentage of heterochromatin in a nucleus must be connected with the presence of histones or histonelike proteins easily forming strong electrostatic complexes with DNA. As it is marked in [6] histones are synthesised in cytoplasm and then transmitted into nucleus. Histones (nuclear proteins) seem to be temporal components, which synthesis is realized by matrix RNA (mRNA). They play essential role in regulation of genetic apparatus activity. The latter (phosphorylation activity) proceeds more intensively in nucleus than in cytoplasm especially when this process concerns high-molecular proteins of nucleus matrix and in addition nonspecific antigens are presented there. There is a feed-back between nucleus and cytoplasm which helps to regulate nucleus activity in correspondence with needs from the side of cytoplasm [7]. Under the influence of signals coming from cytoplasm redistribution of nucleus genes being in passive state and activation of genes take place. This connection in our material appeared to be broken.

M. Asatiani Institute of Psychiatry, Tbilisi

Scientific-Research Institute of Narcology

REFERENCES

1. K. Dan. Behaviour of Sulphydryl Groups in Synchronons division, NY, 1986, 1-138.
2. E. de Robertis et al. Biologia kletki. M., 1983 (Russian).
3. L. Wolper. Biol.Rev. 33, 1978, 108.
4. D. Mazia. Sci. Amer. 40, 1990, 129.
5. T. Stent. Molekulyarnaya genetika, M., 1986 (Russian).
6. V. Bonner. Am.Rev. Physiol. 13, 1991, 45.
7. J. Watson. Molekulyarnaya biologiya gena. M., 1987 (Russian).

M. Gagua, D. Dzidziguri, E. Mikadze, Corr. Member of the Academy V. Bakhutashvili

Study of Plaferon LB Influence on White Rat Hepatocytes Morphofunctional Activity

Presented October 26, 1998

ABSTRACT. The present paper provides for the study of the influence of Plaferon LB on the morphofunctional activity and in particular on the transcriptional activity of hepatocytes in white rats. It has been demonstrated, that Plaferon LB induces intensification of the RNA synthesis activity in hepatocyte nuclei *in vivo* and *in vitro* systems. Activation of the liver tissue due to the Plaferon LB influence was also observed by morphological studies. Our results led to the conclusion, that Plaferon LB, a composition obtained from the amniotic covering of placenta, has the ability to stimulate functional activity of liver cells, which first of all is expressed through intensification of their RNA-synthesis activity.

Key words: Plaferon LB, hepatocyte, transcription

The study of endogenic bioactive substances is one of the most important problems of modern cell biology and experimental medicine. Determination of molecular mechanisms of pharmacologically admissible drugs carried out recently in Georgia is of particular interest. Plaferon LB created and produced in the Institute of Medical Biotechnology was introduced in clinical practice as an antiischemic [1], antiinflammatory [2] and immunomodulative [3] remedy. Pharmacological effects of remedies should result in cell functional activity changes. It is known, that changes of functional activity of cell mainly are based on mutabilities in its gene expression. It is shown also that regulation of gene expression is mainly performed on the transcription level. According to this it was interesting to reveal the influence of Plaferon LB on transcriptional activity of cells. In

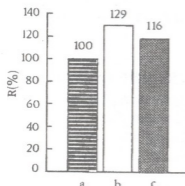


Fig. 1 Plaferon LB effects on the transcription activity of isolated nuclei of mature white rats hepatocytes.

a) control; b) *in vivo*; c) *in vitro*.

particular we have studied the effects of remedy on morphofunctional activity of hepatic cells nuclei both *in vivo* and *in vitro*. The experiments have been carried out on mature white rats (100-120 g), the isolation of nuclei have been performed according to the method in Georgiev's modification [4]. DNA quantity in nuclei have been determined by Sadovsky and Stern method [5]. RNA synthesis intensity in isolated nuclei have been estimated by labelled precursor [C^{14}]-UTP (with relative activity 4.3 GBq/mM) uptake in acid-insoluble fraction. Semithin sections have been studied under light microscope ("Rattennom ROWM").

The experiments detected the transcriptional activity changes after 5 days of daily intraperitoneal infusion of Plaferon LB (single dose 0.1mg protein/kg weight) in in-

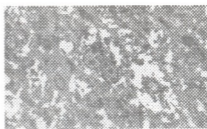
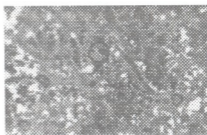
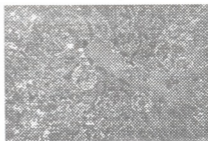
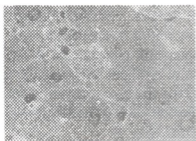


Fig.2 The structure of rat intact hepatic tissue.

Fig.3 The structure of rat hepatic tissue on the 5th day after daily infusion of Plaferon LB

tact animals. In particular the intensity of labelled precursor uptake increased by approximately 29% compared to control (Fig.1.a,b). The studies of Plaferon LB effect on the RNA synthesis activity of hepatocytes *in vitro* have shown that the effect of remedy (dose 25mg protein per 100mg DNA) results in increasing of nuclei transcription activity by approximately 16% (Fig.1.c). Thus, the drug stimulates transcriptional activity of intact hepatic cell both *in vivo* and *in vitro*. It is well known that changes in RNA-synthesis activity in eucaryotic cell nuclei affect their structural organization. That is why in parallel with biochemical analysis the morphological study was performed.

It is clearly shown on the semithin sections, that intact hepatic tissue is characterized by trabecular structure, composed of closely located polyhedral hepatocytes (Fig.2). The average size of the hepatocytes is 21X19 mkm; their nuclei size 7,5X6,0 mkm. Nuclei contain 1-3 large nucleoli. In cytoplasm there is a large number of mitochondria in the form of chaotically disposed dark separated and combined granules. The content of double-nuclei hepatic cells reaches 5%.

After 5 days of daily intraperitoneal injections of Plaferon LB the visible changes of hepatic tissue structure have been observed. Although trabecular structure of tissue is maintained the increase of intratrabeccular spaces is notable, the hepatocytes instead of a

typical polyhedral forms are round-, stretch- or irregular- shaped. The size of hepatic cells increases and is mainly $24 \times 21 \mu\text{m}$, the content of double-nuclei is three times reduced in comparison with intact hepatic tissue, the increasing number of nucleoli and at the same time the expansion of their size indicates the activation of synthetic processes. Together with the activation of nuclei the same tendency is observed in the cytoplasm, where one can detect clearly visible light, the so-called "impoverished" regions indicating the growth of cell functional activity [6].

The obtained results (biochemical and morphological parameters) lead to the conclusion, that Plaferon LB obtained from human amniotic coverings stimulates the functional activity of rat hepatocytes, that considers mainly the activation of hepatocyte transcriptional apparatus. It is known, that Plaferon LB is a multicomponent mixture of proteins and peptides [7] and thus our future studies will be directed to the active basis of the remedy and establish the molecular mechanisms of its effect.

Georgian Academy of Sciences
 Institute of Medical Biotechnology

Tbilisi I. Javakhishvili State University

REFERENCES

1. N. A. Javakhishvili, Z. G. Tsagareli et al. Tezisy dokladov vsesoyuz. konferentsii po aktual. probl. serdech. nedostatochnosti, Tbilisi, 1989, 115-116 (Russian).
2. A. V. Bakhutashvili. Doctor Thesis. Tbilisi, 1991.
3. T. I. Chikovani. Doctor Thesis. Tbilisi, 1997, 90 (Georgian).
4. J. Chauveau, Y. Moule, Ch. Rouiller. Exp. Cell. Res., **11**, 1956, 317-321.
5. P. P. Sadovsky, J. W. Stern. J. Cell. Biol., **37**, 1968, 147-164.
6. E. N. Popova, C. K. Lanin, G. N. Krivitskaya. Morphology of adaptive changes in neural structures, Moscow, 1976, 262.
7. M. G. Gagua, L. U. Rusia, R. M. Kupatadze, M. Sh. Simonidze, V. I. Bakhutashvili. Bull. Georg. Acad. Sci., **153**, 3, 1996, 450-452.

J. Oniani, A. Kudriashov, E. Esebua, Kh. Mebonia

Biological Monitoring of Ecological Danger of Sewage Waters of Various Production Activities

Presented by Corr. Member of the Academy N. Aleksidze, December 17, 1998

ABSTRACT. Using the *Chlorella vulgaris* breed A cells an integral evaluation of ecologico-genetical danger of sewage waters of two plants prior and after purification has been carried out. In both cases a significant decrease in mutagenic activity of the water after passing through the system of purifying equipment was observed. The evaluation of the residual genotoxicity is necessary for establishing minimum multiplicity of dilution of sewage waters at the places of waste water discharge in water bodies.

Key words: sewage waters, genotoxicity, ecology.

While estimating the biological activity of chemical compounds and their combinations in sewage and natural waters, a high-priority problem is the establishing of the "close" effects (general toxicity) and their further manifestations (cancerogenesis, mutagenicity, etc.). The establishment of biological danger of sewage waters is of primary importance; it may be due to at least two causes. First, there is a danger in their direct impact on people who are in permanent contact with it during production activities. Second, the discharge of toxic substances in natural water reservoirs and waterways also has a negative impact on the living systems.

The investigation of the influence of waste waters of various plants on the cells of kharo-algae carried by us earlier revealed their significant impact on the membranes [1-3].

In sewage waters of many plants, in particular, those connected with direct processing of crude oil, as well as using the products of its processing (e. g. paraffin) there is a large number of polynuclear aromatic carbohydrates and other compounds, which may possess cancerogenic and mutagenic properties [4]. In order to reveal possible ecological consequences we have carried out toxico-genetic evaluation of industrial sewage waters prior and after purification.

Methods. Determination of toxico-genetical danger of sewage water samples of microbiological and processing plants was carried out by use of procedures described in [5,6]. As test-objects the cells of *Chlorella vulgaris* breed A, grown in laboratory conditions on Tamiya area were used [7].

The testing of general toxicity was carried out by use of two methods, based on registration of growth and development processes during cultivation on the surfaces of agarized areas during 24 and 72 hours. For the genetic testing statistically certain calculations for the appearance of the number of colonies of alga *Chlorella vulgaris* A, modified in morphology, color, size and with abnormal cell number was carried out.

Results and discussion. Waste water of a plant producing the protein-vitamin concentrates (PVC) possess different toxicity depending on the degree of their dilution. So at 10^3 fold dilution of common sewage samples the number of single cell amount to $14.8 \pm 1.1\%$ against $2.4 \pm 0.4\%$ in control. Increase in concentration (decrease in dilution) leads to an increase in the number of single cells and in undiluted samples amounts to $90.5 \pm 3.7\%$, whereas reproduction inhibition of *Chlorella* takes place $20.3 \pm 2.1\%$, at higher degrees of dilution this index is $72.2 \pm 8.0\%$.

In tests of abnormal sporulations potential genetic impact is detected while treating waste water samples from averaging equipment diluted 10^1 fold. The number of microcolonies with abnormal number of cell amounts to $10.0 \pm 0.9\%$ of control value. Further increase in concentration (decrease in dilution) leads to increase in this index.

The treatment of *Chlorella* cells with samples of sewage water of microbiological production leads to the formation of colonies with abnormal number of cells and sings of growth inhibition, and to the creation of visible mutant colonies. A large number of dotty and dwarf colonies was formed; the number of the latter ones the influence of undiluted sewage water made $69.3 \pm 10.9\%$ in regard with other "nonstandard" colonies.

The samples of PVC plant water, discharged in waterways (after passing through purifying equipment) in $10^4 - 10^0$ fold dilution do not produce significant toxicological and genetical effects. Juxtaposition of the chemical analyze records of plant laboratory with the data of toxico-genetical tests show that the presence of ether-dissolvable and suspended substances, as well as of iron and zinc in sewage water samples, probably, determines its toxicity. So, the reduced contents of these substances after the purification of water does not cause significant toxic and mutagenic effects.

Water samples from oil refinery plant prior purification contained about 4.10 3 mg/l oil products. Toxic effect determined by survival rate (number of single cells in a colony) was rather high in 10^2 fold diluted samples - $30.2 \pm 1.9\%$ against $1.2 \pm 0.1\%$ in control. Certain changes in registered data were observed at 10^4 fold dilution ($14.2 \pm 2.0\%$), at 10^1 fold dilution the number of single cells is $50.2 \pm 4.8\%$ and goes up to 100% in undiluted sewage-water. It must be mentioned that in $10^4 - 10^2$ fold dilution range the number of single cells changes very little, and increases abruptly at 10^1 fold dilution. Average number of autospores formed by one cell is stimulated by treating cells with sewage water within $10^4 - 10^2$ fold dilution range, and drops abruptly under the influence of undiluted water.

After passing through purifying equipment (at the places of discharge) water samples do not affect practically the registered parameters at $10^4 - 10^1$ fold dilutions. In undiluted samples the number of single cells and average number of autospores formed by one cell are $49.7 \pm 3.1\%$ and $29.8 \pm 1.7\%$ respectively.

Tested sewage waters of oil refineries cause the disturbance of spore formation of *Chlorella* cells. Microcolonies with abnormal number of cells were registered, although in small quantities ($3.9 \pm 0.3\%$), at 10^4 fold dilutions of sewage water. The increase in the sewage water concentration (up to 10^1 fold dilution) had very little influence on this index, which fluctuates in the range of $2.1 \pm 0.2\% - 5.0 \pm 0.7\%$; under the action of undiluted sewage water samples the number of colonies drops to $6.5 \pm 0.9\%$ relative to control. The registration of visible mutagenic colonies showed the formation of dwarf, wrinkled,

segment and other kinds of algae colonies. The level of mutagenic activity of all tested samples of sewage water remains rather high. In the sewage water samples of the oil refinery plant wrinkled colonies dominated. Their number accounted for $85.0 \pm 12.0\%$ - $98.7 \pm 11.9\%$ of the total number of the grown colonies.

Purification of the water of given plant results in a little alteration in the number of single *Chlorella* cells ($5.5 \pm 0.7\%$) that is of the order of the control one. Tested undiluted samples of the water after purification still inhibit the reproduction ability of the breed as far as $16.2 \pm 0.7\%$, though these indices were much smaller at 10^4 - 10^2 fold dilutions.

The number of the microcolonies with abnormal number of cells is $1.2 \pm 0.2\%$ - $1.5 \pm 0.2\%$ at 10^4 - 10^1 fold dilutions and increases ($3.9 \pm 0.5\%$) after treatment of the cells with undiluted samples; purification induces outcome of colonies with altered sizes. As in previous series of experiments the wrinkled mutant colonies dominated, though their number was significantly smaller than in the water prior purification.

Thus, sewage water (with oil product concentration of $4 \cdot 10^3$ mg/l) supplied at purification equipment have significant toxic effect on *Chlorella* cells, that is confirmed by the values of all test parameters. Besides toxic action the tested sewage water of oil refinery plant had significantly high mutagenic activity and used to induce specific spectrum of the *Chlorella* mutation changes.

Dispite of decrease in the mutagenic activity level, the complete elimination of mutagenic effects in purified sewage water does not take place, that is confirmed by the presence of oil product remnants, among them benzopirene, in the testing samples. The last fact shows the need for the elaboration of the procedures for removal of benzopyrene from the water discharged into the waterways.

Tbilisi I. Javakhishvili State University

Belorussia State University

REFERENCES

1. E. Moteyunene. In: Indication of natural processes and areas. Vilnius, 1976, 103-105 (Russian).
2. Y. M. Yurin, L. A. Borova, T. G. Sheliaeva. Water Chemistry and Technology, 3, 1981, 455-457 (Russian).
3. J. Oniani, Y. Yurin, M. Chokhonelidze, A. Kudriashov. Bull. Georg. Acad. Sci. 156, 2, 1997, 290-292.
4. I. Tinsli. Environmental behavior of chemical pollutants. M., 1982, 280 (Russian).
5. V. P. Tulchinskaya, G. A. Koshanova et al. Water chemistry and Technology, 6, 1984, 355-364 (Russian).
6. V. P. Tulchinskaya et al. Complex methods of environment quality control. Chernogolovka, 1986, 181-182 (Russian).
7. H. Tamiya. Ann. Rev. Plant Physiol. 17, 1966, 1-21.

V. Yurin, J. Oniani, L. Abadovskaia, E. Esebua, G. Ermolenko

Comparison of Electroalgalogical Testing Results with the Data of other Testing Procedures Using Hydrobionates

Presented by Corr. Member of the Academy N. Aleksidze, December 30, 1998

ABSTRACT. Analysis of our own data, as well as the ones available in literature shows, that bioelectric reaction on kharo-algae cells by their sensitivity is not inferior to other testing procedures carried out on hydrobionates, and by its expressiveness, simplicity and fitness for automated gathering and processing of information exceeds them by far.

Key words: kharo-algae, pollution, chemical compound toxicity.

It has been proposed quite a number of methods for biological testing of water areas and test-objects [1-4]. Some tests are based on mere visual evaluations and their shortcoming is their duration, since by use of them set in irreversible shifts may be registered. However in the number of cases a quick estimation of the established situation is needed, especially in the system of control of accidental discharge of sewage water in natural water reservoirs and waterways. Besides it is very important to detect the starting stage of the pollution, i. e. moment when the concentration of toxic agents still does not result irreversible changes in an organism.

In this respect the use of electroalgalogic tests may have number of advantages in regard with other test-systems. It is obvious that in tests like that the deterioration of sensitivity characteristics in comparison with more long-term tests may take place.

In this connection it seems expedient to compare the sensitivity of the tests based on the biological reactions of kharo-algae cells with other procedures used in different kinds of investigations.

For electroalgalogic tests there were used 2nd - 3rd cells of kharo-algae *Nitella*. As test-reactions served biological responses of a cell on the action of testing preparations. Detailed description of the procedure of the biological testing is given in [2,3].

Results and discussion. The sensitivity threshold and character of the bioelectric reactions of kharo-algae cells, as it has been mentioned several times, is determined considerably by the type of chemical compound affecting them [5].

Let us compare the data of electroalgalogic analysis and some other evaluation methods of estimating chemical compound toxicity, mainly those based on hydrophytes, for three main groups of pollutants: phenol compounds; surface-active substances (SAS); pesticides.

The data in the Table give insight about the values of certain threshold concentrations for the bioelectric reaction of cells *Nitella* in our experiments.

Some of the phenol compounds cause notable bioelectric reactions at rather low concentrations (2.4 - DNF, n- benzoquinone, hydroquinone - 10^{-5} M), but pyrocatechine

and phenol itself have effects only at more higher concentrations ($5 \times 10^3 \text{ M}$). The same is true for 2,4-dichlorophenol [5].

In traditional test-schemes durability of various kinds of algae relative to phenol varies in the range of 2-4 orders. The comparison of our data with the results of inhibiting by phenol the growth of 24 species of algae [6] testifies that only with seven species the complete inhibition of growth takes place at the phenol concentrations higher than C_n . First signs of the inhibition can be observed with all species at concentrations less than C_n .

Using photometric method for the evaluation of *Chlorella* suspension density, G. K. Barashkov and N. M. Kiristaeva [7] worked out a sensitive method for testing the pollution of water areas. According to their observations the presence of $\sim 10^{-5} \text{ M}$ of phenol caused the alteration in the doubling time of the unsynchronized *Chlorella* cultures by 4.2%, 10^{-4} M - by 20.0%. For raising the sensibility and accuracy of the evaluation the test-object was subjected to double shock - they were transferred prior measuring to the area which was different from the growth area in its mineral content, and were treated with ultrasonic waves. The impact of the phenol on the photosynthesis and breathing of the same *Chlorella* shows itself at more lower concentrations (photosynthesis - at 7.5×10^{-4} - $2.6 \times 10^{-3} \text{ M}$; breathing - at $5 \times 10^{-5} \text{ M}$) [8]. By higher algae phenol caused notable shift in water regime indices at concentrations 2.5×10^{-6} - $7.5 \times 10^{-6} \text{ M}$ [9]. It should be mentioned that the kharo-algae cell reaction showed itself only at n-benzoquinone and hydroquinone concentrations of 10^{-3} M [10].

Biocidal effects of the pollutants from SAS group were intensively studied on the sea test-objects [11]. The values of threshold concentrations obtained in our experiments were by 1-3 order lower than the values of threshold concentrations of sea algae, crustacea, fish, test-objects etc. Just for the early detection of the presence in water reservoirs of similar SAS, the methods based on the bioelectric reactions of Kharo-algae cells may be useful. It should be noted that the values of C_n in the case of SAS is also much lower than the concentrations causing notable daphne reactions [12].

The most manifold in chemical content and toxicology group of pollutants - pesticides 2,4-D - in rather high concentrations - 10^{-4} - 10^{-3} M - causes reduction in growth and metabolism of green, diatomic and pyrophite algae [13].

The study of the impact of over 15 kinds of herbicides on the afterglow intensity of *Chlorella* cell suspension showed that the most preparations (phenuron, atrazine, discrill, meturine, etc.) inhibited the glow by 50% at concentrations of 10^{-6} - 10^{-5} M , some of them (diuron, prometin) - at 10^{-7} M [14]. Comparatively less active, as in other experiments, it turned out to be 2,4-D - $4 \times 10^{-5} \text{ M}$. Although, it should be noted that in [15] there was registered the influence of 2,4-D on *Nitellopsis obtusa* cells at concentrations of 10^{-7} M . A considerable reduction in afterglow under atrazin and monuron (10^{-7} - 10^{-6} M) action was observed also on the synchronized *Chlorella* cultures [16]. In our experiments 2,4-D has shown its effects at concentrations of $5 \times 10^{-7} \text{ M}$.

Monuron in concentrations of 2×10^{-6} - $5 \times 10^{-5} \text{ M}$ causes notable changes in the ratio of photosynthesis and breathing in *Vallisneria spiralis* [17], whereas in our experiments a certain bioelectric reaction of a *Nitella* cell was observed at concentrations of 10^{-6} M .

According to our studies, as well as to the data in [18], diuron causes some shift in biological reactions of *Nitella* cells at concentrations of 10^{-6} - $4 \times 10^{-7} \text{ M}$. Daphne-test (reproduction capability and dying-off-rate) has shown almost the same threshold of sensitivity.

Table
 Threshold concentrations causing certain shifts in
 bioelectrical reaction of *Nitella* cells.

Compound	Threshold concentration (C_n), M
Atrazine	$5 \cdot 10^{-3}$
n-Benzoquinone	10^{-5}
Hydroquinone	10^{-5}
Dinitrophenol	10^{-5}
Monuron	10^{-6}
Diuron	$4 \cdot 10^{-7}$
2,4 - D	$5 \cdot 10^{-7}$
Hexachlorane	10^{-7}
2M-4x	$5 \cdot 10^{-8}$
Metaphos	10^{-7}
Propanide	$5 \cdot 10^{-7}$
Satum	$4 \cdot 10^{-7}$
Simazine	10^{-7}
Phenol	$5 \cdot 10^{-3}$
Anionoactive surfactants	10^{-6}
Nonionoactive surfactants	10^{-9}
Ampholytic surfactants	$5 \cdot 10^{-8}$

More sensitive in our experiments was bioelectric reaction of *Nitella* cells on the action of atrazine (5×10^{-8} M) and simazine (10^{-7} M); insecticides metaphos and hexachloran show their effects in concentrations similar those of simazine (10^{-7} M). In other experiments atrazine at more higher concentration (5×10^{-7} M) caused changes in chlorophyll content of *Clorella* cells [19], a little more higher hexachloran concentration (7×10^{-7} M) reduces CO_2 assimilation by rush leaves by 37% compared with control the sample [20], and atrazine at concentration of 10^{-6} M causes general inhibition of photosynthesis and breathing in *Chlorella desulferi* [21].

Thus, electrophysiological analysis based on the use of kharao-algae as test-objects is by its sensitivity no worse than many biological testing procedures commonly used, and by its simplicity,

expressness and fitness for the use in automated monitoring equipment exceeds them by far.

Tbilisi I. Javakhishvili State University

REFERENCES

1. V. M. Yurin. Doctor thesis. Minsk, 1980 (Russian).
2. J. A. Oniani. Ciclosis regulation in algae cells. Tbilisi, 246 (Russian).
3. Bioindication and biotesting methods of natural waters. Leningrad, 1987 (Russian).
4. Water biotesting methods. Chernogolovka, 1988 (Russian).
5. V. M. Yurin, V. M. Ivanchenko, S. G. Galaktionov. Nauka i tehnika. 1979, 200 (Russian).
6. V. Y. Kostiaev. Transactions of Inst. of inter. water biol., 1973, 24, 98-113.
7. G. K. Barashkov, N. M. Kiristaeva. Hydrobiological Journal. 13, 1977, 104-108 (Russian).
8. G. A. Lukina. In Water toxicology algae. M., 1970, 183-185 (Russian).
9. A. I. Mereshko et al. In: Formation and monitoring of water surface quality. 1975, 1, 100-105.
10. M. N. Saksonov, T. G. Atavina. Water biotesting methods. Chernogolovka. 1988, 94-97.
11. S. A. Patin. Impact of the pollution on biological resources and productivity of word ocean. M., 1979, 304.
12. L. A. Koskova, V. I. Kozlovskaya. Hydrobiological Journal. 11, 1979, 77-84.
13. M. E. Kobrali, D. S. White. Arch. Environ. Contam. and Toxicol. 31, 1966, 517-580.
14. D. N. Motorin, P. S. Venediktov, M. G. Makevina. Biological sciences, 12, 1975, 122-125.
15. J. Stolarek. Pr. nauk. USI. Karawicach. 90, 1975, 45-53.
16. A. Murkovski. In Mechanisms of operation of herbicides and synthetic growth regulators their fate in the biosphere, Pushchino. 1970, 187-193 (Russian).
17. A. I. Merezko, E. A. Pasichnaya, A. P. Pasichny. Hydrobiological Journal. 32, 1996, 87-94.
18. V. Y. Petrushenko. In: Kharao-algae and their use in the research of cell biological process. Vilnius, 1973, 404-411.
19. A. EL Jay. Arch. Environ. Contam. and Texicol. 31, 1996, 84-90.
20. L. P. Braginsky, F. L. Komarovsky, A. I. Merezko. Persistent pesticides in fresh-water ecology. Kiev, 1979, 141.
21. M. M. El-shefkh, H. Kotkat, O. H. E. Hammouda. Ecotoxicol. and Environ. Safety. 29, 1994, 349-358.



S. Mgebrishvili

Denture Functional Efficiency during Orthopedic Treatment of Secondary Complete Adenty

Presented by Corr. Member of the Academy T. Dekanosidze, June 25, 1998

ABSTRACT. The artificial teeth displacing was carried out with account of individual motions of the lower jaw particularly by the individual occlusion curves which are formed by means of plaster blocks fixed in the wax occlusion rollers. The sagittal articulation path angle was measured by means of the angle measuring instrument designed by us and the artificial teeth were placed in the articulator constructed by us. To study the efficiency of ready dentures we used I. S. Rubinov's physiological masticatory method of testing.

Key words: central occlusion, occlusion base, occlusion plain, articulator , sagittal occlusion curve, transversal occlusion curve.

Denture for toothless jaws in therapy of the maxillo dental system is of special importance. Complete absence of teeth causes not only anatomic and functional disorder of the masticatory system but it has negative effect on a number of vitally important processes.

Despite the fact that the study of the ways of jaws restoration by dentures after complete loss of all the teeth has a long history, the problem of creation of functional perfect complete dentures has not been solved yet [1].

The methods of displacing artificial teeth as to restore toothless jaws by equipping with dentures are revised in special literature. Some authors, consider that occlusion surface of each artificial tooth as well as complete lines of teeth should repeat the natural teeth occlusion surfaces the patients had before losing the teeth. This view has no grounds as it is important to take into account new conditions connected with losing the teeth when making dentures [2].

The goal of the present paper is to elaborate such method of modification of artificial teeth arrangement in dentures during secondary complete adenty orthopedic treatment, which provides the existence of numerous contacts between the upper and lower jaws teeth lines in different phases of masticatory motions. This stimulates complete denture stability, improvement of masticatory efficiency and raise of its functional value.

120 patients have been equipped with denture; the diagnosis was the secondary complete adenty of the lower and upper jaws, aged 65-94 males 108, females 12. After modelling functional imprints we prepared occlusion basis and rollers of wax. The occlusion plane was formed on the upper occlusion roller, and we established height of occlusion and defined central occlusion. The models were placed in the articulator in the position of central occlusion. A flat piece of metal was fixed in the frontal areas of the lower occlusion roller opposite to the alveolar extension: the metal piece is the size of the lower

central teeth and is sticking out from the roller surface by 1/3 of the previously defined central incisor teeth of the upper occlusion roller. The upper occlusion roller frontal area is softened by means of a warmed up spadel in the direction of the palate as to keep the side from inside the lips untouched. The occlusion basis together with the rollers were placed in the mouth cavity of the patient asking him/her to close mouth in the position of central occlusion and then to make side movements of the lower jaw. As a result, a gap-line was formed on the softened surface of the upper occlusion roller frontal area, which corresponds to the lower jaw transversal movement. Then, we asked the patient to move the lower jaw forward in the so-called sagittal occlusion position and the metal piece fixed in the lower roller came in touch with the upper roller frontal area untouched part. In this position a space is formed in the side area between the upper and lower occlusion rollers; the space enabled us to form the sagittal occlusion curve, bending quality of which corresponds to the lower occlusion roller side space sagittal displacement angle. The sizes of this angle were established by means of the angle measuring instrument designed by us; immobile spindle of the measuring instrument was fixed in the side area of the lower occlusion roller and the mobile spindle - in the corresponding area of the lower occlusion roller, and it moves together with the lower jaw when moving sagittally. According to the established angle sizes we bended the side plates of the articulator; the articulator upper frame is able to move on these plates and the upper jaw model moves with the frame at a time. The occlusion bases and roller were placed back on the models and as a result, in the side area of the articulator upper frame to the background direction a slit is formed, as it was in the mouth cavity. At the same time, the metal piece fixed in the occlusion roller frontal area rested on the untouched part of the upper occlusion roller frontal area again, according to which the front vertical pin of articulator is fastened and the incision plain is bended. The slit formed in the side area of the upper and lower occlusion rollers was filled with soft wax adding to the lower occlusion rollers and a corresponding piece of wax is cut from the upper occlusion roller side areas and the articulator was returned to the central occlusion position again. Afterwards, the upper and lower occlusion rollers side areas were softened opposite each other by means of a warmed up spadle and plaster standard blocks were fixed in them, which correspond to the roller side area by length and width for the upper and lower plaster blocks to bring into close contact. When the plaster blocks are placed on each other closely, we started to move the upper frames articulator back and forth. As a result, the sagittal occlusion curve is formed by the plaster blocks friction. To make the mentioned curves formation more precise and perfect, the occlusion bases and rollers with the plaster blocks fixed in them were removed from the models, moistened with cold water, placed in the patients mouth cavity asking him/her to make the lower jaw movements back and from side to side. As a result, we had the sagittal and transversal curves on the plaster blocks. After having formed the mentioned curves finally, the occlusion bases and rollers were removed from the patient's mouth, placed on the model in articulator. Then we started to displace artificial teeth first on the upper jaw according to the lower occlusion curves, then on the lower jaw according to the upper false teeth arch. The following stages of making the dentures were fulfilled according to the existing rules.

We made use of the Rubinov's physiological masticatory efficiency method of testing to study masticatory efficiency. The testings were carried out after the day of making the dentures 1 month later, 6 months later and 12 months later.

The researches carried out have revealed that masticatory efficiency of the first dentures was 71.4% after 1 month, 81.1% after 6 months, 89.3% after 12 months.

The patients with secondary dentures had masticatory efficiency as following 84.5% 1 month later, 88.7% - 6 months later, 91.6% - 6 months later.

Thus, complete dentures made according to the modification of the method of placing artificial teeth suggested by us are characterized with good indices of masticatory efficiency and they are easier to make both for dentists and patients.

Tbilisi State Medical Academy of Post-Diploma
Training

REFERENCES

1. E. D. Valova. *J. Stomatologia M.*, 5, 1956, 5, str. 37-42 (Russian).
2. A. I. Katz. *J. Stomatologia M.*, 2, 1955, 42-43 (Russian).
3. I. S. Rubinov. In: *Voprosy orthopedicheskoi stomatologii*" L., 1960, 19-36 (Russian).
4. I. M. Hait, *J. Stomatologia M.*, 6, 1961, 71-76 (Russian).



T. Shatilova, M. Beraia

Glaucoma with Normal Pressure and Blood Circulation Disorders in Carotid Artery

Presented by Corr. Member of the Academy P. Todua, July 19, 1999

ABSTRACT. Patient with normal tension glaucoma of the left eye was examined by dopplerography and magnetic resonance imaging. The study showed that extracranially in the left carotid signal intensity was decreased; MRI examination showed diffuse atrophy of the brain and multiple infarction. In spite of stable normal intraocular pressure the hydrodynamics of the eye was pathologic.

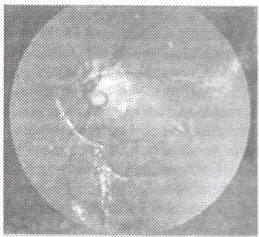
Key words: normal tension glaucoma, excavation, optic nerve head, visual field hydrodynamic, dopplerography, arteria carotis, brain atrophy.

Glaucoma with normal intraocular pressure attracts more and more attention of ophthalmologists. This disease is characterized with function condition typical to glaucoma, progressive loss of vision and characteristic changes of field of view, and optic nerve disk excavation in spite of normal intraocular pressure (IOP). In the past this disease was also called optic nerve disk excavation without glaucoma.

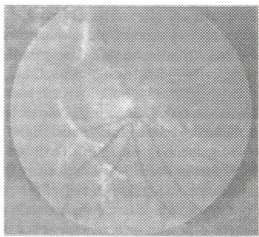
Discussion concerning this disease is given in [1]. Members of the discussion Quigley, Wer, Greenfeld proposed an idea about importance of moderate hypertension and exfoliates in the angle of anterior chamber of the eye. The version concerning IOP increase during the night-time was also proposed. Kitizara considered those versions to be important, as the patient used to lie on the damaged eye side. As an alternative he proposed eye blood flow study.

We describe the case: 76 years old male first payed attention to deprivation of the vision in the left eye. In 1991 he was examined by ophthalmologist at the regional clinic, who proposed diagnosis of retinal central vein thrombosis. The patient was sent for the consultation to the City Hospital no.1, where he first heard the phrase "left eye optic nerve disk excavation". At the Institute of Neurology cranial vessel dopplerography was performed. Insignificant failure of the left-side vertebral vessels was found, carotid arteries without notable stenosis. No signs of tumoral process. 16.05.1991.

The patient was periodically seen and treated at the Ophthalmology clinic of Tbilisi State Medical University. Condition in 1992: external parts of both eyes without changes. In both eyes initial cataracta in the area of lens equator. In the right eye mild opacity of the vitreous body, vessels moderately sclerotic, optic nerve head (ONH) pink, with clear outlines. In the left eye moderate angiosclerosis of retina ONH with deep glaucomatous excavation. Visual acuity of the right eye 0.6-0.7, of the left eye -0.002. Visual field of the right eye was normal, on the left was small island in the upper outer area of the visual field. IOP did not exceed 17-19-21 mm of mercury column. 24-hour tonometry gave the same results. Patient was seen in 1994, 1996, 1997, 1998. Vision worsening is noted since

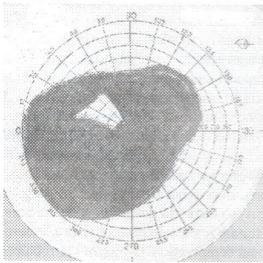


a

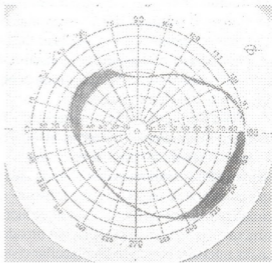


b

Fig. 1. Fundus oculi of the left (a) and the right eye (b)



a



b

Fig. 2. Visual field of the left (a) and the right eye (b)



Fig. 3. CT image of the cranium



Fig. 4. Left common carotid artery

1996. Angles of anterior chamber of the eye are open by gonioscopy with moderate pigmentation. Arterial pressure varies from 130/70 to 120/70. On the 13.09.98 the right eye hydrodynamic was examined: Po-8.3, C- 0.09, F-Po/C=92, C true - 0.06. Left eye: Po-13.8, C- 0.03, F-0.11, Po/C=453, C true - 0.01. The patient was prescribed Timolol malet. Hydrodynamics improved a week later; right eye: Po-8.3, C- 0.19, F-Po/C=44; left eye: Po-10, C- 0.03, F-Po/C=125. A week later Bekker's coefficient was 44 in the right and 54 in the left eye. Neurology status: slightly expressed trembling of upper extremities, flaccid osso-ligamental reflexes in all extremities. Mixed type muscle tonus. Deformation of the vertebrae is noted - spondilosis. Conclusion was "Cerebral encephalopathy". High intelligence and good memory of the patient needs to be mentioned.

Common blood analysis and urinalysis showed no anomaly. Regularly coagulatory system was examined. The presence of B fibrinogen which varied from +++ to + was noted. The patient was regularly receiving medicaments: Kavinton, Nootropil, Cinarisin, Heparin as a course; endonasal ionogalvanisation with 2.4 % Eufillin. Patient was receiving Taufon drops and catachrom instillation into the eyes. The patient was examined at the Research Institute of Radiology and Interventional Diagnostics, Tbilisi, Georgia. On CT study no pathological changes of the both orbits and retrobulbar areas, also of osseous system of basis of cranium and nasal and ethmoidal sinuses were marked. Significant both-side dilatation of Sylvian fissures of the temporal lobes and moderate dilatation of the lateral ventricles system.

MRT of the brain was performed (T1, T2 se; tse regimes; MR-angiography of the intra- and extracranial magistral blood vessels). On the received images in T2tse regime on both sides in the area of basal nuclei, more on the left side, hyperintense areas with sharp outlines are noted without mass-effect. Basal cisternae and convexital subarachnoidal spaces dilatated mostly on the left-side in the area of Sylvian fissures and insulae. No circulated liquor in the level of aqueductus cerebri is noted. No deviation of the median structures is seen. Sella turcica not broadened. Pituitary gland is represented as a homogenous intensity structure. Supracellar cistern without compression. Orbits and retrobulbar area on both sides symmetrical, without seen pathology. On the left side in the ethmoidal sinus hypertrophy of the mucosa is noted. Intracranial magistral arteries, circle of Willis and its branches on both sides are symmetrical and represented by similar intensity signals, without deformation. Perivascular space not dilatated. Extracranially in the left carotid artery distally from the bifurcation signal intensity decrease is noted. The study showed diffuse atrophy of the brain, multiple infarctions.

We explain these processes as follows.

It needs to be mentioned, that few systems are involved in case of glaucoma. The increase of the ophthalmotonus is mostly associated with the anterior drainage system; in this case this system apparently works well, but retinal blood flow is damaged. Dopplerography shows obvious signs of internal carotid artery damage. Retinal blood flow deficit causes death of the ganglial cell and axons; carotid artery stenosis influenced not only on the eye blood circulation, but also on the brain. Subatrophy of the brain matter of the parietal lobe is noted. Significant broadening of the sylvian fissures and subarachnoidal space. These conditions enable the possibility of decrease of the liquor pressure.

Optic disk atrophy is caused by the death of the ganglial cells axons. This is understandable. But what caused glaucoma at nerve excavation, when intraocular pressure was all the time normal?! We consider it was the disbalance between intracranial and intraocular pressure. First time the idea concerning this factor in the aethiology of excavation was proposed [2], and then theoretically worked out [3]. These authors gave this factor principal significance in the process of optic nerve damage in case of glaucoma. We think, that this was the secondary factor, whereas the principal role belongs to blood flow abnormality [4-7].

Retinal blood circulation pathology causes its hypoxia and ganglial cell death, this process spreads to their axons, which are more resistant to the IOP because of Schwann's membrana. In our case carotid artery stenosis caused brain damage, as well as damage of the retina.

There is one more interesting detail in our case: even in case of normal IOP (17-19 mm /Hg) obvious disturbance of eye hydrodynamics is noted – increase of the Becker's coefficient in the damaged eye up to 453. After the local administration of the betaadrenoblockers (Timoptic) this index decreased to the 125 in a week, then down to 54. In the right eye from 92 0 to 54, which means increase of the sympatic nerval system tonus. This attracted our attention and we performed special investigation [7]. Natural experiment – normal pressure glaucoma is the process of great interest and gives keys to the pathological processes in case of glaucoma.

Our investigation is in the contact with [8]. The authors evaluated the reasons of central nervous system degeneration in 10 patients with low tension glaucoma who underwent magnetic resonance imaging, where greater extent of cerebral infarctions and corpus callosum atrophy in patients with low tension glaucoma was noted comparatively to controls.

Tbilisi State Medical Institute of Radiology
 Reserch Institute of Radiology and Interventional
 Diagnostics

REFERENCES

1. *Y. Kitzawa*. J. Glaucoma, 1976, **50-5**.
2. *K. N. Noishevsky*. Glaucoma and its ethiology, 1915, 944 (Russian).
3. *V. V. Vólkov*. Glaucoma, L., 1985, 24-27 (Russian).
4. *T. A. Shatilova*. Doctor Thesis, Tbilisi, 1959 (Russian).
5. *T. A. Shatilova*. Materials of the Russian Congress of the ophthalmologists and XX session after Helmholtz, 1958, 118-127 (Russian).
6. *T. A. Shatilova*. Primary glaucoma, Ch. XXXVII, Pathological anatomy manual TI 1963, 514-524, (Russian).
7. *T. A. Shatilova, T. A. Aleksidze et al.* In: Book of works Medicina. Tbilisi, 1981 (Russian).
8. *K. Oha, K. Favinnella, F. Billeson, Y. Hanong, M. Stern*. Ophthalmology, **102**, 11, 1995, 1632-1638.



K. Gogilashvili, M. Iverieli

Evaluation of Decompensated Caries Reoccurrence Risk

Presented by Corr. Member of the Academy T. Dekanosidze, November 16, 1998

ABSTRACT. We present the tables of reoccurrence risk used for prognosis of disease of a next child in family on the basis of clinical research of ethnic Georgian individuals aged 16 - 25 with decompensated caries, and of probands of the same age group and their relatives, with application of mathematical analysis method.

Key words: reoccurrence risk, decompensated caries.

According to the results of our research the decompensated caries is a multi-factoral disease with polygenic basis, which means that it is determined by mutual influence of genetic inclinations and environmental factors.

Per data provided in the bibliography decompensated caries is characterized by all marks relevant to multi-factoral disease: 1. Relatively high frequency of disease in general population and family based trend towards the disease; 2. Existence of pathogenic and associated markers of predisposition; 3. Chronic proceeding; 4. Manifestation of disease in relatively young age and complication of clinical symptoms with every generation that follows; 5. Similarity of symptoms of disease in diseased individuals and their relatives.

Accordingly, the prognosis of reoccurrence risk is required for prevention of disease.

For this purpose the Tables of empirical risk designed by us reflect reoccurrence risk of decompensated caries in connection to existence of one or more diseased sibling in the family.

Resources and Methods. The resource of the research is data based on clinical, genealogical, and genetic-mathematical analysis of 178 ethnic Georgian probands of 16 - 25 age group diseased with decompensated caries, and their siblings (66/244) and parents (198/356). Also, the research of 162 control probands (not diseased) of the same parameters and their family members has been implemented.

Reoccurrence risk will be calculated with different methods [1-4]. Risk tables are designed according to three types of marriage:

- N x N - neither of parents are diseased;
- N x A - when one parent is diseased;
- A x A - when both parents are diseased.

Results and Discussion. In the studied families the maximum number of siblings did not exceed four. According to the research data, in the cases when neither of parents is diseased with decompensated caries, the reoccurrence risk equals to 22.6% and is not different from population data. The data on reoccurrence risk of decompensated caries in cases of other types of marriages are presented in the Tables 1 and 2.

The sources suggest, that the multi-factoral disease is characterized by increase or decrease of disease reoccurrence risk. As demonstrated in the tables, when one or both

Table 1

Evaluation of reoccurrence risk of decompensated caries in families with one diseased parent

Ordinal number of children	Reoccurrence risk for following children			
	Ordinal number of diseased children			
	0	1	2	3
1	34.8	-	-	-
2	30.2	43.4	-	-
3	26.6	38.3	50.1	-
4	23.8	34.4	44.8	55.3

Table 2

Evaluation of reoccurrence risk of decompensated caries in families with both parents diseased

Ordinal number of children	Reoccurrence risk for following children			
	Ordinal number of diseased child			
	0	1	2	3
1	63.0	-	-	-
2	50.0	70.6	-	-
3	41.5	58.5	75.6	-
4	35.4	50.0	64.6	79.2

parents are diseased together with increased number of diseased children, the risk of reoccurrence increases within following children as well, but the existence of each healthy child decreases the risk of disease in following siblings.

In addition, the reoccurrence risk of DC is higher in the families where both parents are diseased, rather than in the families with only one diseased parent.

Tbilisi State Medical University

REFERENCES

1. *N. E. Morton*. Segregation Analysis. 1969, 129-139.
2. *N. E. Morton, C. S. Ching*. Human Genet, 3, 1967.
3. *C. Smith*. Ann. Hum. Genet, 37, 1974, 275.
4. *F. Figell, A. Motulski*. Human Genetics. 1989, 312.



L. Danelishvili, E. Shilakadze

Drug-Resistance of *M.tuberculosis* and the Future Challenges of Bacteriological Service in Georgia

Presented by Member of the Academy T. Chanishvili, June 22, 1998

ABSTRACT: The object of our consideration is resistance to drugs of cultures isolated from the patients suffering from pulmonary tuberculosis. On the basis of material existing from 1981 to 1991, total of 3574 strains isolated from the patients with pulmonary form were examined for resistance. 2023 of them appeared to be resistant, i.e. 56.5%. From year to year resistance is varied from 38% to 75%. 182 strains were isolated from the patients with pulmonary tuberculosis in 1992-97. 120 of them (66%), appeared to be resistant, 91 strains (76%), appeared polyresistant thus increasing in years.

Key words: *Mycobacterium tuberculosis*, polyresistance.

The socioeconomic shifts taking place in the world have dramatically changed the situation of spreading of tuberculosis. One of the alarming factors of increase in the incidence of tuberculosis in certain parts of the world is the outbreak of polyresistant forms of this disease, especially in the places where medical care is taken of HIV-positive persons. It should be noted that infection of tuberculosis spreads readily and progresses rapidly especially among HIV-infected patients. A wave of tuberculosis outbreak embraced almost all the countries. It penetrated and was spread over the North American States, most of European countries and in the countries of Eastern Europe. Even in England and Sweden the specific tendency towards reduction of incidence of this disease ceased [1].

It is necessary to develop new antituberculosis drugs, which would act on drug-resistant microbes [2].

Situation is desperate in the countries of the former Soviet Union. The disease was widely spread over Russia. Publications indicate an acute, more than two-fold increase in epidemiological index and mortality, especially in some regions, in Western Siberia and Far East where a lot of cases of acute tuberculosis, such as cheesy pneumonia, miliary tuberculosis, etc. are observed [3-6]

The situation has become desperate in Georgia. The antituberculosis combating system has been deranged: the activity of the whole network of institutions of tuberculosis was paralyzed. Due to a deficit of chemical drugs and extreme economic hardship treatment of tuberculosis was stopped. This situation lasted for 3-4 years. During this period people could afford only self-treatment and monotherapy until the end of 1995 when WHO started to carry a project of intensive two-stage chemotherapy with bacterioscopic control, followed by national project including bacteriological studies.

Table 1

Drug-resistance of *M.tuberculosis* in patients with pulmonary tuberculosis in 1981-91

Years	Number of studied strains	Number of resistant strains		Number of mono-resistant strains		Number of poly-resistant strains	
		Abs	%	Abs	%	Abs	%
1981	251	97	38.6	37	38	60	62
1982	398	200	50	78	36.5	127	63.5
1983	325	287	54.6	105	36.6	182	63.4
1984	426	238	55.8	62	26	176	74
1985	303	185	61	52	28.1	133	71.9
1986	379	195	51.5	74	38	121	62
1987	393	295	75	78	26.5	217	73.5
1988	282	164	58	40	24.4	124	75.6
1989	206	138	67	45	33	93	67
1990	231	126	54.5	48	38	78	62
1991	180	98	54.4	45	46	53	54
Total	3574	2023	56.6	659	32.6	1364	67.4

Since 1997 the International Organization of Red Cross started mass bacterioscopic and bacteriologic studies of prisoners (internal project).

Table 2

Drug-resistance of *M.tuberculosis* in patients with pulmonary tuberculosis in 1992-97

Years	Number of studied strains	Number of resistant strains		Number of mono-resistant strains		Number of poly-resistant strains		Double genuine stable strains among poly-resistant strains						
		Abs	%	Abs	%	Abs	%	S+H	%%	H+R	%%	S+H and H+R	%%	
1992	53	32	60.4	12	-	20	62.5	14	-	-	-	-	-	-
1993	35	21	60	9	-	12	57	2	-	-	-	-	-	-
1994	16	9	56.3	2	-	7	77.7	2	-	-	-	-	-	-
1995	17	12	70.6	3	-	9	75	2	-	-	-	-	-	-
1996	6	6	100	3	-	3	50	3	-	-	-	-	-	-
1997	55	40	72.7	-	-	40	100	8	-	8	-	-	10	-
Total	182	120	66	29	24	91	76	31	26	8	6	10	8	-

Nowadays it is hard to judge about the patient's resistance to the drugs of *M.tuberculosis* in this country, since studies in this direction have been scarce recently. And for more or less proper use of chemotherapy it is necessary to know the patient's initial resistance to the microbe. We have made an attempt to consider this question on the available material and make a definite conclusion. The object of our consideration is drug-resistance of the cultures isolated from the patients suffering from pulmonary tuberculosis, since the contingent of such patients is the main reservoir and the source of the infection. We used the material of 1981-91 years.

As seen from Table 1, 3574 strains isolated from the patients with pulmonary form were examined for resistance. 2023 of them appeared to be resistant i.e. 56.5%, including 32.6% of mono-resistant and 67.4% of poly-resistant strains. Resistance to Streptomycin predominates in them, then follows resistance to Isoniazide and to Riphampicin.

Table 2 demonstrates 182 strains isolated from the patients with pulmonary tuberculosis since 1992 up to 1997; 120 of them i.e. 66% appeared to be resistant, 91 strains i.e. 76% appeared to be polyresistant, thus increasing in years.

Double really stable to Streptomycin-Isoniazide, Isoniazide-Rifampicin and both together resistant strains extremely increased in 1997. It is a grave fact, since it makes chemotherapy difficult and actually inefficient.

Proceeding from the foregoing and the situation created in this country, we consider it reasonable to assign the following tasks.

1. For the purpose of early reveal of tuberculosis: a wide application of bacterioscopic method in all suspected patients for detection of *M.tuberculosis* in all somatic curative institutions.

2. To increase the chemotherapy efficiency: a wide use of cultivation method with antibioticograms should be carried out in dynamics prior to treatment, in the course of treatment and at the end of treatment, and on this basis a rational and an adequate chemotherapy should be conducted in all the institutions of tuberculosis.

3. From epidemiological point of view: for the IV group chronic patients who appear to be the infection reservoir and present the source of disease and whose number can considerably increase, it is necessary to create or restore the hitherto existing hospitals (sanatoria) where they would be provided with nursing and treatment. From time to time cultural studies for antibiotics should be made in case of recovery of sensitivity (microbe reversion) to treat them with proper drugs.

Finally, one ought to consider perennial 15-year complex work in search of tuberculostatic drugs, that has been pursued by Microbiological Laboratory of this Institute, Department of Inorganic Chemistry at the Technical University of Georgia and the staff of relevant department at the Institute of Electrochemistry, Georgian Academy of Sciences, by supervision of Academician G.Tsintadze.

A great number of complex and original compounds have been synthesized for these years and examined *in vitro* experiments in this Institute. Rather good results have been obtained *in vivo* (guinea pigs). The studies had been reported and printed, but have not been used so far.

With the use of similar works home chemical preparations could be made.

Institute of Phthysiology and Pulmonology, Tbilisi

REFERENCES

1. A. G. Khomenko. In: Proc. of conf. dedicated to 50th anniversary of foundation of Institute of Phthysiology, Baku, 1995 (Russian).
2. A. G. Khomenko. Problemy tuberculyoza, 5, 1996 (Russian).
3. A. G. Khomenko, V. V. Punga, et al. Problemy tuberculyoza, 5, 1995 (Russian).
4. G. G. Zakopailo. Problemy tuberculyoza, 3, 1996 (Russian).
5. A. G. Khomenko. Problemy tuberculyoza, 4-6, 1997 (Russian).
6. L. P. Kapkov. Problemy tuberculyoza, 6-8, 1997 (Russian).



M. Jebashvili

The Importance of Psychoadaptational and Personality Peculiarities in Development of Early Menopause

Presented by Member of the Academy N. Kipshidze, September 30, 1998

ABSTRACT. In present paper we investigate the influence of psychosocial factors and the importance of personality peculiarities in early menopause development. For this a complex psychological study was conducted on 44 women with early menopause aged 30-40 and 35 practically healthy women, of the same age, without menopause. Thus, women with psychoadaptation disorders are predisposed to early menopause, especially when they are stressed at this age. We think that it is necessary to study psychological factors in women with early menopause. The obtained data received from such a study will help to identify high risk in women and take preventive measures.

Key words: menopause, psychological factors

Problems, connected with menopause, are observed in many countries [1-9]. Menopause often causes prolonged disability and changes in a patient's psychics can be one of the reasons of this.

Menopause can be considered as a developmental stage in a life cycle, when women little by little are becoming adjusted to the biological, social and psychological changes, which accompany ovarian failure and menses cessation.

As tendency to early menopause became more frequent in women of our country, we aimed to investigate the influence of psychological factors and the importance of personality peculiarities in early menopause development. For this purpose a complex psychological study was conducted on 44 women with early menopause aged 30-40 (I group) and 35 practically healthy women, of the same age without menopause (II group - control).

The method of fixed set by D. Uznadze was used during investigation. In his scientific works D. Uznadze had studied those aspects of set, which allow to understand and explain the nature of an individual's mental activity. D. Uznadze had created the general psychological theory of set, which changes unilateral views about human psyche. According to this theory, set is an integral psychophysical state of an individual [10-13].

In our complex psychological investigation MMPI (Minnesota Multiphasic Personality Inventory), which is one of the popular methods of psychometry, was used as well.

In our study special attention was paid to filling in the psychosocial questionnaire, which gives a detailed information about individuals's development, family and interpersonal relations, psychic trauma history and premorbid characteristics.

The analysis of the data received by the application of the method of set has shown that among women with early menopause static (40.9%) and variable (36.4%) set types prevailed, and only 22.7% were of dynamic set type, while most women without meno-

pause were of dynamic set type (65.7%); 14.3% of such women had static set type and 20% had variable set type.

According to the MMPI, most women without menopause had almost all scale indices in norm, while most women (65.9%) with early menopause had significantly higher scores on depression and hypochondria scales.

Summarizing the obtained data we can conclude, that most women with early menopause are characterized by difficulties in adaptation to the environment, deep and heavy interval conflicts, negative emotions, egocentrism, latent aggression, sensitiveness, autoaggression, pessimism, autistic emotions, apathy and hypochondria, which are limiting interpersonal relations and individual's activities.

Psychosocial investigations revealed that most women with early menopause had histories of stresses in childhood: death or illness of loved person, divorce of parents, conflicts in the families, oppressive influence of their parents on them. Such women often were raised by a single parent (mostly mothers). Hence, psychic status of the women with early menopause is somehow related to the type of care for them in childhood, casual emotional stresses, emotional atmosphere in the family and parent's characters.

Women with early menopause often mentioned, that before the beginning of menopause they had psychic traumas: conflicts with relatives - 20.4%; death or serious illness of a loved person - 22.7%, conflicts at a job - 15.9%; 31.8% of these women were experiencing unconscious stresses; in particular, dissatisfaction with family relationships, job, profession.

Thus, disharmony of personality structure may play a certain role in early menopause formation. So the women with psychoadaptation disorders are predisposed to early menopause, especially when they are stressed at this age.

We support psychosocial studies in women with early menopause, which will help to identify high risk and take preventive measures.

Institute of Experimental and Clinical Therapy,
Tbilisi

REFERENCES

1. L. Dennerstein. *Maturitas*, 23, 2, 1996, 147-157.
2. M. Porter, G. C. Penny, D. Russel et al. *British Journal Obstetrics and Gynaecology*. 103, 10, 1996, 1025-1028.
3. S. Fox-Young, M. Sheehan, O' Connor et al. *Journal of Psychosomatic Obstetrics and Gynaecology*. 16, 4, 1995, 215-221.
4. S. Bemederfer. *Journal of the American Psychoanalytic Association*. 1996; 351-369.
5. B. Saletu, N. Brandstatter, M. Metka et al. *Maturitas*. 23, 1, 1996, 91-105.
6. N. F. Woods, E. S. Mitchell. *Research in Nursing and Health*. 19, 2, 1996, 111-123.
7. B. B. Sherwin. *Obstetrics and Gynaecology* 82, (2 Suppl.) 1996, 20S-26S.
8. M. A. Diez, M. M. Gonzales-Tablas, C. Lopez-Sosa et al. *Actas Luso-Espanolas de Neurologia, Psiquiatria y Ciencias Afines*. 23, 4, 1995, 172-177.
9. M. J. Boulet, B. J. Oddens, P. Lehert et al. *Maturitas* 19, 3, 155-156.
10. A. S. Prangishvili. In: *The Unconscious*, Tbilisi. Vol. IV, 1985, 16-24.
11. V. V. Grigolava. *Ibidem*, 24-36.
12. T. T. Iosebade, T. Sh. Iosebade. *Ibidem*, 36-56.
13. V. G. Norakidze. *Ibidem*, 366-377.

Member of the Academy L. Gabunia, O. Bendukidze

On the First Find of the Land Mammal Remains in the Paleogene Deposits of Tbilisi Environs

Presented July 6, 1998

ABSTRACT. The find of the *Rhinoceroidea* remains from the Paleogene deposits of Tbilisi is described. This find is supposed to be the representative of the genus *Rhonzotherium* characteristic for the early Oligocene epoch of Eurasia.

Key words: Oligocene, *Rhinoceroidea*, prohoereses.

During the Paleogene period on the territory of Tbilisi and its surroundings the marine conditions generally prevailed. But from the end of the Eocene the intensification of tectonic development (Pirenean orophasa) caused the raise of some parts of this territory and the formation of land [1,2]. If not at the end of the Eocene, at least, at the beginning of the Oligocene, such terrestrial surrounding surely have existed, which is confirmed by the recent find of the fossil remains of humerus of the early Oligocene land mammal in sandstone of the Vere river valley. The site is about 3 km far from the new building of the Tbilisi State University and geologically belongs to the north wing of the Mamadaviti anticline, and its stratigraphic location corresponds to the Akhalsopelian Eocene-Oligocene formation [4].

The humerus (№V-1) is represented by a badly preserved lower end (Figure 1) with damaged articular surface and trochlea. The upper part of trochlea is broken.

The humerus is relatively large (the width of its lower end is 78 mm, the antero-posterior diameter of the medial pulley-approximately 60 mm, the diameter of the lateral pulley 50 mm, the width at the middle of diaphysis 39.5 mm, antero-posterior diameter on same level - 40 mm. The articular surface has a sand-glass like and manifestly remains of the humeri distal end of primitive perissodactyls [5].

The diameter of the lateral part of trochlea humeri is noticeably smaller than the diameter of the medial part (its index is approximately 80). The trochlea is somewhat inclined to the axis. Its trochlea groove is moderately wide and relatively deep. The surface of the medial part of the trochlea is almost flat and lateral one a bit convexed. There is a slight eminence on the outward edge of the lateral part. The olecranon fossa is very damaged, but obviously it was not very deep. The preserved parts of both epicondyles reflect their considerably strong development. The lower end of the medial epicondylus is relatively wide and bends outwards. All marked features of the fossil bone from the Vere river indicate the resemblance to the humerus of the primitive representatives of the superfamily of *Rhinoceroidea*, but the scarcity of our material does not permit more precise determination. However, it can't be associated with the representatives of *Amyndontidae*, whose lateral part of the humerus is much less in size than the medial part, which makes clear difference between two families of *Rhinoceroidea*

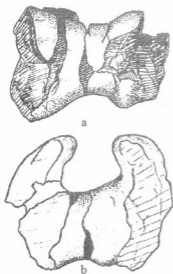


Fig. The distal end of the fossil humerus №V-1 (*Rhinocerozoidea* indet. a) frontal view; b) from below.)

- the forms of the *Hyracodontidae* and *Rhinocerotidae* [6]. But we can't indicate surely to which of these two families of *Rhinocerozoidea* and genus may the humerus from the Vere river be attributed. And yet it can be related with the early Oligocene *Ronzotherium* by its relatively wide articular block and by its relatively slight depth of its medium groove. At the same time it is visibly less by size than the typical species of the mentioned one the *Ronzotherium* - *R. filholi* and some other European forms of this genus [7]. However, our form may approach and even exceed the Mongolian early Oligocene *R. orientalis* [8]. Before some additional data is obtained, we'd better give up more detailed determination of the *Rhinocerotidae*-like perissodactyl form the Vere river and relate it to the group of the superfamily of *Rhinocerozoidea*. Finally, we can assume that the Vere river *Rhinocerozoidea* belongs to the beginning of the early Oligocene, rather than

to the late Eocene. This can be evidenced, in particular, its relatively large sizes (Eocene forms, apart from the gigantic rhinoceroses, are mostly small or smaller than medium animals) and similarity with the *Ronzotherium*. The fossil *Rhinocerozoidea* described from the Paleogene deposits of Vere river indicates that in the early Oligocene epoch Tbilisi region was inhabited by mammalian faunas which probably immigrated from the land in the south-west, populated by rich terrestrial mammal faunas [9, 10]. This land was probably a Paleogene bridge between Asia and Europe providing migration of the mammalian faunas of the two continents in both directions by this way.

Georgian Academy of Sciences
 L. Davitashvili Institute of Palaeobiology

REFERENCES

1. D. Papava. Bull. Geogr. Acad. Sci. XLI, 2, 1966, 365-368 (Russian).
2. V. Alpaidze. Bull. Geogr. Acad. Sci. XLV, 2, 1967, 131-138 (Georgian).
3. The Geology of the USSR, X, 1, Georgian SSR. 1964, Tbilisi, 1-655 (Russian).
4. V. Alpaidze. Doctor Thesis, 1969, Tbilisi, 1-27 (Russian).
5. W. O. Kowalewski. The paleontology of the horses, M., 1948, 1-523 (Russian).
6. V. Gromova. In: Trudy LV, 3, 1954, 85-189 (Russian).
7. Michel Brunet. Les grands mammifères chefs de file de l'immigration Oligocène et le problème de la limite Eocène-Oligocène en Europe. Editions de la foundation Singer-Polignac, Paris, 1979, 1-281.
8. D. Dashzeveg. Palaeovertebrata. 21, 1-2, 1991, Montpellier, 1-84.
9. L. Gabunia. The Benara fauna of Oligocene vertebrates, 1964, Tbilisi, 1-264 (Russian).
10. L. Gabunia. Bull. Geogr. Acad. Sci. 116, 1, 1957, 137-140 (Russian).



M. Murvanidze

To the Study of Quantitative Dynamics of Oribatid Mites (*Acari*, *Oribatei*) in Urban Conditions

Presented by Corr. Member of the Academy I. Eliava, November 16, 1998

ABSTRACT. The quantitative dynamics of oribatid mites in the ravine of the Vere river (within Tbilisi city boundaries) is discussed. Seasonal distribution of *Punctoribates punctum* (Koch), *Eupelops acromios* (Herm) and *Galumna tarsipennata* (Oudemans) is given. Spring and autumn quantitative maxima and summer and winter minima are fixed.

Key words: quantitative dynamics, *Punct. punctum*, *E. acromios*, *G. tarsipennata*.

From ecological viewpoint city is a comparatively new, different from the natural ecosystem environment for the animals including oribatid mites, because by its structure and cenotic peculiarities it has the middle position between the natural and artificial ecosystems. Therefore the establishment of the taxonomic structure and quantitative dynamics of the oribatid mites is of importance in the study of the urban environment.

The researched material was collected in the ravine of the river Vere (within the city boundaries) monthly, from December 1996, till March 1998. The samples have been taken in "Mziuri", from the different grass meadow where some specimens of *Acacia*, *Buxus*, and *Cupressus* are grown.

Soil sampling and isolation of mites was carried out by the methods known in soil zoology [1]. Three 10 cm³ volume samples had been taken from the material. Afterwards we counted the number of specimens of the 1m² area and took out arithmetical mean for the three samples together. Identification of the material was performed by special guides.

On the herb meadow of "Mziuri", which is developed on the brown soil of the field, 21 species of the oribatid mites have been recorded: *Hypochthonius rufulus* (Koch.), *Norhrus bitiliatus* (Koch.), *Oppia clavipectinata* (Mich.), *Belba sculpta* (Mich.), *Metabelba pulverulenta* (Koch.), *Aleurodamaeus setosus* (Berl.), *Liacarus bravilamellatus* (Mihelcic), *Doricranosus morabiacus* (Herm.), *Tectocephus velatus* (Mich.), *Lucopia orientalis* (sp.nov.), *Oribatula tibialis* (Nic.), *Liebstadia similis* (Mich.), *Scheloribates laevigatus* (Koch.), *Trichoribates novus* (Sell.), *Punctoribates punctum* (Koch.), *Eupelops acromios* (Herm.), *E. torulosus* (Koch.), *Galumna flagellata* (Willm.), *G. tarsipennata* (Oudemans.), *Pilogalumna alifera* (Oudemans), *Pergalumna myrmophila* (Oudemans), which belong to the 19 genera and 13 families.

From the mentioned species *P. punctum*, *E. acromios* and *G. tarsipennata* are constant through the whole year. They have quantitative dominant from the different periods of research. The quantitative dynamics of the dominant species defines the dynamic character of the whole fauna. Therefore, we consider the quantitative dynamics of the oribatid mites on the basis of the above mentioned species.

The whole quantity of the oribatid mites made 4 498 sp/m² in December 1996. From 8 appeared species, the most distinguished by its particular multiplicity, is *P. punctum*, which quantity composed 2000 sp/m². During this period, *G. tarsipennata* and *E. acromios* are presented with less quantity. In January 1997, the minimum quantity was fixed, which was conditioned by freezing of the soil surface, but the number of *P. punctum* is still high enough during this period. In our opinion it indicates the resistance of these species to cold as compared with the other species. The quantity of *G. tarsipennata* was unchangeable, but the number of the *E. acromios* noticeably increased. Hence the winter minimum was stipulated not by the quantitative decrease of the background species, but by their falling out of the fauna complex.

From February, the quantity and variety of the oribatid mites species rose again. This process had been continued in spring. Their quantitative maximum 32 929 sp/m² was fixed in May. The increase of the quantity mainly happened at the expense of the increasing of the quantity of *G. tarsipennata*, *E. acromios* and some other individual species. The quantity and share of *P. punctum* in the fauna complex had been progressively decreased. But in May, with the rising of the whole number of oribatid mites, its number rose too.

From June, decrease of oribatid mites number is noticeable, however their whole density is still quite high (9 929 sp/m²). Decrease of quantity mainly happened because of decrease of quantity of *E. acromios* and *P. punctum*; however the number of *G. tarsipennata* is still quite high -3000 sp/m².

In July the number of oribatid mites falls down again -3 396 sp/m². In August the second quantity minimum has fixed, which depends on drying of the soil, due to a high temperature. The density of the oribatid mites during this period is 498 sp/m². A high temperature and lack of humidity restricts the development of *E. acromios*, which is not registered at all in August. However, *G. tarsipennata* and *P. punctum* are presented with less quantity (166 sp/m²), which reveals comparatively more resistance to the extreme conditions.

From September the quantity of oribatid mites increases again. Again appeared *E. acromios*. In December autumn maximum has been fixed - 12 829 sp/m². This mainly amount of *P. punctum*, which made 8 833 sp/m². We should mention that the seasons in the soil delay for about a month as compared with the surface. That means, that in December there is still autumn for the soil. That's why the autumn maximum comes on December.

In January 1998, winter minimum was recorded again, which is higher, than that of 1997 (5531 sp/m²). The quantity of *P. punctum* as compared with other species is higher again 3666 sp/m². *G. tarsipennata* is found with less quantity and *E. acromios* was not found at all.

In February number of oribatid mites rises insignificantly - 5 999 sp/m², but the number of species decreases (only 4 species had been marked). Observation results are given in the Table.

Thus, for the herb meadow "Mziuri", spring and autumn quantitative maximum and winter and summer minima for oribatid mites has been marked. Spring and autumn quantitative maxima were also recorded by Sh. Darejanashvili [2] and V. Piven [3]. Maximum and minimum of mites quantity does not always coincide with maximum and

minimum of species, which shows again the quantity definators usually are found species.

Table
Quantitative dynamics of the oribatid mites from the different grass, meadow ("Mziuri").

Month	Genus number	Species number	Mites number m ²
December, 1996	6	8	4498
January, 1997	6	5	3664
February	11	14	9554
March	10	12	5229
April	8	8	6763
May	12	14	32 926
June	9	11	9929
July	6	9	3396
August	3	3	498
September	12	14	5458
October	8	8	2162
November	12	14	6829
December	9	9	12829
January, 1998	5	5	5331
February	4	4	5999

It should be mentioned, that observations were carried out on imago, but the whole quantity picture including nymphs might be different.

Georgian Academy of Sciences
Institute of Zoology

REFERENCES

1. *D. A. Krivolutski*. In: *Metody pochvenno - zoologicheskikh issledovaniy*. M., 1973, 44-48.
2. *Sh. D. Darejanashvili, L. A. Gomelauri*. *Materialy k faune Gruzii*, 5, 1975, Tbilisi, 47-60.
3. *V. B. Piven*. *Sibirskii vestnik selskokhoziastvennoi nauki*. 5, 1973, Novosibirsk, 1973, 103-106.



K. Tabagari, M. Tsitskishvili, N. Lomsadze

Strontium-90 and Cesium-137 Content in Food Products of Georgia

Presented by Member of the Academy K. Nadareishvili, May 28, 1999

ABSTRACT. The material on artificial radionuclides content in various food products for many years is gathered and generalized. The ratio pollution of food for urban and rural population before and after Chernobyl has been studied.

Key words: long-living radionuclides, Sr-90, Cs-137, alimentary inner-body radiation.

Literary data about long-living Sr-90 and Cs-137 level content and their correlation in the body, food products, environment etc., testify that these parameters significantly vary in different regions.

The aim of our research is to define Sr-90 and Cs-137 content and their correlation in human organism, food products and environment.

The results of investigations of radiation precipitation (level, isotope structure, annual course, dynamics); Sr-90 and Cs-137 content in some products; food ration in different regions (their variety in different regions); the ratio of radioactive precipitation compared with the average of the former USSR made it possible to define the level of radioactive substances in food for a person compared with the average and metabolism of the human organism correspondingly.

Tables 1, 2 show the results of systematic control of radionuclides contents in the food products being carried by Sanitary-Epidemiological Services (SES) of the Georgian Health Ministry. Analysis for many years has been carried out by the laboratory of Republican SES according to the standard methods. A great many analyses were carried out and no doubt there could be an error because of the non-uniformity of the samples. However the results of analyses more or less show general dynamics of the pollution changes by the radionuclides of technogene origin in the products. Local industry products in the individual regions were researched.

We have chosen the main local food products mostly used by people in Georgia for food ration. These basic products contain different amounts of artificial radionuclides in various regions and we found that they were in the limits of average.

The detailed analysis of the material (Tables 1,2) makes it possible to estimate the loadings provoked by artificial radionuclides in human organism being got with food.

Table 1
 Radioactive Sr-90 content in the food products in Georgia (x 10 Bq/kg)
 (coordinated daily permissible dose (DPD)) = 37 Bq/kg)

Years	Milk	Bread	Potatoes	Greenary	Meat	Beans
1963	11.8	13.0	5.0	5.5	1.2	16.7
1964	8.6	9.2	3.4	3.3	1.0	18.9
1965	3.0	3.7	2.9	3.0	0.8	11.1
1966	1.5	2.8	1.7	2.7	0.5	11.1
1967	0.8	3.1	0.9	2.0	0.3	4.1
1968	0.6	1.1	0.5	1.9	0.2	2.6
1969	0.4	0.8	0.7	1.8	0.2	2.3
1970	0.3	0.9	0.5	1.8	0.2	1.4
1971	0.3	0.5	0.4	2.2	0.4	1.1
1972	0.2	0.6	0.7	2.2	0.4	1.3
1973	0.2	0.5	0.6	1.8	0.5	1.0
1974	0.2	0.5	0.7	1.8	0.7	1.2
1975	0.2	0.6	0.8	1.5	0.8	1.2
1976	0.2	0.5	0.7	1.7	0.6	1.0
1977	0.2	0.4	0.4	1.2	0.5	0.7
1978	0.1	0.2	0.4	0.9	0.4	0.6
1979	0.2	0.2	0.4	0.8	0.3	0.4
1980	0.1	0.2	0.3	0.6	0.3	0.4
1981	0.1	0.2	0.2	0.7	0.2	0.7
1982	0.1	0.1	0.2	0.7	0.2	0.9
1983	0.1	0.2	0.3	0.6	0.3	0.5
1984	0.1	0.1	0.3	0.6	0.2	0.5
1985	0.2	0.2	0.3	0.5	0.3	0.5
1986	10.7	4.6	4.6	5.9	1.3	15.5
1987	7.9	3.3	2.9	2.6	1.0	14.8
1988	1.8	2.8	1.9	1.9	0.9	8.9
1989	1.3	2.4	1.2	1.9	0.5	6.8
1990	0.6	2.2	1.0	1.8	0.4	5.9
1991	0.4	1.6	0.9	1.8	0.5	4.0
1992	0.5	1.3	0.9	1.8	0.5	3.4
1993	0.5	1.1	0.9	1.8	0.3	1.9
1994	0.5	0.9	0.9	1.8	0.2	1.4
1995	0.4	0.8	0.8	1.8	0.3	1.2
1996	0.4	0.8	0.8	1.8	0.2	1.1
1997	0.4	0.8	0.8	1.8	0.2	1.0

We conclude:

- nuclear weapon tests provoked radioactive pollution of the environment and, in particular, agrarian production and food ration;
- long-living Sr-90 and Cs-137 (their half-life is more than tens of years) became the fundamental elements in the pollution of ration together with short-living elements (C-141 and 144, La and Ba-140, Zr and Nb-95);
- ratio of these two basic technogene radionuclides almost didn't change for years;

Table 2
 Radioactive Cs (137 and 134) content in the food products in Georgia (x 10 Bq/kg)
 (coordinated DPD = 37 Bq/kg)

Years	Maize	Milk	Potatoes	Greenary	Meat	Beans
1963	2.5	12.9	2.5	17.3	12.0	36.8
1964	2.2	11.7	2.4	16.1	11.1	28.1
1965	1.7	9.2	2.2	13.7	9.2	10.7
1966	1.5	4.4	1.8	8.9	5.6	7.8
1967	1.5	1.8	1.2	4.4	4.4	4.1
1968	1.0	1.5	0.7	2.0	2.8	1.5
1969	0.9	1.0	0.4	1.3	1.8	1.4
1970	1.3	0.9	0.5	2.0	2.9	1.3
1971	1.7	0.9	0.7	1.7	4.4	1.3
1972	1.6	1.0	0.6	1.5	5.9	1.3
1973	1.3	0.8	0.5	1.8	3.7	1.3
1974	1.5	1.0	0.6	1.7	4.4	1.3
1975	2.2	1.2	0.8	1.9	1.8	1.4
1976	1.5	0.9	0.8	1.1	1.7	0.6
1977	1.2	0.8	0.7	1.3	1.8	0.6
1978	0.9	0.3	0.7	0.6	1.5	0.3
1979	0.4	0.2	0.7	0.5	1.7	0.4
1980	0.4	0.2	0.7	0.5	1.7	0.3
1981	0.3	0.3	0.6	0.4	1.6	0.4
1982	0.3	0.2	0.5	0.3	1.6	0.2
1983	0.63	0.2	0.6	0.4	1.4	0.3
1984	0.4	0.2	0.7	0.2	1.4	0.1
1985	0.4	0.2	0.6	0.3	1.4	0.2
1986	22.8	20.4	1.4	33.3	12.4	17.4
1987	2.6	1.6	2.6	5.2	5.3	7.4
1988	2.8	1.4	2.4	0.8	6.5	6.4
1989	3.0	1.3	2.2	0.8	5.0	4.9
1990	2.2	0.4	2.1	0.9	3.3	5.1
1991	1.8	0.4	1.8	0.8	2.6	2.4
1992	1.6	0.4	1.4	0.7	2.4	1.9
1993	1.4	0.4	1.2	0.7	1.9	1.7
1994	1.2	0.4	1.0	0.6	1.7	1.4
1995	0.9	0.3	0.7	0.6	1.6	1.0
1996	0.6	0.3	0.7	0.6	1.6	1.0
1997	0.5	0.2	0.6	0.5	1.6	0.9

- after Chernobyl pollution compiled the same level as it was before Chernobyl, but the correlation of the main pollutants sharply changed. Cs-137 became dominant.

Georgian Academy of Sciences
 Scientific-Research Centre of Radiobiology and
 Radiation Ecology

G. Tevzadze

The Calculation Rule of Real Rhythm Variants of Various Rhythmic Structures

Presented by Member of the Academy G. Tsitsishvili, August 10, 1998

ABSTRACT. We have calculated the real rhythm for N-variants of rhythmic structure. A detailed analysis of N-variants of metric scheme for all permissible rhythmic modifications is given. The classification of various structures allows the author to suggest the method for calculation of real rhythm.

Key words: real rhythm, classification, structure.

As it is generally known the rhythm of verse is determined by the syllable component of the structural item (real rhythm) besides of its main rhythmic structure.

It is very interesting to know how many rhythm variants the same length metre (different structures) has and which length metre has more diversity in this respect.

Analogous studies were made in regard to the concrete writers and concrete metre [1, 2]. It should be noted that such task in its general way hasn't been put forward in verse theory.

Let us set two problems:

- 1) the quantity of real rhythmic variants in rhythmic structures: $(m_1 || m_2)$ and $(m_1 || m_1 || m_3)$
- 2) The theoretical potential of N-syllable metre.

Solution:

Table 1

The syllable component of rhythmic scheme

N ^o	Quantity of syllables	Variant of rhythmic scheme	Quantity of variants
1	2	11;2	2
2	3	111;12;21;3	4
3	4	1111;112;121;13;211;22;31;4	8
4	5	11111;1112;1121;122;113;131;14; 2111;212;221;23;311;32;41;5;1211	16
...	2^{m-1}

According to the syllables composition the general formula of rhythmic variants is expressed as:

$$R_1(m) = 2^{m-1}, \tag{1}$$

where m is a quantity of syllables.

Let us introduce the following nominations:

- | - grammatical or distinct logical pause or caesura;
- || - the metric boundary;
- a - syllable.

Table 2

The variants with account of pause

N ^o	Quantity of rhythmic scheme components	Scheme	Variant of rhythmic scheme	Quantity of variants
1	1	a	a;a//	2
2	2	aa	aa;a/a;a/a//;aa//	4
3	3	aaa	aaa;a/aa;aa/a;aaa//; a/a/a//;a//aa//;aa/a//;a/a/a//	8
4	4	aaaa	aaaa;a/aaa;aa/aa;aaa/a; a/a/aa;a/aa/a;a/aaa//; aaaa//;aa/a/a;aa/aa//; aaa/a;a/a/a/a//;a/a/aa//; aa/a/a//;a/aa/a//;a/a/a/a//	16
5	5	aaaaa	32

According to all kinds of pauses the calculated formula is generally expressed as:

$$R_2^{(n)} = 2^n, \quad (2)$$

where n is the length of rhythmic component (the quantity of syllables in it).

Table 3

The potential of m-syllable component

N ^o	Length of the component	Rhythmic scheme of the component	Frequency of each variant	Potential of rhythmic variants of the component
1	2	3	4	5
1	2	aa	1	4'1+2'1=6
		a	1	
2	3	aaa	1	8'1+4'2+2'1=18
		aaa	2	
		a	1	
3	4	aaaa	1	16'1+8'3+4'3+2'1=54
		aaa	3	
		aa	3	
		a	1	
4	5	aaaaa	1	32'1+16'4+8'6+4'4+2'1=162
		aaaa	4	
		aaa	6	
		aa	4	
		a	1	

The calculated formula of m-syllable is expressed as:

$$R(m) = 2^m C_{m-1}^0 + 2^{m-1} C_{m-1}^1 + \dots + 2 + 2 C_{m-1}^{m-1}, \quad (3)$$

where m is the length of component; C_p^k is a grouping number from p to r

Now we can solve the problems. The solution of the first problem is

$$R(m_1 || m_2) = R(m_1) \cdot R(m_2)$$

$$R(m_1||m_2||m_3) = R(m_1) \cdot R(m_2) \cdot R(m_3),$$

where $R(m_i)$ ($i = 1, 2, 3$) magnitudes are calculated by the formula (3).

The solution of the second problem is:

$$R(N) = \sum_{k=1}^p \prod_{i=1}^k R(m_i)$$

where $(m_1||m_2||\dots||m_k)$ are all permissible rhythmic structure of N length metre.

The analysis of the above Tables and formulas makes it possible to formulate the calculated rule of rhythmic variant for all kinds of rhythmic structures.

Let's make up the Table where the Pascal triangle is located in the central column.

Table 4

The calculated algorithm of real rhythmic variants

m-1	C_{m-1}^k	$\Sigma = 2^{m-1}$	m
1	1 1	2	2
2	1 2 1	4	3
3	1 3 3 1	8	4
4	1 4 6 4 1	16	5
5	1 5 10 10 5 1	32	6
...
m-1	1 C_{m-1}^1 C_{m-1}^2 ... C_{m-1}^{m-2} 1	2^{m-1}	m

If we consider the formula (3), we shall see, that each member of $(m-1)$ line of the Pascal triangle corresponding to m is multiplied by each member of Σ column from the bottom to top.

The arrows indicate the calculated algorithm in case of $m = 4$.

From the above stated follows:

Theorem. The quantity of real rhythmic variants of m length component is $2 \cdot 3^{m-1}$

$$\begin{aligned} & 2^m C_{m-1}^0 + 2C_{m-1}^{m-1} + 2^{m-2} C_{m-1}^2 + \dots + 2^2 C_{m-1}^{m-2} + 2C_{m-1}^{m-1} = \\ & = 2(C_{m-1}^0 \cdot 2^{m-1} \cdot 1^0 + C_{m-1}^1 \cdot 2^{m-2} \cdot 1^1 + \dots + C_{m-1}^{m-2} \cdot 2 \cdot 1^{m-2} + C_{m-1}^{m-1} \cdot 2^0 \cdot 1^{m-1}) = \\ & 2(2+1)^{m-1} = 2 \cdot 3^{m-1} \end{aligned}$$

Georgian Academy of Sciences
Sh. Rustaveli Institute of Georgian Literature

REFERENCES

1. G. Nadareishvili. Galaktion Tabidze's Seven-Syllable Rhythm. Tbilisi, 1977.
2. Idem. The issues of Georgian Prosody. 1984, 140-157.
13. "პროზა", ტ. 160, №2, 1999

O. Petriashvili

Distinctive Features of Literary Grotesque

Presented by Member of the Academy G. Tsitsishvili, June 11, 1998

ABSTRACT. The paper defines literary grotesque as a satirical phantasmagoria. As a result of the investigation of a great number of literary studies of the last decade twenty most important different specifications have been stated. Applied to a literary work they make it possible to characterize it as grotesque or non-grotesque.

Key words: literary grotesque, satire, phantasmagoria, convention, aloofness, implication, irony, paradox.

Grotesque is a special bizarre type of artistic thinking, convention, the essence of which is defined as a satirical phantasmagoria. This feature distinguishes grotesque from ordinary fiction which may be even scientific (i.e. science fiction), that is the reason of not regarding it as a literary grotesque. As far as grotesque is represented in all art forms (architecture, sculpture, painting, music, ballet, circus, etc.), it is important to identify literary grotesque as specific variety. That's why it would be appropriate to distinguish general, essential and distinctive properties of a literary grotesque. These properties help to distinguish whether a literary work is to be called grotesque or not.

On the basis of theoretical analysis of literary material general [1-4] distinctive features of grotesque were summarized as a special literary method of expressing conventionality and we arrived to the following conclusions.

1. Grotesque as a special method of expressing conventional figurative thinking in fiction has ancient mythological root, which gave peculiarities to basic characteristic features of literary grotesque.

2. A carnival, laugh, a joke, a practical joke, buffoonery may be considered as the basis of literary grotesque, but it differs from them as far as literary grotesque depicts them in fiction having its own aesthetic conception.

3. Literary grotesque is related to mocking, castigating and unmasking satire, which is only a part of it, but doesn't fully coincide with it.

4. Literary grotesque is equally represented in all the forms and genres of fiction: (i.e. lyrics, epic literature, drama) where comical is implied.

5. Literary grotesque includes not latent but on the contrary, vividly, openly and even scandalously expressed irrationalism, illogic closely related to logical paradox.

6. Trust ideas and at the same time deliberate tangle of phantasmagoria and reality, beauty and ugliness, tragedy and comedy, sublimity and meanness, chivalry and vulgarity constitute the obligatory components of literary grotesque.

7. Overstatement or understatement, hyperbolisation, excessiveness sometimes increasing to universal, cosmic dimension and vice versa, are characteristic features of literary grotesque.

8. Alterations of real proportions (of things, human dimensions, parts of the body, etc.) exaggerated to caricature and sometimes deliberately transformed into ludicrous figures are to be regarded as important peculiarities of literary grotesque.

9. For the literary grotesque the concrete, fixed object of satirical mockery is necessary with obligatory effect of "recognition" ("finding out") without which neither caricature, parody, satire nor grotesque attain the aim without "recognising" ("finding out") grotesque become a mere entertaining reading. The examples are the adapted books for children "Gargantua and Pantagruel" by Rabelais or "The Gulliver's Travels" by Swift, where the prototypes, political parties and social problems are not of main point for the reader.

10. In most cases mystification, magic, devilishness and other forces of the other world or "magical", "bewitching" forces are presented in literary grotesque.

11. The literary grotesque may embrace irony, malicious mockery, from their crudest to their most refined, exquisite and intellectual forms.

12. The literary grotesque may equally embrace parody, though parody exists independently as an original literary phenomenon independent of grotesque.

13. The literary grotesque implies tale, fable, pamphlet, allegory, but it is not a tale, fable, pamphlet or allegory. It is a special literature phenomenon.

14. The characteristic features of the literary grotesque are the violation of the natural cause and effect relations and they manifest incongruity between the causes and the effects: insignificant trivial causes may provoke great catastrophic effect, whereas truly deep effects, as a rule, cause slight, superficial effects and the causes and results of phenomena are often deliberately confused.

15. The most popular methods of the literary grotesque are turning to the remote historical past or to as much distant future, mysterious countries and distant planets, dreams, intoxication, insanity, phantasmagoric assumptions or zoo-morphic transformations.

16. The grotesque composition is mainly free, easy, subordinated not to the strict logic order but to the fantasy and will of the author or his personages in the phantasmagoric world of grotesque.

17. The literary grotesque is characterized by a particular language expressed in juggling with words, nicknames, names of places or institutions, ridiculous words, combinations or modifications of the words.

18. Implication plays essential role in the literary grotesque when by recognition reminiscences, allusions and implications the desired comic effect achieved.

19. In the historical development of the literary grotesque one can trace its own inner logic of movement from the ancient "Dionysius's laugh" of Renaissance and further to ironical and sceptical "Voltaire's laugh" growing into the merciless and crushing "Stchedrin's laugh" of the XIX century which in the XX century ends with the modern gloomy "non-laugh of Kafka".

20. The literary grotesque is a part of the national culture reflecting national colours and shades but in its best manifestations common to all human.

None of the above mentioned characteristics of the literary grotesque taken separately creates in itself grotesque but only taken together they can create the grotesque. This

méans that in grotesque a fictional world is created: special, abnormal, affected ridiculous, turned over and inside out, exactly out of the interlacement of the above-mentioned numerous characteristics plus the talent and the imagination of the writer, even if he is not acquainted with the specific theoretical rules of the literary grotesque.

The farther in time the literary grotesque deviates from the ancient myth, the medieval and Renaissance carnival and Rabelais laugh, the less grotesque remains in literature in its original form and the more are the proper rules of this grotesque modified. That's why any deviation from the carnival laugh and other West European attributes should not be regarded as breach of the original nature of the literary grotesque. The XX century provides a great number of examples to it.

Sokhumi Branch of Tbilisi State University

REFERENCES

1. *M. M. Bakhtin*. Tvorchestvo Fransua Rable i narodnaia kultura srednevekovia i renessansa. M., 1990 (Russian).
2. *I. Mann*. O groteske v literature. Moskva, 1966 (Russian).
3. *V. Kayser*. Das Groteske in Malerei und Dichtung. Bonn, 1957 (Russian).
4. *D. P. Nikolaev*. Satira Shchedrina i realisticheskii grotesk. M., 1977 (Russian).

M. Khukhunaishvili-Tsiklauri

On Genetic Roots of Tamar According to Folklore Materials

Presented by Member of the Academy G. Tsitsishvili, June 14, 1999

ABSTRACT. This work contains an attempt to study genetic roots of Tamar presenting materials from Georgian and British folklore. In author's opinion Tamar etymologically is connected with the water world.

Key words: Deity-Tamar, Mistress of the water, God's Plant, earthly world, celestial world.

Tamar is a widely spread name among Georgian women. From this name are derived names of geographical places (Tamarasheni, Tamarisi), the surname (Tamarashvili) [1]. Tamar was the name of the historical person, the Georgian monarch called Tamar the Queen. During her reign (1184-1213) Georgia reached the golden Era and her crown exercised authority over much of the territories of the North Caucasus, Armenia, Azerbaijan and Turkey. She was canonized by the church. Tamar the Queen occupies a special place in the hearts of her people. Her name appears frequently in the Georgian folk literature. Folk stories, legends and folk poetry are dedicated to her, in which we meet pagan and Christian beliefs [2]. Analyzing the image of Tamar the Queen in the folk literature, the Georgian scientist, the late Vakhtang Kotetishvili expressed the opinion that the precursor of Tamar the Queen had to be a pagan deity and the historical Tamar had taken on her mythical biography, the motifs from the myths of the deity [3]. Tamar the Queen is credited with conquest of the Kajes, a race of demons with magical powers frequently mentioned in the Georgian folklore, at her command the swallows brought sand and the cranes brought stones for building churches, monasteries and fortresses on inaccessible mountains and cliffs. The creatures of the sky and the Earth were placed under her command and used for noble deeds. She captured the ruler of the seasons of the year, the Morning Star and after that she did down the winter and there was no winter in her kingdom. She used to hold the serpent by the blessed bridle and to ride it quickly and easily. She dominated the sea with the help of fire and became the mistress of the water too, as well as of lands [4].

From the folklore motifs connected with Tamar the Queen we pick out the motifs of domination of the water-sea by Tamar. The semantic meaning of Tamar is well known, in Hebrew it means a date palm [5]. The plant likes water places. In the vegetable world there are also known other plants by the name of Tamar, growing near water places – near rivers, lakes. In Georgia in the province Kakheti there grows a plant called Tamriko Kvavili (Tamar Flower), its Latin name is *Poligonum orientale*. [6]. In Georgia another plant is found under the name Tamarhindi (Latin – *Tamarindus indica*) [7]. There is also other plant Ialguni or Chaluri (Latin – *Tamarix*) [8]. Russians call it Grebenchuk or God's tree [9].

In Pshavi and Khevsureti (provinces of Georgia) the population respect Dobilebi (Dobilebi are maids accepted by a person as sisters) of local Khakhmati Deity-among them is Tamar Kali (Tamar the maid) [10].

There is a place in Benjamin near Gibeah and Bethel (O.T. Judg. 20; 33) called Baal-Tamar. The word Baal in Hebrew means Lord, Possessor, Husband. Sometimes it is used in the primary sense of "master" or "owner". Most often the word refers to the Semitic Deity or deities, called Baal. Baal is not the name of one god, but the name of the presiding deity of any given locality. [11]. To summarize the above mentioned examples we see that Tamar is a mistress of the sea, a plant growing near water places, a God's tree, a sister (Dobili) of a Deity and together with the word Baal-Tamar (Deity-Tamar) is a name of the place.

Russian scientist O. Freidenberg in her work "Thamyris" collected and analyzed the motifs of Thamyris, where a water occupies a special place and the emblem of all the plots of the motifs is lowering or disappear ance into the world of death or of water, searching and appearance in the life, coming out in the light. She also drew attention to the fact that many words related to Thamyris-Tamar, such as Timer, Taimur, Taimir, Tamir, Temir are the names of a river, of a lake, of a bay and cape [12]. This idea was approved half a century later by T. V. Gamkrelidze and V. V. Ivanov. They compiled a semantic vocabulary of Proto-Indo-European, where the words having a semantical meaning of water basins, such as: sea, lake, bay, water body have similar roots mar/mer/mor [13].

Tamar from the British legend also leads us to the world of water [14]. The legend of Tamar, Tavy and Taw tells the story of the lovely nymph Tamara, the daughter of the earth spirits. She used to come and visit the Upper World. Two sons of Dartmoor giants Tavy and Tawrage had seen the fair maid and fell in love. One day the parents saw their daughter sitting between the sons of the giants whom they hated. The gnome father caused a deep sleep to fall on Tavy and Tawrage and took the daughter to his subterranean cell. Tamara did not want to leave her lovers. The father cursed her and changed her into a river which should flow on for ever to salt waters. "Tamara dissolved into tears, and as a crystal stream of exceeding beauty the waters glided onward to the ocean". when Tavy awoke his father who knew of the metamorphosis transformed him into a stream. Tavy runs by the side of Tamara and they glide together to the eternal sea. Tawrage also awakened after a long sleep and was changed to a stream, but he mistook the road along which Tamara had gone and flows away from Tamara for ever [14]. In her remarks to the legend Katherine M. Briggs wrote that this story seemed unconvincing as a folk legend and that it is read rather like a tale founded on classical myths [15].

Summarizing Tamar's synonymous line we have the following picture: Tamar mistress of the sea – plant which likes water places – god's plant, deity's sister (Dobili) – Deity –Tamar (Baal-Tam the name of the place) – nymph, a daughter of the earth spirits, turned into a river. The spacial localization of Tamar is the earthly world.

In the Georgian folklore, in the Tale of Amirani (Amirani is Georgian Prometheus) there is a character by the name of Kamar. She is Amirani's sweetheart. Tamar and Kamar have common root "mar", which in Indo-European has a semantic meaning of the water world. In the Tale of Amirani Kamar is a daughter of the Lord of the Sky and his troops cause changing of weather, provoke rain. According to one of the version of the

Tale rain is tears of Kamar's mother [16]. So water occupies special places in the emblem of the family of Kamar too. This water is a celestial water. Kamar's and her family's spacial place is the celestial world.

Investigating the image of Tamar in the Georgian and the British folklore, the motifs and semantic meanings of the words related to Tamar, we may conclude that the etymologically their roots go to the water world. We find in them traces of myths on water, one of the main elements of the Cosmos.

Georgian Academy of Sciences

Sh. Rustaveli Institute of Georgian Literature

REFERENCES

1. Z. *Chumburidze*. Dedaena kartuli, Tbilisi, 1987, 388 (Georgian).
2. Kartuli khalkhuri saistorio sitkviereba, I, red. Ks. Sikharulidze, Tbilisi, 1961, 24-27 (Georgian).
3. V. *Kotetishvili*. Khalkhuri poezia, Tbilisi, 1961, 374-378 (Georgian).
4. Kartuli khalkhuri saistorio sitkviereba, I, 202-256 (Georgian).
5. The Zondervan Pictorial Bible Dictionary, General Editor Merrill C. Tenney, Grand Rapids, Michigan, USA, 1967, 827.
6. A. *Makashvili*. Botanicuri Lexikoni, Tbilisi, 1961, 91 (Georgian).
7. *Idem, Ibidem*, 30.
8. *Idem, Ibidem*, 32.
9. F. A. *Brokgauz*, I. A. *Efron*. Entsiklopedicheski slovar, S. Peterburg, 1893, tom 18, IX A, 586 (Russian).
10. V. *Kotetishvili*. Khalkhuri poezia, Tbilisi, 378 (Georgian).
11. The Zondervan Pictorial Bible Dictionary, 87-88.
12. O. *Freidenberg*. Thamyris, Iafeticheski Sbornik, V, Leningrad, 1927, 72-81 (Russian).
13. T. V. *Gamkrelidze*, V. V. *Ivanov*. Indoeuropeiski iazik i indoeuropeitsi, rekonstruktsia i istoriko-tipologicheski analiz praiazika i protokulturi, Tbilisi, 1984, II, 672-673 (Russian).
14. M. *Katherine*. Briggs. "Tamar, Tavi and Taw". A Dictionary of British Folk Tales in the English Language, Incorporating The F. I. Norton Collection, Part B, Volume I, folk Legends, London and New York, Routledge, 1991, 367-368.
15. *Idem, Ibidem*, 368.
16. M. *Chikovani*. Mijachvuli Amirani, TSU, Tbilisi, 1947, 329, 320.

T. Evdoshvili

Armenian Historical Source of Tamerlan's First Invasions of Georgia

Presented by Corr. Member of the Academy Z. Aleksidze, June 28, 1998

ABSTRACT: The article represents the Armenian chronicle written at the end of the 14th century. This historical source is contemporary to the Tamerlan's first invasions of Georgia and includes important information about the events in 1386-1387.

Key words: chronicle, bishop, vardapet, Georgia, Armenia, Tamerlan.

Contemporary Georgian written sources about the Tamerlan's invasions of Georgia are very scarce. The preserved documents — inscription of the monastery of Rkoni [1, 204], colophon of the paracliton from Largvisi [2, 204] (both written in 1400), several chronicle notes [2, 191, 193, 201] and the only narrative source «Dzegli Eristavta» (the history of one of the Georgian noble families) [3, 305-374] — can't recreate well enough the situation in Georgia at the end of the 14th and at the beginning of the 15th centuries. So it is necessary to pay a special attention to all foreign-language sources (Persian, Armenian, Greek, Spanish, Arabian) telling us about «Great Asian Conqueror's» [4, 216] invasions of Georgia. Although, Armenian sources aren't so many and versatile as Persian, they still contain very interesting material helping us to study the socioeconomical and political condition of our country of the mentioned period and give more specific information about concrete historical facts. On the other hand, it is very important to determine and ascertain the relation between the historical works of the 18th century's Georgian authors (Beri Egnatashvili's «New Georgian Chronicle» (Akhali Kartlis Tskhovreba) and the prince Vakhushti's «History of Georgian Kingdom» (Aghtsera Sameposa Sakartvelosa) and Armenian sources.

In 1972 an Armenian scientist L. Khachikian published two short historical chronicles, containing the information about the Tamerlan's invasions of Armenia. The publication represents the research and the notes as well. These chronicles are the parts of the old manuscript, kept in the Mashtots Matenadaran under No 9832 [5, 231-48].

The manuscript was found in the middle of the 20th century in Turkey (Diarbekhir) by native ecclesiastic. From March 17, 1950 it was kept in Konstantinopol, at the library of Armenian collector T. Azatian. The manuscript together with the valuable archives was transferred to the possession of E. Charents Museum of Literature and Art, by the widow of the late collector. In 1958-1961 all medieval manuscripts of Azatian's archives were taken from the museum and placed in the Mashtots Matenadaran [6, 127].

In the catalogue of Matenadaran's manuscripts the manuscript No 9832 is called «Collection». Here we present the full description of the «Collection»: 15th c.; 17th c.; 38 pages.; paper; 14 X 5 X 10; written in one column; in Bolorgir and Notrgir (different types of Armenian writing); 17-23 lines; binding: pasteboard covered with fabric; colo-

phons 38 v (15th c.), 24 v (1735), 18 r 37 v (18th c.); contents: from the history of Thomas of Metsoph (1387-1441); the tale of Ephonia's son Kagheba – from the chronicle of priest Jacob; from holly Fathers lives; Arabian prayer-book written with Armenian letters [7, 1000].

The part of the manuscript we are interested in and have translated (19r - 24r p.p.) contains two stories: a) Tamerlan's invasions of Armenia and neighboring countries in 1386-1387 (19r - 22r pg.); b) Armenian history from 1387 to 1443 (22r- 24r p.p.). There is no dividing line between these two chronicles [5, 235]. In the research added to the published texts L. Khachikian has expressed the opinion, that this part of the manuscript doesn't belong to Thomas of Metsoph, as it is shown in the description, but has been written by two different persons and the first of them is the origin of Thomas' historical work. According to the information preserved in the chronicle it is impossible to define exact personality of the author. At first we read: «and I - vardapet Stephan of Metsoph and bishop Nerses took the escaped Christians...», but below we see a phrase: «I too - bishop Nerses was among them». It seems to be, that in one case the author is vardapet Stephan, but in other case - bishop Nerses. Without certain additional knowledge it is impossible to show the preference to any of these two probable authors. According to this L. Khachikian named the chronicle – « History of Tamerlan's First Invasions Written by Stephan and Nerses of Metsoph» [5, 235].

At the end of the 14th and the beginning of the 15th centuries the monastery of Metsoph was one of the best-known educational centers in Armenia. It was founded at the beginning of the 14th century by a well-known clergyman — Mkhitar of Sasun. But it must be said, that the monastery school achieved its golden age in 90-ies of the 14th century under the guidance of John of Metsoph, the disciple of Gregory of Tatev and John of Vorotan. From that time till 50-ies of the 14th century the most popular Armenian vardapets were living and working in this center. Among them were: Gregory of Tatev, Gregory of Khlat, Jacob of the Crimea and Thomas of Metsoph [8, 440-41].

Thomas of Metsoph is the author of some works, that are very interesting from historical point of view. One of them is «Memories» [9]. It is dedicated to the story of the moving of the Catholicos' throne from Sis (Cilicia) to Echmiatsin (Armenia). The second and most valuable work is the «History of Tamerlan and His successors» [10]. The author tells the history of Armenia during the last quarter of the 14th century and the first half of the 15th century. At the same time, the «History» is one of the most important sources in studying the contemporary Caucasian and especially Georgian history. This historical work made the author the only representative of the Armenian historical literature of the 15th-16th centuries [11, 161].

Vardapet Stephan and bishop Nerses, the authors of our chronicle, appear as the well-known representatives of the educational school of Metsoph. They are not only contemporaries, but often the direct participants of the events they tell about. Vardapet Stephan and bishop Nerses took an active part in rescuing the settlement of different regions of Armenia, that left their native places because of the battle between Tamerlan and Khara-Mahmad. The ecclesiastics met the refugees in the region of Mush and led them to the St. Karapet monastery. Together with local bishop and vardapet they fed refugees and encouraged them with the prayer. After leaving the monastery, on their way

to Artshesh they were imprisoned by Tamerlan's troops, but a little later they got freedom. Then the authors and refugees thanked God for saving their lives.

Besides our source, references to authors can be found in Thomas of Metsoph's «History». Specifically, Stephan and Nerses are mentioned together in the description of Tamerlan's invasion of Armenia in 1387, when they helped and encouraged refugees together with the other priests [10, 25]. According to Thomas' information it was the bishop Nerses, who sanctified John of Metsoph (mentioned above) as priest [10, 45]. There are also short references to Stephan. He was a priest of Metsoph's monastery. After John's sanctification (about 1374) they became friends and went to John of Vorotan to study and to take the order of vardapet [10, 42]. According to Thomas of Metsoph vardapet Stephan died in 1395 [10, 38].

Stephan and Nerses of Metsoph's chronicle includes very important information about Georgia and the Georgians. The principle reference, we are interested in, connected with Tamerlan's invasions of Georgia contains information about the origin of the Georgian Royal family name and ethnic structure of Georgian settlement in the 14th-15th centuries.

Stephan and Nerses of Metsoph's story about the invasion of Tbilisi in 1386 by Tamerlan and the events after the taking King Bagrat prisoner, are very important for Georgian historiography. Specifically, the story tells about the King Bagrat the V, who pretended to take Islam, took Tamerlan's troops fraudulently and afterwards Georgians annihilated them completely.

Information like that, but more extended can be found in the «History» by Thomas of Metsoph [12, 19-20], and in «New Georgian Chronicle» by Beri Egnatashvili [13, 329-330]. Here must be mentioned, that these references caused contradiction between the Georgian scientists.

Historians of the 18th-19th centuries trusted the information given in these sources. A critical point of view was given by I. Javakhishvili. He considered, this reference to be tendentious and it appeared to excuse Bagrat the V's unexpected, unpleasant defeat and nothing like that could happen in reality. His opinion is based on the following arguments: 1) Tamerlan was clever and perfidious politician and he never trusted his forces to his former enemy; 2) and if so, Tamerlan would try to take vengeance, but he never invaded Georgia till 1393; 3) In 1387 Thomas «could be a child of eleven», that is why he had to know about that event by verbal information. And besides, when Thomas tells us the story of the crush of Tamerlan's troops, he writes «as they say». I. Javakhishvili explained the appearance of such information in «New Georgian Chronicle» through the Thomas' original work [1, 188-190]. In Persian sources available to the scientist there was no information like this, also there were not discovered any other sources that could define this question.

The argumentation of I. Javakhishvili was completely proved by some of the scientists [14, 38]. The others expressed the opposite opinion about this problem [14, 38], [16], [10, 88]. According to them the information given in Thomas' work and in «New Georgian Chronicle» corresponds to the historical truth. Although this opinion is not proved in their works.

K. Tabatadze analyzed and compared the references of Armenian and Georgian historians to the materials found in Persian sources. The scientist concluded, that the information about the forces that were trusted to King Bagrat had to be true. In this case

Tamerlan's behavior corresponded to his conqueror policy and it is impossible to attach it to Bagrat's enterprise or naivety of Tamerlan. The story of the crash of Tamerlan's troops by Georgians also had to be true. That is why Tamerlan invaded Georgia once more at the beginning of spring in 1387 [17, 71-86].

In the chronicle of Stephan and Nerses of Metsoph we have the following interpretation of the crash of Tamerlan's troops: the crash of Tamerlan's forces by Georgians and set out of Georgian princes (George, Constantine and David) against Tamerlan are not the simultaneous actions, as it is performed in Thomas' «History» and in «New Georgian Chronicle», but these events took place one after the other. So it might be that Bagrat V sons' setting out against Tamerlan is connected with his second invasion in 1387 and proposes the version of the development of events that is different from traditional one.

In our opinion it is interesting to perform this new historical source for several reasons: 1) We have obtained one more source, which is contemporary to Tamerlan's invasions, and proves the crash of Chaghata's troops trusted to King Bagrat V; 2) It gives the right to deny the common skeptic opinion about Thomas' reference spread among Georgian scientists; 3) It is possible to obtain some new information about Tamerlan's second invasion of Georgia in 1387; 4) In spite of its small size, the document gives us the possibility to compare it to other foreign and Georgian materials and to make certain questions of the Georgian history of the end the 14th century more precise.

Tbilisi I. Javakishvili State University

REFERENCES

1. *I. Javakishvili*. History of the Georgian People, v. III, Tbilisi, 1982 (Georgian).
2. *Chronicles and Other Materials of Georgian History and Writing*, collected, put in chronological order, commentary by T. Jordania, II, Tiflis, 1897 (Georgian).
3. *Sh. Meskhia*. Dzegli Eristavta, Family History of the Nobles of Ksani, Materials of Georgian and Caucasian History, section 30, Tbilisi, 1954 (Georgian).
4. *V. Gabashvili*. Tamerlan. Researches of the History of the Near East, 1957 (Georgian).
5. *L. Khachikian*. Patma-Banasirakan Handes, N4, Yerevan, 1972 (Armenian).
6. *L. Khachikian*. Patma-Banasirakan Handes, N3, Yerevan, 1970 (Armenian).
7. *Catalogue of the Manuscripts of Mashtots Matenadaran*, v. II, Yerevan, 1970 (Armenian).
8. *History of the Armenian People*, IV, Yerevan, 1972 (Armenian).
9. *Memories of Thomas of Metsoph*, published and furnished with preface by Karapet Kostaneants, Tiflis, 1892 (Armenian).
10. *Thomas of Metsoph, The History of Tamerlan and his Successors*, translated from old Armenian, furnished with preface, commentary by K. Kutsia, Sources of Georgian History, Tbilisi, 1987 (Georgian).
11. *L. Melikset-Beg*. History of Old Armenian Literature, Tbilisi, 1941 (Georgian).
12. *Thomas of Metsoph, Armenian text together with Georgian translation*, published, furnished with preface, commentary by L. Melikset-Beg, The Notes of Foreign Writers about Georgia, section III: Armenian Authors, Tbilisi, 1937 (Georgian).
13. *Georgian Chronicle*, text established according to the principle manuscripts by S. Kaukhchishvili, v. II, Tbilisi, 1959 (Georgian).
14. *D. Katsitadze*. Georgia at the End of the 14th and the Beginning of the 15th Centuries (According to Persian Sources), Tbilisi, 1975 (Georgian).
15. *V. Gabashvili*. The Tatar Invasions of Georgia, Tbilisi, 1943 (Georgian).
16. *K. Grigolia*. Tsignis Samkharo, N1, 1973 (Georgian).
17. *K. Tabatadze*. Struggle of the Georgian People against Foreign Conquerors at the End of the 14th and the Beginning of the 15th Centuries, Tbilisi, 1974 (Georgian).



A. Arveladze

To the Problem of Correlation of the Pianist's Hearing and Moving System

Presented by Member of the Academy V. Beridze, May 31, 1999

ABSTRACT. Hearing and moving systems work simultaneously in the process of music performing. Both of these systems have hierarchical structure: from the lowest phonic to the highest cortical level where intonational performative anticipation is leading. Correlation of hearing and moving systems and artificial continuity of a performance are discussed.

Key words: coordination, correlation, anticipation

Musical performance is the basic form of music as an art. Creative world is inexhaustible for analytical mind. Correspondingly, the area of problematic study of the performance is rather wide. One of the actual and less studied questions is the problem of artistic continuity of performance. This problem is many-sided: the wholeness of performance, performance and experience of performance time, conception of performance and basic conditions of its sounding, excitation of public performance and possibility of its regulation, etc.

The aim of the present study is to find those conditions which can provide artistic continuity of a performing process while performing of the studied piece of music on public. Due to the fact that musical performance is a complicated psychophysiological act of man's creative work we suppose it is quite natural to seek the key just within the psychophysiological regularities. The moving side of musical performance is significant and it is comparatively well studied in [1-3]. The most vivid expression of the performer's hearing activity is the hand itself which represents a kind of performative apparatus.

The above mentioned authors regard the moving system of a performer according to B4. Bernstein's [] classification, i. e. from the simplest level to the highest cortical one. But the moving system is not decisive and single in the artistic continuity of musical piece. The moving system is in the closest connection with hearing system, which consists of six levels. This classification is based on hearing reaction to the certain properties of the sound, namely, frequency, intensity, duration. It should be noted that dynamic and timbre characteristics of hearing are comparatively less researched in physiology.

In the process of hearing system of a musician hearing expression, real sounding and hearing control should be in harmony with each other. Very often strong developed hearing expression diminishes the hearing control and insufficient clearness of hearing reduces the activity of hearing control. It is clear that in this complicated coordinative system the function of musician-performer is impossible without prognostic and directing work of anticipation mechanism.

the meaning of the linguistic units only on the ground of their interrelations or within the limits of "pure verbalism" and say that certain unit has a meaning as its compatibility with the same level units within the limits of the next, higher level unit is somehow restricted and these combinative restrictions are defined by some rules or without, when one concrete unit is incompatible with the other concrete unit or units. In fact, the phrase is tautological since linguistic units are to be identified following from the combinative restrictions of their constituents and of the supposed units themselves within the higher level units. Hence we can say that every linguistic unit has some "meaning".

As an illustration of the above-stated we'll dwell upon the meanings of words (lexemes) and consider some outlines of constituting admissible syntagmas on the basis of distributional characteristics of lexemes. Evidently, it is impossible to deduce the compatibility of words or, more exactly, lexemes within syntagmas from their structure (we don't mean, of course, the mythical "semantic structures" of words). we wouldn't be able to decide whether a combination of two lexemes forms permissible syntagma even if we had taken into consideration the "meanings" (distributions) of their constituent syllables, their positions within the words and their number. But in order to clear up whether the syntagma corresponds to the linguistic usage it not necessary to know the lexical composition of all the permissible syntagmas of the given language. Syntagmas may be constituted on the grounds of analogy as well. The restrictions in compatibility between certain level units within the next, higher level units may be considered regular so that as the compatibility of some classes of units, not of the individual units, was regulated and the classes in its turn were identified not by the structure and constituents of the units but deduced from the relational paradigms of the units on the basis of the functional analogies. Suppose lexeme "a" within the higher level unit (some syntagma) is combined with each of the units of its level (lexemes) "c", "d", "e", "f", "g". We shall obtain the syntagmatic paradigm "ac", "ad", "ae", "af", "ag" with "a" as a "constant" component of its members. Now imagine that the paradigm as a whole is just one member of some larger paradigm, constituted on the basis of variability of the very "a", i. e., in such a way that "a" being substituted in turns by some of its level units "l", "m", "n", "o". As a result the second member of the new paradigm would be "lc, ld, le, lf, lg", the third "mc, md, me, mg", etc. We can conclude that the unit "b", which is compatible with each of "c", "d", "e", "f" would be compatible with "g" as well. The "logic" of the relational structure of the units is as follows: the units (lexemes) "c", "d", "e", "f", "g" compose a class the members of which have one feature in common: they all are compatible with the same set of units. If some unit "b" was actually compatible with each member of the class except "g" (we didn't know whether it is compatible with "g"), it would be compatible with "g" as well because the latter belongs to the same class as the others. Besides, the more units are compatible with the members of the mentioned class the more "features" in common would have its members and the more stable would be the class itself and therefore with the more certainty we could assert the permissibility of "bg" combination. It is evident that such a "logic" is nothing more but the application of analogy, certain unification of the relational structure.



A. Arveladze

To the Problem of Correlation of the Pianist's Hearing and Moving System

Presented by Member of the Academy V. Beridze, May 31, 1999

ABSTRACT. Hearing and moving systems work simultaneously in the process of music performing. Both of these systems have hierarchical structure: from the lowest phonic to the highest cortical level where intonational performative anticipation is leading. Correlation of hearing and moving systems and artificial continuity of a performance are discussed.

Key words: coordination, correlation, anticipation

Musical performance is the basic form of music as an art. Creative world is inexhaustible for analytical mind. Correspondingly, the area of problematic study of the performance is rather wide. One of the actual and less studied questions is the problem of artistic continuity of performance. This problem is many-sided: the wholeness of performance, performance and experience of performance time, conception of performance and basic conditions of its sounding, excitation of public performance and possibility of its regulation, etc.

The aim of the present study is to find those conditions which can provide artistic continuity of a performing process while performing of the studied piece of music on public. Due to the fact that musical performance is a complicated psychophysiological act of man's creative work we suppose it is quite natural to seek the key just within the psychophysiological regularities. The moving side of musical performance is significant and it is comparatively well studied in [1-3]. The most vivid expression of the performer's hearing activity is the hand itself which represents a kind of performative apparatus.

The above mentioned authors regard the moving system of a performer according to B4. Bernstein's [] classification, i. e. from the simplest level to the highest cortical one. But the moving system is not decisive and single in the artistic continuity of musical piece. The moving system is in the closest connection with hearing system, which consists of six levels. This classification is based on hearing reaction to the certain properties of the sound, namely, frequency, intensity, duration. It should be noted that dynamic and timbre characteristics of hearing are comparatively less researched in physiology.

In the process of hearing system of a musician hearing expression, real sounding and hearing control should be in harmony with each other. Very often strong developed hearing expression diminishes the hearing control and insufficient clearness of hearing reduces the activity of hearing control. It is clear that in this complicated coordinative system the function of musician-performer is impossible without prognostic and directing work of anticipation mechanism.

The problem of correlation of hearing and moving systems is supposed in the nature of continuity anticipation. A well known musicologist and pianist S.M.Mal'tzev [5] states: "The hands of the improvisator-performer must be ready unconsciously, easily and instantly to obey every direction of hearing and perform just those harmonic sounds which possess the hearing imagination of the performer in advance".

The pianist's hands as individualized functional system set up anticipation ties between musician's ear and motoric system. Instant reaction of the hand to the directions of the ear, its readiness to respond every demand of ear imagination occurs on the basis of anticipation.

The pianist R.Khojava states [6]: "The whole penetration into the composition becomes possible not only by means of developed inner sounding imaginations and memory mechanisms but also by hearing in advance. If the performer masters the mechanism of advance hearing then his excitement on the scene becomes significantly reduced, because in such case his attention will be directed on emotional, intonational and logical development of music. Therefore every outside stimuli disappears for the performer and he will be absorbed completely in performing composition".

Our practical observations and analysis of corresponding literature make us to arrive to the necessity of anticipation mechanism specificity in relation to music's intonation nature. Music is a creative process developing in time. The more this time subjectively connected and intonationally excited, the more tense the intonation tonus and dynamics is. And performance is characterized by these properties when the level of penetration of musical intonation is high. The more intensive inner hearing intonation, the more complete is the process of performing, because inner intonation promotes continuity of sounds interrelation of tones. These arguments are also proved by B. Asafiev in [7]. "The activity of hearing is in the fact that in every instant of musical performance (if you don't "read" but play) consciously must be listened earlier that it really will sound in your fingers".

As it is seen from the present study hearing (moving coordinations have a rising hierarchy which is directed to maximum switch of cortical levels where basic and leading is intonation-performative anticipation which provides hearing and moving systems correlation and artistic continuity of performance.

V. Sarajishvili Tbilisi State Conservatory

REFERENCES

1. *V. Grigor'ev*. In: *Voprosy muzykal'noi pedagogiki*. 7, M., 1986 (Russian).
2. *V. Sradzhev*. *Problemy razvitiia fortepiannoi tekhniki*. Tashkent, 1987 (Russian).
3. *I. Kvirikadze*. Candidate thesis. Tbilisi, 1990.
4. *N. Bernshtein*. In: *Problemy kibernetiki*. 6, M., 1961 (Russian).
5. *S. Mal'tsev*. *J. Voprosy psikhologii*. 3, 1988.
6. *R. Khozhava*. *J. Religion*. 9, 1992 (Georgian).
7. *B. Asafiev*. *Muzykal'naia forma kak protses*. 1, L., 1963 (Russian).

Subscription Information

Correspondence regarding subscriptions, back issues should be sent to:

Bulletin of the Georgian Academy of Sciences

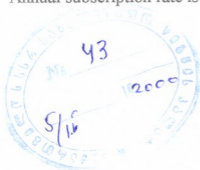
Georgian Academy of Sciences,
52, Rustaveli Avenue, Tbilisi, 380008, Georgia

Phone : + 995-32 99-75-93;

Fax/Phone : + 995-32 99-88-23

E-mail : BULLETIN@PRESID.ACNET.GE

Annual subscription rate is US \$ 400



© საქართველოს მეცნიერებათა აკადემიის შოამბე, 1999
Bulletin of the Georgian Academy of Sciences, 1999

გადაეცა წარმოებას 8.09.1999. ხელმოწერილია დასაბეჭდად 2.12.1999.

ფორმატი 70×108 1/16, აწეობილია კომპიუტერზე, ოფსეტური ბეჭდვა.

პირობითი ნაბ. თ. 13, სააღრიცხვო-საგამომცემლო თაბახი 13.

ტირაჟი 250. შეკვ. 274 ფასი სახელმწიკრულეზო.

რედაქციის მისამართი: 380008, თბილისი-8, რუსთაველის პრ. 52, ტელ. 99-75-93.
საქართველოს მეცნიერებათა აკადემიის საწარმო-საგამომცემლო გაერთიანება „მეცნიერება“,
380060, თბილისი, დ. გამრეკელის ქ. 19, ტელ. 37-22-97.

